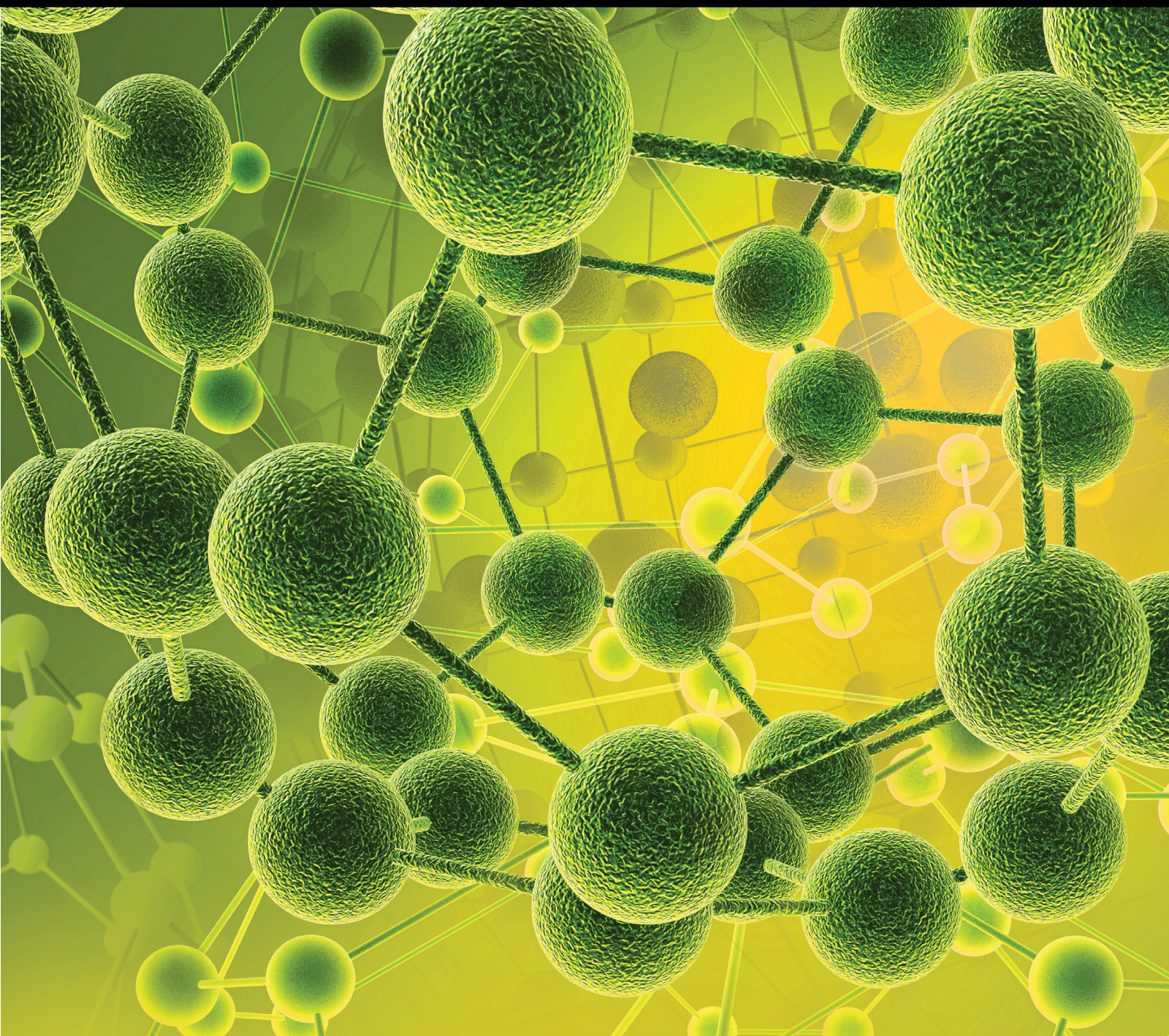


# Extraction and Sample Preparation

Guest Editors: Mohammad Rezaee, Faezeh Khalilian,  
Mohammad Reza Pourjavid, Shahram Seidi, Alberto Chisvert,  
and Mohamed Abdel-Rehim





---

# **Extraction and Sample Preparation**

International Journal of Analytical Chemistry

---

## **Extraction and Sample Preparation**

Guest Editors: Mohammad Rezaee, Faezeh Khalilian,  
Mohammad Reza Pourjavid, Shahram Seidi,  
Alberto Chisvert, and Mohamed Abdel-Rehim



---

Copyright © 2015 Hindawi Publishing Corporation. All rights reserved.

This is a special issue published in "International Journal of Analytical Chemistry." All articles are open access articles distributed under the Creative Commons Attribution License, which permits unrestricted use, distribution, and reproduction in any medium, provided the original work is properly cited.

## Editorial Board

Mohamed Abdel-Rehim, Sweden  
Yoshinobu Baba, Japan  
Barbara Bojko, Canada  
Günther K. Bonn, Austria  
Lawrence A. Bottomley, USA  
Richard G. Brereton, UK  
Bogusław Buszewski, Poland  
Farid Chemat, France  
Alberto Chisvert, Spain  
Pawel Ciborowski, USA  
Stephen P. Cramer, USA  
Neil D. Danielson, USA  
Ibrahim Darwish, Saudi Arabia  
Adil Denizli, Turkey  
Geraldine Dowling, Ireland  
Francis D'souza, USA  
Josep Esteve-Romero, Spain  
Luca Evangelisti, Italy  
Antonio Facchetti, USA  
Jiu-Ju Feng, China  
Frantisek Foret, Czech Republic  
Ruth Freitag, Germany  
Chris D. Geddes, USA  
Dimosthenis L. Giokas, Greece

Lo Gorton, Sweden  
Andras Guttman, Austria  
Paul R. Haddad, Australia  
John P. Hart, UK  
Josef Havel, Czech Republic  
Lei Hong, USA  
Xiaolin Hou, Denmark  
Jan Åke Jönsson, Sweden  
Teizo Kitagawa, Japan  
Spas D. Kolev, Australia  
Roger M. LeBlanc, USA  
Hian Kee Lee, Singapore  
Shaoping Li, China  
Shaorong Liu, USA  
David M. Lubman, USA  
John H. Luong, Canada  
Roland Marini, Belgium  
Mitsuo Miyazawa, Japan  
Shoji Motomizu, Japan  
Eric J. Munson, USA  
Boris F. Myasoedov, Russia  
Mu Naushad, Saudi Arabia  
Pavel Nesterenko, Australia  
Dimitrios P. Nikolelis, Greece

Francesco Palmisano, Italy  
Gabor Patonay, USA  
Stig Pedersen-Bjergaard, Norway  
Hans Puxbaum, Austria  
Peter L. Rinaldi, USA  
Aldo Roda, Italy  
Israel Schechter, Israel  
Steven A. Soper, USA  
Giuseppe Spoto, Italy  
Paul Stevenson, Australia  
Shi-Gang Sun, China  
Greg M. Swain, USA  
Kamchiu Tam, Canada  
Peter A. Tanner, Hong Kong  
David Touboul, France  
Ashley Townsend, Australia  
Dimitrios Tsikas, Germany  
Valentina Venuti, Italy  
Joseph Wang, USA  
Charles L. Wilkins, USA  
Philip M. Williams, UK  
Troy D. Wood, USA  
Jyhmyng Zen, Taiwan

## Contents

**Extraction and Sample Preparation**, Mohammad Rezaee, Faezeh Khalilian, Mohammad Reza Pourjavid, Shahram Seidi, Alberto Chisvert, and Mohamed Abdel-Rehim  
Volume 2015, Article ID 397275, 2 pages

**Arsenic, Antimony, Chromium, and Thallium Speciation in Water and Sediment Samples with the LC-ICP-MS Technique**, Magdalena Jabłońska-Czapla  
Volume 2015, Article ID 171478, 13 pages

**A Rapid and Accurate Extraction Procedure for Analysing Free Amino Acids in Meat Samples by GC-MS**, Trinidad Pérez-Palacios, Miguel A. Barroso, Jorge Ruiz, and Teresa Antequera  
Volume 2015, Article ID 209214, 8 pages

**An Optimized High Throughput Clean-Up Method Using Mixed-Mode SPE Plate for the Analysis of Free Arachidonic Acid in Plasma by LC-MS/MS**, Wan Wang, Suzi Qin, Linsen Li, Xiaohua Chen, Qunjie Wang, and Junfu Wei  
Volume 2015, Article ID 374819, 6 pages

**Pregabalin and Tranexamic Acid Evaluation by Two Simple and Sensitive Spectrophotometric Methods**, Nawab Sher, Nasreen Fatima, Shahnaz Perveen, Farhan Ahmed Siddiqui, and Alisha Wafa Sial  
Volume 2015, Article ID 241412, 7 pages

**Antibacterial, Antifungal, and Insecticidal Potentials of *Oxalis corniculata* and Its Isolated Compounds**, Azizur Rehman, Ali Rehman, and Ijaz Ahmad  
Volume 2015, Article ID 842468, 5 pages

**Dramatic Improvement of Proteomic Analysis of Zebrafish Liver Tumor by Effective Protein Extraction with Sodium Deoxycholate and Heat Denaturation**, Jigang Wang, Yew Mun Lee, Caixia Li, Ping Li, Zhen Li, Teck Kwang Lim, Zhiyuan Gong, and Qingsong Lin  
Volume 2015, Article ID 763969, 11 pages

**Application of an Activated Carbon-Based Support for Magnetic Solid Phase Extraction Followed by Spectrophotometric Determination of Tartrazine in Commercial Beverages**, José A. Rodríguez, Karen A. Escamilla-Lara, Alfredo Guevara-Lara, Jose M. Miranda, and Ma. Elena Páez-Hernández  
Volume 2015, Article ID 291827, 8 pages

**Extraction of HCV-RNA from Plasma Samples: Development towards Semiautomation**, Imran Amin, Tania Jabbar, Fawad Niazi, and Muhammad Saeed Akhtar  
Volume 2015, Article ID 367801, 4 pages

**Comparison of Electrospray Ionization and Atmospheric Chemical Ionization Coupled with the Liquid Chromatography-Tandem Mass Spectrometry for the Analysis of Cholesteryl Esters**, Hae-Rim Lee, Sunil Kochhar, and Soon-Mi Shim  
Volume 2015, Article ID 650927, 6 pages

**Sample Preparation and Extraction in Small Sample Volumes Suitable for Pediatric Clinical Studies: Challenges, Advances, and Experiences of a Bioanalytical HPLC-MS/MS Method Validation Using Enalapril and Enalaprilat**, Bjoern B. Burckhardt and Stephanie Laeer  
Volume 2015, Article ID 796249, 11 pages



---

**QuEChERS Method Followed by Solid Phase Extraction Method for Gas Chromatographic-Mass Spectrometric Determination of Polycyclic Aromatic Hydrocarbons in Fish**, Mona Khorshid, Eglal R. Souaya, Ahmed H. Hamzawy, and Moustapha N. Mohammed  
Volume 2015, Article ID 352610, 7 pages

**A High Throughput Method for Measuring Polycyclic Aromatic Hydrocarbons in Seafood Using QuEChERS Extraction and SBSE**, Edward A. Pfannkoch, John R. Stuff, Jacqueline A. Whitecavage, John M. Blevins, Kathryn A. Seely, and Jeffery H. Moran  
Volume 2015, Article ID 359629, 8 pages

**Estimation of Measurement Uncertainties for the DGT Passive Sampler Used for Determination of Copper in Water**, Jesper Knutsson, Sebastien Rauch, and Gregory M. Morrison  
Volume 2014, Article ID 389125, 7 pages

## Editorial

# Extraction and Sample Preparation

**Mohammad Rezaee,<sup>1</sup> Faezeh Khalilian,<sup>2</sup> Mohammad Reza Pourjavid,<sup>1</sup> Shahram Seidi,<sup>3</sup> Alberto Chisvert,<sup>4</sup> and Mohamed Abdel-Rehim<sup>5</sup>**

<sup>1</sup>*Nuclear Fuel Cycle Research School, Nuclear Science & Technology Research Institute, Atomic Energy Organization of Iran, P.O. Box 14395-836, Tehran, Iran*

<sup>2</sup>*Department of Chemistry, College of Basic Science, Islamic Azad University, Yadegar-e-Imam Khomeini (RAH) Branch, P.O. Box 18155-144, Tehran, Iran*

<sup>3</sup>*Department of Chemistry, K.N. Toosi University of Technology, P.O. Box 15875-4416, Tehran, Iran*

<sup>4</sup>*Department of Analytical Chemistry, University of Valencia, 46100 Burjassot, Valencia, Spain*

<sup>5</sup>*Department of Analytical Chemistry, Stockholm University, 10691 Stockholm, Sweden*

Correspondence should be addressed to Mohammad Rezaee; [chem.rezaee219@gmail.com](mailto:chem.rezaee219@gmail.com)

Received 1 March 2015; Accepted 1 March 2015

Copyright © 2015 Mohammad Rezaee et al. This is an open access article distributed under the Creative Commons Attribution License, which permits unrestricted use, distribution, and reproduction in any medium, provided the original work is properly cited.

As everyone knows, the role played by extraction and sample preparation in the analytical sciences cannot be overemphasized. Despite tremendous advances in chromatography, detection, and other aspects of analysis, extraction and sample preparation remain a preanalysis ritual of critical importance. It has been estimated that around 50% to 70% possibly even more of the time and effort that goes into an analytical process comprises extraction and sample preparation. Sample preparation procedure can vary in the degree of selectivity, speed, and convenience, depending on the approach and conditions used, as well as on the geometric configurations of the extraction phase and conditions. Proper design of the extraction devices and procedures facilitates rapid and convenient on-site implementation, coupled with separation/quantification and/or automation.

This special issue addresses the research studies on the sample preparation, analytical extraction, and sample clean-up techniques. For example, M. Jabłońska-Czapla reported a review on chemical speciation and provided numerous examples of the hyphenated technique usage (e.g., the LC-ICP-MS application in the speciation analysis of chromium, antimony, arsenic, or thallium in water and bottom sediment samples). T. Pérez-Palacios et al. investigated the use of a mixer mill as the homogenization tool for the extraction of free amino acids in meat samples, with the main goal of

analyzing a large number of samples in the shortest time and minimizing sample amount and solvent volume. It takes less time and requires lower amount of sample and solvent than conventional techniques. N. Sher et al. studied colorimetric visible spectrophotometric quantification methods for amino acids, namely, tranexamic acid and pregabalin. Both drugs contain the amino group, and when reacted with 2,4-dinitrophenol and 2,4,6-trinitrophenol they give rise to yellow colored complexes showing absorption maximum at 418 nm and 425 nm, respectively, based on the Lewis acid base reaction.

J. A. Rodríguez et al. reported magnetic solid phase extraction of tartrazine from nonalcoholic beverages. The method involves the extraction and clean-up by activated carbon covered with magnetite dispersed in the sample, followed by the magnetic isolation and desorption of the analyte by basified methanol. The proposed methodology saves time and is less expensive than the reference method. M. Khorshid et al. reported QuEChERS (quick, easy, cheap, effective, rugged, and safe) method for extraction followed by solid phase extraction for sample purification and gas chromatography mass spectrometer, GCMS, for determination of 16 PAHs in fish at low LOQ level. E. A. Pfannkoch et al. reported combination QuEChERS and SBSE methods for extraction and concentration PAHs from fish and shellfish. I. Amin et al.

reported a semiautomated extraction protocol of HCV-RNA using Favorgen RNA extraction kit. The kit provided protocol was modified by replacing manual spin steps with vacuum filtration. The assay performance was evaluated by real time qPCR based on Taqman technology. W. Wang et al. reported a high throughput sample preparation method utilizing mixed-mode solid phase extraction (SPE) in 96-well plate format for the determination of free arachidonic acid in plasma by LC-MS/MS. J. Knutsson et al. reported an uncertainty budget for the determination of fully labile Cu in water using a DGT passive sampler. H.-R. Lee et al. reported two different ionization techniques including electrospray ionization (ESI) and atmospheric pressure chemical ionization (APCI) coupled with liquid chromatography-tandem mass spectrometry (LC-MS/MS) for the analysis of cholesteryl esters (CEs). The ESI technique proved to be effective in ionizing more kinds of CEs than the APCI technique. J. Wang et al. evaluated various existing protein extraction buffers with zebrafish liver tumor samples and found that sodium deoxycholate (DOC) based extraction buffer with heat denaturation was the most effective approach for highly efficient extraction of proteins from complex tissues such as the zebrafish liver tumor. B. B. Burckhardt and S. Laeer developed sample preparation exemplified by solid phase extraction for the bioanalytical method development of low-volume assays for pediatric studies according to international agency guidelines. A. Rehman et al. suggested that *Oxalis corniculata* has good antibacterial, antifungal, and insecticidal properties and can be used for the treatment of infections and control of insects. The plant extracts could be a new source for antibiotics and pesticides with minimum noxious effects on the environment. Further studies may also lead to isolating and characterizing the active compounds of the plant extracts and elucidating their biological mechanisms of action.

## Acknowledgments

Finally, the guest editors would like to express sincere appreciation to all the authors for their contributions. Moreover, thanks are extended to all reviewers for their time enhancing the quality of these papers.

Mohammad Rezaee  
Faezeh Khalilian  
Mohammad Reza Pourjavid  
Shahram Seidi  
Alberto Chisvert  
Mohamed Abdel-Rehim

## Review Article

# Arsenic, Antimony, Chromium, and Thallium Speciation in Water and Sediment Samples with the LC-ICP-MS Technique

**Magdalena Jabłońska-Czapla**

*Institute of Environmental Engineering, Polish Academy of Sciences, M. Skłodowskiej-Curie 34 Street, 41-819 Zabrze, Poland*

Correspondence should be addressed to Magdalena Jabłońska-Czapla; [magdalena.jablonska-czapla@ipis.zabrze.pl](mailto:magdalena.jablonska-czapla@ipis.zabrze.pl)

Received 4 September 2014; Revised 24 November 2014; Accepted 25 November 2014

Academic Editor: Mohamed Abdel-Rehim

Copyright © 2015 Magdalena Jabłońska-Czapla. This is an open access article distributed under the Creative Commons Attribution License, which permits unrestricted use, distribution, and reproduction in any medium, provided the original work is properly cited.

Chemical speciation is a very important subject in the environmental protection, toxicology, and chemical analytics due to the fact that toxicity, availability, and reactivity of trace elements depend on the chemical forms in which these elements occur. Research on low analyte levels, particularly in complex matrix samples, requires more and more advanced and sophisticated analytical methods and techniques. The latest trends in this field concern the so-called hyphenated techniques. Arsenic, antimony, chromium, and (underestimated) thallium attract the closest attention of toxicologists and analysts. The properties of those elements depend on the oxidation state in which they occur. The aim of the following paper is to answer the question why the speciation analytics is so important. The paper also provides numerous examples of the hyphenated technique usage (e.g., the LC-ICP-MS application in the speciation analysis of chromium, antimony, arsenic, or thallium in water and bottom sediment samples). An important issue addressed is the preparation of environmental samples for speciation analysis.

## 1. Introduction

The beginning of the 21st century is a time of great challenges in the analytical chemistry, which also includes the environmental analytics. Such a situation is mainly related to the new information on the toxicological properties of elements, their forms of occurrence, and the necessity to detect and determine lower and lower analytes levels, which are very often observed in the complex matrix samples. Speciation (a term borrowed from biology) describes the occurrence of various chemical and physical forms of a given element. The determination of such forms is known as speciation analytics [1]. Chemical speciation is an important subject in the environmental protection, toxicological and analytical research because toxicity, availability, and reactivity of trace elements depend on the chemical forms in which such elements occur. Two aspects can be differentiated within the speciation analytics framework, that is, determining man-made substances that are emitted into the environment by humans and analysing natural compounds formed as a result of biochemical transformations in the environment or living

organisms. The first group is particularly interesting for the environmental analysis, whereas the other one concerns biochemists and ecotoxicologists. The fate and influence of trace elements are directly related to their chemical forms. They can occur as free ions, small organometallic formations, or bigger biomolecules included in the biological systems [1–5].

Due to the fact that metals and metalloids have a strong impact on the environment, the methods of their determination and speciation have received special attention in recent years. What is more, they have become one of the most important fields of application in the modern analytical chemistry. Arsenic, antimony, and thallium are examples of toxic elements.

Antimony is a very popular element in the environment, and its trivalent chemical species is about ten times more toxic as oxidized Sb(V) [6–10]. Another important and interesting metalloid is arsenic, whose inorganic species are much more toxic than organic ones [1, 11].

There are also elements that are very important for the health and life of living organisms.

Such an element is chromium, which reduced; inorganic form has a major role for the functioning of a living organism [12]. Unfortunately, hexavalent, oxidized chromium form is carcinogenic and mutagenic for humans. Similarly, thallium and its compounds are very toxic.

The element is also toxic in the dust form as it oxidizes in the contact with air. Food and respiratory thallium poisonings are possible. One of the characteristic poisoning symptoms is hair loss preceded by hair follicle atrophy. Other signs include digestion disorders, pain, neuropsychiatric complications, and cardiovascular system damage. In the past, thallium salts were often added to rodenticides [13]. The described elements have complex physical and chemical characteristics and are of great interest for both toxicologists and analytical chemists. Among them, arsenic and its compounds are the best known and described. Less information on antimony is available while thallium and its compounds are still the most mysterious and unfamiliar [14]. Unfortunately, the environmental pollution caused by human activity is still increasing, and hence the supply of metals and nonmetals is growing.

## 2. Speciation by Classical Methods or Rather by Using Hyphenated Techniques

The information obtained from toxicological tests and research into the influence of the specific chemical species on living organisms requires continuous lowering of the analyte detection limits to extremely low concentration levels. Such knowledge needs the development of the applied analytical methods. The progress enables the researchers to examine elements occurring at very low concentration levels and their chemical species, interactions, transformations, and functions in the biological systems. Such data is extremely important to understand the toxicology and metabolic routes of toxic elements, such as arsenic (As), antimony (Sb), chromium (Cr), or thallium (Tl).

Conventional methods are usually labor-intensive, time-consuming, and susceptible to interferences [15–20]. The most common tools for trace chemical speciation are the combination of separation techniques coupled with highly sensitive detector. In the early days, the separation consisted of a special off-line sample preparation followed by the detection step. The evolution and development of nonchromatographic methodologies based on chemical speciation are still growing because they can offer simple and inexpensive ways to make speciation, or, at least, for the determination of specific or toxic forms of trace elements [5]. The following analytical techniques are used in the thallium analytics: atomic absorption spectrometry, coulometry, spectrophotometry, ICP-MS, laser induced fluorescence spectrometry, or differential pulse stripping voltamperometry [1].

The hyphenated techniques, in which separation method is coupled with multidimensional detectors, have become useful alternatives. The main advantages of those techniques consist in extremely low detection and quantification limits, insignificant interference influence, and high precision and repeatability of the determinations. Even though speciation analytics is relatively expensive, it plays an important role

in the following fields: research into biochemical cycles of selected chemical compounds, determination of the toxicity and ecotoxicity of selected elements, quality control of food products and pharmaceuticals, control of technological processes, health risk assessment, and clinical analytics

In order to be able to continuously lower the detection and quantification limits, various separation and detection methods are combined. Such couplings are known as the hyphenated methods. Effective separation techniques for various chemical species and appropriate detectors are necessary to determine individual element forms. Most chromatographic methods, such as liquid chromatography (LC), are coupled with inductively coupled plasma-mass spectrometry (ICP-MS). ICP-MS offers many benefits, such as high element selectivity, broad linear range, and relatively low limit of detection (LOD). The basic separation mechanisms in the high-performance liquid chromatography (HPLC) that are applied in the environmental speciation analytics encompass the exclusion process, ion exchange, and chromatography in the reversed phase system. The use of the inductively coupled plasma collision cell-quadrupole mass spectrometry (ICP-CC-QMS), inductively coupled plasma dynamic reaction cell-quadrupole mass spectrometry (ICP-DRC-QMS) [2], or inductively coupled plasma-sector field mass spectrometry (ICP-SF-MS) [21–23] decreases the signal background (caused by molecular interferences) by separating the analyte signal from the signal of a given molecular ion.

Nonetheless, ICP-MS itself does not allow the researchers to obtain information on the chemical species of the examined element as full ionization of molecules in the plasma does not retain any molecular data. Liquid chromatography (LC), gas chromatography (GC), and capillary electrophoresis (CE) can be coupled with ICP-MS to determine various chemical species. Importantly, the coupling of CE with ICP-MS is not as the direct as the couplings with LC or GC. Coupling LC, GC, or CE (as separation methods) with ICP-MS opens up opportunities for the speciation analysis of elements in various samples. LC enables relatively simple coupling with the ICP spectrometer plasma torch without any major modifications in the standard system of the sample introduction in the ICP-MS spectrometer. LOD for liquid chromatography-inductively coupled plasma-mass spectrometry (LC-ICP-MS) may not be sufficient. Consequently, ultrasonic or pneumatic nebulizers [24, 25] can be used to improve LOD. One of the main limitations of LC-ICP-MS is the application of a suitable eluent. Only a mobile phase with the appropriate (limited) salt concentration and pH can be used. Importantly, it is advisable not to use organic solvents. Chromatographic techniques with the liquid mobile phase can be used to separate different chemical species, both in the off-line and on-line modes. When compared to the direct on-line separation of chemical species, the off-line separation has many disadvantages. The coupling of the isotopic analysis with the direct chromatographic separation can be performed with the multicollector-inductively coupled plasma-mass spectrometry (MC-ICP-MS). The advantages of the liquid chromatography-multicollector-inductively coupled plasma-mass spectrometry (LC-MC-ICP-MS) include sensitivity, selectivity, high ionization efficiency, and the ICP source

resistance, which enables the coupling of chromatography and simultaneous monitoring of the relevant isotopes. At the same time, it provides the high precision of isotope correlations. Two separation methods are usually applied in LC-MC-ICP-MS, that is, ion-exchange columns or reversed phase [26].

### 3. Why Is Arsenic, Antimony, Chromium, and Thallium Speciation so Important?

Arsenic, antimony, chromium, and the underestimated thallium attract most interest of toxicologists and analysts. Their properties depend on the oxidation state in which they occur.

Antimony is common in the natural environment and comes both from natural processes and human activity. Over the years, the human activity brought about the significant increase in its concentration in the environment due to its applications in the car industry (i.e., as an additive in the car tyre vulcanization process). The geochemical behaviour of antimony is similar to that of arsenic and bismuth [6, 27, 28]. Its biological role is not fully recognized, but it is toxic at a low level (similarly to arsenic). Sb(III) is approximately 10 times more toxic than Sb(V). That is why there is such an interest in its speciation analysis [8, 9, 28]. Antimony and its salts mainly affect the central nervous system (CNS) and blood in the toxic way. They also cause conjunctivitis and skin inflammation and damage the heart muscle and liver. The antimony compounds demonstrate mutagenic and carcinogenic effects [27, 29].

Arsenic is a toxic metalloid that is common in various biological systems and the environment. The number of its speciation forms in the environment is still increasing due to the economic growth. As the industrial pollution has not been reduced in the recent decades, the arsenic emission from the industry, steelworks, animal waste, and the dust from fuel fossil combustion is currently rising. As arsenic is very mobile, it occurs in all the environment elements. The toxicity of arsenic itself and its compounds differs. However, its inorganic chemical species are about 100 times more toxic than the organic ones. The contact with arsenic can cause various health effects, such as dermatologic, inhalation, cardiologic, genetic, genotoxic, or mutagenic lesions [11]. It accumulates in the keratin-rich tissues, such as hair, skin, or nails. Arsenic and its inorganic forms can provoke cancers of the respiratory system or skin. They can also cause multiple organ cancer lesions. The dominant arsenic effects in humans are skin and mucous membrane lesions and nerve damage. Drinking water is one of the most important sources of the exposure to arsenic.

The most frequent poisonings are those caused by arsenic and its compounds. It has been used for approximately 1,000 years as the rodenticide because it is colourless and has neither taste nor smell. The toxic dose of arsenic is approximately 10–50 mg. It is lethal in the acute poisoning when the level is 70–200 mg or 1 mg/kg body weight. DMPS (2,3-Dimercapto-1-propanesulfonic acid) is validated in Germany as a medicine used in the acute or chronic mercury or lead poisoning (commercial names in Germany are Dimaval, oral capsules, and Heyl DMPS that is used for injections).

In the USA, the DMPS application is considered experimental as the medicine has no approval of its effectiveness and safety granted by the U.S. Food and Drug Administration (FDA). Nonetheless, the reports presented in the literature prove its safety and effectiveness, when compared to other chelators. There is also a report that states that the oral application of DMPS is more effective than the injections. DMPS has been successfully used in the peripheral neuropathy caused by the arsenic poisoning [30].

Chromium is a classic example of an element whose two chemical species differ significantly in their chemical and toxicological properties. It is believed that the Cr(III) compounds have a positive influence on the functioning of living organisms. They are responsible for the appropriate glucose metabolism in mammals. They easily undergo complexation with various substances present in the environmental samples. On the other hand, the Cr(VI) compounds are extremely toxic. Their inhalation causes pneumonia and asthma, whereas their contact with skin provokes allergies and dermatoses [29]. The International Agency for Research on Cancer (IARC) classified the Cr(VI) compounds in the B-2 group, that is, substances carcinogenic and mutagenic for humans [31]. The Cr(VI) toxic effect results from its strong oxidising properties and also from the formation of free radicals in the reduction of Cr(VI) to Cr(III), which occurs in the cells. The Cr(VI) compounds are usually more easily soluble, mobile, and bioavailable, which maximizes their toxic effect. Even though the modern speciation analytics methods are developing fast, the standards and legal regulations still concern the total chromium and not its particular forms. Cr(VI) is 1,000 times more toxic than Cr(III), which is related to the fact that it easily penetrates the cell membrane (impermeable to the reduced chromium form). This ability results from the fact that the  $\text{CrO}_4^{2-}$  ion is similar to the orthophosphoric and sulphate ions, which are transported in the appropriate ion channels into the interior of the cell. When the chromium ions are inside, they can react with the enzymes responsible for the metabolism of phosphate and sulphate ions. They can also react with DNA and RNA and disturb their normal functions. As a result, such reactions cause anomalies in the cell structure. The properties of chromium and its compounds and the methods used for their determination are described in detail in the study [32]. The literature examples of the Cr(III) and Cr(VI) ion determinations with the hyphenated methods are given in [33, 34].

Thallium was discovered by Sir William Crookes in 1861 and, independently, by Claude-Auguste Lamy in 1862. The element was introduced relatively quickly, that is, in 1880, as a medicine in the treatment of syphilis and mycosis. It was also used in depilation. Nonetheless, as thallium is highly toxic, its use was stopped at the beginning of the 20th century. Additionally, it has been abolished in pesticides in many countries in recent years as it was considered too toxic [35]. As the thallium application in various types of metal alloys has been increasing since the beginning of the digital revolution, it seems that the element has been accumulating in various elements of the environment. It is also used as a catalyst, in laser devices and in the production of optical fibres and high

refractive index glass. The element occurs in two oxidation states, that is, +1 and +3. The Tl(I) compounds are colourless, and Tl(OH) is a strong and soluble base. The Tl(III) ions exist in the solution only when pH is close to 0. When it is higher, Tl(OH)<sub>3</sub> precipitates [21]. The inorganic Tl(I) compounds are far more stable in a water solution with neutral pH than the Tl(III) compounds. On the other hand, the covalent organic thallium compounds are only stable for Tl(III). Each ionic form has different bioavailability and toxic properties. The Tl(III) cations are much more reactive and toxic than the Tl(I) ones. However, the number of Tl(III) cations is so low that Tl(I) is believed to be the most bioactive thallium form in the water environment, particularly for living organisms as it can replace the K<sup>+</sup> ion. Thallium is highly toxic. Its average lethal dose for humans is 4–60 mg/kg. The Tl(III) toxicity is difficult to define because it is easily reduced in the biological systems [36]. The recent research has shown that Tl(III) can be even 50,000 times more toxic than Tl(I). Therefore, it is more toxic than Cd(II), Cu(II), Ni(II), or even Hg(II) [37, 38]. The Tl(I) salts are easily absorbed through skin and this is how they normally penetrate living organisms. Food is another source of thallium and its compounds. For this reason, food quality monitoring is very important at present. In clinical analyses, thallium is normally determined in urine, saliva, tissues, and blood. Balding preceded with the hair follicle darkening is a characteristic symptom of the thallium poisoning. Apart from these, digestion problems, psychological changes, and damage in the cardiovascular system occur. In the past, thallium salts were often used in rodenticides. Thallium is very common in the environment even though it usually occurs at very low concentration levels. The mean thallium concentration in the Earth crust is 0.3–0.5 mg/kg. Its content in soils is 0.02–2.8 mg/kg and depends on the geological bedrock composition and pollution. That is why the thallium contents vary in different countries (Austria, 0.076–0.911 mg/kg; China, 0.292–1.172 mg/kg; and Germany, in the vicinity of a lead and zinc mine, 8–27.8 mg/kg) [39].

#### 4. Sample Preparation for Analyses

The analyte determination is one of the last stages of the analytical procedure that includes sampling, sample preservation, transport, storage, preparation for analyses, determination, and result processing. If the sample is collected, stored, or prepared for analyses in an inappropriate way, the most sophisticated analytical method and the most experienced analyst are not able to provide reliable results. The sample preparation stage is normally the most laborious part of the analysis. It is usually the most important source of errors. The sampling time should be as short as possible, which can be easily provided for water or bottom sediment samples. Factors that influence the analyte speciation in the real samples ought to be taken into account when storing the samples. For example, the storage of the samples for antimony determinations is very difficult, because Sb(III) easily transforms into Sb(V) in the oxidising environment [40]. To preserve the samples, the researchers often use chelating reagents, such as the ethylenediaminetetraacetic acid (EDTA). Studies on the stability of arsenic compounds

in water samples chiefly concern the inorganic forms of this element, arsenite, and arsenate. There are many pieces of information about the redox stability of inorganic arsenic. The authors do not agree on the stability and permanence of arsenic forms in water, especially at different pH and in the presence of other substances [41]. Generally, in river water, As(V) is partially converted to As(III), but after 2 days, this is followed by gradual oxidation of As(III) into As(V) to reach an equilibrium. Storage at 5°C delays this oxidation by about 6 days [42].

In the case of thallium, diethylenetriaminepentaacetic acid (DTPA) (Merck) was used for stabilization of Tl(III) and sodium dodecyl sulfate (SDS) was used for extraction plant samples [43]. Other authors provide that river water samples, after sampling, were transported back to the laboratory and separation processes were finished within 8 hours of sample collection [39]. DTSP and HNO<sub>3</sub> were used as extractants for the determination of Tl(I) and Tl(III) in the sediments of the Kłodnica River. This extractant was later used as an eluent during the chromatographic separation [44].

Trace elements can be present in the environmental samples at the ppb and lower concentration levels. It is often a great challenge for an analyst to extract the demanded analyte forms from the samples without changing their oxidation states. Additionally, sample storage is a very important issue in the speciation analysis. The environmental samples are normally frozen or stored in a refrigerator at 4°C and without the light access. Importantly, even such routinely used processes as dilution, changes in pH caused by the sample preservation, or pressure and temperature changes can bring about irreversible changes in the primary analyte form. There are particular difficulties when sampling takes place under conditions that differ significantly from those under which the sample is later analysed. The oxidation state change can occur in both directions due to the oxidation and reduction. For chromium, it is very unlikely (under normal conditions) to oxidise to Cr(VI), as Cr(III) oxidation to Cr(VI) takes place under drastic conditions (high temperature and oxygen presence or strong oxidation agent presence, such as Mn(IV) in a highly alkaline environment). It is very important to prevent the Cr(VI) reduction to Cr(III). For liquid samples (e.g., water samples), sampling, transport, and storage procedures should be as short as possible. Normally, the samples are frozen directly after sampling (transport). Such an action reduces the redox reaction kinetics [45].

Analysts often encounter problems related to the extraction of the suitable speciation analyte forms from the sample. It is particularly difficult when the analytes must be extracted from a complex matrix so that there are no changes in the oxidation state of a given chemical species. Usually, weak acids, buffers, or complexing reagents are used to extract inorganic or organic forms of low molecular weight. A proper extractant should not influence the analyte oxidation state and should be selected in such a way as to provide the highest extraction efficiency. The extraction efficiency test is performed through introducing an additive into the standard sample or extracting certified reference materials for soils or bottom sediments. It is assumed that the extraction procedure is correct, when the relative standard deviation (RSD) is ±5%.

When the repeatability of results is poorer, there is no process control [46].

The use HPLC as time-resolved introduction techniques into the atomic spectrometer establishes some physicochemical requirements for the analytes. This usually makes a sample preparation procedure that includes the pretreatment of the sample with some type of reagent to condition the matrix or leach the species for the extractions step in which the species are completely isolated from the matrix necessary.

Most living organisms reduce the toxicity of arsenic and antimony by incorporating them into organometallic molecules through metabolic pathways [41]. Therefore, speciation methods have to be capable of extracting these compounds without structural modifications. More ubiquitous organoarsenic environmental molecules are monomethylarsonic acid (MMA), dimethylarsinic acid (DMA), arsenobetaine (AsB), and arsenocholine (AsCh) and extraction procedures can be developed to isolate them from matrices. Due to the stability of methylated arsenic species, they are leached together with total inorganic arsenic, using warm [47] or cold [48] concentrated HCl from sediments and biological tissues. Arsenic chemical species could be leaching using acidic solvents (pH = 2.3) for As(III) or basic leaching (pH = 11.9) for As(V), MMA, and DMA. Other weak leaching reagents such as acetate, citrate, and oxalate buffers selectively leach As(III) and phosphoric acid efficiently extracts total arsenic from soils [41]. Phosphate buffer (5 mM Na<sub>2</sub>HPO<sub>4</sub>/50 mM NaH<sub>2</sub>PO<sub>4</sub> (pH = 6.0) and ultrasonic bath were used for extraction of inorganic arsenic species in sediment samples [49]. As most of the arsenic is usually associated with iron oxides, a selective extraction method using hydroxylammonium hydrochloride as extractant with special emphasis on the different arsenic chemical species (As(III), As(V), MMA, and DMA) in the extract has been performed [50].

## 5. Application of Chromium, Arsenic, Antimony, and Thallium Speciation Analyses in Water Samples

Generally, it is known that the contents of chromium, arsenic, antimony, and thallium are very low in the uncontaminated samples. It is necessary to use very sensitive methods, such as ICP-MS, to determine such low analyte contents [51]. Over the last two decades, there have been many studies concerning the determination methods and occurrence of Cr(III) and Cr(VI) in the natural environment. The chromium chemistry is very complex. The concentration of oxidising substances is another important factor that affects the chromium redox behaviour. Even though there are a few substances that are able to oxidise Cr(III), only a few of them have sufficiently high concentrations that enable the oxidation of Cr(III) to Cr(VI) in the environment. The situation is different when compared to the Cr(VI) reduction to Cr(III). In this case, the concentrations of the reducing substances are high enough and play the main part even though the reduction is less thermodynamically privileged. The precipitation and dissolution processes also influence the contents of the chromium chemical species [12].

The research into chromium speciation with hyphenated techniques is very popular. Bednar et al. [32] examined various water types (surface, ground, and tap water) with the anion-exchange AG-11 and AS-11 columns (Dionex) coupled with the ICP-MS detection. There was also the research into three water reservoirs (Pławniowice and Goczałkowice Reservoirs, and Rybnickie Lake) that differed in the anthropopressure type. The chromium content in the Pławniowice reservoir demonstrated variations in the chemical species concentrations, which depended on the sampling month. Cr(III) dominated in winter and spring months, whereas the Cr(VI) dominance was observed in the surface water in June (probably related to the oxygen content of 135%). The Cr(III) concentration in the bottom water was the lowest in July–October period. There was also a strong correlation between the Cr(VI) concentration and pH in the bottom water [33]. Cr(III) also dominated the chromium content in the Goczałkowice reservoir and Rybnickie Lake. The water research indicated the seasonal variations in the concentrations of the chromium chemical species. The high oxygen content and highly reducing conditions were also responsible for the lack of Cr(VI) in the porous water of the bottom sediments [34], which were collected from a river near a tannery.

It is necessary for the hyphenated methods used in the arsenic speciation analytics (at low concentration levels) to be both appropriately selective and sensitive. There are many studies in the literature on the instrumental methods used in the speciation of 5 arsenic chemical species. Most of them are based on the chromatographic separation techniques, such as HPLC [52].

The researchers determined arsenic chemical species in the Ohio River water samples with the ion-pairing reversed phase chromatography with inductively coupled plasma-mass spectrometry (IPRP-ICP-MS) with tetrabutylammonium hydroxide (TBAH) and C-18 column. The obtained LODs were at the ng/L level [53]. Bednar et al. [54] examined surface, ground, and even acidic waters from a coal mine with the hyphenated system of HPLC-ICP-MS. They used various columns and eluents.

In 1990s, there were many successful studies into the chromium [55] and arsenic [56, 57] chemical species and subsequently into the simultaneous determination of the chromium and arsenic speciation forms [58]. At the beginning, only water samples were examined and the obtained LODs were at the  $\mu\text{g/L}$  level.

HPLC coupled with a sector mass analyser and ICP-MS was used for the arsenic speciation in the environmental samples collected from Moira Lake and the Moira River (Ontario, Canada) [59]. The researchers proved that the Moira River water was highly polluted with arsenic, particularly in summer. The total arsenic content in the river water exceeded 140 mg/L. On the other hand, the arsenic concentration in the Moira Lake water was 40–50 mg/L. The arsenic speciation proved that As(V) was dominant in the surface water. The content of the totally dissolved As(III) in water was approximately 2% of the total content. Such results are typical for waters with a high oxygen content and fast flow. Nonetheless, As(III) was dominant in the bottom water.

The analysis suggests that three processes affect the distribution of As(III) and As(V) in the water column, that is, diffusion of As(V) from the interstitial waters to the upper layers; As(III) formation resulting from biological transformations; and dissolution of the suspension and atmospheric dusts that contain As(III).

As(V) was also the main arsenic chemical species in the Kamo and Ichonakawa Rivers (Japan) [60]. The study indicates similarities between the geochemical behaviour of arsenic and antimony under the oxygen conditions in the researched rivers.

The stability of the environmental and biological samples, and particularly waters, in the speciation analysis largely depends on the sample matrix. The published data demonstrates that storing water samples at 5°C delay the oxidation of As(III) to As(V), whereas acidification can affect the changes in the distribution of particular chemical species in the samples. The performed research clearly shows that approximately 10% of As(III) oxidizes to As(V) under the sample matrix effect after 24 hours of the surface water sample storage. After the 3-day storage, 10–90% of As(III) turns into As(V), which depended on the sample. At the same time, the research into the Cr(VI) content in the same samples reveals that its concentration did not change even after 15 days [61, 62].

The arsenic speciation in the surface and well waters showed that arsenites and arsenates were the main forms found in the samples. In the surface waters, both DMA(V) and AsB were also observed. The presence of the methyl derivatives is probably related to the occurrence of microorganisms. No methyl derivatives of arsenic were observed in the well and mineral waters [52].

There are also publications which discuss simultaneous determinations of the chemical species of various elements. For example, in the study [61], the authors researched arsenic speciation forms and Cr(VI) using HPLC-ICP-MS with the anion-exchange Hamilton PRP-X100 column. The application of HPLC-ICP-MS in the arsenic speciation for water samples was described in detail in the study [63].

In China, antimony speciation was performed with HPLC-ICP-MS to examine water from the biggest antimony mine in the world. The authors determined Sb(V) and Sb(III) in the samples. It turned out that the Sb(V) form was the dominant one. Only trace amounts of Sb(III) were found [64]. Asaoka et al. [60] obtained similar results. They examined arsenic and antimony chemical species in the waters and bottom sediments of the Kamo and Ichinokawa Rivers (Japan). They observed that Sb(V) was the dominant speciation form in each water sample. It was probably dissolved as  $\text{Sb(OH)}_6^-$ .

Analysts also investigated hot spring water sold as drinking water to determine the contents of the arsenic and antimony chemical species with HPLC-ICP-MS [65]. The researchers observed that only inorganic arsenic species, such as As(III) and As(V), were present in the analysed waters. No antimony chemical species were found.

In another study, tap water was examined and inorganic antimony chemical species were determined in the samples. Sb(V) was the dominant form, while the Sb(III) content

was below LOD [66]. Similarly [67], when tap water was researched, it was observed that the mean Sb(V) concentration was 20 ng/L, whereas the Sb(III) and  $\text{TSbCl}_2$  contents were below the method LOD.

Other authors used the complexation reactions to form stable Sb(III) and Sb(V) complexes, which were afterwards separated in the HPLC-ICP-MS system with the PRP-X100 column. The obtained low LODs were 0.05  $\mu\text{g/L}$  for Sb(III) and 0.07  $\mu\text{g/L}$  for Sb(V) [68].

Apart from the antimony inorganic chemical species, trimethylstiboxide (TMSbO) was examined in the surface water [69]. TMSbO is stable in water and can be reduced to trimethylantimony (TMSb). It can be formed either in the bacteriological process (e.g., in the soil) or during trimethylantimony oxidation in the biomethylation process of the antimony compounds. Waters polluted due to the industrial activities and mining processes were investigated. The researchers found the contents of Sb(V) and Sb(III) at the levels of 90% and 10%, respectively. No TMSbO was found in the polluted water samples. Nevertheless, some chromatograms showed peaks of the unknown antimony species that originated from certain stable antimony complexes.

The research into the contents of the arsenic, antimony, and chromium chemical species is very popular. The same situation is observed for the analyses of thallium speciation forms in the environmental samples [70, 71]. The application of HPLC-ICP-MS enables determining thallium species in the samples of the sea [72] and surface [14, 44] waters. The flow injection analysis coupled with atomic absorption spectrometry (FIA-AAS) is another technique often applied in the thallium speciation [73]. However, the most popular, in the case of thallium, are speciation methods of combining extraction procedures with very sensitive detection techniques [74]. In this study, a simple and novel sequential mixed micelle cloud point extraction procedure for the separation of Tl species in environmental water samples for their determination by ICP-MS, without using any additional salts or chelating agents was used. The anionic mixed micelle comprising sodium dodecyl sulfate (SDS) and Triton X-114 is used for selective extraction of positive Tl(III), DTPA species into the surfactant-rich phase. To improve the preconcentration factor, ultrasound was used for back-extraction of Tl(III). Other authors studied thallium speciation in river waters, using Chelex-100 resin and atomic absorption spectroscopy technique [39].

## 6. Application of Chromium, Arsenic, Antimony, and Thallium Speciation Analyses in Bottom Sediment Samples

The high chromium content in bottom sediments is often caused by the close vicinity of tanneries, steelworks, or galvanic shops. The tanning industry is a typical source of Cr(III), including mainly sulphates [34]. Under the redox and slightly oxidising conditions, Cr(VI) is reduced to Cr(III) within the period that ranges between a few minutes and a few days. Cr(III) is the chromium chemical species that is most often adsorbed on bottom sediments. The Cr(VI) adsorption

is significantly lower than that of Cr(III). It depends on pH and occurs more easily under acidic conditions.

Jabłońska et al. [33] investigated bottom sediments sampled from the Pławniowice and Goczałkowice Reservoirs and Rybnickie Lake. In the Pławniowice Reservoir [60], the bottom sediment analysis indicated high contents of the easily leached fractions (metals in the porous solution, carbonate, and ion-exchange fractions). The chromium speciation analysis of the Pławniowice bottom sediment revealed slight dominance of its reduced form (Cr(III), 56%; Cr(VI), 44%). In Rybnickie Lake, the high Cr(VI) content was observed in the bottom sediment, which was most probably related to the phytoplankton bloom. Phytoplankton is able to accumulate, i.e., chromium (particularly Cr(VI)), both inside the cell and on its surface (phytosorbent). The organic matter that lands on the lake bottom enriches the Rybnickie Lake bottom sediments with Cr(VI). The chromium speciation analysis in the easily leached fractions demonstrated significant dominance of the oxidised form, Cr(VI), whose percentage in the heated water discharge zone and dam zone was 75% and 62%, respectively.

In the study [69], the authors focused on the sample preparation methods. They particularly concentrated on the extraction of the solid samples (including bottom sediments) for the analysis with HPLC-ICP-MS. The harbour water and sediments (Baltimore, USA) had low concentrations of Cr(VI), which was reduced to Cr(III) under the conditions existing in the harbour. The application of the Brownlee C8 column in the HPLC-ICP-MS system helped to determine highly saline samples [75].

Inorganic arsenic compounds are the most toxic arsenic forms that occur naturally in the environment. The arsenate toxic effect results from the mechanism of oxidative phosphorylation uncoupling. The research into the contents of the arsenic chemical species in Lake Moira, which is one of the biggest lakes in Canada, indicated the complexity of the undergoing processes. The total arsenic concentration in the bottom sediments was determined after acid digestion. The result was many times higher than the background value. The arsenic extraction from the bottom sediments was performed with the mixture of the phosphoric acid (1 mol/L) and ascorbic acid (0.1 mol/L). The concentration of the arsenic species was determined in the HPLC-ICP-SF-MS system. It was observed that the As(III) concentration decreased with the increasing depth of the particular bottom sediment layers. The As(III)/As-complex ratio in the extracts also indicated the tendency to decrease with the increasing depth. The highest As(III)/As-complex ratio was obtained in the surface layer of the Lake Moira bottom sediments. The authors suggest that As(III) was released from the surface layer of the bottom sediments in the redox or decomposition process. Subsequently, it was moved into water through the bottom sediment/bottom water exchange. The research points to the complexity of the forming organic species of arsenic and the necessity to investigate fresh, not dried, and bottom sediments [59].

In another study, 0.3 M phosphoric acid was used as the extractant of the arsenic chemical species from the bottom

sediment samples that were determined with the HPLC-ICP-MS system [76].

The research into the bottom sediments of the Godavari River Estuary (the third biggest river in India) shows that the increase in the salinity of the water column above the bottom sediments also affects the arsenic distribution and speciation in the sediments. The researchers determined the As(III) and As(V) with the spectrophotometric methods. They also used sequential extraction procedure proposed by the Community Bureau of Reference (BCR) [77].

The concentrations of arsenic and antimony in bottom sediments are often correlated. The research demonstrates that the Sb(V) content is 60–84% of the total antimony content. The authors point to the important adsorption influence on the arsenic and antimony concentrations in the bottom sediments. They also reveal that the distribution and migration of arsenic and antimony in the water bottom sediment system were similar under the oxygen conditions observed in the river. When taking into consideration the redox conditions in the river, it is not surprising that As(V) and Sb(V) forms dominated. The coefficients for arsenic and antimony in water and bottom sediments were similar (approximately 4.7 at Eh > 200 mV) [59].

The literature does not provide many reports on the thallium speciation in bottom sediments with HPLC-ICP-MS [44]. Most investigations concern bottom sediment fractionation [78] and extraction of particular chemical species [79, 80]. Table 1 presents the application of LC-ICP-MS techniques in chromium, arsenic, antimony, and thallium speciation in water and sediment samples.

## 7. Conclusions

Even though speciation analytics has been rapidly developing over the last 30 years, it is still a relatively new field of the analytical chemistry. Its further progress depends on many factors, such as the new sample preparation methods, separation and detection techniques, and the availability of the new certified reference materials. The element speciation has more and more applications in various scientific areas. Both the elaboration of the measurement methods and usage of the research results should be interdisciplinary. The speciation investigations call for the mutual cooperation of chemical analysts with biologists and toxicologists [46].

Hyphenated methods provide new research opportunities [102, 103]. Their main advantages are extremely low detection and quantification limits, insignificant influence of the interferences in determinations, and very high determination precision and repeatability. Obviously, they also have limitations, such as the high price and complexity of the apparatus. Consequently, they are not normally available and used in the laboratories. Using hyphenated techniques requires full understanding of the analytical methodologies and apparatus operations. The systems are expensive and are used for scientific studies rather than routine analyses. Nonetheless, the development of these methods is becoming more and more important, which is corroborated by the growing number of applications and studies [104].

TABLE 1: Application of LC-ICP-MS techniques in chromium, arsenic, antimony, and thallium speciation in water and sediment samples.

Analytes	Analytical column	Mobile phase	Method of separation and detection	Matrix	References
As <sup>3+</sup> , As <sup>5+</sup> , MMA, DMA	Hamilton PRP-X100 Dionex IonPac AS7, AG7	75 mM Na <sub>3</sub> PO <sub>4</sub> , 2.5–50 mM HNO <sub>3</sub>	HPLC-ICP-MS	Surface water, mining water, underground water	[54]
As <sup>3+</sup> , As <sup>5+</sup> , MMA, DMA, AB, AC	Waters IC-Pak CM/D Waters Guard-Pak CM/D	NaHCO <sub>3</sub> /Na <sub>2</sub> CO <sub>3</sub> , HNO <sub>3</sub>	HPLC-ICP-MS	Water	[56]
As <sup>3+</sup> , As <sup>5+</sup> , MMA, DMA, AB	Hamilton PRP-X100	20 mM NH <sub>4</sub> H <sub>2</sub> PO <sub>4</sub>	HPLC-ICP-DRC-MS	Polluted waters	[81]
As <sup>3+</sup> , As <sup>5+</sup>	Hamilton PRP X-100	Na <sub>2</sub> CO <sub>3</sub>	HPLC-ICP-MS	Surface water	[61]
As <sup>3+</sup> , As <sup>5+</sup> , MMA, DMA	Dionex IonPac AS7	HNO <sub>3</sub>	HPLC-ICP-MS	Waters	[82]
As <sup>3+</sup> , As <sup>5+</sup>	Wescan Anion-S Cl8	EDTA	HPLC-ICP-MS	River waters	[83]
As <sup>3+</sup> , As <sup>5+</sup>	Waters IC-Pak A HC	NaOH, KNO <sub>3</sub>	HPLC-ICP-MS	Water	[58]
As <sup>3+</sup> , As <sup>5+</sup>	Dionex IonPac AG12A/AS12A	Sodium carbonate, sodium hydroxide, methanol	HPLC-ICP-MS	Iron rich water samples	[84]
As <sup>3+</sup> , As <sup>5+</sup> , MMA, DMA	Hamilton PRP X100	NH <sub>4</sub> NO <sub>3</sub>	HPLC-ICP-MS	Water	[62]
As <sup>3+</sup> , As <sup>5+</sup> , MMA, DMA, AB	Supelcosil LC-SCX	Pyridine, NaHCO <sub>3</sub> , Na <sub>2</sub> CO <sub>3</sub>	HPLC-ICP-MS	Aqueous extracts	[85]
As <sup>3+</sup> , As <sup>5+</sup> , MMA, DMA, AB	Dionex IonPac AS7	NH <sub>4</sub> H <sub>2</sub> PO <sub>4</sub> , NH <sub>4</sub> OH	HPLC-ICP-MS	Waters	[86]
As <sup>3+</sup> , As <sup>5+</sup>	Hamilton PRP X100	CH <sub>3</sub> COOH, NH <sub>4</sub> NO <sub>3</sub> , EDTA	HPLC-ICP-MS	Drinking water	[87]
As <sup>3+</sup> , As <sup>5+</sup> , MMA, DMA, AC, AB	Spherisorb ODS/NH <sub>2</sub>	5 mM NaH <sub>2</sub> PO <sub>4</sub> , 5 mM Na <sub>2</sub> HPO <sub>4</sub>	HPLC-ICP-MS	Water	[57]
As <sup>3+</sup> , As <sup>5+</sup> , MMA, DMA	Hamilton PRP-X100	10–200 mM NH <sub>4</sub> H <sub>2</sub> PO <sub>4</sub>	HPLC-ICP-DRC-MS	Sediments	[77]
As <sup>3+</sup> , As <sup>5+</sup> , MMA, DMA, AB, AC	Develosil C30-UG-5, Chemcosorb 7SAX	Sodium butanesulfonate, malonic acid, tetramethylammonium hydroxide, methanol, ammonium tartrate	HPLC-ICP-MS	Environmental samples	[65]
As <sup>3+</sup> , As <sup>5+</sup>	Dionex IonPac AG-7 Hamilton PRP-X100	10 mM HNO <sub>3</sub>	HPLC-ICP-MS	Water	[33]
Sb <sup>3+</sup> , Sb <sup>5+</sup>	Hamilton PRP-X100	20 mM EDTA, 2 mM KHP	HPLC-ICP-MS	Waters	[64]
Sb <sup>3+</sup> , Sb <sup>5+</sup>	Hamilton PRP-X100	10 mM EDTA, 1 mM phthalic acid	HPLC-ICP-MS	Moat water	[68]
Sb <sup>3+</sup> , Sb <sup>5+</sup>	Hamilton PRP-X100	20 mM EDTA, 2 mM KHP	HPLC-ICP-MS	Mineral water	[88]
Sb <sup>3+</sup> , Sb <sup>5+</sup> , TMSbCl <sub>2</sub>	Hamilton PRP-X100	20 mM EDTA, 2 mM KHP	HPLC-HG-AFS	Sea water,	[89]
Sb <sup>3+</sup> , Sb <sup>5+</sup> , TMSbO	Hamilton PRP-X100	2 mM phthalic acid 2 mM 4-hydroxybenzoic acid	HPLC-ICP-MS	Surface water	[69]
Sb <sup>3+</sup> , Sb <sup>5+</sup> , TMSbCl <sub>2</sub>	CETAC ION-120 Dionex IonPac AS14	2 mM NH <sub>4</sub> HCO <sub>3</sub> , 1 mM tartaric acid, 1.25 mM EDTA	HPLC-ICP-MS	Tap water	[67]
Sb <sup>3+</sup> , Sb <sup>5+</sup> , TMSbCl <sub>2</sub> , TMS(OH) <sub>2</sub>	Hamilton PRP-X100, Hamilton PRPX-200, Supelcosil LC-SCX, Hamilton PRPI, Phenomenex Intersil 5 ODS	KH <sub>2</sub> PO <sub>4</sub> /K <sub>2</sub> HPO <sub>4</sub> 0.5–5 mM, KHCO <sub>3</sub> /K <sub>2</sub> CO <sub>3</sub> 1–50 mM, Pyridine, 2,6 dicarboxylic acid (PDCA): 5–20 mM EDTA, 5–50 mM HNO <sub>3</sub> , 1–4 mM Ethylenediamine	HPLC-ICP-MS	Environmental samples	[90]

TABLE 1: Continued.

Analytes	Analytical column	Mobile phase	Method of separation and detection	Matrix	References
Sb <sup>3+</sup> , Sb <sup>5+</sup>	Synchropak Q300	5 mM EDTA, 2 mM phthalic acid	HPLC-ICP-MS	Tap water	[66]
Sb <sup>3+</sup> , Sb <sup>5+</sup> , TMSbCl <sub>2</sub>	Hamilton PRP-X100, Dionex IonPac AS4A-SC	12 mM tetra-methylammonium hydroxide 3 mM tetra-methylammonium hydroxide	HPLC-ICP-MS	Environmental samples	[91]
Sb <sup>3+</sup> , Sb <sup>5+</sup>	Dionex IonPac AS-7	1 mM Phthalic acid, 10 mM EDTANa <sub>2</sub>	IC-ICP-MS	Water and bottom sediments	[49]
Tl <sup>1+</sup> , Tl <sup>3+</sup>	Dionex IonPac CG12A	0.015 M HNO <sub>3</sub>	IC-ICP-MS	Water	[92]
Tl <sup>1+</sup> , Tl <sup>3+</sup>	Dionex IonPac AG12A CG12A	HNO <sub>3</sub> , HCl	IC-ICP-MS	Water	[70]
Tl <sup>1+</sup> , Tl <sup>3+</sup>	Dionex IonPac AS7	1.5 mM phthalic acid, 10 mM EDTA, 15 mM HNO <sub>3</sub> , 2 mM DTPA	IC-ICP-MS	Water; bottom sediments	[44]
Cr <sup>3+</sup> , Cr <sup>6+</sup> , Se <sup>4+</sup> , Se <sup>6+</sup>	Dionex IonPac AG-II Dionex IonPac AS-II	20 Mm NaOH	IC-ICP-DRC-MS	Surface water, groundwater, tap waters	[32]
Cr <sup>3+</sup> , Cr <sup>6+</sup>	Waters Guard-Pak CM/D Waters IC-Pak A	0.4–40 mM HNO <sub>3</sub>	IC-ICP-DRC-MS	Sludge	[55]
Cr <sup>3+</sup> , Cr <sup>6+</sup>	Waters IC-Pak CM/D Waters Guard-Pak CM/D	0.4–40 mM HNO <sub>3</sub>	IC-ICP-DRC-MS	Water	[93]
Cr <sup>3+</sup> , Cr <sup>6+</sup>	G3145A/101 G3145A/102	30 mM NH <sub>4</sub> H <sub>2</sub> PO <sub>4</sub>	IC-ICP-MS	Sludge	[94]
Cr <sup>3+</sup> , Cr <sup>6+</sup>	G3145A/101 G3145A/102	20 mM NH <sub>4</sub> NO <sub>3</sub>	IC-ICP-DRC-MS	Saline water with a high content of Cl <sup>-</sup>	[95]
Cr <sup>3+</sup> , Cr <sup>6+</sup>	Shodex RS-pak NN-814 4DP	90 mM (NH <sub>4</sub> ) <sub>2</sub> SO <sub>4</sub> 10 mM NH <sub>4</sub> NO <sub>3</sub>	IC-ICP-DRC-MS	Water	[96]
Cr <sup>3+</sup> , Cr <sup>6+</sup>	Prepared in the laboratory	0.70 M HNO <sub>3</sub>	IC-ICP-MS	Seawater	[97]
Cr <sup>3+</sup> , Cr <sup>6+</sup>	Dionex IonPac CS5	2 mM PDCA + 2 mM NaHPO <sub>4</sub> + 1 mM NaI + 5 mM CH <sub>3</sub> COONH <sub>4</sub>	IC-ICP-MS	Drinking water	[98]
Cr <sup>3+</sup> , Cr <sup>6+</sup>	Excelpak ICS-A23	1 mM EDTA-2NH <sub>4</sub> + 10 mM H <sub>2</sub> C <sub>2</sub> O <sub>4</sub>	IC-ICP-MS	Drinking water, sludge	[99]
Cr <sup>3+</sup> , Cr <sup>6+</sup>	Dionex IonPac CS5	PDCA + (NH <sub>4</sub> ) <sub>2</sub> HPO <sub>4</sub> + CH <sub>3</sub> COONH <sub>4</sub> + NH <sub>4</sub> OH + NH <sub>4</sub> I	IC-ICP-MS	Water	[100]
Cr <sup>3+</sup> , Cr <sup>6+</sup>	Dionex IonPac CS5A	40 mM MgSO <sub>4</sub> + 30 mM HClO <sub>4</sub>	IC-ICP-MS	Drinking water, sludge	[101]
Cr <sup>3+</sup> , Cr <sup>6+</sup>	Dionex IonPac AG7	0.1 M NH <sub>4</sub> NO <sub>3</sub> , pH = 4 0.8 M HNO <sub>3</sub>	IC-ICP-MS	Water and bottom sediments	[49]

## Abbreviations

CE:	Capillary electrophoresis
CNS:	Central nervous system
DMA:	Dimethylarsenine
DMPS:	2,3-Dimercapto-1-propanesulfonic acid
DNA:	Deoxyribonucleic acid
EDTA:	Ethylenediaminetetraacetic acid
FDA:	Food and Drug Administration
FIA-AAS:	Flow injection analysis atomic absorption spectrometry
GC:	Gas chromatography
HPLC:	High performance liquid chromatography
HPLC-ICP-MS:	High performance liquid chromatography inductively coupled plasma-mass spectrometry
HPLC-ICP-SF-MS:	High performance liquid chromatography sector field inductively coupled plasma-mass spectrometry
IARC:	International agency for research on cancer
ICP-CC-QMS:	Inductively coupled plasma collision cell quadrupole mass spectrometry
ICP-DRC-QMS:	Inductively coupled plasma dynamic reaction cell quadrupole mass spectrometry
ICP-MS:	Inductively coupled plasma-mass spectrometry
ICP-SF-MS:	Inductively coupled plasma sector field mass spectrometry
IPRP-ICP-MS:	Ion-pairing reversed phase chromatography inductively coupled plasma mass spectrometry
LC:	Liquid chromatography
LC-ICP-MS:	Liquid chromatography inductively coupled plasma-mass spectrometry
LC-MC-ICP-MS:	Liquid chromatography-multicollector inductively coupled plasma-mass spectrometry
LOD:	Limit of detection
MC-ICP-MS:	Multicollector inductively coupled plasma-mass spectrometry
MMA:	Monomethylarsonic acid
RNA:	Ribonucleic acid
RSD:	Relative standard deviation
TBAH:	Tetrabutylammonium Hydroxide
TMSb:	Trimethylantimony
TMSbO:	Trimethylstiboxide
TSbCl <sub>2</sub> :	Trimethylantimony dichloride.

## Conflict of Interests

The author declares that there is no conflict of interests regarding the publication of this paper.

## References

- [1] R. Cornelis, J. Caruso, H. Crews, and K. Heumann, *Handbook of Elemental Speciation: Techniques and Methodology*, John Wiley & Sons, Chichester, UK, 2003.
- [2] L. A. Ellis and D. J. Roberts, "Chromatographic and hyphenated methods for elemental speciation analysis in environmental media," *Journal of Chromatography A*, vol. 774, no. 1-2, pp. 3-19, 1997.
- [3] R. A. Shalliker, *Hyphenated and Alternative Methods of Detection in Chromatography*, vol. 104 of *Chromatographic Science Series*, CRC Press, New York, NY, USA, 2011.
- [4] G. Purcaro, S. Moret, and L. Conte, "Hyphenated liquid chromatography-gas chromatography technique: recent evolution and applications," *Journal of Chromatography A*, vol. 1255, pp. 100-111, 2012.
- [5] A. Gonzalez, M. L. Cervera, S. Armenta, and M. de la Guardia, "A review of non-chromatographic methods for speciation analysis," *Analytica Chimica Acta*, vol. 636, no. 2, pp. 129-157, 2009.
- [6] P. Smichowski, "Antimony in the environment as a global pollutant: a review on analytical methodologies for its determination in atmospheric aerosols," *Talanta*, vol. 75, no. 1, pp. 2-14, 2008.
- [7] M. Filella, N. Belzile, and Y.-W. Chen, "Antimony in the environment: a review focused on natural waters I. Occurrence," *Earth-Science Reviews*, vol. 57, no. 1-2, pp. 125-176, 2002.
- [8] S. Marcellino, H. Attar, D. Lièvremon, M.-C. Lett, F. Barbier, and F. Lagarde, "Heat-treated *Saccharomyces cerevisiae* for antimony speciation and antimony(III) preconcentration in water samples," *Analytica Chimica Acta*, vol. 629, no. 1-2, pp. 73-83, 2008.
- [9] A. Léonard and G. B. Gerber, "Mutagenicity, carcinogenicity and teratogenicity of antimony compounds," *Mutation Research: Reviews in Genetic Toxicology*, vol. 366, no. 1, pp. 1-8, 1996.
- [10] S. Garboś, E. Bulska, A. Hulanicki, Z. Fijalek, and K. Soltyk, "Determination of total antimony and antimony(V) by inductively coupled plasma mass spectrometry after selective separation of antimony(III) by solvent extraction with N-benzoyl-N-phenylhydroxylamine," *Spectrochimica Acta B*, vol. 55, no. 7, pp. 795-802, 2000.
- [11] C.-H. S. J. Chou and C. T. de Rosa, "Case studies—arsenic," *International Journal of Hygiene and Environmental Health*, vol. 206, no. 4-5, pp. 381-386, 2003.
- [12] R. Cornelis, H. Crews, J. Caruso, and K. G. Heumann, *Handbook of Elemental Speciation II: Species in the Environment, Food, Medicine & Occupational Health*, John Wiley & Sons, New York, NY, USA, 2005.
- [13] T. Shibamoto and M. Dekker, *Chromatographic Analysis of Environmental and Food Toxicants*, CRC Press, New York, NY, USA, 1998.
- [14] R. Michalski, S. Szopa, M. Jabłońska, and A. Łyko, "Application of hyphenated techniques in speciation analysis of arsenic, antimony, and thallium," *The Scientific World Journal*, vol. 2012, Article ID 902464, 17 pages, 2012.
- [15] N. Ulrich, "Determination of antimony species with fluoride as modifier and flow injection hydride generation inductively-coupled plasma emission spectrometry," *Analytica Chimica Acta*, vol. 417, no. 2, pp. 201-209, 2000.
- [16] S. Garboś, E. Bulska, A. Hulanicki, N. I. Shcherbinina, and E. M. Sedykh, "Preconcentration of inorganic species of antimony by sorption on Polyorgs 31 followed by atomic absorption spectrometry detection," *Analytica Chimica Acta*, vol. 342, no. 2-3, pp. 167-174, 1997.

- [17] R. Torralba, M. Bonilla, L. V. Pérez-Arribas, M. A. Palacios, and C. Cámara, "Comparison of three multivariate calibration methods as an approach to arsenic speciation by HG-AAS," *Mikrochimica Acta*, vol. 126, no. 3-4, pp. 257-262, 1997.
- [18] N. M. M. Coelho, A. C. da Silva, and C. M. da Silva, "Determination of As(III) and total inorganic arsenic by flow injection hydride generation atomic absorption spectrometry," *Analytica Chimica Acta*, vol. 460, no. 2, pp. 227-233, 2002.
- [19] J. Chwastowska, W. Skwara, E. Sterlińska, and L. Pszonicki, "Speciation of chromium in mineral waters and salinas by solid-phase extraction and graphite furnace atomic absorption spectrometry," *Talanta*, vol. 66, no. 5, pp. 1345-1349, 2005.
- [20] M. A. Vieira, P. Grinberg, C. R. R. Bobeda, M. N. M. Reyes, and R. C. Campos, "Non-chromatographic atomic spectrometric methods in speciation analysis: a review," *Spectrochimica Acta—Part B Atomic Spectroscopy*, vol. 64, no. 6, pp. 459-476, 2009.
- [21] S. D. Tanner, V. I. Baranov, and D. R. Bandura, "Reaction cells and collision cells for ICP-MS: a tutorial review," *Spectrochimica Acta B*, vol. 57, no. 9, pp. 1361-1452, 2002.
- [22] J. S. Becker, *Inorganic Mass Spectrometry: Principles and Applications*, John Wiley & Sons, Chichester, UK, 2008.
- [23] J. M. Marchante-Gayón, C. Thomas, I. Feldmann, and N. Jakubowski, "Comparison of different nebulizers and chromatographic techniques for the speciation of selenium in nutritional commercial supplements by hexapole collision and reaction cell ICP-MS," *Journal of Analytical Atomic Spectrometry*, vol. 15, no. 9, pp. 1093-1102, 2000.
- [24] J. Szpunar and R. Łobinski, "Hyphenated techniques in speciation analysis," in *RSC Chromatography Monographs*, R. M. Smith, Ed., Royal Society of Chemistry, Cambridge, Mass, USA, 2003.
- [25] R. Michalski, M. Jabłńska, S. Szopa, and A. Łyko, "Application of ion chromatography with ICP-MS or MS detection to the determination of selected halides and metal/metalloids species," *Critical Reviews in Analytical Chemistry*, vol. 41, no. 2, pp. 133-150, 2011.
- [26] F. Vanhaecke and P. Degryse, *Isotopic Analysis. Fundamentals and Applications Using ICP-MS*, Wiley-VCH GmBH&Co. KGaA, Weinheim, Germany, 2012.
- [27] A. Kabata-Pendias and H. Pendias, *Biogeochemia pierwiastków śladowych*, Wydawnictwo Naukowe PWN, Warszawa, Poland, 1999.
- [28] P. Niedzielski, M. Siepak, and J. Siepak, "Występowanie i zawartości arsenu, antymonu i selenu w wodach i innych elementach środowiska," *Rocznik Ochrony Środowiska*, vol. 1, pp. 317-341, 2000.
- [29] W. Semczuk, *Toksykologia*, Państwowy Zakład Wydawnictw Lekarskich, Warszawa, Poland, 1990.
- [30] H. V. Aposhian, D. E. Carter, T. D. Hoover, C.-A. Hsu, R. M. Maiorino, and E. Stine, "DMSA, DMPS, and DMPA-as arsenic antidotes," *Fundamental and Applied Toxicology*, vol. 4, no. 2, pp. S58-S70, 1984.
- [31] *Guidelines for Drinking-Water Quality: Volume 2: Health Criteria and Other Supporting Information*, WHO, Geneva, Switzerland, 2nd edition, 1996.
- [32] A. J. Bednar, R. A. Kirgan, and W. T. Jones, "Comparison of standard and reaction cell inductively coupled plasma mass spectrometry in the determination of chromium and selenium species by HPLC-ICP-MS," *Analytica Chimica Acta*, vol. 632, no. 1, pp. 27-34, 2009.
- [33] M. Jabłńska, M. Kostecki, S. Szopa, A. Łyko, and R. Michalski, "Specjacja nieorganicznych form arsenu i chromu w wybranych zbiornikach zaporowych Górnego Śląska," *Ochrona Środowiska*, vol. 34, no. 3, pp. 25-32, 2012.
- [34] D. J. Burbridge, I. Koch, J. Zhang, and K. J. Reimer, "Chromium speciation in river sediment pore water contaminated by tannery effluent," *Chemosphere*, vol. 89, no. 7, pp. 838-843, 2012.
- [35] J. O. Nriagu, *Thallium in the Environment*, Advances in Environmental Science and Technology, Wiley-Interscience, New York, NY, USA, 1998.
- [36] G. Repetto, A. del Peso, and M. Repetto, "Human thallium toxicity," in *Thallium in the Environment*, J. O. Nriagu, Ed., John Wiley & Sons, New York, NY, USA, 1998.
- [37] C.-H. Lan and T.-S. Lin, "Acute toxicity of trivalent thallium compounds to *Daphnia magna*," *Ecotoxicology and Environmental Safety*, vol. 61, no. 3, pp. 432-435, 2005.
- [38] L. Ralph and M. R. Twiss, "Comparative toxicity of thallium(I), thallium(III), and cadmium(II) to the unicellular alga *Chlorella* isolated from Lake Erie," *Bulletin of Environmental Contamination and Toxicology*, vol. 68, no. 2, pp. 261-268, 2002.
- [39] T.-S. Lin and J. O. Nriagu, "Thallium speciation in river waters with Chelex-100 resin," *Analytica Chimica Acta*, vol. 395, no. 3, pp. 301-307, 1999.
- [40] S. Garboś, M. Rzepecka, E. Bulska, and A. Hulanicki, "Microcolumn sorption of antimony(III) chelate for antimony speciation studies," *Spectrochimica Acta B*, vol. 54, no. 5, pp. 873-881, 1999.
- [41] L. Ebdon, L. Pitts, R. Cornelis, H. Crews, O. F. X. Donard, and P. Quevauviller, *Trace Element Speciation for Environment, Food and Health*, The Royal Society of Chemistry, Cambridge, UK, 2001.
- [42] M. L. Peterson and R. Carpenter, "Biogeochemical processes affecting total arsenic and arsenic species distributions in an intermittently anoxic fjord," *Marine Chemistry*, vol. 12, no. 4, pp. 295-321, 1983.
- [43] B. Krasnodębska-Ostręga, M. Asztemborska, J. Golimowski, and K. Strusińska, "Determination of thallium forms in plant extracts by anion exchange chromatography with inductively coupled plasma mass spectrometry detection (IC-ICP-MS)," *Journal of Analytical Atomic Spectrometry*, vol. 23, no. 12, pp. 1632-1635, 2008.
- [44] S. Szopa and R. Michalski, "Simultaneous determination of inorganic forms of arsenic, antimony, and thallium by HPLC-ICP-MS," *LCGC Europe*. In press.
- [45] B. Radke, L. Jewell, and J. Namieśnik, "Analysis of arsenic species in environmental samples," *Critical Reviews in Analytical Chemistry*, vol. 42, no. 2, pp. 162-183, 2012.
- [46] B. Godlewska-Żyłkiewicz, "Sztuka przygotowywania próbek w analizie specjacyjnej," in *Specjacja Chemiczna, Problemy i Możliwości*, D. Barańkiewicz and E. Bulska, Eds., Malamut, Warszawa, Poland, 2009.
- [47] A. W. Fitchett, E. H. Daughtrey Jr., and P. Mushak, "Quantitative measurements of inorganic and organic arsenic by flameless atomic absorption spectrometry," *Analytica Chimica Acta*, vol. 79, pp. 93-99, 1975.
- [48] A. Yasui, C. Tsutsumi, and S. Toda, "Selective determination of inorganic arsenic (III), (V) and organic arsenic in biological materials by solvent extraction-atomic absorption spectrophotometry," *Agricultural and Biological Chemistry*, vol. 42, no. 11, pp. 2139-2145, 1978.
- [49] M. Jabłńska-Czapla, S. Szopa, K. Grygoyć, A. Łyko, and R. Michalski, "Development and validation of HPLC-ICP-MS method for the determination inorganic Cr, As and Sb speciation forms and its application for Pławniowiec reservoir (Poland) water and bottom sediments variability study," *Talanta*, vol. 120, pp. 475-483, 2014.

- [50] J. L. Gómez-Ariza, D. Sánchez-Rodas, and I. Giraldez, "Selective extraction of iron oxide associated arsenic species from sediments for speciation with coupled HPLC-HG-AAS," *Journal of Analytical Atomic Spectrometry*, vol. 13, no. 12, pp. 1375–1379, 1998.
- [51] M. Popp, S. Hann, and G. Koellensperger, "Environmental application of elemental speciation analysis based on liquid or gas chromatography hyphenated to inductively coupled plasma mass spectrometry—a review," *Analytica Chimica Acta*, vol. 668, no. 2, pp. 114–129, 2010.
- [52] S. N. Ronkart, V. Laurent, P. Carboneille, N. Mabon, A. Copin, and J.-P. Barthélemy, "Speciation of five arsenic species (arsenite, arsenate, MMAA<sup>V</sup>, DMAA<sup>V</sup> and AsBet) in different kind of water by HPLC-ICP-MS," *Chemosphere*, vol. 66, no. 4, pp. 738–745, 2007.
- [53] S. Afton, K. Kubachka, B. Catron, and J. A. Caruso, "Simultaneous characterization of selenium and arsenic analytes via ion-pairing reversed phase chromatography with inductively coupled plasma and electrospray ionization ion trap mass spectrometry for detection: applications to river water, plant extract and urine matrices," *Journal of Chromatography A*, vol. 1208, no. 1-2, pp. 156–163, 2008.
- [54] A. J. Bednar, J. R. Garbarino, M. R. Burkhardt, J. F. Ranville, and T. R. Wildeman, "Field and laboratory arsenic speciation methods and their application to natural-water analysis," *Water Research*, vol. 38, no. 2, pp. 355–364, 2004.
- [55] M. Pansar-Kallio and P. K. G. Manninen, "Speciation of chromium in waste waters by coupled column ion chromatography-inductively coupled plasma mass spectrometry," *Journal of Chromatography A*, vol. 750, no. 1-2, pp. 89–95, 1996.
- [56] P. Teräsahde, M. Pansar-Kallio, and P. K. G. Manninen, "Simultaneous determination of arsenic species by ion chromatography-inductively coupled plasma mass spectrometry," *Journal of Chromatography A*, vol. 750, no. 1-2, pp. 83–88, 1996.
- [57] M. Moldovan, M. M. Gómez, M. A. Palacios, and C. Cámara, "Arsenic speciation in water and human urine by HPLC/ICP/MS and HPLC/MO/HG/AAS," *Microchemical Journal*, vol. 59, no. 1, pp. 89–99, 1998.
- [58] M. Pansar-Kallio and P. K. G. Manninen, "Simultaneous determination of toxic arsenic and chromium species in water samples by ion chromatography-inductively coupled plasma mass spectrometry," *Journal of Chromatography A*, vol. 779, no. 1-2, pp. 139–146, 1997.
- [59] J. Zheng, H. Hintelmann, B. Dimock, and M. S. Dzurko, "Speciation of arsenic in water, sediment, and plants of the Moira watershed, Canada, using HPLC coupled to high resolution ICP-MS," *Analytical and Bioanalytical Chemistry*, vol. 377, no. 1, pp. 14–24, 2003.
- [60] S. Asaoka, Y. Takahashi, Y. Araki, and M. Tanimizu, "Comparison of antimony and arsenic behavior in an Ichinokawa River water-sediment system," *Chemical Geology*, vol. 334, pp. 1–8, 2012.
- [61] A. F. Roig-Navarro, Y. Martínez-Bravo, F. J. López, and F. Hernández, "Simultaneous determination of arsenic species and chromium(VI) by high-performance liquid chromatography-inductively coupled plasma-mass spectrometry," *Journal of Chromatography A*, vol. 912, no. 2, pp. 319–327, 2001.
- [62] Y. Martínez-Bravo, A. F. Roig-Navarro, F. J. López, and F. Hernández, "Multielemental determination of arsenic, selenium and chromium(VI) species in water by high-performance liquid chromatography-inductively coupled plasma mass spectrometry," *Journal of Chromatography A*, vol. 926, no. 2, pp. 265–274, 2001.
- [63] I. Komorowicz and D. Baralkiewicz, "Arsenic and its speciation in water samples by high performance liquid chromatography inductively coupled plasma mass spectrometry—last decade review," *Talanta*, vol. 84, no. 2, pp. 247–261, 2011.
- [64] F. Liu, X. C. Le, A. McKnight-Whitford et al., "Antimony speciation and contamination of waters in the Xikuangshan antimony mining and smelting area, China," *Environmental Geochemistry and Health*, vol. 32, no. 5, pp. 401–413, 2010.
- [65] Y. Morita, T. Kobayashi, T. Kuroiwa, and T. Narukawa, "Study on simultaneous speciation of arsenic and antimony by HPLC-ICP-MS," *Talanta*, vol. 73, no. 1, pp. 81–86, 2007.
- [66] J. Zheng, M. Ohata, and N. Furuta, "Antimony speciation in environmental samples by using high-performance liquid chromatography coupled to inductively coupled plasma mass spectrometry," *Analytical Sciences*, vol. 16, no. 1, pp. 75–80, 2000.
- [67] M. Krachler and H. Emons, "Speciation analysis of antimony by high-performance liquid chromatography inductively coupled plasma mass spectrometry using ultrasonic nebulization," *Analytica Chimica Acta*, vol. 429, no. 1, pp. 125–133, 2001.
- [68] J. Zheng, A. Iijima, and N. Furuta, "Complexation effect of antimony compounds with citric acid and its application to the speciation of antimony(III) and antimony(V) using HPLC-ICP-MS," *Journal of Analytical Atomic Spectrometry*, vol. 16, no. 8, pp. 812–818, 2001.
- [69] N. Ulrich, "Speciation of antimony(III), antimony(V) and trimethylstiboxide by ion chromatography with inductively coupled plasma atomic emission spectrometric and mass spectrometric detection," *Analytica Chimica Acta*, vol. 359, no. 3, pp. 245–253, 1998.
- [70] U. Karlsson, A. Düker, and S. Karlsson, "Separation and quantification of Tl(I) and Tl(III) in fresh water samples," *Journal of Environmental Science and Health Part A: Toxic/Hazardous Substances and Environmental Engineering*, vol. 41, no. 7, pp. 1155–1167, 2006.
- [71] O. F. Schedlbauer and K. G. Heumann, "Development of an isotope dilution mass spectrometric method for dimethylthallium speciation and first evidence of its existence in the ocean," *Analytical Chemistry*, vol. 71, no. 24, pp. 5459–5464, 1999.
- [72] B. Krasnodębska-Ostręga, M. Sadowska, K. Piotrowska, and M. Wojda, "Thallium (III) determination in the Baltic seawater samples by ICP MS after preconcentration on SGX C18 modified with DDTc," *Talanta*, vol. 112, pp. 73–79, 2013.
- [73] S. Dadfarnia, T. Assadollahi, and A. M. Haji Shabani, "Speciation and determination of thallium by on-line microcolumn separation/preconcentration by flow injection-flame atomic absorption spectrometry using immobilized oxine as sorbent," *Journal of Hazardous Materials*, vol. 148, no. 1-2, pp. 446–452, 2007.
- [74] N. N. Meeravali and S. J. Jiang, "Ultra-trace speciation analysis of thallium in environmental water samples by inductively coupled plasma mass spectrometry after a novel sequential mixed-micelle cloud point extraction," *Journal of Analytical Atomic Spectrometry*, vol. 23, no. 4, pp. 555–560, 2008.
- [75] N. Unceta, F. Séby, J. Malherbe, and O. F. X. Donard, "Chromium speciation in solid matrices and regulation: a review," *Analytical and Bioanalytical Chemistry*, vol. 397, no. 3, pp. 1097–1111, 2010.
- [76] A. M. Graham, A. R. Wadhawan, and E. J. Bouwer, "Chromium occurrence and speciation in Baltimore harbor sediments and porewater, Baltimore, Maryland, USA," *Environmental Toxicology and Chemistry*, vol. 28, no. 3, pp. 471–480, 2009.
- [77] L. Orero Iserte, A. F. Roig-Navarro, and F. Hernández, "Simultaneous determination of arsenic and selenium species in

- phosphoric acid extracts of sediment samples by HPLC-ICP-MS," *Analytica Chimica Acta*, vol. 527, no. 1, pp. 97–104, 2004.
- [78] Z. Lukaszewski, B. Karbowska, W. Zembrzuski, and M. Siepak, "Thallium in fractions of sediments formed during the 2004 tsunami in Thailand," *Ecotoxicology and Environmental Safety*, vol. 80, pp. 184–189, 2012.
- [79] B. Krasnodbska-Ostrga, M. Sadowska, and S. Ostrowska, "Thallium speciation in plant tissues—Tl(III) found in *Sinapis alba* L. grown in soil polluted with tailing sediment containing thallium minerals," *Talanta*, vol. 93, pp. 326–329, 2012.
- [80] P. Chakraborty, S. Jayachandran, P. V. R. Babu et al., "Intra-annual variations of arsenic totals and species in tropical estuary surface sediments," *Chemical Geology*, vol. 322–323, pp. 172–180, 2012.
- [81] Z. Chen, N. I. Khan, G. Owens, and R. Naidu, "Elimination of chloride interference on arsenic speciation in ion chromatography inductively coupled mass spectrometry using an octopole collision/reaction system," *Microchemical Journal*, vol. 87, no. 1, pp. 87–90, 2007.
- [82] W. D. James, T. Raghvan, T. J. Gentry, G. Shan, and R. H. Loeppert, "Arsenic speciation: HPLC followed by ICP-MS or INAA," *Journal of Radioanalytical and Nuclear Chemistry*, vol. 278, no. 2, pp. 267–270, 2008.
- [83] R. T. Gettar, R. N. Garavaglia, E. A. Gautier, and D. A. Batis-toni, "Determination of inorganic and organic anionic arsenic species in water by ion chromatography coupled to hydride generation-inductively coupled plasma atomic emission spectrometry," *Journal of Chromatography A*, vol. 884, no. 1–2, pp. 211–221, 2000.
- [84] B. Daus, J. Mattusch, R. Wennrich, and H. Weiss, "Investigation on stability and preservation of arsenic species in iron rich water samples," *Talanta*, vol. 58, no. 1, pp. 57–65, 2002.
- [85] A. Raab and J. Feldmann, "Arsenic speciation in hair extracts," *Analytical and Bioanalytical Chemistry*, vol. 381, no. 2, pp. 332–338, 2005.
- [86] S. N. Ronkart, V. Laurent, P. Carbonnelle, N. Mabon, A. Copin, and J.-P. Barthélemy, "Speciation of five arsenic species (arsenite, arsenate, MMAA<sup>V</sup>, DMAA<sup>V</sup> and AsBet) in different kind of water by HPLC-ICP-MS," *Chemosphere*, vol. 66, no. 4, pp. 738–745, 2007.
- [87] P. A. Creed, C. A. Schwegel, and J. T. Creed, "Investigation of arsenic speciation on drinking water treatment media utilizing automated sequential continuous flow extraction with IC-ICP-MS detection," *Journal of Environmental Monitoring*, vol. 7, no. 11, pp. 1079–1084, 2005.
- [88] H. R. Hansen and S. A. Pergantis, "Detection of antimony species in citrus juices and drinking water stored in PET containers," *Journal of Analytical Atomic Spectrometry*, vol. 21, no. 8, pp. 731–733, 2006.
- [89] I. De Gregori, W. Quiroz, H. Pinochet, F. Pannier, and M. Potin-Gautier, "Simultaneous speciation analysis of Sb(III), Sb(V) and (CH<sub>3</sub>)<sub>3</sub>SbCl<sub>2</sub> by high performance liquid chromatography-hydride generation-atomic fluorescence spectrometry detection (HPLC-HG-AFS): application to antimony speciation in sea water," *Journal of Chromatography A*, vol. 1091, no. 1–2, pp. 94–101, 2005.
- [90] J. Lintschinger, I. Koch, S. Serves, J. Feldmann, and W. R. Cullen, "Determination of antimony species with high-performance liquid chromatography using element specific detection," *Fresenius' Journal of Analytical Chemistry*, vol. 359, no. 6, pp. 484–491, 1997.
- [91] J. Lintschinger, O. Schramel, and A. Kettrup, "The analysis of antimony species by using ESI-MS and HPLC-ICP-MS," *Fresenius' Journal of Analytical Chemistry*, vol. 361, no. 2, pp. 96–102, 1998.
- [92] P. P. Coetzee, J. L. Fischer, and M. Hu, "Simultaneous separation and determination of Tl(I) and Tl(III) by IC-ICP-OES and IC-ICP-MS," *Water SA*, vol. 29, no. 1, pp. 17–22, 2003.
- [93] M. Panssar-Kallio and P. K. G. Manninen, "Speciation of chromium in aquatic samples by coupled column ion chromatography-inductively coupled plasma-mass spectrometry," *Analytica Chimica Acta*, vol. 318, no. 3, pp. 335–343, 1996.
- [94] Z. Chen, M. Megharaj, and R. Naidu, "Speciation of chromium in waste water using ion chromatography inductively coupled plasma mass spectrometry," *Talanta*, vol. 72, no. 2, pp. 394–400, 2007.
- [95] Z. Chen, M. Megharaj, and R. Naidu, "Removal of interferences in the speciation of chromium using an octopole reaction system in ion chromatography with inductively coupled plasma mass spectrometry," *Talanta*, vol. 73, no. 5, pp. 948–952, 2007.
- [96] H. Hagendorfer and W. Goessler, "Separation of chromium(III) and chromium(VI) by ion chromatography and an inductively coupled plasma mass spectrometer as element-selective detector," *Talanta*, vol. 76, no. 3, pp. 656–661, 2008.
- [97] S. Hirata, K. Honda, O. Shikino, N. Maekawa, and M. Aihara, "Determination of chromium(III) and total chromium in sea-water by on-line column preconcentration inductively coupled plasma mass spectrometry," *Spectrochimica Acta, Part B: Atomic Spectroscopy*, vol. 55, no. 7, pp. 1089–1099, 2000.
- [98] M. Sikovec, M. Novic, V. Hudnik, and M. Franko, "On-line thermal lens spectrometric detection of Cr(III) and Cr(VI) after separation by ion chromatography," *Journal of Chromatography A*, vol. 706, no. 1–2, pp. 121–126, 1995.
- [99] P. M. Paquet, J.-F. Gravel, P. Nobert, and D. Boudreau, "Speciation of chromium by ion chromatography and laser-enhanced ionization: optimization of the excitation-ionization scheme," *Spectrochimica Acta Part B: Atomic Spectroscopy*, vol. 53, no. 14, pp. 1907–1917, 1998.
- [100] T. Williams, P. Jones, and L. Ebdon, "Simultaneous determination of Cr(III) and Cr(VI) at ultratrace levels using ion chromatography with chemiluminescence detection," *Journal of Chromatography*, vol. 482, no. 2, pp. 361–366, 1989.
- [101] R. Michalski, "Trace level determination of Cr(III)/Cr(VI) in water samples using ion chromatography with UV detection," *Journal of Liquid Chromatography & Related Technologies*, vol. 28, pp. 2849–2862, 2005.
- [102] R. Michalski, M. Jabłońska, and S. Szopa, "Role and importance of hyphenated techniques in speciation analysis," in *Speciation Studies in Soil, Sediment and Environmental Samples*, S. Bakirdere, Ed., pp. 242–262, Science Publishers/CRC Press/Taylor&Francis Group, 2013.
- [103] R. Michalski, M. Jabłońska-Czapla, A. Łyko, and S. Szopa, "Hyphenated methods for speciation analysis," in *Encyclopedia of Analytical Chemistry*, John Wiley & Sons, New York, NY, USA, 2013.
- [104] J. Feldmann, P. Salaün, and E. Lombi, "Critical review perspective: elemental speciation analysis methods in environmental chemistry—moving towards methodological integration," *Environmental Chemistry*, vol. 6, no. 4, pp. 275–289, 2009.

## Research Article

# A Rapid and Accurate Extraction Procedure for Analysing Free Amino Acids in Meat Samples by GC-MS

Trinidad Pérez-Palacios,<sup>1</sup> Miguel A. Barroso,<sup>1</sup> Jorge Ruiz,<sup>2</sup> and Teresa Antequera<sup>1</sup>

<sup>1</sup>Department of Animal Production and Food Science, Faculty of Veterinary Sciences, University of Extremadura, Avenida de la Universidad s/n, 10003 Cáceres, Spain

<sup>2</sup>Dairy, Meat and Plant Product Technology, Department of Food Science, University of Copenhagen, Rolighedsvej 30, 1958 Frederiksberg C, Denmark

Correspondence should be addressed to Trinidad Pérez-Palacios; trinity@unex.es

Received 2 September 2014; Revised 12 January 2015; Accepted 20 January 2015

Academic Editor: Shahram Seidi

Copyright © 2015 Trinidad Pérez-Palacios et al. This is an open access article distributed under the Creative Commons Attribution License, which permits unrestricted use, distribution, and reproduction in any medium, provided the original work is properly cited.

This study evaluated the use of a mixer mill as the homogenization tool for the extraction of free amino acids in meat samples, with the main goal of analyzing a large number of samples in the shortest time and minimizing sample amount and solvent volume. Ground samples (0.2 g) were mixed with 1.5 mL HCl 0.1 M and homogenized in the mixer mill. The final biphasic system was separated by centrifugation. The supernatant was deproteinized, derivatized and analyzed by gas chromatography. This procedure showed a high extracting ability, especially in samples with high free amino acid content (recovery = 88.73–104.94%). It also showed a low limit of detection and quantification ( $3.8 \cdot 10^{-4}$ – $6.6 \cdot 10^{-4} \mu\text{g mL}^{-1}$  and  $1.3 \cdot 10^{-3}$ – $2.2 \cdot 10^{-2} \mu\text{g mL}^{-1}$ , resp.) for most amino acids, an adequate precision (2.15–20.15% for run-to-run), and a linear response for all amino acids ( $R^2 = 0.741$ – $0.998$ ) in the range of 1–100  $\mu\text{g mL}^{-1}$ . Moreover, it takes less time and requires lower amount of sample and solvent than conventional techniques. Thus, this is a cost and time efficient tool for homogenizing in the extraction procedure of free amino acids from meat samples, being an adequate option for routine analysis.

## 1. Introduction

Meat and meat products are a good source of amino acids and their proteins are considered of high biological quality. After consumption of meat, free amino acids are rapidly absorbed, while proteins are easily hydrolysed into peptides and amino acids, which in turn are also absorbed. Apart from their nutritional importance, amino acids also influence meat palatability [1] and flavour [2], through the generation of volatile compounds by Maillard reactions and Strecker degradations [3–6]. During the processing of dry-cured meat products, such as dry-cured ham or loin, there happens an increase in free amino acid content as a consequence of proteolytic activity [4, 7]; indeed, the amount of most amino acids increases with processing time and with higher processing temperatures [3, 8, 9]. Glutamic acid and phenylalanine have been found to be the major amino acids in fresh meat, while in

dry-cured products glutamic acid, arginine, and lysine have shown the highest levels [10].

Traditionally, the most common method to analyze free amino acids in food matrices has been reverse phase-high performance liquid chromatography (RP-HPLC) with a precolumn derivatization step [10]. Gas chromatography coupled with mass spectrometry (GC-MS) can be also used as an alternative method, especially when sample amounts are limited and high sensitivity is required [11]. In addition GC presents higher resolution and speed of analysis and lower instrumental cost than HPLC [12]. When GC was first used for the analysis of amino acids, its main drawback was the time consuming and tedious derivatization steps (esterification + acylation) required. Then, the simultaneous silylation of the amino and carboxyl groups in a single step, first using bis(trimethylsilyl)trifluoroacetamide (BSTFA) [13] and later with N-methyl-N-(tert-butyl)dimethylsilyl)trifluoroacetamide

(MTBSTFA) [14], was developed. MTBSTFA allows the use of milder derivatization conditions [15]. Jiménez-Martín et al. [10] have demonstrated the suitability of using MTBSTFA for the determination of free amino acids in different animal source foods.

A previous free amino acid extraction is required before their derivatization and further analysis. Most extraction methods for amino acids in food products involve using perchloric acid or hydrochloric acid (HCl) diluted in water or in ethanol [9, 10, 12, 16–20]. Other solvents for the extraction of amino acids have also been described in the scientific literature, such as ethanol [21], and solvent mixtures, such as water/acetonitrile (50 : 50, v/v) [22] or 0.1% (v/v) formic acid in 20% (v/v) methanol [23]. After mixing the sample with the solvent, the homogenization step is essential for the amino acids to be extracted. For this purpose, different techniques have been used, that is, stirring [12], ultraturax [16, 17], stomacher [10, 17], omni mixer [9], rotary mixer at 50 °C [21], vortex [23], and a heating block at 40 °C with stirring [18]. Then, centrifugation is usually carried out, followed by the collection of the supernatant [20] and its filtration through glass wool [9, 10], nylon membrane [23], or Whatman 42 paper [17]. Some authors clean up the supernatant through a cartridge [12, 21] and others do not specify the filtration procedure [9, 20].

The search for new and accurate methods for amino acid analysis in meat and meat products is challenging. The development of derivatization and chromatographic procedures has been thoroughly studied, while less attention has been paid to the extraction methods [24]. Recently, Jiménez-Martín et al. [10] described a GC-MS method for the determination of free amino acids in animal source food. In this methodology, the sample is homogenized with HCl 0.1 M by using a stomacher. Acetonitrile is used for deproteinizing and MTBSTFA for derivatizing. The application of this GC-MS method for the determination of amino acids in meat and meat products constitutes an important reduction in time and solvents in the separation and detection procedures in comparison to RP-HPLC with diode array detector method [3, 4, 8, 9]. However the extraction protocol is time consuming and requires a large amount of sample and solvent, which makes it frequently not suitable for routine analysis.

The present work is focused on the homogenization step for the amino acid extraction from meat samples, with the main goal of reducing sample amount, solvent volume, and extraction time. Recently, Segura and Lopez-Bote [25] developed a new procedure to extract intramuscular fat from pork based on homogenizing the samples using a mixer mill, which allowed minimizing the sample amount, the solvent use, and the analysis time, which are important advantages for routine analysis. The mixer mill is a compact versatile bench-top unit, which has been developed specially for homogenizing small amounts of sample quickly and efficiently by impact and friction. The grinding jars perform radial oscillations in a horizontal position. The inertia of the grinding balls causes them to impact with high energy on the sample material at the rounded ends of the grinding jars and pulverizes it. Also, the movement of the grinding jars combined with the movement of the balls results in the intensive mixing of the sample.

The degree of mixing can be increased even further by using several smaller balls.

Thus, the objective of this study was to evaluate the use of the mixer mill as homogenization tool in the extraction of free amino acids from meat samples, in order to analyze a large number of samples in the shortest time, minimizing sample amount and solvent volume.

## 2. Material and Methods

**2.1. Samples.** This study was developed with two different meat samples, fresh pork loin and dry-cured ham. These samples were obtained from a local store. First, samples were ground using a commercial grinder. Subsequently, the moisture content of the products was determined according to the method of the Association of Official Analytical Chemists [26] (moisture reference 935.29). The rest of the ground samples were stored at –80 °C until free amino acid analysis.

**2.2. Reagents.** Hydrochloric acid (HCl), 37% extra pure, was used for the amino acid extraction (Scharlau, Barcelona, Spain). Acetonitrile of HPLC-gradient grade (Panreac, Barcelona, Spain) and dichloromethane (Merck, Darmstadt, Germany) were used for the amino acid deproteinization and derivatization procedures. MTBSTFA (Sigma-Aldrich, Madrid, Spain) was the derivatization reagent. Standard amino acids (Sigma-Aldrich) purchased for preparing the standard solutions were alanine, glycine, valine, leucine, isoleucine, proline, methionine, serine, threonine, phenylalanine, aspartic acid, hydroxyproline, cysteine, glutamic acid, arginine, asparagine, lysine, glutamine, histidine, tyrosine, tryptophan, and cystine. DL-Norleucine (Sigma-Aldrich) was used as internal standard (IS).

**2.3. Amino Acid Extraction Methods.** Two methods for the amino acid extraction were compared. They mainly differ in the homogenization procedure, carried out with stomacher (S) or mixer mill (M). Both methods used HCl 0.1 M as solvent extraction and the sample:solvent ratio was 1:7.5. The free amino acid content of fresh loin ( $n = 6$ ) and dry-cured ham ( $n = 6$ ) was analysed by using the two extraction methods. Each sample was analysed in triplicate.

**2.3.1. Stomacher Method.** Samples (2 g) were weighed, mixed with HCl 0.1 M (15 mL), and subsequently homogenized in a stomacher (Stomacher 400, Lab-Blender, Barcelona, Spain) for 4 min, as described by Jiménez-Martín et al. [10]. From the stomacher bag, 2 mL was transferred to a safe-lock micro test tube and centrifuged (10000 rpm) (Eppendorf Centrifuges, model 5810R) for 15 minutes at 4 °C. The supernatant was stored at –80 °C until analysis.

**2.3.2. Mixer Mill Method.** Ground samples (0.2 g) were homogenized with HCl 0.1 M (1.5 mL) and three stainless steel balls (2 mm of diameter) in the mixer mill (MM400, Retsch technology, Haan, Germany) during 2 min and centrifuged (10000 rpm, 15 min, 4 °C). After then, the supernatant was stored at –80 °C until analysis.

**2.4. Deproteinization and Derivatization.** To deproteinize the sample, 250  $\mu\text{L}$  of acetonitrile was mixed with 100  $\mu\text{L}$  of the extract in safe-lock micro test tube and centrifuged at 10000 rpm for 3 min. 100  $\mu\text{L}$  of the supernatant was transferred to heat-resistant tubes and 100  $\mu\text{L}$  of IS solution ( $5 \mu\text{g mL}^{-1}$ ) was added. Then, tubes were dried under nitrogen. The residual water was removed adding 50  $\mu\text{L}$  of dichloromethane to the dried samples and again evaporated under nitrogen. Finally, 50  $\mu\text{L}$  of MTBSTFA and 50  $\mu\text{L}$  of acetonitrile were added to the dried tubes, which were shaken and subsequently incubated at  $100^\circ\text{C}$  for 60 min to induce the derivatization reaction to occur. Then, tubes were stored at refrigeration and analyzed by GC-MS within the next 24 hours.

**2.5. Instrumentation.** The chromatographic analysis was carried out in a GC equipment 5890 series II (Hewlett-Packard, Barcelona, Spain) coupled to a mass selective detector (MSD) electron impact (EI), model 5973 (Agilent, Barcelona, Spain). A  $1 \mu\text{L}$  portion of the derivatized extract was injected in splitless mode onto the column. The column used was a  $50 \text{ m} \times 0.32 \text{ mm i.d.}, 1.05 \mu\text{m}$ , HP-5 (Hewlett-Packard), being a 5% phenyl-methyl polysiloxane bonded phase fused silica capillary column. Column head pressure was 12.8 psi, resulting in a flow of  $1.2 \text{ mL/min}$  at  $280^\circ\text{C}$ . The oven program was as follows:  $170^\circ\text{C}$  for 5 min,  $4^\circ\text{C/min}$  ramp to  $200^\circ\text{C}$ , held at  $200^\circ\text{C}$  for 3 min,  $4^\circ\text{C/min}$  ramp to  $290^\circ\text{C}$ , held at  $290^\circ\text{C}$  for 1 min,  $20^\circ\text{C/min}$  ramp to a final temperature of  $325^\circ\text{C}$ , and held for 15 min. The transfer line to the mass spectrometer program was as follows:  $280^\circ\text{C}$  for 35 min,  $10^\circ\text{C/min}$  ramp to  $320^\circ\text{C}$ . Total run time was 55.75 min. Free amino acids were identified both by their retention time and by comparison of their characteristic  $m/z$  ions with those published in the literature [9, 10]. The quantification was carried out in the selected ion monitoring (SIM) mode. Table 1 shows retention time (Rt), ions selected in SIM mode, and the selected ion for quantification of each amino acid in this study. A calibration curve (quantification ion AA peak area/quantification ion IS peak area versus AA amount/IS amount) was constructed, obtaining  $R^2$  values of 0.9999. The final results, expressed in microgram per 100 gram sample dry weight, take into account the moisture content and the exact weight of the sample.

**2.6. Standard and Calibration Curves.** A standard calibration solution containing  $200 \mu\text{g mL}^{-1}$  for each AA was prepared (0.5 g of each amino acid was dissolved in 250 mL of HCl 0.1 M). From this solution, seven decreasing dilutions were made (150, 100, 50, 25, 10, 5, and  $1 \mu\text{g mL}^{-1}$ ). A stock solution of IS at  $5 \mu\text{g mL}^{-1}$  was prepared in 0.1 M HCl.

**2.7. Quality Control.** Quality control of the GC-MS analysis was performed through the routine analysis of procedural blanks and quality control standards and samples to ensure the absence of contaminants and the possible carryover between samples and to assess the quality of the results. Limit of detection (LOD) and quantification (LOQ) based on a signal/noise ratio of 3:1 and 10:1, respectively, were determined using aqueous standard solutions ( $n = 5$ ) with the following equations:  $\text{LOD} = 3\text{SD}/b$  and  $\text{LOQ} = 10\text{SD}/b$ ,

TABLE 1: Ions selected in SIM mode (quantification ions in bold) and retention time (Rt) for the analysis of free amino acids.

Aminoacid	Rt (min)	Ions ( $m/z$ )
Alanine	12.86	<b>158</b> , 260, 232
Glycine	13.37	<b>218</b> , 246
Valine	16.60	<b>186</b> , 288, 260
Leucine	17.89	<b>200</b> , 302, 274
Isoleucine	18.98	<b>200</b> , 302, 274
Norleucine (IS)	19.45	<b>200</b> , 147, 274
Proline	20.38	<b>184</b> , 286, 258
Methionine	26.20	<b>218</b> , 320, 292
Serine	26.76	<b>362</b> , 390
Threonine	27.69	<b>404</b> , 376, 303
Phenylalanine	29.56	<b>336</b> , 302, 234
Aspartic acid	30.98	<b>316</b> , 418, 390
Hydroxyproline	31.78	<b>388</b> , 416, 314
Cysteine	32.35	<b>406</b> , 378
Glutamic acid	33.73	<b>432</b> , 330, 272
Asparagine	34.54	<b>417</b> , 302
Lysine	36.14	<b>300</b> , 431, 329
Glutamine	37.14	<b>329</b> , 431, 357, 338
Arginine	38.48	<b>442</b> , 340
Histidine	40.49	<b>196</b> , 489, 440, 338
Tyrosine	41.09	<b>466</b> , 438, 364, 302
Tryptophan	45.10	<b>244</b> , 489, 302
Cystine	50.18	<b>639</b> , 589, 537, 348

where, for each free amino acid, SD is the standard deviation of the average of the signal obtained for the calibration solution of lowest concentration ( $0.1 \text{ mg}/100 \text{ mL}$ ) and  $b$  is the slope of the analytical curve calculated with the calibration solutions. For calculating the relative standard deviation (RSD) run-to-run, five replicate analyses of samples were done. In these determinations, ions were selected in SIM mode.

In order to study the recovery for each AA, loin and dry-cured ham samples were spiked with appropriate amounts of AA ( $7.5\text{--}40 \mu\text{g}$ ) each and were extracted using  $S$  and  $M$  methods. Moreover, the recovery was also calculated in unspiked samples, using the aqueous standard solutions.

**2.8. Statistical Analysis.** The effect of the extraction method on total chromatographic area as well as on the content of each detected amino acid was analysed by the Student's  $t$ -test for independent samples. Linear regression analysis was carried out in order to compare the response of the different homogenization tools. The SPSS package (v 18.0) was used.

### 3. Results and Discussion

**3.1. Evaluation of the Mixer Mill as Homogenization Tool for Free Amino Acid Extraction.** The chromatographic areas of each free amino acid detected in fresh loin and dry-cured ham samples homogenized by using  $S$  and  $M$  are shown in Figure 1. Most AA showed no statistical differences in

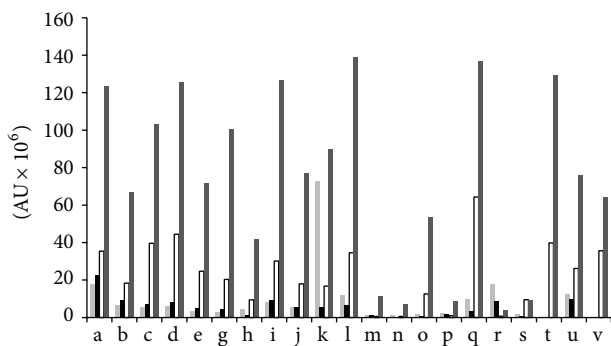


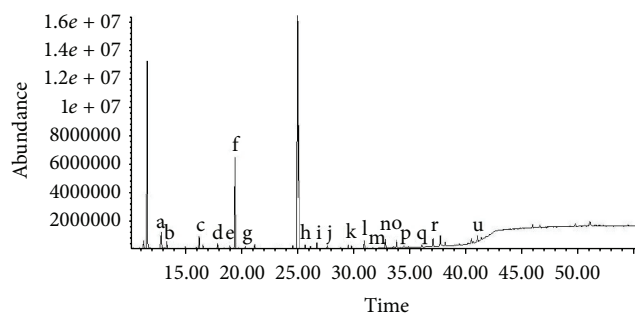
FIGURE 1: Area units (AU) of chromatographic area of each free amino acid detected in fresh loin and dry-cured ham samples by using stomacher (light grey and white, resp.) and mixer mill (black and dark grey, resp.) as homogenization tools. Alanine (a), glycine (b), valine (c), leucine (d), isoleucine (e), proline (g), methionine (h), serine (i), threonine (j), phenylalanine (k), aspartic acid (l), hydroxyproline (m), cystine (n), glutamic acid (o), asparagine (p), lysine (q), glutamine (r), arginine (s), histidine (t), tyrosine (u), and tryptophan (v).

fresh loin between *S* and *M*, whereas in dry-cured hams chromatographic areas of free amino acids were significantly higher ( $P < 0.05$ ) when using *M* than *S* for extraction.

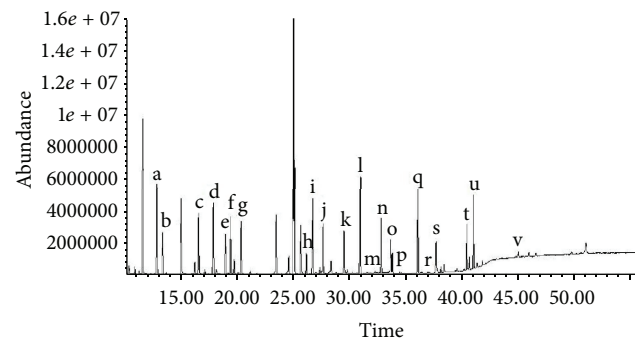
Figure 2 shows a GC-MS chromatogram of the free amino acids detected in fresh loin (Figure 2(a)) and dry-cured ham (Figure 2(b)) when using *M*. Twenty-one free amino acids were detected in dry-cured samples: alanine, glycine, valine, leucine, isoleucine, proline, methionine, serine, threonine, phenylalanine, aspartic acid, hydroxyproline, cysteine, glutamic acid, asparagine, lysine, glutamine, arginine, histidine, tyrosine, and tryptophan, while fresh loin samples presented 18 free amino acids, the same as dry-cured hams except for arginine, histidine, and tryptophan.

Results on free amino acid content in fresh and dry-cured hams using *S* and *M* homogenization tools are shown in Table 2. As expected, most amino acids showed a higher content in dry-cured ham than in fresh loin, which is in agreement with previous results [10]. This can be ascribed to the longer time during which the proteolytic activity takes place in the processing of the hams [4, 8, 9].

Content of most amino acids from fresh loin did not show statistical differences between *S* and *M*, and nor did the sum of total amino acids. However, hydroxyproline and glutamic acid were only detected when using *M*. In addition, the profile of free amino acid did not vary with the homogenization method. Major free amino acids in loins were glutamine (148.33 and 153.93 mg/100 g sample dry matter in *S* and *M*, resp.), cysteine (100.99 and 103.71 mg per 100 g sample dry matter in *S* and *M*, resp.), while leucine (12.22 and 11.77 mg per 100 g simple dry matter in *S* and *M*, resp.), isoleucine (11.30 and 10.75 mg per 100 g simple dry matter in *S* and *M*, resp.), hydroxyproline (nondetected and 10.24 mg per 100 g simple dry matter in *S* and *M*, resp.), and valine (11.20 and 8.80 mg per 100 g simple dry matter in *S* and *M*, resp.) showed the lowest content. The levels of the other amino acids detected in fresh loin were between 29 and 69 mg



(a)



(b)

FIGURE 2: Chromatogram of free amino acids detected in fresh loin (a) and dry-cured ham (b) samples. Alanine (a), glycine (b), valine (c), leucine (d), isoleucine (e), norleucine (f, internal standard), proline (g), methionine (h), serine (i), threonine (j), phenylalanine (k), aspartic acid (l), hydroxyproline (m), cystine (n), glutamic acid (o), asparagine (p), lysine (q), glutamine (r), arginine (s), histidine (t), tyrosine (u), and tryptophan (v).

per 100 g sample dry matter. These results are in agreement with previous findings. Glutamine has been described as the major amino acid in fresh meat [27, 28]. In relation to the tryptophan, it has been detected in low concentration in fresh meat [29]. According to results found by Jiménez-Martín et al. [10], glutamic acid is the major amino acid in fresh pork, followed by glutamine, cysteine, and phenylalanine.

In dry-cured ham samples, most amino acids detected and the sum of total amino acids showed higher content when using *M* for extraction as compared to *S*. The *M* procedure could break more effectively the meat gel structure formed during the processing of the dry-cured hams than the *S* one. In fact, other authors [29, 30] observed a difficulty of protein extraction during the processing of Iberian hams, even using solutions with high ionic strength for their extraction. The observed suitability of the *M* in the extraction procedures for the analyses of these compounds could be related to the combined movement of the grinding jars with the balls, which results in an intensive mixing of the ham sample with the solvent.

The obtained results highlight the accuracy of the *M* homogenization tool, which is crucial in the case of samples containing high amino acid content, as dry-cured hams do. This is in concordance with results found by Segura and

TABLE 2: Amino acid content (mg per 100 g sample dry matter) extracted from fresh loin and dry-cured ham samples by using two extraction procedures, with stomacher (*S*) and mixer mill (*M*).

	Fresh loin			Dry-cured ham			<i>P</i> (fresh loin versus dry-cured ham)
	<i>S</i>	<i>M</i>	<i>P</i>	<i>S</i>	<i>M</i>	<i>P</i>	
Alanine	41.82 ± 15.38	52.43 ± 19.48	0.500	234.86 ± 31.25	307.04 ± 22.74	0.032	<0.001
Glycine	<LOQ.	<LOQ.	—	69.49 ± 11.51	113.69 ± 10.23	0.008	<0.001
Valine	11.20 ± 1.63	8.80 ± 3.04	0.295	177.39 ± 28.43	242.10 ± 5.44	0.018	<0.001
Leucine	12.22 ± 2.10	11.77 ± 2.06	0.806	181.12 ± 29.86	254.25 ± 4.47	0.014	<0.001
Isoleucine	11.30 ± 1.45	10.75 ± 1.81	0.705	130.22 ± 20.76	174.52 ± 2.58	0.021	<0.001
Proline	36.74 ± 1.12	29.64 ± 0.97	0.001	186.77 ± 24.13	244.28 ± 15.73	0.026	<0.001
Methionine	29.38 ± 2.94	30.26 ± 9.03	0.881	77.04 ± 11.38	99.87 ± 0.41	0.026	<0.001
Serine	30.40 ± 1.46	27.98 ± 1.41	0.108	156.65 ± 30.08	244.85 ± 21.07	0.014	<0.001
Threonine	32.84 ± 2.87	37.13 ± 10.87	0.545	293.38 ± 66.02	488.86 ± 31.09	0.010	<0.001
Phenylalanine	28.23 ± 0.96	27.48 ± 4.83	0.804	118.40 ± 20.92	172.00 ± 2.26	0.012	<0.001
Aspartic acid	43.67 ± 4.24	43.43 ± 6.56	0.960	201.95 ± 38.71	281.37 ± 11.33	0.027	<0.001
Hydroxyproline	n.d.	10.24 ± 2.34	0.002	17.45 ± 1.17	20.48 ± 2.01	0.087	<0.001
Cysteine	100.99 ± 22.64	103.71 ± 26.27	0.898	154.55 ± 29.13	206.79 ± 23.52	0.073	0.001
Glutamic acid	n.d.	42.28 ± 2.86	<0.001	352.89 ± 80.64	520.02 ± 11.65	0.024	<0.001
Asparagine	56.75 ± 1.06	44.28 ± 2.10	0.001	47.83 ± 2.29	37.09 ± 0.90	0.002	0.059
Lysine	69.53 ± 8.15	48.94 ± 3.35	0.016	356.36 ± 91.72	554.92 ± 109.00	0.073	<0.001
Glutamine	148.33 ± 21.24	153.93 ± 28.16	0.797	69.34 ± 1.12	54.27 ± 0.90	<0.001	<0.001
Arginine	n.d.	n.d.	—	130.22 ± 8.08	224.19 ± 4.81	<0.001	<0.001
Histidine	n.d.	n.d.	—	119.13 ± 5.96	145.60 ± 7.29	0.008	<0.001
Tyrosine	66.39 ± 12.21	46.71 ± 6.01	0.066	91.05 ± 12.70	119.52 ± 2.73	0.019	<0.001
Tryptophan	n.d.	n.d.	—	26.82 ± 7.49	207.58 ± 3.76	<0.001	—
Cystine	n.d.	n.d.	—	n.d.	n.d.	—	—

LOQ: limit of quantification.

n.d.: not detected.

Lopez-Bote [25], who tested the mixer mill for the extraction of intramuscular fat. These authors noticed that the higher extracting ability of the mixer mill was more evident in samples with high levels of intramuscular fat rather than in low lipid content ones.

In spite of the influence of the homogenization tool on the free amino acid content in dry-cured hams, the overall profile of amino acids was similar with *M* and *S* extraction methods. Glutamic acid (352.89 and 520.02 mg per 100 g sample dry matter in *S* and *M*, resp.) and lysine (356.36 and 554.91 mg per 100 g sample dry matter in *S* and *M*, resp.) were the major amino acids in dry-cured ham samples, with hydroxyproline (14.45 and 20.48 mg per 100 g sample dry in *S* and *M*, matter, resp.) and asparagine (47.83 and 37.09 mg per 100 g sample dry in *S* and *M*, matter, resp.) being the minor ones. The content of the other amino acids in dry-cured ham was between 54 and 307 mg per 100 g sample dry matter. Previous research on dry-cured ham showed similar results [4, 8–10]. Nevertheless, considering results from different works, it can be noticed a high variability in the content of some amino acids from hams; that is, Jurado et al. [7] found higher content of glutamic acid (1269 mg per 100 g sample dry matter) than Martín et al. [4] (650 mg per 100 g sample dry matter), Pérez-Palacios et al. [9] (271 mg per 100 g sample dry matter), and Jiménez-Martín et al. [10] (271 mg per 100 g sample dry matter). These differences may be ascribed to the

different processing of hams (salting time, temperature, and moisture conditions). Moreover, several factors may affect aminopeptidase activity during dry-cured ham processing, such as sodium chloride, which is a potent inhibitor for these enzymes [31]. In addition, the water loss and the subsequent reduction in water activity that takes place during dry-cured ham processing also influence the proteolytic activity [32]. Free amino acid accumulation has a feedback effect, reducing aminopeptidase activity [33]. Finally, the variability in the content of free amino acids among works can be also related to the differences in the extraction method. In fact, this work shows significant differences in the content of amino acids of the same samples analyzed under the same conditions, except for the procedure of the extraction method.

Correlation analysis between amino acid content obtained using the *S* and *M* extraction methods was carried out in order to compare the response of two methodologies. Table 3 shows regression equations and coefficient of determination for each amino acid detected. It can be observed that the response is linear for all amino acids ( $R^2 = 0.741$ – $0.998$ ), suggesting that the validity of the *M* homogenization tool is similar to that of *S* one, which has been previously validated [10].

Amount of sample and volume of solvent used and time consumed are notable aspects to take into account when comparing methodologies. At this respect, time analysis,

TABLE 3: Regression equations and coefficient of determination ( $R^2$ ) between the content of each amino acid extracted with stomacher (S) and mixer mill (M) as homogenization tools.

Aminoacid	Regression equation	$R^2$
Alanine	$y_M = 1.2674x_S + 4.4005$	0.946
Glycine	$y_M = 1.5921x_S + 1.5241$	0.971
Valine	$y_M = 1.3580x_S - 2.6046$	0.971
Leucine	$y_M = 1.3769x_S - 0.0915$	0.958
Isoleucine	$y_M = 1.3245x_S - 1.0850$	0.962
Proline	$y_M = 1.3859x_S - 17.9915$	0.965
Methionine	$y_M = 1.3385x_S - 6.1658$	0.888
Serine	$y_M = 1.6283x_S - 15.8795$	0.955
Threonine	$y_M = 1.6032x_S - 1.4932$	0.922
Phenylalanine	$y_M = 1.4914x_S - 9.6092$	0.926
Aspartic acid	$y_M = 1.4050x_S - 10.1634$	0.941
Hydroxyproline	$y_M = 0.5893x_S + 10.2204$	0.905
Cysteine	$y_M = 1.4952x_S - 37.4279$	0.741
Glutamic acid	$y_M = 1.2701x_S + 57.0415$	0.941
Asparagine	$y_M = 0.8251x_S - 2.7964$	0.841
Lysine	$y_M = 1.5545x_S - 29.1033$	0.832
Glutamine	$y_M = 1.2664x_S - 33.7431$	0.998
Arginine	$y_M = 1.7126x_S + 0.5797$	0.994
Histidine	$y_M = 1.2203x_S + 0.1130$	0.997
Tyrosine	$y_M = 1.9083x_S - 72.6416$	0.851
Tryptophan	$y_M = 7.0101x_S + 9.7883$	0.905

TABLE 4: Estimation of analysis time, amount of sample, and solvent volume for the extraction of free amino acids in twenty samples by using stomacher (S) and mixer mill (M).

	S	M
Time (min)	80	2
Sample (g)	40	4
Solvent volume (mL)	300	30

sample quantity, and solvent volume for the extraction of free amino acids in twenty samples by using S and M homogenization tools were estimated (Table 4). M takes less time and requires lower amount of sample and solvent than S (2 versus 80 min, 4 versus 40 g, and 30 versus 300 mL, resp.).

The observed ability of the M method in the homogenization process for extraction of free amino acids in meat samples, reducing notably sample and solvent amount as well as time consuming, makes it appropriate for routine analysis.

**3.2. Quality Control.** The performance of the GC-MS method was examined by determining quality parameters for each individual amino acid. Good linearity was obtained for the range 1–100  $\mu\text{g mL}^{-1}$  for the 22 standard amino acids. The correlation coefficients were  $>0.90$ , except for tryptophan ( $R^2 = 0.837$ ). Most amino acids showed a poor linearity above 150  $\mu\text{g mL}^{-1}$ ; thus, curve point at this concentration or higher was avoided. A similar behaviour was reported previously [10]. LOD and LOQ of the analytical procedure ranged from

TABLE 5: Recoveries (%) in aqueous standard solution (ASS) and in spiked samples extracted by using stomacher (S) and mixer mill (M).

	ASS	Fresh loin		Dry-cured ham	
		S	M	S	M
Alanine	94.49	65.45	82.04	69.13	104.94
Glycine	99.17	69.95	98.94	85.96	90.99
Valine	96.96	91.10	71.62	71.83	104.71
Leucine	96.62	83.78	80.73	69.82	98.01
Isoleucine	97.72	87.70	83.46	71.13	98.35
Proline	105.75	90.45	78.62	72.20	102.96
Methionine	99.97	72.24	74.38	74.95	99.65
Serine	98.33	96.48	88.81	61.47	97.58
Threonine	95.99	66.45	75.13	54.97	94.74
Phenylalanine	99.90	85.49	83.21	68.14	98.79
Aspartic acid	102.18	85.70	101.23	73.05	95.66
Hydroxyproline	97.90	54.63	82.80	40.41	88.84
Cysteine	102.52	80.12	82.28	69.12	100.45
Glutamic acid	102.27	77.27	103.47	82.24	98.75
Asparagine	105.38	91.76	77.05	91.16	93.79
Lysine	104.34	91.53	64.44	57.43	92.89
Glutamine	100.78	79.56	82.56	90.66	85.62
Arginine	102.76	92.47	78.43	54.80	97.67
Histidine	104.79	90.27	74.04	85.52	98.60
Tyrosine	102.02	84.13	89.19	81.99	88.73
Tryptophan	95.06	93.14	87.74	79.39	98.14
Cystine	106.87	88.21	99.31	84.29	92.69

$3.8 \cdot 10^{-4}$ – $6.6 \cdot 10^{-4}$   $\mu\text{g } \mu\text{L}^{-1}$  to  $1.3 \cdot 10^{-3}$ – $2.2 \cdot 10^{-2}$   $\mu\text{g } \mu\text{L}^{-1}$ , respectively, for alanine, glycine, valine, leucine, isoleucine, proline, methionine, serine, threonine, phenylalanine, aspartic acid, histidine, and tyrosine. For glutamine, asparagine, lysine, glutamic acid, tryptophan, and cysteine these values were around 0.02–0.2  $\mu\text{g } \mu\text{L}^{-1}$  and 0.07–0.66  $\mu\text{g } \mu\text{L}^{-1}$  for LOD and LOQ, respectively. These results are quite in concordance with previous studies [10, 24]. Hydroxyproline and cysteine had higher values for LOD (0.38 and 1.27  $\mu\text{g } \mu\text{L}^{-1}$ , resp.) and LOQ (0.98 and 2.98  $\mu\text{g } \mu\text{L}^{-1}$ , resp.). In fact, previous studies using RP-HPLC-DAD for analyzing amino acids from dry-cured hams did not allow the detection of hydroxyproline and cysteine [8]. Adequate precision was achieved with a RSD of 2.15–20.15% for run-to-run.

Table 5 shows the recovery of AA in aqueous standard solution and in spiked samples (loin and dry-cured ham) extracted by using both S and M extraction methods. In aqueous standard solution all AA showed high recoveries (94.49–105.75%), indicating the accuracy of the chromatographic procedure. In the samples, most AA showed higher recoveries when using the M method for the extraction in comparison to the S one, especially in dry-cured ham. This result points out the suitability of the mixer mill for the extraction of AA and it is in concordance with other studies in AA from meat samples [34].

## 4. Conclusions

The mixer mill is an appropriate tool for the homogenization step in the extraction procedure of free amino acids from meat samples, especially in samples with high free amino acids content. In addition, this technique notably reduces sample amount and solvent volume as well as analysis time. Thus, it could be an adequate option for routine analysis of free AA in meat and meat products.

## Conflict of Interests

The authors declare that there is no conflict of interests regarding the publication of this paper.

## Acknowledgments

This study was supported by the CONSOLIDER-Ingenio 2010 project (CARNISENUSA, Comisión Interministerial de Ciencia y Tecnología) and by the Gobierno de Extremadura (GR10180).

## References

- [1] N. Barylko-Pikielna and E. Kostyra, "Sensory interaction of umami substances with model food matrices and its hedonic effect," *Food Quality and Preference*, vol. 18, no. 5, pp. 751–758, 2007.
- [2] P.-D. Chiang, C.-T. Yen, and J.-L. Mau, "Non-volatile taste components of various broth cubes," *Food Chemistry*, vol. 101, no. 3, pp. 932–937, 2006.
- [3] J. Ruiz, C. García, M. D. Carmen Díaz, R. Cava, J. Florencio Tejada, and J. Ventanas, "Dry cured iberian ham non-volatile components as affected by the length of the curing process," *Food Research International*, vol. 32, no. 9, pp. 643–651, 1999.
- [4] L. Martín, T. Antequera, J. Ventanas, R. Benítez-Donoso, and J. J. Córdoba, "Free amino acids and other non-volatile compounds formed during processing of Iberian ham," *Meat Science*, vol. 59, no. 4, pp. 363–368, 2001.
- [5] A. I. Carrapiso, J. Ventanas, and C. García, "Characterization of the most odor-active compounds of Iberian ham headspace," *Journal of Agricultural and Food Chemistry*, vol. 50, no. 7, pp. 1996–2000, 2002.
- [6] F. Toldrá, "Meat: chemistry and biochemistry," in *Handbook of Food Science, Technology and Engineering*, Y. H. Hui, Ed., pp. 1–18, CRC Press, Boca Raton, Fla, USA, 2006.
- [7] Á. Jurado, C. García, M. L. Timón, and A. I. Carrapiso, "Effect of ripening time and rearing system on amino acid-related flavour compounds of Iberian ham," *Meat Science*, vol. 75, no. 4, pp. 585–594, 2007.
- [8] J. J. Córdoba, T. Antequera Rojas, C. G. González, J. V. Barroso, C. L. Bote, and M. A. Asensio, "Evolution of free amino acids and amines during ripening of Iberian cured ham," *Journal of Agricultural and Food Chemistry*, vol. 42, no. 10, pp. 2296–2301, 1994.
- [9] T. Pérez-Palacios, J. Ruiz, J. M. Barat, M. C. Aristoy, and T. Antequera, "Influence of pre-cure freezing of Iberian ham on proteolytic changes throughout the ripening process," *Meat Science*, vol. 85, no. 1, pp. 121–126, 2010.
- [10] E. Jiménez-Martín, J. Ruiz, T. Pérez-Palacios, A. Silva, and T. Antequera, "Gas chromatography-mass spectrometry method for the determination of free amino acids as their dimethyl-*tert*-butylsilyl (TBDMS) derivatives in animal source food," *Journal of Agricultural and Food Chemistry*, vol. 60, no. 10, pp. 2456–2463, 2012.
- [11] M. W. Duncan and A. Poljak, "Amino acids analysis of peptides and proteins on the femtomole scale by gas chromatography/mass spectrometry," *Analytical Chemistry*, vol. 70, no. 5, pp. 890–896, 1998.
- [12] B. M. Silva, S. Casal, P. B. Andrade, R. M. Seabra, M. B. Oliveira, and M. A. Ferreira, "Development and evaluation of a GC/FID method for the analysis of free amino acids in quince fruit and jam," *Analytical Sciences*, vol. 19, no. 9, pp. 1285–1290, 2003.
- [13] C. W. Gehrke and K. Leimer, "Trimethylsilylation of amino acids derivatization and chromatography," *Journal of Chromatography A*, vol. 57, pp. 219–238, 1971.
- [14] H. J. Chaves das Neves and A. M. P. Vasconcelos, "Capillary gas chromatography of amino acids, including asparagine and glutamine: sensitive gas chromatographic-mass spectrometric and selected ion monitoring gas chromatographic-mass spectrometric detection of the N,O(S)-*tert*-butyldimethylsilyl derivatives," *Journal of Chromatography*, vol. 392, pp. 249–258, 1987.
- [15] T. G. Sobolevsky, A. I. Revelsky, B. Miller, V. Oriedo, E. S. Chernetsova, and I. A. Revelsky, "Comparison of silylation and esterification/acetylation procedures in GC-MS analysis of amino acids," *Journal of Separation Science*, vol. 26, no. 17, pp. 1474–1478, 2003.
- [16] N. Erkan and Ö. Özden, "The changes of fatty acid and amino acid compositions in sea bream (*Sparus aurata*) during irradiation process," *Radiation Physics and Chemistry*, vol. 76, no. 10, pp. 1636–1641, 2007.
- [17] M. Erbas, M. F. Ertugay, M. Ö. Erbas, and M. Certel, "The effect of fermentation and storage on free amino acids of tarhana," *International Journal of Food Sciences and Nutrition*, vol. 56, no. 5, pp. 349–358, 2005.
- [18] A. Becalski, B. P.-Y. Lau, D. Lewis et al., "Acrylamide in French fries: influence of free amino acids and sugars," *Journal of Agricultural and Food Chemistry*, vol. 52, no. 12, pp. 3801–3807, 2004.
- [19] O. Pinho, I. M. P. L. V. O. Ferreira, E. Mendes, B. M. Oliveira, and M. Ferreira, "Effect of temperature on evolution of free amino acid and biogenic amine contents during storage of Azeitão cheese," *Food Chemistry*, vol. 75, no. 3, pp. 287–291, 2001.
- [20] R. Pätzold and H. Brückner, "Gas chromatographic determination and mechanism of formation of D-amino acids occurring in fermented and roasted cocoa beans, cocoa powder, chocolate and cocoa shell," *Amino Acids*, vol. 31, no. 1, pp. 63–72, 2006.
- [21] A. Mustafa, P. Åman, R. Andersson, and A. Kamal-Eldin, "Analysis of free amino acids in cereal products," *Food Chemistry*, vol. 105, no. 1, pp. 317–324, 2007.
- [22] V. Gökmen, A. Serpen, and B. A. Mogol, "Rapid determination of amino acids in foods by hydrophilic interaction liquid chromatography coupled to high-resolution mass spectrometry," *Analytical and Bioanalytical Chemistry*, vol. 403, no. 10, pp. 2915–2922, 2012.
- [23] M. S. Nimbalkar, S. R. Pai, N. V. Pawar, D. Oulkar, and G. B. Dixit, "Free amino acid profiling in grain Amaranth using LC-MS/MS," *Food Chemistry*, vol. 134, no. 4, pp. 2565–2569, 2012.
- [24] T. Pérez-Palacios, A. Melo, S. Cunha, and I. M. P. L. V. O. Ferreira, "Determination of free amino acids in coated foods by GC-MS: optimization of the extraction procedure by using

- statistical design,” *Food Analytical Methods*, vol. 7, no. 1, pp. 172–180, 2014.
- [25] J. Segura and C. J. Lopez-Bote, “A laboratory efficient method for intramuscular fat analysis,” *Food Chemistry*, vol. 145, pp. 821–825, 2014.
- [26] Association of Official Analytical Chemists (AOAC), *Official Methods of Analysis*, AOAC International, Arlington, Va, USA, 2000.
- [27] M. Cornet and J. Bousset, “Free amino acids and dipeptides in porcine muscles: differences between ‘red’ and ‘white’ muscles,” *Meat Science*, vol. 51, no. 3, pp. 215–219, 1999.
- [28] M.-C. Aristoy and F. Toldra, “Deproteinization techniques for HPLC amino acid analysis in fresh pork muscle and dry-cured ham,” *Journal of Agricultural and Food Chemistry*, vol. 39, no. 10, pp. 1792–1795, 1991.
- [29] J. J. Córdoba, T. Antequera, J. Ventanas, C. López-Bote, C. García, and M. A. Asensio, “Hydrolysis and loss of extractability of proteins during ripening of iberian ham,” *Meat Science*, vol. 37, no. 2, pp. 217–227, 1994.
- [30] C. G. Zarkadas, C. N. Karatzas, A. D. Khalili, S. Khanizadeh, and G. Morin, “Quantitative determination of the myofibrillar proteins and connective tissue content in selected porcine skeletal muscles,” *Journal of Agricultural and Food Chemistry*, vol. 36, no. 6, pp. 1131–1146, 1988.
- [31] M. Flores, M.-C. Aristoy, A. M. Spanier, and F. Toldrá, “Non-volatile components effects on quality of ‘Serrano’ dry-cured ham as related to processing time,” *Journal of Food Science*, vol. 62, no. 6, pp. 1235–1239, 1997.
- [32] F. Toldrá, E. Rico, and J. Flores, “Activities of pork muscle proteases in model cured meat systems,” *Biochimie*, vol. 74, no. 3, pp. 291–296, 1992.
- [33] M. Flores, M.-C. Aristoy, and F. Toldrá, “Feedback inhibition of porcine muscle alanyl and arginyl aminopeptidases in cured meat products,” *Journal of Agricultural and Food Chemistry*, vol. 46, no. 12, pp. 4982–4986, 1998.
- [34] A. Leggio, E. L. Belsito, R. De Marco, A. Liguori, C. Siciliano, and M. Spinella, “Simultaneous extraction and derivatization of amino acids and free fatty acids in meat products,” *Journal of Chromatography A*, vol. 1241, pp. 96–102, 2012.

## Research Article

# An Optimized High Throughput Clean-Up Method Using Mixed-Mode SPE Plate for the Analysis of Free Arachidonic Acid in Plasma by LC-MS/MS

Wan Wang,<sup>1</sup> Suzi Qin,<sup>2</sup> Linsen Li,<sup>2</sup> Xiaohua Chen,<sup>2</sup> Qunjie Wang,<sup>2</sup> and Junfu Wei<sup>3</sup>

<sup>1</sup>School of Material Science and Engineering, Tianjin Polytechnic University, Tianjin 300387, China

<sup>2</sup>Bonna-Agela Technologies, Tianjin 300462, China

<sup>3</sup>School of Environment & Chemical Engineering, Tianjin Polytechnic University, Tianjin 300387, China

Correspondence should be addressed to Junfu Wei; [jfwei@tjpu.edu.cn](mailto:jfwei@tjpu.edu.cn)

Received 16 October 2014; Revised 2 December 2014; Accepted 20 December 2014

Academic Editor: Shahram Seidi

Copyright © 2015 Wan Wang et al. This is an open access article distributed under the Creative Commons Attribution License, which permits unrestricted use, distribution, and reproduction in any medium, provided the original work is properly cited.

A high throughput sample preparation method was developed utilizing mixed-mode solid phase extraction (SPE) in 96-well plate format for the determination of free arachidonic acid in plasma by LC-MS/MS. Plasma was mixed with 3% aqueous ammonia and loaded into each well of 96-well plate. After washing with water and methanol sequentially, 3% of formic acid in acetonitrile was used to elute arachidonic acid. The collected fraction was injected onto a reversed phase column at 30°C with mobile phase of acetonitrile/water (70:30, v/v) and detected by LC-MS/MS coupled with electrospray ionization (ESI) in multiple reaction monitoring (MRM) mode. The calibration curve ranged from 10 to 2500 ng/mL with sufficient linearity ( $r^2 = 0.9999$ ). The recoveries were in the range of 99.38% to 103.21% with RSD less than 6%. The limit of detection is 3 ng/mL.

## 1. Introduction

Arachidonic acid is a  $\omega$ -6 long chain polyunsaturated fatty acid, a senior unsaturated fatty acid. There is high content of free arachidonic acid in the human body which usually comes from dietary animal sources—meat, eggs, and dairy—or is converted from linoleic acid. Arachidonic acid and its metabolites have a strong biological activity and can regulate a wide variety of physiological processes, such as the regulation of lipid and glucose, prevention of cardiovascular disease, chemoprevention of cancer cells, and improvement of memory [1–5]. Therefore, it is important to determine the concentration of free arachidonic acid in human plasma for medical research and clinical diagnosis (Figure 1).

There are many methods to detect arachidonic acid in plasma, such as gas chromatography coupled with mass spectrometry, liquid chromatography with precolumn derivation fluorescence detection, and ELISA method [6–10]. However, these methods are either too complicated to operate or lack of good reproducibility. In contrast, LC-MS/MS has been well accepted for the determination of arachidonic acid with

high sensitivity [11–17]. In order to detect arachidonic acid in plasma by LC-MS/MS, the samples have to be pretreated to remove interferences which may result in matrix effect on mass spectrometry [18–21]. Although the traditional techniques such as protein precipitation (PPT), liquid-liquid extraction (LLE), and SPE with reversed phase packing material have been reported for clean-up of plasma samples, it is clear that these techniques are insufficient to remove interferences of phospholipids and proteins in plasma [22–24], while the combination of ionic interaction and reversed phase interaction was reported to remove phospholipids and proteins more sufficiently in the clean-up process for plasma samples [25]. Furthermore, the analytical chemists in the field of preclinical researches and routine clinical testing are facing thousands of samples. Therefore, it is necessary to establish a simple, fast, efficient, and high throughput sample clean-up method for LC-MS/MS analysis of numerous samples [26, 27].

The attention of this study was focused on the development of a high throughput and sufficient sample clean-up

TABLE 1: MS parameters.

Analyte	$t_R$ /min	Q1	Q3	DP	CE	IS/V	TEM/°C	GS1/Pa	GS2/Pa	CUR/Pa
Arachidonic acid	3.3	303	259.1	-109	-18	-4500	500	55	35	15
		303	205.1	-107	-20					
Phospholipids	4.1	496.3	184.3	63	20	+5500	600	50	50	15

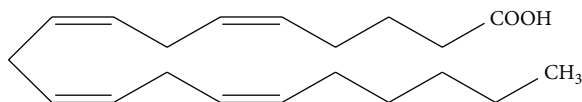


FIGURE 1: Chemical structure of arachidonic acid.

method prior to the analysis of arachidonic acid in plasma by LC-MS/MS. Various sample preparation methods including PPT, LLE, single-mode SPE with nonpolar interaction, and mixed-mode SPE with multiple interaction were studied. The matrix effect of both phospholipids and proteins on the recovery of arachidonic acid was investigated and the final method was applied for the assay of some human plasma samples.

## 2. Experimental

**2.1. Materials and Reagents.** Arachidonic acid (purity of 99%), formic acid, and ammonia were purchased from Sigma-Aldrich (St. Louis, MO, USA). Methanol, acetonitrile, and ethyl acetate were of HPLC-grade and were purchased from Merck (Darmstadt, Germany). Purified water was produced by a Milli-Q Academic System (Millipore, Billerica, MA, USA). Human plasma samples were obtained from local hospital.

Cleanert PPT 96-well plate, Cleanert collection 96-well plate (2 mL), Cleanert PEP 96-well plate (60 mg/well), and Cleanert MAS-M 96-well plate (60 mg/well) were purchased from Agela Technologies (Wilmington, Delaware, USA).

**2.2. Instrumentation.** Positive pressure SPE manifold, vortex mixer, and centrifuge for 96-well plate were purchased from Agela Technologies (Wilmington, Delaware, USA).

The analysis was accomplished with a Shimadzu LC-20A binary HPLC system with an autoinjector coupled with API4000+ triple quadrupole tandem mass spectrometer (AB SCIEX, MA, USA). AB SCIEX Analyst software (version 1.5.1) was used for data acquisition. The HPLC column was a 3  $\mu$ m, 2.1 mm  $\times$  50 mm Venusil ASB C18 (Agela Technologies) operated at 30°C under an isocratic condition with mobile phase of acetonitrile/water (75 : 25, v/v). Flow rate was 0.2 mL/min and injection volume was 5  $\mu$ L. The target compounds eluted from the HPLC column were introduced directly into the MS source. Electrospray ionization (ESI) with negative ion mode was selected for arachidonic acid and that with positive ion mode was selected for phospholipids, respectively. Quantitative analysis was performed under MRM mode by calculating the peak areas. The optimal MS parameters were listed in Table 1. The ions were detected by multiple reaction monitoring (MRM), monitoring the  $[M + H]^+$  transition of the  $m/z$  precursor ion to the  $m/z$  of the product ion

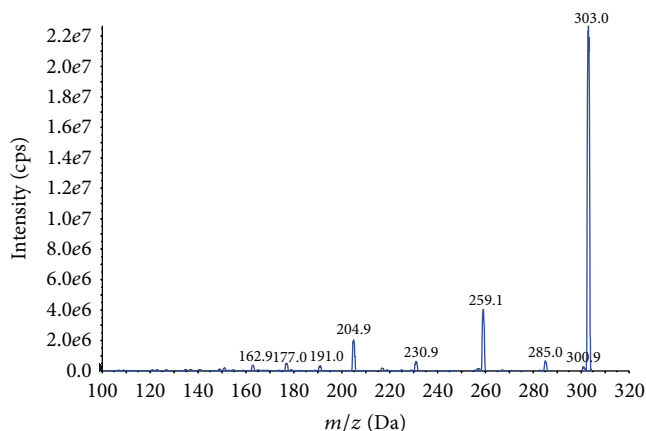


FIGURE 2: Product ion mass spectra of arachidonic acid.

for arachidonic acid. These MS/MS transitions utilized for analysis were  $m/z$  303/259.1 and 303/205.1. An example of the mass spectra of arachidonic acid was shown in Figure 2. A UV detector at 254 nm wavelength was applied for the detection of proteins.

**2.3. Standards and Stock Solutions.** 10 mg of arachidonic acid was dissolved in 100 mL of methanol to prepare a stock solution at 100  $\mu$ g/mL. The stock solution was further diluted with a mixture of acetonitrile : water (70 : 30, v/v) to obtain work solution with the required concentration of arachidonic acid.

**2.4. Sample Pretreatments.** PPT is a widely adopted sample pretreatment for plasma with routine procedures [22], while LLE and single-mode SPE with reversed phase packing material have been reported to pretreat plasma when arachidonic acid was detected [11, 24]. They were compared with Cleanert MAS-M which was a mixed-mode SPE to extract arachidonic acid in plasma. All the procedures for each sample pretreatment method were described as follows.

5 mL of plasma spiked with 50  $\mu$ L of arachidonic acid work solution was mixed by vortex for 30 seconds to get homogenate samples.

**2.4.1. Method A: Protein Precipitation.** 100  $\mu$ L of plasma sample diluted with 100  $\mu$ L of 1% formic acid was loaded into each well of protein precipitation plate followed by 400  $\mu$ L of acetonitrile. The plate was vortexed for 30 sec. After centrifuging at 6000 rpm for 5 min, the plate was set on a positive pressure 96-well plate manifold for eluting the target compound into 96-well collection plate. The eluates were dried at 45°C under a gentle stream of nitrogen. The residues

were reconstituted with 200  $\mu\text{L}$  of acetonitrile : water (70 : 30, v/v) for LC-MS/MS analysis.

**2.4.2. Method B: Liquid-Liquid Extraction.** 100  $\mu\text{L}$  of plasma sample diluted with 100  $\mu\text{L}$  of 1% formic acid was loaded into each well of 96-well collection plate followed by 5  $\mu\text{L}$  of methanol. After 30 sec vortex, 500  $\mu\text{L}$  of ethyl acetate was added to each well of the plate and then vortexed for 3 min. The plate was stood for 1 min and centrifuged at 6000 rpm for 5 min. The supernatants were transferred into a clean collection plate sequentially and were dried at 45°C under a gentle stream of nitrogen. The residues were reconstituted with 200  $\mu\text{L}$  of acetonitrile : water (70 : 30, v/v) for LC-MS/MS analysis.

**2.4.3. Method C: Solid Phase Extraction with Cleanert PEP.** 100  $\mu\text{L}$  of plasma sample diluted with 100  $\mu\text{L}$  of 1% formic acid was loaded into each well of Cleanert PEP, a single-mode SPE plate packed with reversed phase resin. The plate was preconditioned with 1 mL of methanol and 1 mL of water sequentially. 500  $\mu\text{L}$  of methanol : water (5 : 95, v/v) was used to wash each well of the plate. The target compounds were eluted with 2 mL of 5% ammonia in acetonitrile. The eluates were collected into collection plate and further concentrated at 45°C under a gentle stream of nitrogen until dryness. The residues were reconstituted with 200  $\mu\text{L}$  of acetonitrile : water (70 : 30, v/v) for LC-MS/MS analysis.

**2.4.4. Method D: Solid Phase Extraction with Cleanert MAS-M.** 100  $\mu\text{L}$  of plasma sample diluted with 100  $\mu\text{L}$  of 3% ammonium hydroxide was loaded into each well of Cleanert MAS-M, a mixed-mode SPE plate which was preconditioned with 1 mL of methanol and 1 mL of water sequentially. The plate was washed with 500  $\mu\text{L}$  of water followed by 500  $\mu\text{L}$  of methanol. The target compound was eluted with 600  $\mu\text{L}$  of 3% formic acid in acetonitrile and collected into collection plate. The eluates were concentrated at 45°C under a gentle stream of nitrogen until dryness. The residues were reconstituted with 200  $\mu\text{L}$  of acetonitrile : water (70 : 30, v/v) for LC-MS/MS analysis.

### 3. Results

**3.1. Comparison of Sample Pretreatment Methods on the Effect of Eliminating Phospholipids.** It is well known that phospholipids in plasma will result in matrix effect on mass spectrometry [19, 20]. Therefore, it is necessary to remove phospholipids from the samples before injection. Although PPT is a common method for biosample preparation [22], the method is unable to remove the phospholipids from plasma efficiently. As shown in Figure 3 (PPT), the eluate obtained from Method A results in a big phospholipids peak that may influence the analysis of arachidonic acid. Although LLE is a widely used sample preparation method to extract the target compounds from aquatic samples [23], the result of Method B (Figure 3 LLE) indicates that a wide peak of phospholipids appeared. Comparing with LLE, SPE has become a popular sample preparation technique in terms of reproducibility,

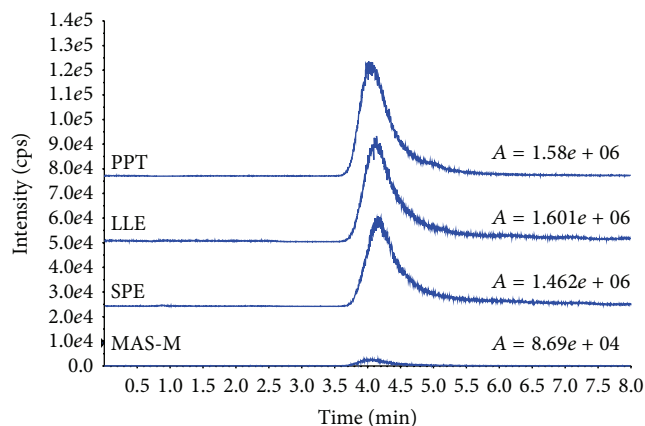


FIGURE 3: Chromatograms and peak areas of phospholipids in plasma treated with various clean-up methods, where "A" = peak area of phospholipids.

less usage of organic solvents, and ease of use. Moreover, SPE is very compatible with an automatic system for high throughput analysis. Arachidonic acid is a hydrophobic compound with Log Kow 7.27; in Method C, therefore, a Cleanert PEP plate packed with nonpolar polymer material was used. However, as shown in Figure 3 (SPE), a broad high peak of phospholipids still remains after SPE clean-up. It is apparent to see from Figure 3 (MAS-M) that Method D is the best one for removing phospholipids from plasma. Cleanert MAS-M plate is packed with mixed resins with nonpolar, anion exchange, and cation exchange interactions. Since the pKa of arachidonic acid is 4.77, it is retained on the plate by both anion exchange and nonpolar interactions while the phospholipids and some proteins are retained on the plate by cation exchange and nonpolar interactions under experiment conditions during sample loading. Water soluble interferences are washed out with water and the nonpolar interferences are removed by methanol. Since the arachidonic acid is adsorbed on the plate by anion interaction, there is no loss when the plate is washed by methanol. Finally, after optimizing, 600  $\mu\text{L}$  of 3% formic acid in acetonitrile is applied to release arachidonic acid from the plate while phospholipids with choline groups and proteins with poly amino-groups are retained by the Cleanert MAS plate.

**3.2. Comparison of Sample Pretreatment Methods on the Effect of Eliminating Proteins.** Proteins with larger molecular weight have similar retention behaviors as arachidonic acid on reversed phase HPLC column. They would cause matrix effect on the determination of arachidonic acid. As shown in Figure 4 (PPT), there are two big peaks that appeared in Method A while the rest of sample pretreatment methods are effective enough to remove proteins from plasma (Figure 4: LLE, SPE, and MAS-M). Combined with the capability for removing phospholipids and proteins, Method D with Cleanert MAS-M plate was selected for further investigation of the analysis of arachidonic acid by LC-MS/MS.

TABLE 2: Recoveries of arachidonic acid in spiked samples treated by four sample pretreatment methods.

Concentration of arachidonic acid spiked in plasma	PPT ( $n = 5$ )		LLE ( $n = 5$ )		SPE ( $n = 5$ )		MAS-M ( $n = 5$ )	
	Recoveries (%)	RSD (%)	Recoveries (%)	RSD (%)	Recoveries (%)	RSD (%)	Recoveries (%)	RSD (%)
500 ng/mL	129.32	11.14	85.48	55.90	132.95	19.60	103.21	5.17
2 $\mu$ g/mL	130.42	2.06	67.05	82.21	94.66	9.21	99.38	5.34

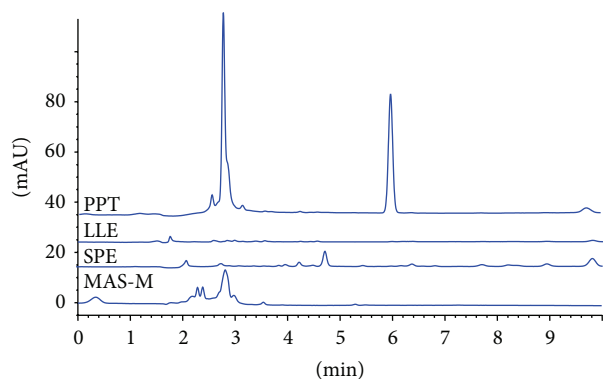


FIGURE 4: Chromatograms of proteins in samples treated with various clean-up methods, where PPT is Method A, LLE is Method B, SPE is Method C, and MAS-M is Method D.

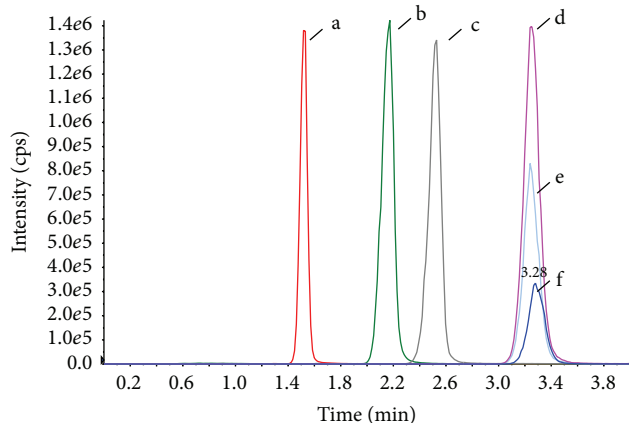


FIGURE 5: Chromatograms of arachidonic acid in different samples. a: unspiked plasma of Method C, b: unspiked plasma of Method B, c: unspiked sample of Method A, d: spiked plasma of Method D at a concentration of 500 ng/mL, e: unspiked plasma of Method D, and f: arachidonic acid standard, 500 ng/mL.

**3.3. Comparison Study on the Chromatographic Behaviors and Recoveries of Arachidonic Acid of Various Sample Pretreatment Methods.** It is noted that, as shown in Figure 5, the retention time of arachidonic acid in samples treated by Methods A to C is shifted compared with that of arachidonic acid standard. This phenomenon may be due to the accumulation of residual phospholipids and proteins on reversed phase HPLC column. In contrast, the endogenous interferences are removed efficiently in Method D by Cleanert MAS-M; the retention of arachidonic acid is stable. Also, the results listed in Table 2 reveal the advantage of Cleanert MAS-M.

The recoveries of arachidonic acid by various sample pretreatment methods in two concentration levels are listed in Table 2. As discussed in Sections 3.1 and 3.2, the elimination of phospholipids and proteins is not satisfactory by Method A (PPT), Method B (LLE), and Method C (single-mode SPE with Cleanert PEP). The matrix effect caused by phospholipids and proteins is considered as the main factor to cause the variable recoveries of arachidonic acid. In contrast, Method D with Cleanert MAS-M results in efficient removing of impurities and obtains a sufficient, robust recovery of arachidonic acid.

For quantitation, in order to compare the absolute recoveries of various sample preparation methods, the external standard method is used so that the matrix effect on the absolute recoveries can be observed clearly by contrast with Method D and others.

### 3.4. Method Validation

**3.4.1. Linearity, Limits of Detection, and Quantitation.** The calibration curve range of 10~2500 ng/mL was calculated by a regression analysis of the data to a linear fit with a weighting factor of  $1/x^2$  for the ratio of the peak area of arachidonic acid against the nominal concentration. In this range, a linear curve was obtained with correlation coefficients ( $r^2$ ) better than 0.9999; the result of the linear regression analysis for arachidonic acid is  $y = 5.18e + 3x + 9.45e + 4$  ( $r^2 = 0.9999$ ).

The limit of detection, defined as the concentration giving the signal to noise ratio of 3, was estimated to be 3 ng/mL for arachidonic acid.

**3.4.2. Precision and Accuracy.** The recoveries and precision of the proposed method with Method D are summarized in Table 2. Two concentration levels at 500 ng/mL and 2  $\mu$ g/mL were measured. The average recoveries are in the range of 99.38%~103.21% with RSD ranged from 5.17% to 5.34%.

It is found that adding 100  $\mu$ L of 3% ammonium hydroxide to dilute plasma is critical to improve the recovery of arachidonic acid, because it will damage the binding of analyte and proteins in plasma by ionizing arachidonic acid. Also, the ionized arachidonic acid will be adsorbed strongly in the loading process by the resin with the combination of anion exchange and nonpolar interaction. By contrast, the recovery of arachidonic acid was insufficient when 100  $\mu$ L of water was used to dilute plasma.

**3.5. Applications of the Proposed Methods.** The optimized clean-up method using Cleanert MAS-M plate coupled with LC-MS/MS was applied to analyze free arachidonic acid in human plasma samples obtained from local hospital. The results are listed in Table 3.

TABLE 3: Free arachidonic acid in some human plasma samples.

Sample number	1	2	3	4	5	6	7	8
Concentration of arachidonic acid ( $\mu\text{g/mL}$ )	1.51	0.83	1.15	0.98	1.83	2.11	2.18	1.82

The method was also applied in medical research center of local hospital to determine more than 100 actual plasma samples from patients of coronary heart disease and healthy people. With the high throughput sample clean-up method utilizing 96-well plate, the efficiency of the analysis was improved and well accepted by the researchers from local hospital. The results showed the average concentration of free arachidonic acid in the plasma from patients was lower than that from healthy people, which fit the law of pathology.

#### 4. Conclusion

An effective clean-up procedure is developed by comparing four different sample pretreatment methods. The selected method (Method D) is simple, accurate, and precise and has high throughput for the determination of arachidonic acid in plasma samples. In contrast to protein precipitation (Method A), liquid-liquid extraction (Method B), and SPE on Cleanert PEP (Method C), Cleanert MAS-M (Method D) method has better effect on eliminating matrix effect of phospholipids and proteins in the analysis of arachidonic acid in plasma by LC-MS/MS. A sufficient recovery with acceptable precision is reached. The proposed method is successfully applied for determining arachidonic acid in human plasma. The results indicate that the method can be used for routine analysis of arachidonic acid in pharmaceutical industries, hospitals, and research laboratories effectively. Since the 96-well plate was used, the clean-up method can easily be automated. This study has shown the possibility to apply Cleanert MAS-M plate for the pretreatment of hydrophobic analytes in plasma which are usually coeluted with phospholipids and proteins on reversed phase HPLC column.

#### Conflict of Interests

All authors declare that there is no conflict of interests in their submitted paper.

#### Acknowledgments

This publication is financially supported by the National Key Technology R&D Program of China (no. 2012BAK25B00) and the National High Technology Research and Development Program of China (no. 2013AA065600).

#### References

- [1] T. Fukaya, T. Gondaira, Y. Kashiyae et al., "Arachidonic acid preserves hippocampal neuron membrane fluidity in senescent rats," *Neurobiology of Aging*, vol. 28, no. 8, pp. 1179–1186, 2007.
- [2] Z. J. Wang, C. L. Liang, G. M. Li, C. Y. Yu, and M. Yin, "Neuroprotective effects of arachidonic acid against oxidative stress on rat hippocampal slices," *Chemico-Biological Interactions*, vol. 163, no. 3, pp. 207–217, 2006.
- [3] W. S. Harris, D. Mozaffarian, E. Rimm et al., "Omega-6 fatty acids and risk for cardiovascular disease: a science advisory from the American Heart Association nutrition subcommittee of the council on nutrition, physical activity, and metabolism; council on cardiovascular nursing; and council on epidemiology and prevention," *Circulation*, vol. 119, no. 6, pp. 902–907, 2009.
- [4] M. F. Leitzmann, M. J. Stampfer, D. S. Michaud et al., "Dietary intake of n-3 and n-6 fatty acids and the risk of prostate cancer," *The American Journal of Clinical Nutrition*, vol. 80, no. 1, pp. 204–216, 2004.
- [5] G. J. Nelson, P. C. Schmidt, G. Bartolini et al., "The effect of dietary arachidonic acid on plasma lipoprotein distributions, apoproteins, blood lipid levels, and tissue fatty acid composition in humans," *Lipids*, vol. 32, no. 4, pp. 427–433, 1997.
- [6] A. M. Rizzo, G. Montorfano, M. Negroni et al., "A rapid method for determining arachidonic: eicosapentaenoic acid ratios in whole blood lipids: correlation with erythrocyte membrane ratios and validation in a large Italian population of various ages and pathologies," *Lipids in Health and Disease*, vol. 9, article 7, 2010.
- [7] C. M. Zghibeh, V. R. Gopal, C. D. Poff, J. R. Falck, and M. Balazy, "Determination of trans-arachidonic acid isomers in human blood plasma," *Analytical Biochemistry*, vol. 332, no. 1, pp. 137–144, 2004.
- [8] S. Hauff and W. Vetter, "Quantitation of cis- and trans-monounsaturated fatty acids in dairy products and cod liver oil by mass spectrometry in the selected ion monitoring mode," *Journal of Agricultural and Food Chemistry*, vol. 57, no. 9, pp. 3423–3430, 2009.
- [9] A. D. Ilyina, J. L. Martinez Hernandez, C. Estrada Badillo et al., "Determination of arachidonic acid based on the prostaglandin H synthase catalyzed reaction," *Applied Biochemistry and Biotechnology—Part A Enzyme Engineering and Biotechnology*, vol. 88, no. 1–3, pp. 33–44, 2000.
- [10] Y. Arai, T. Fukushima, M. Shirao, X. Yang, and K. Imai, "Sensitive determination of anandamide in rat brain utilizing a coupled-column HPLC with fluorimetric detection," *Biomedical Chromatography*, vol. 14, no. 2, pp. 118–124, 2000.
- [11] T. Y. Zhan, L. Shi, S. J. Zhao et al., "HPLC-MS/MS determination of arachidonic acid in human plasma," *Chinese Journal of Pharmaceutical Analysis*, vol. 32, no. 3, pp. 388–391, 2012.
- [12] L. M. Gonzalez-Reche, A. K. Musiol, A. Müller-Lux, T. Kraus, and T. Göen, "Method optimization and validation for the simultaneous determination of arachidonic acid metabolites in exhaled breath condensate by liquid chromatography-electrospray ionization tandem mass spectrometry," *Journal of Occupational Medicine and Toxicology*, vol. 1, article 5, 2006.
- [13] Y. Gu, X. Z. Shi, S. M. Zhao, Q. Gu, X. Lu, and G. W. Xu, "Determination of arachidonic acid and its endogenous eicosanoid metabolites in mice tissues using liquid chromatography/electrospray ionization tandem mass spectrometry," *Chinese Journal of Analytical Chemistry*, vol. 38, no. 8, pp. 1089–1094, 2010.
- [14] D. D. Shinde, K. B. Kim, K. S. Oh et al., "LC-MS/MS for the simultaneous analysis of arachidonic acid and 32 related metabolites in human plasma: basal plasma concentrations and aspirin-induced changes of eicosanoids," *Journal of Chromatography B: Analytical Technologies in the Biomedical and Life Sciences*, vol. 911, no. 1, pp. 113–121, 2012.

- [15] M. Aslan, F. Özcan, I. Aslan, and G. Yücel, "LC-MS/MS analysis of plasma polyunsaturated fatty acids in type 2 diabetic patients after insulin analog initiation therapy," *Lipids in Health and Disease*, vol. 12, no. 1, article 169, 2013.
- [16] R. C. Murphy, R. M. Barkley, K. Z. Berry et al., "Electrospray ionization and tandem mass spectrometry of eicosanoids," *Analytical Biochemistry*, vol. 346, no. 1, pp. 1–42, 2005.
- [17] D. Tsikas and A. A. Zoerner, "Analysis of eicosanoids by LC-MS/MS and GC-MS/MS: a historical retrospect and a discussion," *Journal of Chromatography B: Analytical Technologies in the Biomedical and Life Sciences*, vol. 964, pp. 79–88, 2014.
- [18] R. King, R. Bonfiglio, C. Fernandez-Metzler, C. Miller-Stein, and T. Olah, "Mechanistic investigation of ionization suppression in electrospray ionization," *Journal of the American Society for Mass Spectrometry*, vol. 11, no. 11, pp. 942–950, 2000.
- [19] Y. Q. Xia and M. Jemal, "Phospholipids in liquid chromatography/mass spectrometry bioanalysis: comparison of three tandem mass spectrometric techniques for monitoring plasma phospholipids, the effect of mobile phase composition on phospholipids elution and the association of phospholipids with matrix effects," *Rapid Communications in Mass Spectrometry*, vol. 23, no. 14, pp. 2125–2138, 2009.
- [20] O. A. Ismaiel, M. S. Halquist, M. Y. Elmamly, A. Shalaby, and H. T. Karnes, "Monitoring phospholipids for assessment of matrix effects in a liquid chromatography-tandem mass spectrometry method for hydrocodone and pseudoephedrine in human plasma," *Journal of Chromatography B: Analytical Technologies in the Biomedical and Life Sciences*, vol. 859, no. 1, pp. 84–93, 2007.
- [21] E. Chambers, D. M. Wagrowski-Diehl, Z. Lu, and J. R. Mazzeo, "Systematic and comprehensive strategy for reducing matrix effects in LC/MS/MS analyses," *Journal of Chromatography B*, vol. 852, no. 1-2, pp. 22–34, 2007.
- [22] A. P. Watt, D. Morrison, K. L. Locker, and D. C. Evans, "Higher throughput bioanalysis by automation of a protein precipitation assay using a 96-well format with detection by LC-MS/MS," *Analytical Chemistry*, vol. 72, no. 5, pp. 979–984, 2000.
- [23] C. Kousoulos, G. Tsatsou, C. Apostolou, Y. Dotsikas, and Y. L. Loukas, "Development of a high-throughput method for the determination of itraconazole and its hydroxy metabolite in human plasma, employing automated liquid-liquid extraction based on 96-well format plates and LC/MS/MS," *Analytical and Bioanalytical Chemistry*, vol. 384, no. 1, pp. 199–207, 2006.
- [24] L. Kortz, J. Dorow, S. Becker, J. Thiery, and U. Ceglarek, "Fast liquid chromatography-quadrupole linear ion trap-mass spectrometry analysis of polyunsaturated fatty acids and eicosanoids in human plasma," *Journal of Chromatography B: Analytical Technologies in the Biomedical and Life Sciences*, vol. 927, pp. 209–213, 2013.
- [25] S. T. Wu, D. Schoener, and M. Jemal, "Plasma phospholipids implicated in the matrix effect observed in liquid chromatography/tandem mass spectrometry bioanalysis: evaluation of the use of colloidal silica in combination with divalent or trivalent cations for the selective removal of phospholipids from plasma," *Rapid Communications in Mass Spectrometry*, vol. 22, no. 18, pp. 2873–2881, 2008.
- [26] A. P. Watt, D. Morrison, and D. C. Evans, "Approaches to higher-throughput pharmacokinetics (HTPK) in drug discovery," *Drug Discovery Today*, vol. 5, no. 1, pp. 17–24, 2000.
- [27] N. Zhang, K. Rogers, K. Gajda, J. R. Kagel, and D. T. Rossi, "Integrated sample collection and handling for drug discovery bioanalysis," *Journal of Pharmaceutical and Biomedical Analysis*, vol. 23, no. 2-3, pp. 551–560, 2000.

## Research Article

# Pregabalin and Tranexamic Acid Evaluation by Two Simple and Sensitive Spectrophotometric Methods

Nawab Sher,<sup>1</sup> Nasreen Fatima,<sup>1</sup> Shahnaz Perveen,<sup>2</sup>  
Farhan Ahmed Siddiqui,<sup>3</sup> and Alisha Wafa Sial<sup>4</sup>

<sup>1</sup>Department of Chemistry, Faculty of Science, University of Karachi, Karachi 75270, Pakistan

<sup>2</sup>PCSIR Laboratories Complex Karachi, Shahr-e-Dr. Salimuzzaman Siddiqui, Karachi 75280, Pakistan

<sup>3</sup>Faculty of Pharmacy, Federal Urdu University of Arts, Science and Technology, Karachi 75300, Pakistan

<sup>4</sup>Faculty of Medicine, Ziauddin University, Karachi 75600, Pakistan

Correspondence should be addressed to Nawab Sher; [nawabsherafridi@gmail.com](mailto:nawabsherafridi@gmail.com)

Received 8 September 2014; Accepted 6 December 2014

Academic Editor: Mohamed Abdel-Rehim

Copyright © 2015 Nawab Sher et al. This is an open access article distributed under the Creative Commons Attribution License, which permits unrestricted use, distribution, and reproduction in any medium, provided the original work is properly cited.

This paper demonstrates colorimetric visible spectrophotometric quantification methods for amino acid, namely, tranexamic acid and pregabalin. Both drugs contain the amino group, and when they are reacted with 2,4-dinitrophenol and 2,4,6-trinitrophenol, they give rise to yellow colored complexes showing absorption maximum at 418 nm and 425 nm, respectively, based on the Lewis acid base reaction. Detailed optimization process and stoichiometric studies were conducted along with investigation of thermodynamic features, that is, association constant and standard free energy changes. The method was linear over the concentration range of 0.02–200  $\mu\text{g mL}^{-1}$  with correlation coefficient of more than 0.9990 in all of the cases. Limit of detection was in range from 0.0041 to 0.0094  $\mu\text{g mL}^{-1}$  and limit of quantification was in the range from 0.0137 to 0.0302  $\mu\text{g mL}^{-1}$ . Excellent recovery in Placebo spiked samples indicated that there is no interference from common excipients. The analytical methods under proposal were successfully applied to determine tranexamic acid and pregabalin in commercial products. *t*-test and *F* ratio were evaluated without noticeable difference between the proposed and reference methods.

## 1. Introduction

Pregabalin (PG) chemically is 3-amino methyl hexanoic acid, with the chemical formula  $\text{C}_8\text{H}_{17}\text{NO}_2$ . Its structural and pharmacological features correspond to the mammalian neurotransmitter gamma-aminobutyric acid (GABA), and it is primarily used as anticonvulsant drug. However, its effects are much broader being analgesic, antiepileptic, antidiabetic, and anti-inflammatory drug. Further more, it has been recommended for gastrointestinal damage, alcoholism, and insomnia [1]. Exact mechanism is not known; however, it has been an established fact that it binds to calcium channel in the central nervous system which decreases calcium influx at nerve endings and therefore reduces the liberation of several associated neurotransmitters which subsequently results in the above-mentioned activities [2]. Tranexamic acid (TXA) is chemically designed as *trans*-4-(aminomethyl) cyclohexanecarboxylic acid, with chemical formula  $\text{C}_8\text{H}_{14}\text{NO}_2$ . It is

the closed cyclic analogous structure of lysine. TXA has been very potent antifibrinolytic agent, vastly used in haemorrhagic diseases. Its significant use is to treat ovarian tumors and it is recommended to manage pregnancy and reduce blood loss in surgery. It is considered as the best substitute to surgery in cases of menorrhagia [3, 4]. Chemical structure of TXA and PG is shown in Figure 1.

PG is not yet part of any pharmacopoeial monograph. However, analytical method reported for PG includes spectrophotometry [5–9], spectrofluorimetry [10], and high pressure liquid chromatography with UV detection [11], with mass detection [12], and with fluorescence detection [13]. TXA quantification has been reported through colorimetric spectrophotometry [14–18], HPLC [19], and spectrofluorimetry [20]. Although chromatographic method offers high level of selectivity and specificity, the associated expenses are alarming and cannot be shouldered by every pharmaceutical

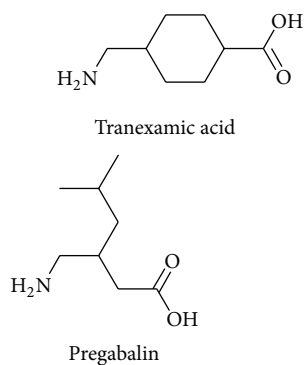


FIGURE 1: Structure of PG and TXA.

industry. Moreover, the molecules of TXA and PG lack UV absorbing chromospheres, so in case of HPLC high load on column will deteriorate and reduce its life which turned out to be huge burden on low and middle economy-based industries. Amino acids like TXA and PG are highly polar and cannot be easily volatilized, so gas chromatographic method would not be easy or straightforward. Spectrofluorometers are not the common instruments in all the labs. All these suggest that the proposed analytical methods are highly important from quality control point of view. The colorimetric reagents used in this study are trinitrophenol (TNP) and dinitrophenol (DNP). These reagents have wide range utility as quality colorimetric analyzing agents in pharmaceutical industry [21–27].

A glance over the literature revealed few reports regarding charge transfer complexes for PG and TXA. A structural analogous of PG and TXA gabapentin has been determined by colorimetry-visible spectrophotometry by reacting with iodine, chloranil, chloranilic acid, 2,3-dichloro-5,6-dicyano-1,4-benzoquinone, tetracyanoethylene, methyl orange, hydroxy benzaldehyde, picric acid and with ninhydrin [28–30]. Colorimetric spectrophotometric methods for PG include reaction with 1,2-naphthoquinone-4-sulphonate sodium and 2,4-dinitrofluorobenzene [5], ascorbic acid and salicylaldehyde [6], 7,7,8,8-tetracyanoquinodimethane, 2,3-dichloro-5,6-dicyano-1,4-benzoquinone, 2,5-dichloro-3,6-dihydroxy-1,4-benzoquinone, tetracyanoethylene and 2,3,5,6-tetrachloro-1,4-benzoquinone [7], quinalizarin and alizarin [8], and vanillin, acetyl acetone, and formaldehyde [9]. Colorimetric quantification reagent for TX includes ninhydrine [14, 15], ferric chloride [15], 1,2-naphthoquinone-4-sulphonate sodium [16], ascorbic acid [17], and Azo dye [18].

There is no report on TXA and PG determination which utilizes TNP or DNP reagents. Most of the reported spectrometric methods are insensitive or need complicated extractions and heating/cooling procedures or use reagents which do not produce linear response. Moreover, most of the methods are based on the absorbance in near UV region and thus specificity is questioned. The method under proposal is highly selective and extremely simple, so it can be usefully adopted for routine analysis in quality control laboratories. The proposed methods are accompanied by the reaction of amine group of amino acid with hydroxyl group, activated

by neighboring nitro groups of both TNP and DNP. As a result, yellow color complexes are formed on simple addition of the two reagents and no extra process is required. Thermodynamics features in respect of association constant and standard free energy changes have been evaluated for both reactions. Both of methods have been proved to be very useful from routine quality control prospective and can be considered as superior to most of the published methods with respect to pace, ease, low cost, and sensitivity.

## 2. Experimental

**2.1. Instrument.** A UV-Visible Shimadzu Spectrophotometer 1601 with 1 cm path length quartz cells controlled by Shimadzu UV Probe 3.9 version software was used. MS Excel sheet was used to evaluate  $F$ ,  $t$  tests, and other statistical parameters.

**2.2. Materials and Reagents.** Analytical grade reagents were used. Pregabalin and tranexamic acid pure drugs were a kind gift from a local pharmaceutical agency having 99% plus purity. Tranex capsules 250 and 500 mg and Syngab capsules 200 mg, 50 mg, and 100 mg (Atco Laboratories Ltd., Karachi, Pakistan) were procured from the market. TNP and DNP were acquired from Merck Sigma Aldrich, Germany. Microcrystalline cellulose (Avicel pH 101, maize starch, magnesium stearate, PVP, Aerosil R-200, crospovidone-X, HPMC (606), and PEG (6000)), titanium dioxide, and isopropyl alcohol were a gift from a local pharmaceutical agency. The entire chemicals were used according to their safety precautionary measures.

### 2.3. General Procedure

#### 2.3.1. Analytical Method Development

**Reagents and Standard Stock Solutions Preparation.** A  $2.27 \text{ gL}^{-1}$  TNP and  $1.84 \text{ gL}^{-1}$  2,4-DNP solutions were prepared individually in dichloromethane corresponding to 10 mMol of the concerned reagent.

$160 \mu\text{g mL}^{-1}$  of PG and  $155 \mu\text{g mL}^{-1}$  of TXA were prepared individually by taking 16 and 15.5 mg weights, respectively, in 100 mL calibrated volumetric flasks, dissolved in 10 mL of water, and diluted to the mark level with the same solvent.

**Stoichiometric Study.** To study stoichiometry of the reaction, Job's method of continuous variation was followed [31]. Equimolar solution (1 mMol) of each of the coloring reagents and drugs were prepared. In a series of 10 mL calibrated amber volumetric flasks, solutions of PG and TXA were prepared individually, comprising different complementary proportions (0:10, 1:9, 2:8, 3:7, 4:6, 5:5, ..., 9:1) each with both of the reagents (TNP and DNP) separately. After 10 minutes of reaction the absorbance of the complex was measured at the wavelength of maximum absorption against the reagent blanks treated similarly.

**DNP Method.** 3 mL of drug PG or TXA stock solution was taken individually in 10 mL amber volumetric flasks to

which 4 mL of the coloring reagent DNP was added. Sample was diluted with acetonitrile up to volume. Absorbance was measured after 10 minutes of reaction at 418 nm using appropriate blank treated similarly.

**TNP Method.** 3 mL of drug PG or TXA stock solution was taken individually in 10 mL amber volumetric flasks to which 4 mL of the coloring reagent TNP was added. Acetonitrile was added up to the mark level. Absorbance was measured after 10 minutes of reaction at 425 nm using appropriate blank treated similarly.

**2.3.2. Procedures for Pharmaceuticals Formulation.** Homogeneous samples were obtained for each drug molecule. Bulk homogenous powder equivalent to 10 mg of pregabalin or tranexamic acid was dissolved in methanol by sonication for 15 min and shaking thoroughly for about 30–40 min. The samples were cooled down and diluted up to the mark level with methanol, mixed well, and filtered using a Whatman number 42 filter paper to give  $100 \mu\text{g mL}^{-1}$  of PG and TXA each, individually. Further dilution and reactions were continued as described above under general procedures.

**2.3.3. Excipients Interference Evaluation.** 10 mg of each PG and 10 mg of TXA were spiked individually with common excipients like magnesium stearate, HPMC (hydroxypropyl methylcellulose), glucose, pyrrolidone, lactose, talc powder, and starch. It was further processed as described under general procedures. Samples were subjected to multiple analyses and percent recovery was calculated.

**2.3.4. Reaction Mechanism.** This reaction is based on the proton transfer reaction from Lewis acid such as TNP and DNP to Lewis base such as TXA and PG, which produces intensely yellow color ion-pair complex as depicted by Saito and Matsunaga [26]. Mechanistic view has been expressed in Figure 2.

**2.3.5. Thermodynamic Studies.** Standard free energy changes ( $\Delta G^\circ$ ) and association constant ( $K_c$ ) were determined for both of the methods to evaluate thermodynamic aspects. The reaction of TNP and DNP each with PG and TXA was investigated for the association constants by the application of Benesi-Hildebrand equation [32]:

$$\frac{C_a}{A} = \frac{1}{\epsilon} + \frac{1}{K_c \cdot \epsilon} \cdot \frac{1}{C_b}, \quad (1)$$

where  $C_a$  and  $C_b$  are the concentrations of the drug (PG or TXA) and coloring reagent (DNP or TNP) respectively,  $A$  is the absorbance of the complex,  $\epsilon$  is the molar absorptivity of the complex, and  $K_c$  is the association constant of the complex.

Utilizing the above equation,  $A$  was plotted against  $C_a$  in both cases and straight lines were obtained. Standard free energy changes were calculated by the following equation:

$$\Delta G^\circ = -2.356RT \log K_c, \quad (2)$$

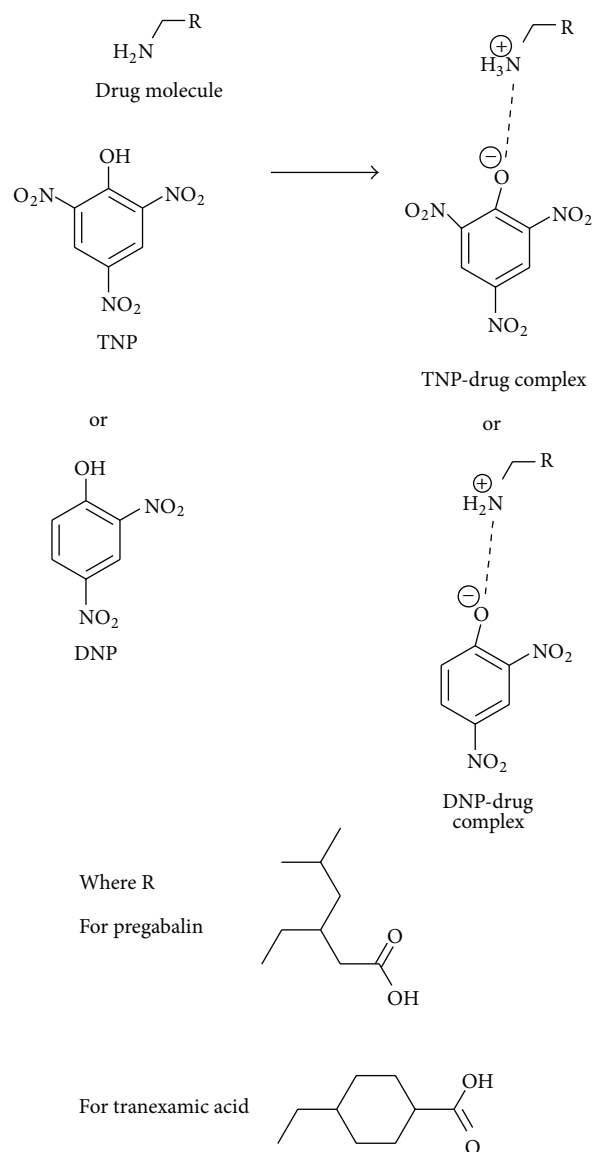


FIGURE 2: Mechanism of reaction.

where  $\Delta G^\circ$  is free energy change associated with complex ( $\text{kJ mol}^{-1}$ ),  $R$  is the thermodynamic gas constant ( $1.987 \text{ cal mol}^{-1} \text{ deg}^{-1}$ ),  $T$  is the Kelvin temperature ( $273 + ^\circ\text{C}$ ), and  $K_c$  is the equilibrium constant.

**2.4. Assay Validation.** ICH guideline was followed for the validation purpose and various experiments were performed [33].

**2.4.1. Linearity.** Linearity is the ability of method to show absorbance correspondingly to the analytes concentration. Least square procedure was adopted to develop the regression equations which showed linear relation of the concentration of complex with absorbance, complying Lambert Beer's law. Under these experimental set-ups, absorbance at the given

wavelength was found to vary directly with the concentrations of both the donor and the acceptor molecules.

**2.4.2. Precision and Accuracy.** Accuracy of the analytical method is that the parameter confirms that the test results obtained with the method are close to the true or accepted values, while precision is the reproducibility of test result when the same homogenous sample is subjected to multiple testing. Solutions containing three different concentrations of pregabalin and tranexamic acid were arranged and investigated in triplicate for accuracy and precision.

**2.4.3. Specificity.** Specificity is the quantification of the analytes in presence of component mixtures, excipients, and additives. The effect of common excipients and additives was evaluated by designing spiking experiments. Both TXA and PG were evaluated with common excipients at different concentration levels individually.

**2.4.4. Limit of Detection (LOD) and Limit of Quantification (LOQ).** Both reactions were evaluated for LOD and LOQ values. The empirical formulas  $3\sigma/S$  and  $10\sigma/S$  were used to establish LOD and LOQ for the method, where  $S$  is the slope and  $\sigma$  is the standard deviation of the response statistically inferred from calibration curve. A signal to noise ratio of 3:1 was defined for LOD and of 10:1 was defined for LOQ, respectively [33].

### 3. Results and Discussion

The reaction of coloring reagent TNP or DNP as Lewis acids with amino acid (PG and TXA) as Lewis base afforded intense yellow charge transfer complex. The intensity in color is attributed to the formation of phenolate ion [26] as shown in reaction scheme in Figure 2.

**3.1. Method Optimization.** In order to achieve optimum experimental condition, various factors were evaluated including time, temperature, solvent of choice, and concentration of drugs and reagent. Those experimental factors which were affecting the absorbing abilities of the resulting complex were optimized to enhance selectivity and sensitivity. The reaction and stability of the complex were evaluated with respect to time in intervals at room temperature. Maximum absorbance was obtained in 5- to 10-minute time period and prolonged period of time did not affect the absorbance of the complex. However, a negative impact was noted when reaction mixture was heated especially beyond 60°C. Similarly, effect of coloring reagent was evaluated by adding it to the fixed concentration of drug substance. To  $100 \mu\text{g mL}^{-1}$  of drug substance, reagents TNP and DNP were added in the range from 1 to 9 mL. The amount of coloring reagent linearly increased the absorbance up to equimolar stage beyond which the absorbance remains constant at maximum absorbance, which corresponds to 4.0 mL of solution of each DNP and TNP. Different solvents systems including chloroform, acetone, 2-propanol, acetonitrile, and dichloromethane were evaluated for optimum results.

TABLE 1: Thermodynamic study.

Drug molecule	DNP		TNP	
	PG	TXA	PG	TXA
Molar absorptivity (Ma)	1326.85	1337.35	1404.77	1418.36
$K_c$	$1.51 \times 10^3$	$1.62 \times 10^3$	$2.74 \times 10^3$	$2.86 \times 10^3$
$\Delta G^\circ$	-2.336	-2.358	-2.498	-2.508

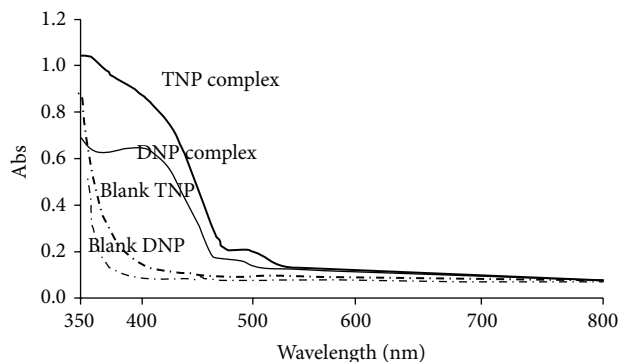


FIGURE 3: Spectrum of complexes and blanks.

Water was used to prepare stock solution of PG and TXA because of the free solubility of the drugs and working range solutions were prepared in acetonitrile. It has been known that methanol interferes in charge transfer complex formation so acetonitrile was used in working range solutions in subsequent analysis [25]. Dichloromethane was found to be suitable for preparation of DNP and TNP solutions. The solutions were scanned in visible range (800 to 350 nm) by spectrophotometer using the corresponding blank. It was found that, for TNP complex,  $\lambda_{\text{max}}$  was 425 nm, while for DNP it was 418 nm which justifies intensity in color of complex derived from TNP as compared to that of DNP as in Figure 3. In view of these results, all working solutions to reaction were prepared in acetonitrile in sequence of drug-reagent solvent, maintained at  $25 \pm 2^\circ\text{C}$ . Absorbance is measured at 418 and 425 nm for DNP and TNP complexes, respectively, after 10 minutes of mixing.

**3.2. Stoichiometry.** Job's continuous variations method suggested a 1:1 molar ratio for both reagents with both drugs. However, experimental design considered the drug molecules to be limiting reactants, so the chromogenic reagent was taken in slight excess in subsequent analysis in order to make the reaction drug concentration dependent and to counter any possible interference.

**3.3. Thermodynamic Study of the Complex.** Complexes were studied in detail by applying Bensi-hilbrand theory. Association constant ( $K_c$ ) was in the range of  $1.51\text{--}1.62 \times 10^3$  for DNP, while it was in the range of  $2.74\text{--}2.86 \times 10^3$  for TNP and standard free energy changes were  $-2.336$  to  $-2.358$  for complex derived from DNP and  $-2.498$  to  $-2.508$  for TNP-based complex. Results are portrayed in Table 1.

TABLE 2: Linearity and range.

Parameter	DNP		TNP	
	PG	TXA	PG	TXA
Linearity range ( $\mu\text{g/mL}$ )	0.02–200	0.02–200	0.02–200	0.02–200
Correlation coefficient ( $r$ )	0.99962	0.99971	0.99948	0.99987
Slope ( $m$ )	0.01002	0.02035	0.01423	0.01553
Intercept ( $c$ )	–0.0012	–0.0028	0.0021	–0.0011
(LOD) ( $\mu\text{g mL}^{-1}$ )	0.0059	0.0094	0.0041	0.0075
(LOQ) ( $\mu\text{g mL}^{-1}$ )	0.0195	0.0302	0.0137	0.0269

TABLE 3: Accuracy and precision.

	Pregabalin (PG)				Tranexamic acid (TXA)							
	50% nominal		100% nominal		50% nominal		100% nominal					
	con. %recovery	%Lc found	con. %recovery	%RSD	con. %recovery	%Lc found	con. %recovery	%RSD				
DNP	98.10	1.235	101.68	0.525	101.93	0.235	99.84	0.545	99.84	0.412	101.85	0.864
TNP	100.60	0.320	99.89	0.536	99.17	0.938	101.60	0.940	100.69	0.526	101.57	0.638

TABLE 4: Recovery studies in commercial products.

Brand name (active molecule): Label claim	Label claim (%) $\pm$ S.D.	
	DNP	TNP
Tranex (TXA): 250 mg	101.23% $\pm$ 0.51	100.15% $\pm$ 0.61
Tranex (TXA): 500 mg	99.95% $\pm$ 0.63	99.19% $\pm$ 0.92
Syngab (PG): 100 mg	99.99% $\pm$ 0.77	99.91% $\pm$ 0.65
Syngab (PG): 200 mg	101.47% $\pm$ 1.13	100.27% $\pm$ 1.22

Standard free energy changes value indicates spontaneity of the reaction. High wavelength, high association constant, and low standard free energy changes with complex involving TNP as compared to DNP justify the resonance phenomenon in the phenolate ion derived from TNP compared to DNP [26].

**3.4. Validation Studies.** After development method validation studies were conducted in line with the above-mentioned protocol. Using linear regression equation, methods showed linear response in concentration range from 0.02 to 200  $\mu\text{g mL}^{-1}$  with correlation coefficient of more than 0.9990 in both cases. In all the cases studied, Beer's law was obeyed with small intercept values (–0.0028 to 0.0021). Slopes were found to be in the range of 0.01018 to 0.0146. Small intercept and insignificant variation of slope are attributes of the excellent response of the methods. Low LOQ values of (0.095–0.109)  $\mu\text{g mL}^{-1}$  explained sensitivity of the method as in Table 2. Obtained results in Tables 3 and 4 are very close to 100% label claim, indicating excellent accuracy, while very good precision is obvious from the % relative standard deviation which is less than 2. During spiking experiments no interference was found which indicated that none of those additives possess enough basicity to cause interference in analysis of TXA and PG. In addition, good % recoveries in common excipients spiked samples that ranged from 98.3

to 101.4% further confirmed the specificity of the projected methods.

**3.5. Application of the Method in Pharmaceuticals.** General procedures described above were followed to determine content of capsule dosage formulations for both of the drugs. The projected colorimetric methods based on charge-transfer complexes were applied to determine PG and TXA, along with the reference methods 9 and 15 for PG and TXA, respectively, to evaluate the test results.  $t$ -test and  $F$  test were carried out with MS Excel, and the proposed methods were found to be comparable to the referenced methods and no considerable variation was found between them which indicated similar precision and accuracy. Results are presented in Table 5.

## 4. Conclusions

To estimate the quantity of tranexamic acid and pregabalin in commercial products, two simple and sensitive colorimetric methods were developed and validated. Picric acid and 2,4-dinitrophenol, the two coloring reagents, have been utilized to develop two simple, much more common but sensitive and selective visible range spectrophotometric methods for routine analysis of tranexamic and pregabalin in bulk raw material and finished or semifinished dosage form. The

TABLE 5: *F* and *t* tests of the method.

Taken (mg)	TNP		DNP		Reference method	
	PG found (mg)	TXA found (mg)	PG found (mg)	TXA found (mg)	PG [9] found (mg)	TXA [15] found (mg)
100.1	100.2	100.6	101.6	100.7	100.3	101.1
101.1	99.8	100.3	98.6	99.4	100.8	99.8
100.2	100.1	99.8	100.9	100.3	99.7	101.2
100.4	100.2	99.6	99.1	98.7	99.3	100.7
100.3	100.6	100.6	98.4	97.9	99.5	100.4
99.6	100.5	101.4	97.5	98.1	100.5	100.3
MEAN	100.23	100.38	99.35	99.13	100.01	100.58
SD	0.288	0.646	1.576	1.184	0.601	0.527
RSD	0.287	0.644	1.586	1.195	0.601	0.524
<i>t</i> -Test	0.44	0.569	0.355	0.022		
<i>F</i> -Test	0.131	0.665	0.054	0.110		

suggested methods are superior to the already established spectrophotometric methods in terms of simplicity. *t* and *F* tests guaranteed high accuracy and precision. Hence, the proposed methods can be eagerly adopted by pharmaceutical quality control laboratories for routine quantitative analysis.

### Conflict of Interests

The authors declare that they have no conflict of interests regarding the publication of this paper.

### References

- L. A. Houghton, C. Fell, P. J. Whorwell, I. Jones, D. P. Sudworth, and J. D. Gale, "Effect of a second-generation  $\alpha_2\delta$  ligand (pregabalin) on visceral sensation in hypersensitive patients with irritable bowel syndrome," *Gut*, vol. 56, no. 9, pp. 1218–1225, 2007.
- S. I. Johannessen and T. Tomson, "Pharmacokinetic variability of newer antiepileptic drugs: when is monitoring needed?" *Clinical Pharmacokinetics*, vol. 45, no. 11, pp. 1061–1075, 2006.
- A. R. Gennaro, *Remington. The Science and Practice of Pharmacy*, Mack, Easton, Pa, USA, 1995.
- L. Good, E. Peterson, and B. Lisander, "Tranexamic acid decreases external blood loss but not hidden blood loss in total knee replacement," *British Journal of Anaesthesia*, vol. 90, no. 5, pp. 596–599, 2003.
- M. I. Walash, F. F. Belal, N. M. El-Enany, and M. H. El-Maghrabey, "Utility of certain nucleophilic aromatic substitution reactions for the assay of pregabalin in capsules," *Chemistry Central Journal*, vol. 5, no. 1, article 36, 2011.
- F. S. Hammad and O. M. Abdallah, "Optimized and validated spectrophotometric methods for the determination of pregabalin in pharmaceutical formulation using ascorbic acid and salicylaldehyde," *Journal of American Science*, vol. 8, no. 12, pp. 118–124, 2012.
- H. Salem, "Analytical study for the charge-transfer complexes of Pregabalin," *E-Journal of Chemistry*, vol. 6, no. 2, pp. 332–340, 2009.
- A. A. Gouda and Z. A. Malah, "Development and validation of sensitive spectrophotometric method for determination of two antiepileptics in pharmaceutical formulations," *Spectrochimica Acta—Part A: Molecular and Biomolecular Spectroscopy*, vol. 105, pp. 488–496, 2013.
- H. M. Saleh, M. M. El-Henawee, G. H. Ragab, and O. F. Mohamed, "Spectrophotometric and spectrofluorimetric determination of pregabalin via condensation reactions in pure form and in capsules," *International Journal of Pharmaceutical, Chemical and Biological Sciences*, vol. 4, no. 3, pp. 738–747, 2014.
- M. I. Walash, F. Belal, N. El-Enany, and M. H. El-Maghrabey, "Simple and sensitive spectrofluorimetric method for the determination of pregabalin in capsules through derivatization with fluorecamine," *Luminescence*, vol. 26, no. 5, pp. 342–348, 2011.
- R. S. Gujral, S. K. M. Haque, and S. Kumar, "A novel method for the determination of pregabalin in bulk pharmaceutical formulations and human urine samples," *African Journal of Pharmacy and Pharmacology*, vol. 3, no. 6, pp. 327–334, 2009.
- V. V. Vaidya, S. M. Yetal, S. M. N. Roy, N. A. Gomes, and S. S. Joshi, "LC-MS-MS determination of pregabalin in human plasma," *Chromatographia*, vol. 66, no. 11-12, pp. 925–928, 2007.
- M. Dousa, P. Gibala, and K. Lemr, "Liquid chromatographic separation of pregabalin and its possible impurities with fluorescence detection after postcolumn derivatization with o-phthalaldehyde," *Journal of Pharmaceutical and Biomedical Analysis*, vol. 53, no. 3, pp. 717–722, 2010.
- T. M. Ansari, A. Raza, and A.-U. Rehman, "Spectrophotometric determination of tranexamic acid in pharmaceutical bulk and dosage forms," *Analytical Sciences*, vol. 21, no. 9, pp. 1133–1135, 2005.
- M. S. Arayne, N. Sultana, F. A. Siddiqui, A. Z. Mirza, and M. H. Zuberi, "Spectrophotometric techniques to determine tranexamic acid: kinetic studies using ninhydrin and direct measuring using ferric chloride," *Journal of Molecular Structure*, vol. 891, no. 1–3, pp. 475–480, 2008.
- S. Agarwal and R. S. R. Murthy, "A novel and sensitive colorimetric method for estimation of tranexamic acid in bulk and in pharmaceutical dosage form," *International Journal of Research in Pharmaceutical and Biomedical Sciences*, vol. 3, no. 2, pp. 947–950, 2012.
- E. A. Gadkariem, M. A. Mohamed, and M. A. A. Jabbar, "Assay of Tranaxamic acid via coupling with Ascorbic acid using kinetic methods," *Elixir Pharmacy*, vol. 54, pp. 12331–12334, 2013.
- M. Y. Dhamra, "Spectrophotometric determination of tranexamic acid by azo-dye formation-application to pharmaceutical preparations," *Journal of Education & Science*, vol. 24, no. 3, pp. 21–33, 2011.

- [19] J. F. Huertas-Pérez, M. Heger, H. Dekker, H. Krabbe, J. Lankelma, and F. Ariese, "Simple, rapid, and sensitive liquid chromatography-fluorescence method for the quantification of tranexamic acid in blood," *Journal of Chromatography A*, vol. 1157, no. 1-2, pp. 142–150, 2007.
- [20] G. Iskender and S. Atmaca, "Spectrofluorometric determination of tranexamic acid in pharmaceutical dosage forms," *Pharmazie*, vol. 43, no. 4, p. 290, 1988.
- [21] M. H. Abdel-Hay, S. M. Sabry, M. H. Barary, and T. S. Belal, "Spectrophotometric determination of bisacodyl and piribedil," *Analytical Letters*, vol. 37, no. 2, pp. 247–262, 2004.
- [22] M. Y. El-Mamli, "Spectrophotometric determination of flucloxacillin in pharmaceutical preparations using some nitrophenols as a complexing agent," *Spectrochimica Acta Part A: Molecular and Biomolecular Spectroscopy*, vol. 59, no. 4, pp. 771–776, 2003.
- [23] E. Regulska, M. Tarasiewicz, and H. Puzanowska-Tarasiewicz, "Extractive-spectrophotometric determination of some phenothiazines with dipicrylamine and picric acid," *Journal of Pharmaceutical and Biomedical Analysis*, vol. 27, no. 1-2, pp. 335–340, 2002.
- [24] I. Hussain, M. I. Tariq, and H. L. Siddiqui, "Structure elucidation of chromogen resulting from Jaffe's reaction," *Journal of the Chemical Society of Pakistan*, vol. 31, no. 6, pp. 937–948, 2009.
- [25] N. Sultana, M. S. Arayne, and S. N. Ali, "Charge transfer complexes of gamma aminobutyric acid-analogue, a neurotransmitter: synthesis and spectrophotometric determination," *Journal of Bioanalysis & Biomedicine*, vol. 528, no. 2, pp. 12–21, 2013.
- [26] G. Saito and Y. Matsunaga, "Charge-transfer and proton-transfer in the formation of molecular complexes. I. The complex isomerization of some anilinium picrates by melting," *Bulletin of the Chemical Society of Japan*, vol. 44, pp. 3328–3335, 1971.
- [27] M. S. Refat, L. A. El-Zayat, and O. Z. Yeşilel, "Spectroscopic characterization of charge-transfer complexes of morpholine with chloranilic and picric acids in organic media: crystal structure of bis(morpholinium 2,4,6-trinitrocyclohexanolate)," *Spectrochimica Acta Part A: Molecular and Biomolecular Spectroscopy*, vol. 75, no. 2, pp. 745–752, 2010.
- [28] M. S. Saleh, A. K. Youssef, E. Y. Hashem, and D. A. Abdel-Kader, "A novel Spectrophotometric method for determination of gabapentin in pharmaceutical formulations using 2,5-dihydroxybenzaldehyde," *Computational Chemistry*, vol. 2, pp. 22–30, 2014.
- [29] F. A. Siddiqui, M. S. Arayne, N. Sultana et al., "Spectrophotometric determination of gabapentin in pharmaceutical formulations using ninhydrin and  $\pi$ -acceptors," *European Journal of Medicinal Chemistry*, vol. 45, no. 7, pp. 2761–2767, 2010.
- [30] F. A. Siddiqui, N. Sher, N. Shafi, H. Shamshad, and A. Zubair, "Kinetic and thermodynamic spectrophotometric technique to estimate gabapentin in pharmaceutical formulations using ninhydrin," *Journal of Analytical Science and Technology*, vol. 4, p. 17, 2013.
- [31] P. Job, "Recherches sur la formation de complexes minéraux en solution, et sur le stabilité (formation and stability of inorganic complexes in solution)," *Annali di Chimica*, vol. 9, pp. 113–203, 1928.
- [32] H. A. Benesi and J. Hidelbrand, "A spectrophotometric investigation of the interaction of iodine with aromatic hydrocarbons," *Journal of the American Chemical Society*, vol. 71, no. 8, pp. 2703–2707, 1949.
- [33] ICH-Q2B Guideline for Industry, "Validation of analytical procedure: methodology," in *Proceedings of the International Conference on Harmonization*, 2005.

## Research Article

# Antibacterial, Antifungal, and Insecticidal Potentials of *Oxalis corniculata* and Its Isolated Compounds

**Azizur Rehman, Ali Rehman, and Ijaz Ahmad**

*Department of Chemistry, Kohat University of Science & Technology (KUST), Khyber Pakhtunkhwa, Kohat 26000, Pakistan*

Correspondence should be addressed to Ijaz Ahmad; [drijaz.chem@yahoo.com](mailto:drijaz.chem@yahoo.com)

Received 21 September 2014; Accepted 25 December 2014

Academic Editor: Faezeh Khalilian

Copyright © 2015 Azizur Rehman et al. This is an open access article distributed under the Creative Commons Attribution License, which permits unrestricted use, distribution, and reproduction in any medium, provided the original work is properly cited.

*Oxalis corniculata* is a common medicinal plant widely used against numerous infectious diseases. The agrochemical potential of methanolic extract, *n*-hexane, chloroform, ethyl acetate, and *n*-butanol fractions were assessed to measure the antibacterial, antifungal, and insecticidal activities of the plant. The crude, chloroform, and *n*-butanol soluble fractions showed excellent activities against *Escherichia coli*, *Shigella dysenteriae*, *Salmonella typhi*, and *Bacillus subtilis* but have no activity against *Staphylococcus aureus*. Similarly the crude, *n*-hexane, and chloroform fractions were also found to have significant activity against fungal strains including *Fusarium solani*, *Aspergillus flexneri*, and *Aspergillus flavus* and have no activity against *Aspergillus niger*. Chemical pesticides have shown very good results at the beginning, but with the passage of time the need was realized to use the natural plant sources for the safe control of insects. The current study will provide minor contribution towards it. High mortality rate was recorded for the crude extract and chloroform fraction against *Tribolium castaneum*. The two isolated compounds 5-hydroxy-6,7,8,4'-tetramethoxyflavone (1) and 5,7,4'-trihydroxy-6,8-dimethoxyflavone (2) were evaluated for antibacterial, antifungal, and insecticidal activities. The results showed that compound 2 was more active than compound 1 against the tested bacterial strains and insects.

## 1. Introduction

The progress in new antimicrobial agents to multidrug resistant pathogens for the treatment of various infectious diseases is of increasing interest. Therefore different plant extracts of many plants have been used locally against various pathogens, which showed positive results [1].

Higher plants and their extracts are used for the treatment of infectious disease as traditional medicines from the very beginning of life. About 80 percent of the world population depends upon the plant extracts [2]. But there are only a small percentage of these plants that have been subjected to pharmacological or biological screening [3]. Microbes which are free to move around the world cause different infections in human races. In developing countries about 43 percent of total deaths are due to infectious diseases. WHO claims significant control in major infectious diseases [4]. Due to jumbled use of existing antimicrobial drugs pathogenic bacteria have developed resistance against wide range of antibiotics. The  $\beta$ -lactamase producers like *Staphylococcus aureus*, *Escherichia coli*, *Klebsiella pneumonia*, and

many others have become a major therapeutic problem, resulting in increased treatment failure and health care cost. Microbiologists from all over the world are in search to formulate new antimicrobial drugs and evaluate the efficiency of plant products to replace chemical antimicrobial agents [5]. Medicinal plants extracts have shown to serve as a cheap source of antimicrobial agents against pathogenic microbes. These extracts have biologically active compounds, which make them attractive fowler for preying these pathogens [6].

Annual postharvest losses are resulting due to insect damage, microbial deterioration, and many other environmental factors such as humidity, aeration, temperature, and cleanliness of the massive storage and are expected to be 10–25% of production throughout the world. Insects are the major problem in stored grain because they destroy the quantity and quality of the grains [7]. Higher plants and their extracts can be used for environmentally safe control of insects. It is claimed that 99 families, 276 genera, and 346 species of medicinal plants have environment- friendly insecticidal properties [8]. Plant extracts or pure compounds control insects in several ways, including antifeedant, growth

inhibitors, toxicity, mortality suppression of reproductive behavior, and fertility [9]. Synthetic chemical pesticides have some serious flaws to environmental and health related concerns. It is expected that only in America about 200 people are dying every year due to this pesticidal poisoning [10]. These problems resulted in renewed interest in formulating new botanical pesticides, which could be nonhazardous, effective, biodegradable, and of low cost and pose less threat to the environment [11].

The aim of the present study was to evaluate the antibacterial, antifungal, and insecticidal activities of different fractions of *Oxalis corniculata*. These include methanol, *n*-hexane, chloroform, ethyl acetate, and *n*-butanol soluble fractions. Selection of *Oxalis corniculata* fractions was based on the fact that these fractions were not previously screened for these activities.

## 2. Material and Methods

**2.1. Collection of Plant Sample.** *Oxalis corniculata* was collected from District Buner, KPK, Pakistan in June 2012. Plant was identified by plant taxonomist Dr. Nisar Ahmad, Chairman Department of Botany, Kohat University of Science & Technology, Kohat, KPK, Pakistan, and a voucher specimen number 169 was stored there in the herbarium.

**2.2. Preparation of Extract.** Plant was shade dried at room temperature and 1 kg dried plant materials were soaked in methanol to obtain methanolic extract. Extract was evaporated under reduced pressure to dryness; the residue was weighed (81 g) and redissolved in distilled water. The aqueous solution of the plant extract was subjected to different solvents on the basis of increasing polarity like *n*-hexane, chloroform, ethyl acetate, and *n*-butanol to get the respective *n*-hexane, chloroform, ethyl acetate, and *n*-butanol solvent soluble fractions with the ratio of 15 g (*n*-hexane fraction), 22 g (chloroform fraction), 16 g (ethyl acetate fraction), 14 g (*n*-butanol fractions), and 10 g (aqueous fraction), respectively. All the fractions were dried at low pressure using rotary evaporator and stored at 4°C.

**2.3. Microbial Strains.** To evaluate the antimicrobial activity of different fractions of *Oxalis corniculata*, nine microbial species were used, five of which were bacterial pathogens including *Bacillus subtilis* (ATCC7966), *Staphylococcus aureus* (ATCC 12600), *Escherichia coli* (ATCC8677), *Shigella dysenteriae* (ATCC29027), and *Salmonella typhi* (ATCC0650) and four fungal species including *Fusarium solani*, *Aspergillus flexneri*, *Aspergillus flavus*, and *Aspergillus niger* were taken from culture collection of Department of Microbiology, Kohat University of Science & Technology, Kohat, Pakistan.

## 3. Antibacterial Assay

**3.1. Preparation of Bacterial Inoculums.** The bacterial strains were subcultured to get fresh cultures of bacteria. For this purpose a single colony from bacterial strain was inoculated on nutrient broth. The broth was incubated for 24 hours

at 37°C. 14 g of nutrient agar media was dissolved in 1 L of distilled water at PH 7 and autoclaved for 20 minutes at 121°C. The media were allowed to cool down to 45°C and poured to petri plates (14 cm) for preparing 75 mL of solid media. Using sterile cork borer (8 mm) 7 wells per plate were made in the solidified media. Agar diffusion method was used for antibacterial activity [12]. Bacterial culture was inoculated on the surface of solid media. The crude extract and fractions were dissolved in dimethyl sulfoxide (DMSO) at the same concentration of 2 mg/mL to prepare stock solutions. From the stock solutions, 100 µL was poured into respective wells. Cefixime was used as positive control while DMSO was used as a negative control. The zones of inhibition of crude extract and fractions were measured in mm after 24 hours of incubation at 37°C and compared with the zone of inhibition of standard drug Cefixime [12].

## 4. Antifungal Assay

**4.1. Preparation of Fungal Inoculums.** Four fungal strains including *Aspergillus flexneri*, *Aspergillus niger*, *Aspergillus flavus*, and *Fusarium solani* were tested for the antifungal activity. Fungal strains were subcultured in potato dextrose agar (PDA) and incubated for 7 days at 28°C. To evaluate the antifungal activity the disk diffusion method was used [3]. Fungal strains were inoculated on the potato dextrose agar plate (PDA) by point inoculation. 100 µL of solution (2 mg/mL in DMSO), pure DMSO (–ve control), and antibiotic terbinafin 2 mg/mL (+ve control) were used. After incubation of 7 days at 28°C, the fungal activities were noted.

## 5. Insecticidal Assay

The insects *Ephestia cautella* and *Tribolium castaneum* were taken from Department of Zoology, Kohat University of Science & Technology, Kohat, Kpk, Pakistan. The insecticidal activity was determined by direct contact application [13]. 60 mm of petri dish was used to conduct the surface film activity of all the extract by dissolving 50 mg/mL of crude extract and fractions in DMSO. Extracts were sprayed on to the lower part of the petri dish and allowed to dry out. The insects were released in these treated petri dishes. Pure DMSO was taken as a standard. These treated petri dishes having insects were kept at room temperature in a secured place. The result was observed from time to time starting from 30 minutes to 48 hours and finally recorded. The mortality of insects was confirmed by using simple microscope to check any movement of their organs. In last, the living (if any) insects were recovered and submitted to their respective department [14].

The percentage mortality rate was determined by the following formula:

$$\text{Mortality (\%)} = \frac{100 - \text{number of survival insamples}}{\text{number of survival in control}} \times 100. \quad (1)$$

TABLE 1: Showing zones of inhibition (mm) against different bacteria.

S. number	Fractions	Gram positive bacteria			Gram negative bacteria	
		<i>B. subtilis</i>	<i>S. aureus</i>	<i>E. coli</i>	<i>S. dysenteriae</i>	<i>S. typhi</i>
1	Crude	24	00	21.3	17	11
2	<i>n</i> -Hexane	14	00	00	14.6	09
3	Chloroform	11.3	00	11	12	00
4	Et. acetate	14.8	00	11.7	00	8.4
5	<i>n</i> -Butanol	24	00	16.5	13.2	08

## 6. Results and Discussion

Medicinal plants are the most prominent source of natural products against various common infectious microbes. The appearance of multidrug-resistant infectious microbes, high cost of synthetic compounds, and uninvited side effects of certain drugs insisted the new era to search for the new curative agents from alternative and low cost sources like medicinal plants.

The current attempt was made due to increasing resistance of different pathogens (bacteria and fungi) and insects against available antibiotics and insecticides, respectively. Plants extracts and compounds are of innovative interest as safe and health friendly antimicrobial and insecticidal agents. As a result the different fractions of *Oxalis corniculata* were screened for their antimicrobial and insecticidal activities.

To assess the antimicrobial activity of *Oxalis corniculata*, the microbial strains used were tested bacterial pathogens including *Escherichia coli*, *Bacillus subtilis*, *Staphylococcus aureus*, *Salmonella typhi*, and *Shigella dysenteriae*; the fungal species including *Fusarium solani*, *Aspergillus flexneri*, *Aspergillus flavus*, and *Aspergillus niger* were used. For the evaluation of insecticidal activity the insects used were *Ephestia cautella* and *Tribolium castaneum*. The plant solvent soluble extracts showed a broad spectrum of activities against used microbes and insects. The crude extract, *n*-butanol, and ethyl acetate soluble fractions showed excellent activities against *Escherichia coli*, *Salmonella typhi*, and *Bacillus subtilis*. Similarly crude extract, *n*-hexane, chloroform, and *n*-butanol soluble fractions were active against *Shigella dysenteriae* but not active in case of ethyl acetate soluble fraction. No activity was recorded against *Staphylococcus aureus* as shown in Table 1. Similarly the crude extract, *n*-hexane, and soluble fractions were also found to have significant activity against fungal strains including *Fusarium solani* and *Aspergillus flexneri*; the crude extract, chloroform, and ethyl acetate soluble fractions were active against *Aspergillus flavus*. The *n*-butanol soluble fraction was only active against *Aspergillus flexneri*; also chloroform, ethyl acetate, and *n*-butanol soluble fractions were inactive against *Fusarium solani*. In case of *Aspergillus niger* all the fractions showed no activity as shown in Table 2. Taley et al., 2012 [15], investigated the methanol and aqueous extracts of *O. corniculata* leaves for antibacterial activities against 5 bacterial strains: *E. coli*, *S. aureus*, *P. aeruginosa*, *P. vulgaris*, and *B. subtilis*. They recorded zone of inhibition in the range of 6–14 mm against these pathogens among which *B. subtilis* showed maximum zone of inhibition

TABLE 2: Showing activity of different fractions against fungi.

S. number	Fractions	<i>A. flavus</i>	<i>A. flexneri</i>	<i>A. niger</i>	<i>F. solani</i>
1	Crude	+	+	-	+
2	<i>n</i> -Hexane	-	+	-	+
3	Chloroform	+	+	-	-
4	Et. acetate	+	-	-	-
5	<i>n</i> -Butanol	-	+	-	-

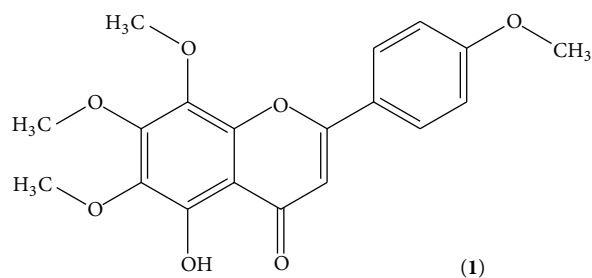


FIGURE 1: 5-Hydroxy-6,7,8,4'-tetramethoxyflavone.

(14 mm), while, in our present investigation, the whole plant (*O. corniculata*) crude extract, its solvent soluble fractions, and the isolated compounds were evaluated for antibacterial and antifungal activities and obtained significant results.

The maximum toxicity of plant against *Ephestia cautella* and *Tribolium castaneum* was recorded for the crud extract and chloroform soluble fraction with highest mortality rate especially for the *Tribolium castaneum* (up to 62%). *n*-Butanol soluble fraction also showed valuable mortality (46%) in 48 hours as shown in Table 3. The lowest mortality rate was recorded for ethyl acetate and *n*-butanol soluble fractions against *Ephestia cautella* (08%) after 48 hours; however it was nonactive till 24 hours. No significant change in toxicity was observed in the experiment with passage of time. The comparative study shows that the plant is more toxic against *Tribolium castaneum* than *Ephestia cautella*. There is no literature available on the insecticidal activity of *Oxalis* species to compare with the present results.

**6.1. Compounds Isolated from *Oxalis corniculata*.** The chloroform soluble fraction was subjected to column chromatography and as a result two known compounds, compound 1 (Figure 1) and compound 2 (Figure 2), were isolated whose structures were elucidated with the help of EI, HREIMS, 1D,

TABLE 3: Showing percentage mortality rate of insects against different fractions of *Oxalis corniculata*.

S. number	Fractions	<i>T. Castaneum</i> 24 hours	<i>T. castaneum</i> 48 hours	<i>E. cautella</i> 24 hours	<i>E. cautella</i> 48 hours
1	Crude	53	57	34	49
2	<i>n</i> -Hexane	15	23	22	25
3	Chloroform	62	62	44	47
4	Et. acetate	11	14	00	08
5	<i>n</i> -Butanol	38	46	00	08

TABLE 4: Zone of inhibition (mm) of compounds 1 and 2 against different bacteria.

S. number	Compounds	<i>E. coli</i>	<i>S. dysenteriae</i>	<i>S. aureus</i>	<i>S. typhi</i>	<i>B. subtilis</i>
1	Compound 1	13.3	14.9	00	10.1	14.3
2	Compound 2	16.5	14.6	00	11.7	15.6

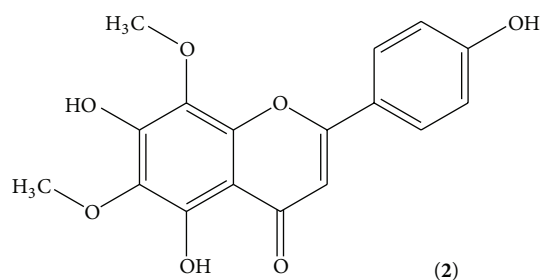


FIGURE 2: 5,7,4'-Trihydroxy-6,8-dimethoxyflavone.

TABLE 5: Percentage mortality rate of *T. castaneum* against compounds 1 and 2.

S. number	Compounds	<i>T. castaneum</i> 24 hours	<i>T. castaneum</i> 48 hours
1	Compound 1	34.21%	38.47%
2	Compound 2	41.56%	45.33%

and 2D NMR techniques. The two isolated compounds 1 and 2 were subjected to antibacterial, antifungal, and insecticidal activities. The result showed that compound 2 was more active than compound 1 against the tested organisms. Antibacterial activity of compound 2 was potent as compared to compound 1. Both the compounds were active against all the tested bacteria except *S. aureus* as shown in Table 4. While compounds 1 and 2 showed negative activity against *Fusarium solani*, *Aspergillus flavus*, *Aspergillus niger*, and *Aspergillus flexneri* which indicates that these compounds are inactive against these species of fungi. Table 5 shows that insecticidal activity of compound 2 was also potent as compared to that of compound 1. Both the compounds showed a good mortality rate against the *Tribolium castaneum*.

## 7. Conclusions

The present study suggests that *Oxalis corniculata* has good antibacterial, antifungal, and insecticidal properties and can

be used for the treatment of infections and control of insects. The plant extracts could be a new source for antibiotics and pesticides with minimum noxious effects on the environment. Further studies may also lead to isolate and characterize the active compounds of the plant extracts and to elucidate their biological mechanisms of action.

## Conflict of Interests

The authors declare that there is no conflict of interests regarding the publication of this paper.

## References

- [1] M. Obeidat, "Antimicrobial activity of some medicinal plants against multidrug resistant skin pathogens," *Journal of Medicinal Plants Research*, vol. 5, no. 16, pp. 3856–3860, 2011.
- [2] M. S. Rahman, M. M. H. Khan, and M. A. H. M. Jamal, "Antibacterial evaluation and minimum inhibitory concentration analysis of *Oxalis corniculata* and *Ocimum santum* against bacterial pathogens," *Biotechnology*, vol. 9, no. 4, pp. 533–536, 2010.
- [3] B. Mahesh and S. Satish, "Antimicrobial activity of some important medicinal plant against plant and human pathogens," *World Journal of Agricultural Sciences*, vol. 4, pp. 839–843, 2008.
- [4] F. Hussain, B. Ahmad, I. Hameed, G. Dastagir, P. Sanauallah, and S. Azam, "Antibacterial, antifungal and insecticidal activities of some selected medicinal plants of polygonaceae," *African Journal of Biotechnology*, vol. 9, no. 31, pp. 5032–5036, 2010.
- [5] S. Maji, P. Dandapat, D. Oja et al., "In vitro anti microbial potentialities of different solvent extracts of ethnomedicinal plants against clinically isolated human pathogens," *Journal of Phytology*, vol. 2, no. 4, pp. 57–64, 2010.
- [6] R. A. Khan, M. R. Khan, S. Sahreen, and J. Bokhari, "Antimicrobial and phytotoxic screening of various fractions of *Sonchus asper*," *African Journal of Biotechnology*, vol. 9, no. 25, pp. 3883–3887, 2010.
- [7] D. Haouas, M. B. Kamel, and M. H. B. Hamouda, "Insecticidal activity of flower and leaf extracts from *Chrysanthemum* species against *Tribolium confusum*," *Journal of Plant Protection*, vol. 3, pp. 87–93, 2008.

- [8] R. K. Singh, R. C. Dhiman, and P. K. Mittal, "Mosquito larvicidal properties of *Momordica charantia* Linn (Family: Cucurbitaceae)," *Journal of Vector Borne Diseases*, vol. 43, no. 2, pp. 88–91, 2006.
- [9] R. Jbilou, A. Ennabili, and F. Sayah, "Insecticidal activity of four medicinal plant extracts against *Tribolium castaneum* (Herbst) (Coleoptera: Tenebrionidae)," *African Journal of Biotechnology*, vol. 5, no. 10, pp. 936–940, 2006.
- [10] P. P. Sharm, A. B. Pardeshi, and D. Vijigiri, "Bioactivity of some medicinal plant extracts against *Musca domestica* L.," *Journal of Ecobiotechnology*, vol. 3, no. 9, pp. 14–16, 2011.
- [11] T. Khan, M. Ahmad, R. Khan, H. Khan, and M. I. Choudhary, "Phytotoxic and insecticidal activities of medicinal plants of Pakistan, *Trichodesma indicum*, *Aconitum laeve* and *Sauromatum guttatum*," *Journal of the Chemical Society of Pakistan*, vol. 30, no. 2, pp. 251–255, 2008.
- [12] A. M. Khan, R. A. Qureshi, S. A. Gillani, and F. Ullah, "Antimicrobial activity of selected medicinal plants of Margalla hills, Islamabad, Pakistan," *Journal of Medicinal Plant Research*, vol. 5, no. 18, pp. 4665–4670, 2011.
- [13] Azizuddin and M. I. Choudhary, "Antibacterial, phytotoxic, insecticidal and cytotoxic potential of *Vitex agnus-castus*," *Journal of Medicinal Plant Research*, vol. 5, no. 23, pp. 5642–5645, 2011.
- [14] M. S. Islam, R. Zahan, M. B. Alam et al., "Studies on antibacterial and insecticidal activities of *Suregada multiflora*," *Libyan Agriculture Research Center Journal International*, vol. 2, no. 2, pp. 62–67, 2011.
- [15] S. L. Taley, A. S. Pethe, and S. P. Rothe, "Studies on antibacterial activity of some plant extracts," *International Multidisciplinary Research Journal*, vol. 2, no. 12, pp. 17–18, 2012.

## Research Article

# Dramatic Improvement of Proteomic Analysis of Zebrafish Liver Tumor by Effective Protein Extraction with Sodium Deoxycholate and Heat Denaturation

Jigang Wang, Yew Mun Lee, Caixia Li, Ping Li, Zhen Li, Teck Kwang Lim, Zhiyuan Gong, and Qingsong Lin

*Department of Biological Sciences, National University of Singapore, 14 Science Drive 4, Singapore 117543*

Correspondence should be addressed to Zhiyuan Gong; [dbsgzy@nus.edu.sg](mailto:dbsgzy@nus.edu.sg) and Qingsong Lin; [dbslinqs@nus.edu.sg](mailto:dbslinqs@nus.edu.sg)

Received 10 October 2014; Revised 17 December 2014; Accepted 17 December 2014

Academic Editor: Mohamed Abdel-Rehim

Copyright © 2015 Jigang Wang et al. This is an open access article distributed under the Creative Commons Attribution License, which permits unrestricted use, distribution, and reproduction in any medium, provided the original work is properly cited.

Majority of the proteomic studies on tissue samples involve the use of gel-based approach for profiling and digestion. The laborious gel-based approach is slowly being replaced by the advancing in-solution digestion approach. However, there are still several difficulties such as difficult-to-solubilize proteins, poor proteomic analysis in complex tissue samples, and the presence of sample impurities. Henceforth, there is a great demand to formulate a highly efficient protein extraction buffer with high protein extraction efficiency from tissue samples, high compatibility with in-solution digestion, reduced number of sample handling steps to reduce sample loss, low time consumption, low cost, and ease of usage. Here, we evaluated various existing protein extraction buffers with zebrafish liver tumor samples and found that sodium deoxycholate- (DOC-) based extraction buffer with heat denaturation was the most effective approach for highly efficient extraction of proteins from complex tissues such as the zebrafish liver tumor. A total of 4,790 proteins have been identified using shotgun proteomics approach with 2D LC, which to our knowledge is the most comprehensive study for zebrafish liver tumor proteome.

## 1. Introduction

It is increasingly important to profile proteins in order to understand biological processes in a postgenomic era as the dynamics of proteins between cells at different times and under different environmental conditions provide an actual biological phenotype. In particular, the presence of posttranslational modifications in proteins further highlights the importance of proteomic analysis which is not replaceable by other genomic approaches [1]. To profile the proteome of tissue samples, the proteins have to be extracted using relevant solvent. Currently, there are two major approaches to prepare the tissue samples for proteome analysis. The first approach, termed as gel-based separation and in-gel digestion, involves the use of detergents like SDS to solubilize the proteins before separation by SDS-PAGE and subsequent digestion of the proteins trapped in the gel [2]. The second approach, termed as in-solution digestion, involves the use of

strong chaotropic reagents like urea and thiourea to solubilize the proteins before digesting the proteins in the solution [3].

Proteomic studies on zebrafish liver tissue had been conducted using the gel-based approaches [4–9]. However, the amount of work required from two-dimensional gel electrophoresis, to protein spot excision, to protein identification using mass spectrometry (MS) can be laborious. In-solution digestion coupled with mass spectrometry (MS) seems to present a better alternative to reduce the labor involved and allow for more high-throughput proteomic analysis. More studies are beginning to adopt this approach for proteomic analysis [10–12]. However, numerous difficulties still exist such as difficult-to-solubilize proteins, poor proteomic analysis in complex tissue samples, and the presence of sample impurities.

In 2009, Wiśniewski et al. [13] developed a protein extraction approach and coined it the filter-aided sample preparation (FASP). FASP incorporates the advantages of

both gel-based and in-solution digestion for subsequent proteomic analysis using MS. FASP uses high concentration of SDS and urea as detergents to solubilize the proteins. This resulted in the need to use an ultrafiltration system consisting of a filter membrane and facilitated via centrifugation to remove these detergents as they are known to interfere with both enzymatic digestion of proteins into peptides and MS analysis. Although the authors demonstrated the effectiveness of FASP in proteomic analysis, multiple steps were included for the removal of the detrimental detergents. These could create unforeseen problems for different types of samples. Hence, there is still a great demand to formulate a highly efficient protein extraction buffer with high protein extraction efficiency from tissue samples, high compatibility with in-solution digestion, reduced number of sample handling steps to reduce sample loss, low time consumption, low cost, and ease of usage.

In this study, we evaluated various existing protein extraction buffers (SDS, RIPA, urea, 2D, sodium deoxycholate (DOC), and triethylammonium bicarbonate (TEAB)/urea/triton-X/SDS (TUTS) [14] buffer) for their protein extraction and solubilization efficiency for in-solution digestion using both 1D SDS-PAGE and shotgun proteomics approaches. Comparison of efficiency using these approaches indicated that DOC was the most efficient protein extraction buffer in our study. Our results provide the evidences for the effective application of DOC-based protein extraction buffer in MS-based proteomic studies on the whole zebrafish liver tumor and our method could be applied to other tissue samples across different organisms for proteomics analysis.

## 2. Materials and Methods

**2.1. Chemicals and Reagents.** All reagents were of ACS grade or higher; all solvents used, including water, were of LC/MS grade. Urea, SDS, DOC, triethylammonium bicarbonate (TEAB), tris(2-carboxyethyl)phosphine (TCEP), phosphoric acid, and formic acid were purchased from Sigma-Aldrich (St. Louis, MO). Sequencing grade trypsin was obtained from Promega (Madison, WI). Methyl methanethiosulfonate (MMTS) was purchased from Pierce, Thermo-Fisher Scientific Inc. (Rockford, IL). Unless otherwise indicated, all the other reagents used for the biochemical methods were purchased from Sigma-Aldrich. LC/MS grade ACN and LC/MS grade water were purchased from Thermo-Fisher Scientific (Waltham, MA).

**2.2. Zebrafish Sample Preparation.** The Tet-on transgenic zebrafish, *TO (xmrk)*, were generated previously by Li et al. [15]. Both male and female *TO (xmrk)* zebrafish were used in this study. The *TO (xmrk)* zebrafish were treated with 60  $\mu\text{g}/\text{mL}$  of doxycycline for 6 weeks to induce the development of liver cancer. The tumor-bearing fish were euthanized in ice-cold water, dissected, and rinsed with phosphate buffered saline (PBS). Liver tumors were collected and stored at  $-80^\circ\text{C}$  until protein extraction. For protein extraction, frozen liver tumors were placed in a ceramic mortar and ground into dry powder using a pestle in the presence of acetone.

Equal amount (10 mg) of tissue powder was transferred to seven Eppendorf tubes containing equal volume (200  $\mu\text{L}$ ) of different protein extraction buffers (Table 1) and placed on ice. Each tube of the mixtures was sonicated using a probe sonicator at 2 s sonication bursts with a 2 s rest between each sonication burst for a total of 1 min. The lysate was then centrifuged in a bench-top centrifuge at 14,000x rpm for half an hour. Each of the supernatants was collected for 1D SDS-PAGE or for in-solution digestion. Samples were aliquoted and stored at  $-80^\circ\text{C}$  for later analysis.

**2.3. 1D SDS-PAGE Comparison of Zebrafish Liver Tumor Proteome Extracted Using Various Buffers.** For SDS buffer and DOC buffer, both raw (without heating) and heat-denatured samples were prepared. The heat denaturation involves heating the samples on a  $95^\circ\text{C}$  heat block for 15 min after sonication. The lysates were then centrifuged in a bench-top centrifuge at 14,000x rpm for half an hour and collected for downstream analysis. Equal volumes (5  $\mu\text{L}$ ) of protein samples extracted by different buffer were mixed with 5  $\mu\text{L}$  of 2x SDS loading buffer. The samples were heated to  $95^\circ\text{C}$  for 10 min and then separated by SDS gel electrophoresis with 10% polyacrylamide gel. After 1D SDS-PAGE, gels were stained using CBB solution (Bio-Rad, Hercules, CA) and destained in accordance with the manufacturer's protocol.

**2.4. Liver Tumor Proteome In-Solution Digestion.** Protein concentration of each lysate was determined using Bradford assay (Bio-Rad). Twenty-microgram samples (extracted by DOC buffer or SDS buffer) were used for the following in-solution digestion. Samples were diluted using 0.5 M TEAB to lower the detergent concentration in order to maintain the activity of the trypsin (0.05% SDS or 1% DOC does not affect the trypsin activity [16, 17]). pH was measured and adjusted to eight for trypsin digestion. The sample was subsequently reduced with 5 mM TCEP in a  $65^\circ\text{C}$  heat block for 60 min and alkylated with 10 mM MMTS for 15 min at room temperature. Following reduction and alkylation, trypsin (1  $\mu\text{g}$ , Promega; protein versus trypsin ratio: 20/1) was added and the sample incubated at  $37^\circ\text{C}$  overnight on a thermoshaker. The digested peptides were stored at  $-20^\circ\text{C}$  pending LC separation and MS analysis.

**2.5. Sample Cleanup before LC-MS/MS.** Before the LC-tandem MS (LC-MS/MS) analysis, the sample must be cleaned up to remove the detergent, dissolution buffer (TEAB), reducing agent (TCEP), alkylating agent (MMTS), SDS, and other unknown interfering substances. To remove most of the DOC, 0.1% TFA was added into the DOC sample. After acidifying the sample, DOC was precipitated and removed by centrifugation at 14,000 rpm for 20 min. Then the DOC sample was subjected to strong cation-exchange chromatography (SCX) using the iTRAQ Method Development Kit (AB SCIEX; Foster City, CA). The bound peptides were eluted with 5% ammonium hydroxide ( $\text{NH}_4\text{OH}$ ) in 30% methanol. The eluate was desalted using a Sep-Pak C18 cartridge (Waters, Milford, MA), dried, and then reconstituted with 100  $\mu\text{L}$  of diluent (98% water, 2% ACN, and 0.05% formic

TABLE 1: Overview of the various lysis buffer and the number of proteins identified using 1D LC-MS/MS shotgun analysis.

Number	Lysis buffer	Buffer component	Heat	Number of protein ID
1	SDS	1% SDS, 0.5 M TEAB	–	NA.
2	SDS	1% SDS, 0.5 M TEAB	+	622
3	RIPA	50 mM Tris, 150 mM NaCl, 1% NP-40, 1% DOC, and 0.1% SDS	–	NA.
4	Urea	9 M urea	–	NA.
5	2D	7 M urea, 2 M thiourea, 4% CHAPS, 20 mM DTT, and 40 mM Tris	–	NA.
6	DOC	5% DOC	–	NA.
7	DOC	5% DOC	+	823
8	TUTS	25 mM TEAB, 8 M urea, 2% triton X-100, and 0.1% SDS	–	NA.

TEAB: triethylammonium bicarbonate; TUTS: TEAB/urea/triton-X/SDS.

acid). For the SDS lysed sample, it was also cleaned up by SCX and Sep-Pak C18 cartridge.

**2.6. Protein Identification and Quantification.** The detailed methods for LC-MS/MS were described previously [18]. Briefly, separation of the peptides was carried out on an Eksigent nanoLC Ultra and ChiPLC-nanoflex (Eksigent, Dublin, CA) in Trap-Elute configuration. Five-microliter samples were loaded onto the LC system. Peptides were separated by a gradient formed by 2% ACN, 0.1% FA (mobile phase A), and 98% ACN, 0.1% FA (mobile phase B): 5–12% of mobile phase B (20 min), 12–30% of mobile phase B (90 min), 30–90% of mobile phase B (2 min), 90% of mobile phase B (5 min), 90–5% of mobile phase B (3 min), and 5% of mobile phase B (13 min), at a flow rate of 300 nL/min. The MS analysis was performed on a TripleTOF 5600 system (AB SCIEX) in information dependent mode.

The detailed method of ProteinPilot analysis was described previously [18]. Briefly, the protein identification was performed with ProteinPilot 4.5 (AB SCIEX) which uses the Paragon algorithm to perform database searches. The database used includes the International Protein Index (IPI) v3.87 zebrafish protein sequences. The search parameters used were as follows: cysteine alkylation of MMTS; trypsin digestion; TripleTOF 5600; and biological modifications. Redundancy was eliminated by the grouping of identified proteins using the ProGroup algorithm in the software. A decoy database search strategy was used to determine the false discovery rate for peptide identification. A corresponding randomized database was generated using the Proteomics System Performance Evaluation Pipeline feature in the ProteinPilot Software 4.5. In this study, a strict unused score cut-off  $\geq 1.3$  was adopted as the qualification criterion, which corresponded to a peptide confidence level of  $\geq 95\%$ . The identification results were then exported into Microsoft Excel for manual data analysis.

**2.7. Gene Ontology and Pathway Analysis.** The identified proteins were subjected to gene ontology (GO) analysis using Software Tool for Rapid Annotation of Proteins (STRAP) v1.5.0.0 [19]. The pathway analysis was performed using Ingenuity Pathway Analysis (IPA) software v21249400 (Qiagen,

Hilden, Germany). The figures generated were abstracted from IPA.

### 3. Results and Discussion

**3.1. 1D SDS-PAGE Showed Better Protein Extraction Efficiency with SDS and DOC.** In order to maximize the efficiency in the protein extraction and solubilisation of the liver tumors for downstream analysis, we compared various extraction buffers commonly used in laboratories worldwide (Table 1). Of these, SDS was chosen because it is one of the most common surfactants used to assist in the solubilisation of proteins, especially membrane proteins, during protein extraction [12, 13, 20]. Urea, a chaotrope, is another commonly used protein solubilizing agent that competes with the protein's native interactions, resulting in the unfolding of the protein and its solubilization [21]. In addition, urea is also found in TUTS buffer (one of the buffers tested in our study) which was formulated for a previous study on the subcellular localization of membrane proteins [14]. Furthermore, thiourea, a component in the 2D extraction buffer, is found to be a stronger denaturant than urea [22]. Henceforth, the 2D extraction buffer was also included in our study. DOC is an inexpensive bile salt surfactant which has been used in studies of membrane proteins [23, 24] and was included in our study due to its comparative protein extraction efficiency as SDS [23]. Lastly, RIPA is another commonly used protein extraction buffer in proteomic studies, and it contains a small percentage of both SDS and DOC.

Following protein extraction from the harvested liver tumor tissue using the various extraction buffers, 1D SDS-PAGE analysis was performed to provide an initial visual indication of protein extraction efficiency. As shown in Figure 1, protein extraction using the DOC extraction buffer was potentially better than the other extraction buffers, as evident from the larger number of protein bands as well as higher intensity bands in the DOC-extracted protein lysate samples. Our results were comparable to a previous study conducted by Proc et al. [23], who demonstrated that both SDS and DOC were more superior denaturants than urea in terms of the greater amount of solubilized human plasma proteins. This could explain the larger number of protein bands in the liver tumor samples extracted with SDS or DOC. However, in

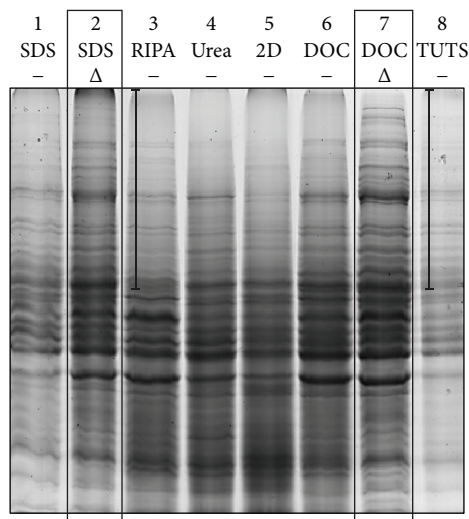


FIGURE 1: CBB stained gel from the 1D SDS-PAGE of proteins extracted from liver tumor samples using various extraction buffers. The loading concentration of each sample reflects the amount of proteins extracted from the liver samples before trypsin digestion. Larger number of protein bands would mean larger number of proteins extracted. Darker protein bands from each lane would mean a higher amount of proteins extracted. Black boxes indicate the two best extraction buffers and conditions in terms of number of protein bands and the intensity of the CBB stain. The highlighted regions for Lanes 2 and 7 show a larger number of visible bands compared to other lanes.  $\Delta$ : heat.

extraction buffers like RIPA and TUTS, the concentration of SDS and DOC could be too low to obtain comparable results with those of SDS or DOC extraction buffers.

Furthermore, as shown in Figure 1, the addition of the heat-denaturing step in our protocol greatly increased the extraction efficiency in SDS-extracted as well as DOC-extracted samples. In contrast, the introduction of the heat denaturing step by Proc et al. [23] did not show a significant increase in the digestion efficiency of human plasma proteins. Our observations were based on the amount of proteins extracted directly from a tissue rather than the digestion efficiency of trypsin investigated by the authors. Additionally, our results were based on the whole liver tumor tissue rather than just plasma proteins. Hence, the addition of heat denaturation step could greatly improve the amount of proteins extracted in our study. Hence, our results indicated the need to include the heat denaturation step to improve the protein extraction efficiency from the whole tissue.

**3.2. 1D LC-MS/MS Shotgun Analysis of SDS- and DOC-Extracted Liver Tumor Samples.** Following the above observations, both SDS-heat-extracted (SDS $\Delta$ X) and DOC-heat-extracted (DOC $\Delta$ X) samples were subjected to 1D LC-MS/MS shotgun proteomics (1D shotgun) analysis to determine the number of proteins that could be identified. In our 1D shotgun results, 659 and 881 unique proteins were identified from SDS $\Delta$ X and DOC $\Delta$ X samples, respectively (Supplementary Tables 1 and 2) (see Supplementary Material available online at <http://dx.doi.org/10.1155/2015/763969>).

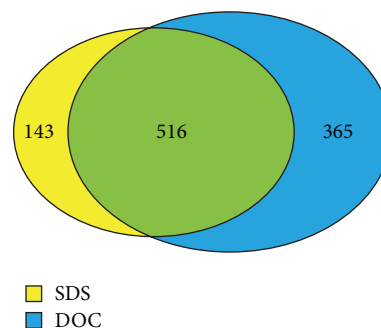


FIGURE 2: A comparison between the identified proteins from SDS-heat- and DOC-heat-extracted samples. A total of 1,024 unique proteins were identified from 1D shotgun analysis.

Between the two sets of identified proteins, there were 516 overlapping proteins, with 143 and 365 proteins uniquely found in SDS $\Delta$ X and DOC $\Delta$ X samples, respectively (Figure 2). Therefore, the use of DOC-heat might be more effective than SDS-heat in extracting liver proteins or DOC-heat might have improved the downstream sample processing mainly including trypsin digestion and MS analysis.

Although no direct comparison of the 1D shotgun profile between SDS $\Delta$ X and DOC $\Delta$ X liver tumor tissue samples has been reported in literature, a study by Zhou et al. [24] on the evaluation of the application of SDS in the proteomic analysis of rat hippocampal plasma membrane has shown that the use of DOC has resulted in a larger, although insignificant, number of total identified plasma membrane proteins or membrane-associated proteins than the SDS method. Our results also showed a difference in the total number of proteins identified between SDS $\Delta$ X and DOC $\Delta$ X samples, with the latter having a significantly larger number of proteins identified.

To determine whether different proteins identified from the two groups differ in terms of their subcellular localization, we conducted a GO analysis of the proteins using the *D. rerio* GOSLIM database. In the GO analysis of SDS $\Delta$ X and DOC $\Delta$ X samples, majority of the proteins are found in the cytoplasm (20% and 25% resp.; Figure 3). The subcellular localization profiles of both samples are observed to be very similar, but the additional proteins identified from the DOC $\Delta$ X samples resulted in more even distribution of protein in the various subcellular locations, even detecting proteins in the endosome, which is absent from the SDS $\Delta$ X sample. Our results highlighted the comparability of DOC- and SDS-based extraction method in their proteome coverage.

**3.3. 2D LC-MS/MS Shotgun Analysis of DOC-Extracted Liver Tumor Sample.** Since the DOC extraction buffer was able to extract more proteins from the nucleus and various organelles compared to the SDS extraction buffer, this could potentially increase the proteome coverage of the whole zebrafish liver using the DOC extraction buffer. To further increase the coverage of the whole proteome for the liver tumors, we conducted a 2D LC-MS/MS shotgun (2D shotgun) analysis on the DOC $\Delta$ X sample since our 1D shotgun analysis revealed a better proteome coverage using DOC extraction buffer.

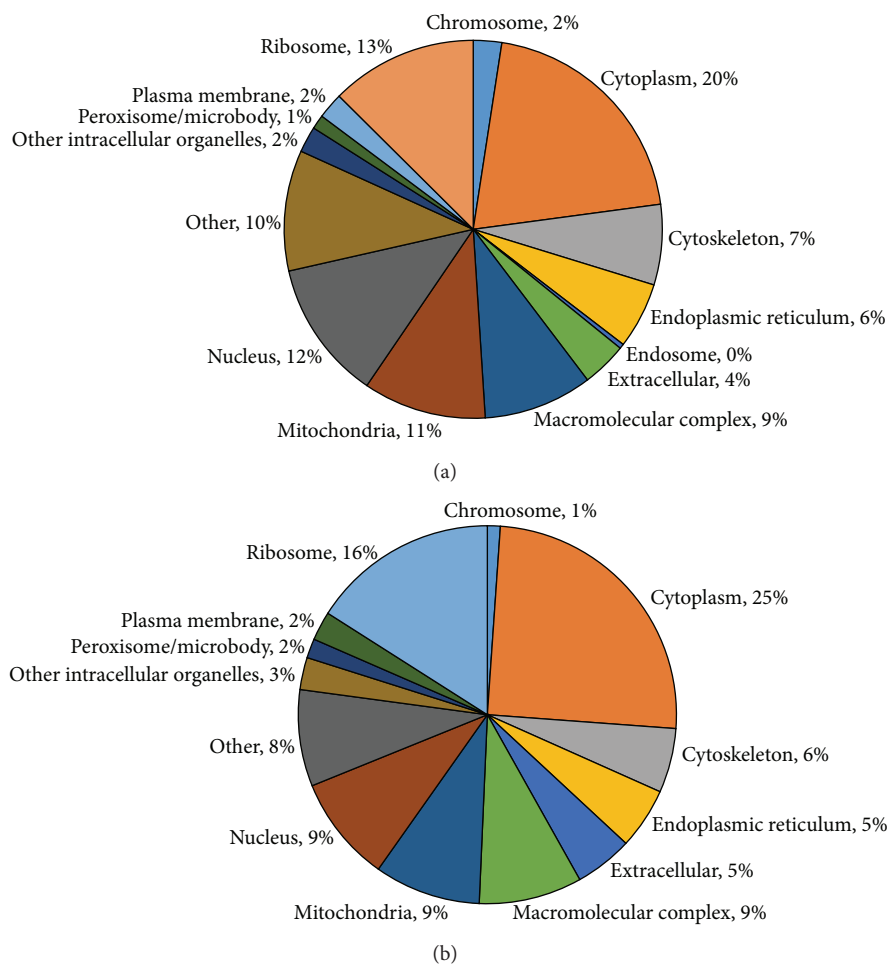


FIGURE 3: Subcellular localization of the identified proteins based on GO analysis. (a) 881 proteins identified in DOC $\Delta$ X samples; (b) 659 proteins identified in SDS $\Delta$ X samples generated using STRAP. The identified subcellular localization profiles are largely similar between both samples, with only the DOC $\Delta$ X samples having proteins located in the endosome. The larger number of proteins identified from the DOC $\Delta$ X samples also showed more even distribution of proteins across all subcellular locations. Percentages are rounded to the nearest whole number.

By 2D shotgun analysis, we identified a total of 4,790 unique proteins from the DOC $\Delta$ X sample. In comparison, a previous study conducted by Wang et al. [12] on the proteomic profiling of cytosolic component of the zebrafish liver has identified a total of 1,204 proteins via the combination of three extraction methods as compared to a single one in our study. In another study by Carlson et al. [11], the investigators have used 8 M urea buffer to extract the proteins from adult zebrafish liver tissue, identifying a total of 745 proteins. Furthermore, Abramsson et al. [10] have employed a mixture of chloroform and methanol to extract proteins from various adult zebrafish organs including the liver and they have identified a total of 1,394 proteins from multiple tissues including blood, brain, fin, heart, intestine, liver, and skeletal muscle.

To the best of our knowledge, our study has by far the largest number of proteins reported to be identified from the zebrafish liver tissue. A full list of the proteins identified is presented in Supplementary Table 3. Using STRAP, the identified proteins were grouped according to their (1) subcellular

locations, (2) biological processes, or (3) molecular functions. The data generated provide an overview of the proteins identified from *xmrk* oncogene induced zebrafish liver tumor (Figure 4).

The grouping of the 2D shotgun dataset indicated that the identified proteins were well represented across various subcellular locations, thus dismissing the possibility of subcellular location biasness. As illustrated in Figure 4(a), the identified proteins were originated from various subcellular locations, importantly from the nucleus (17%), mitochondria (8%), and the various organelles. In particular, the presence of plasma membrane proteins (4%) in our 2D shotgun dataset supports the previous study on the effectiveness of DOC in the extraction of poor water-soluble proteins like plasma membrane proteins by Zhou et al. [24]. This provides a further support in the use of DOC for tissue extraction of liver and other organs.

From our GO analysis for biological processes, we identified proteins involved mainly in cellular process (40%), regulation (19%), developmental process (9%), and localization

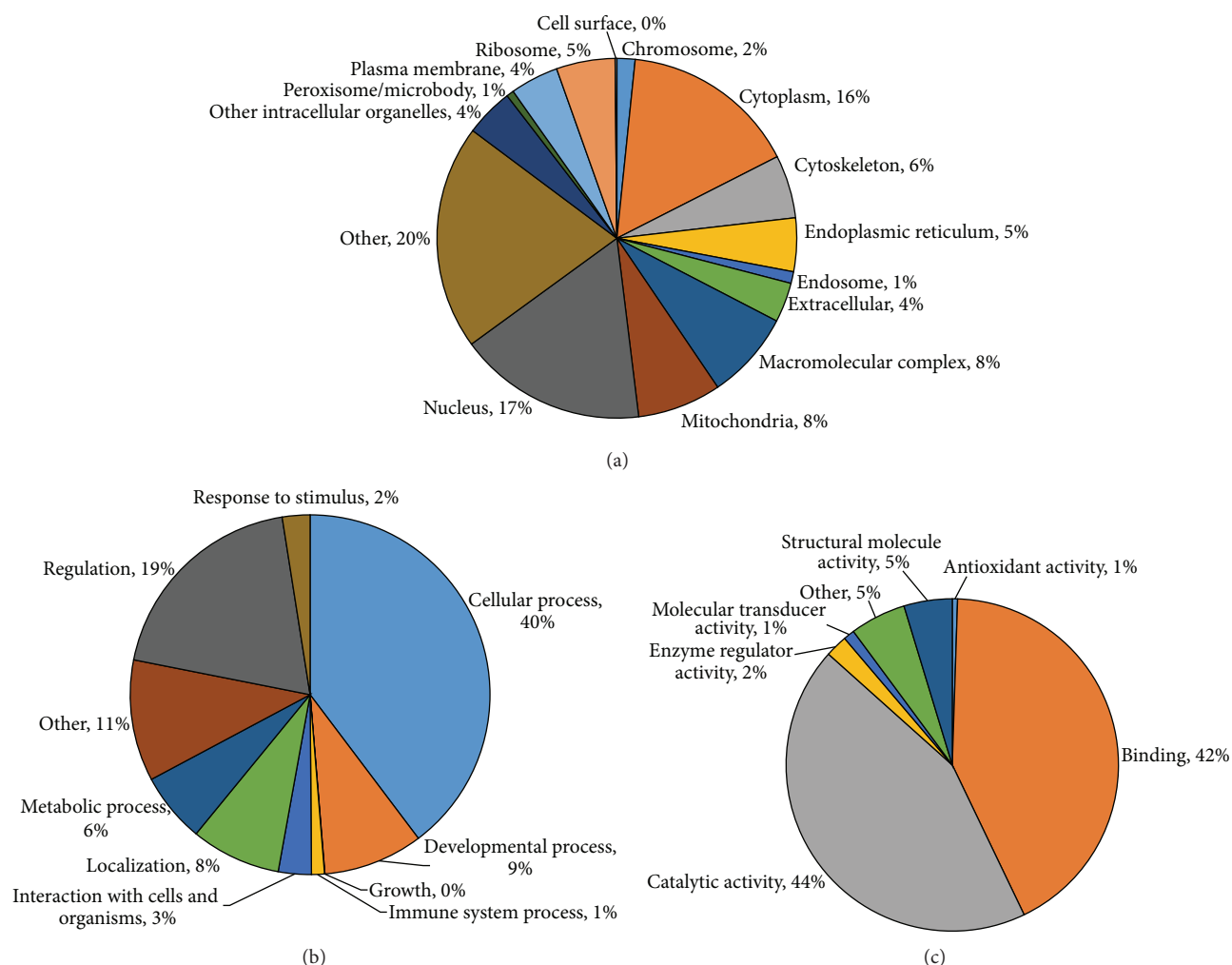


FIGURE 4: Distribution of proteins identified from the 2D shotgun dataset of DOC-extracted liver tumor samples based on (a) subcellular localization; (b) biological processes; (c) molecular functions. A total of 4,790 proteins were used in this GO analysis using STRAP. Percentages are rounded to the nearest whole number.

(8%; Figure 4(b)). Our GO analysis for molecular functions identified proteins mainly with catalytic activity (44%) and binding functions (42%; Figure 4(c)). From our GO analysis, we have demonstrated the capability of our DOC-based protein extraction method to generate proteomic data, providing a platform to allow protein extraction from various organs for the study of diseases via proteomic approaches.

**3.4. Identification of Proteins Involved in Important Signaling Pathways of Liver Cancer.** Since the protein samples for our proteomic analysis were derived from liver tumors induced by expression of the *xmrk* oncogene, it is interesting to see if our DOC-based extraction method was able to identify proteins from pathways related to liver cancer. Our IPA results identified proteins involved in various diseases and biological functions such as cancer (2545 proteins), cell cycle progression (268 proteins), cell death (938 proteins), and proliferation of cells (1009 proteins) which could provide us with insight into liver cancer in future studies. More pieces

of detailed information pertaining to the proteins classified into the respective diseases and biological functions with significance to liver cancer were provided in Supplementary Table 4.

Further analysis using IPA revealed high coverage of our identified proteins in numerous canonical pathways. A close look into the pathways involved in the molecular mechanism of cancer identified a total of 77 associated proteins from our dataset, and Figure 5 shows the coverage of these proteins in the various cancer pathways. The coverage is relatively extensive, with many proteins identified upstream of pathways such as EGFR-Ras-mitogen-activated protein kinase (MAPK) and phosphoinositide 3-kinase/protein kinase B (PI3K/AKT). The carcinogenesis of liver cancer consists of a complex, multifactorial, stepwise development [25]. These include genetic mutations affecting signaling pathway such as Wnt- $\beta$ -catenin, hedgehog, hepatocyte growth factor/mesenchymal-epithelial transition factor (HGF/*c*-Met), insulin-like growth factor (IGF), PI3K/AKT/mammalian

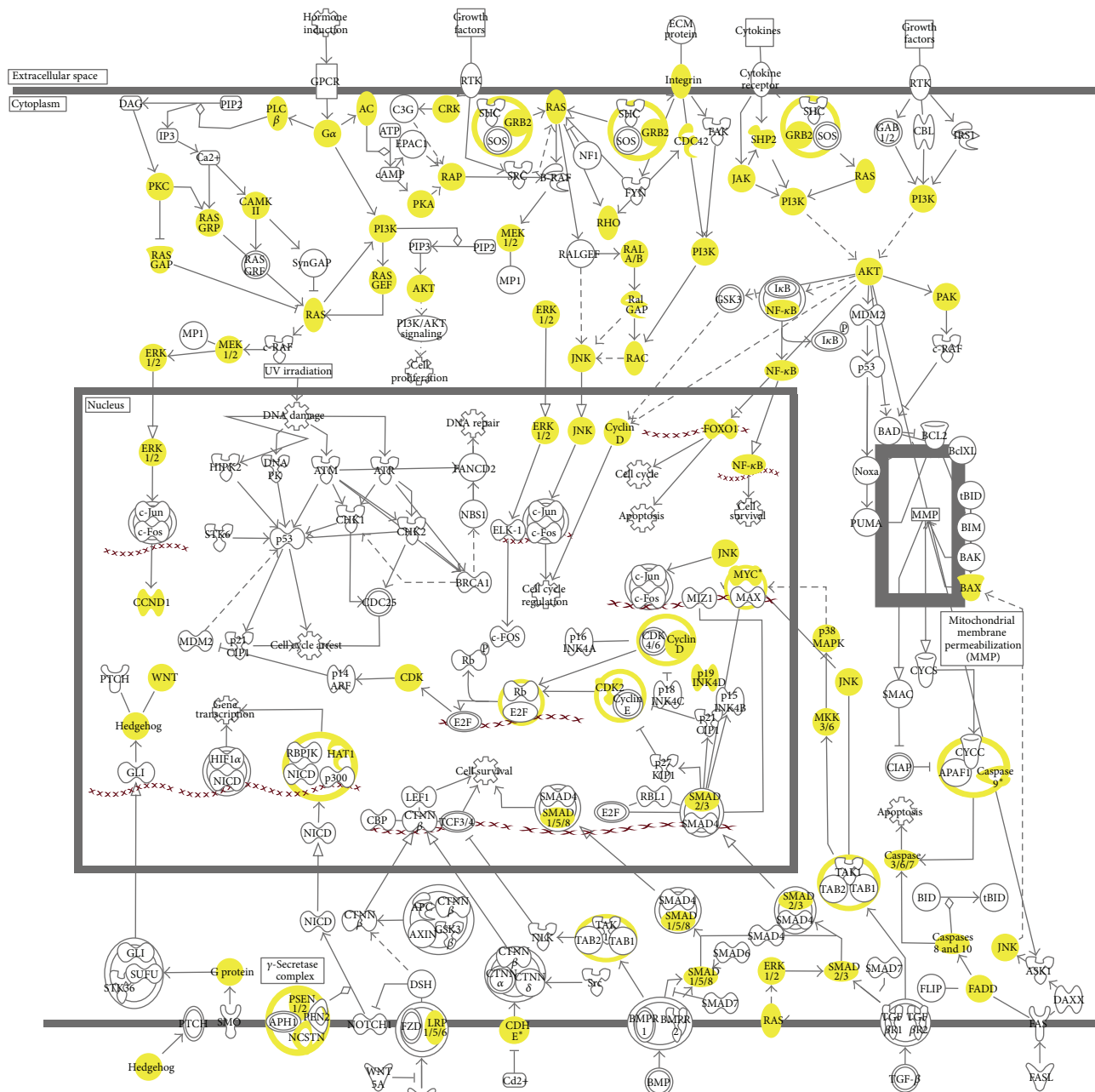


FIGURE 5: The major pathways involved in the molecular mechanisms of cancer as adapted from Ingenuity Pathway Analysis (IPA) database. The highlighted proteins in yellow depict our identified proteins from our 2D-LC-MS/MS analysis. A total of 77 proteins from our identified dataset from our 2D-LC-MS/MS are associated with the molecular mechanisms of cancer.

target of rapamycin (mTOR), MAPK, p53, phosphoinositide-3-kinase (PI3K), Janus kinase-signal transducers and activators of transcription (JAK-STAT), and transforming growth factor- $\beta$  (TGF $\beta$ ) pathways [25–27].

These genetic alternations will result in changes to the cellular proteome; thus the use of comprehensive approaches to profile for these changes might provide insights to the molecular mechanism leading to the development of liver cancer. Our IPA results revealed good representation of our

identified proteins in Wnt- $\beta$ -catenin (28 proteins), HGF/c-Met (28 proteins), IGF (32 proteins), PI3K/AKT/mTOR (79 proteins), MAPK (51 proteins), JAK-STAT (21 proteins), and TGF $\beta$  (21 proteins) pathways. A detailed list of the identified proteins for each pathway is listed in Supplementary Table 4. These results again demonstrated the potential of our DOC-based protein extraction method in high-throughput proteomic studies to elucidate the molecular progression of diseases.

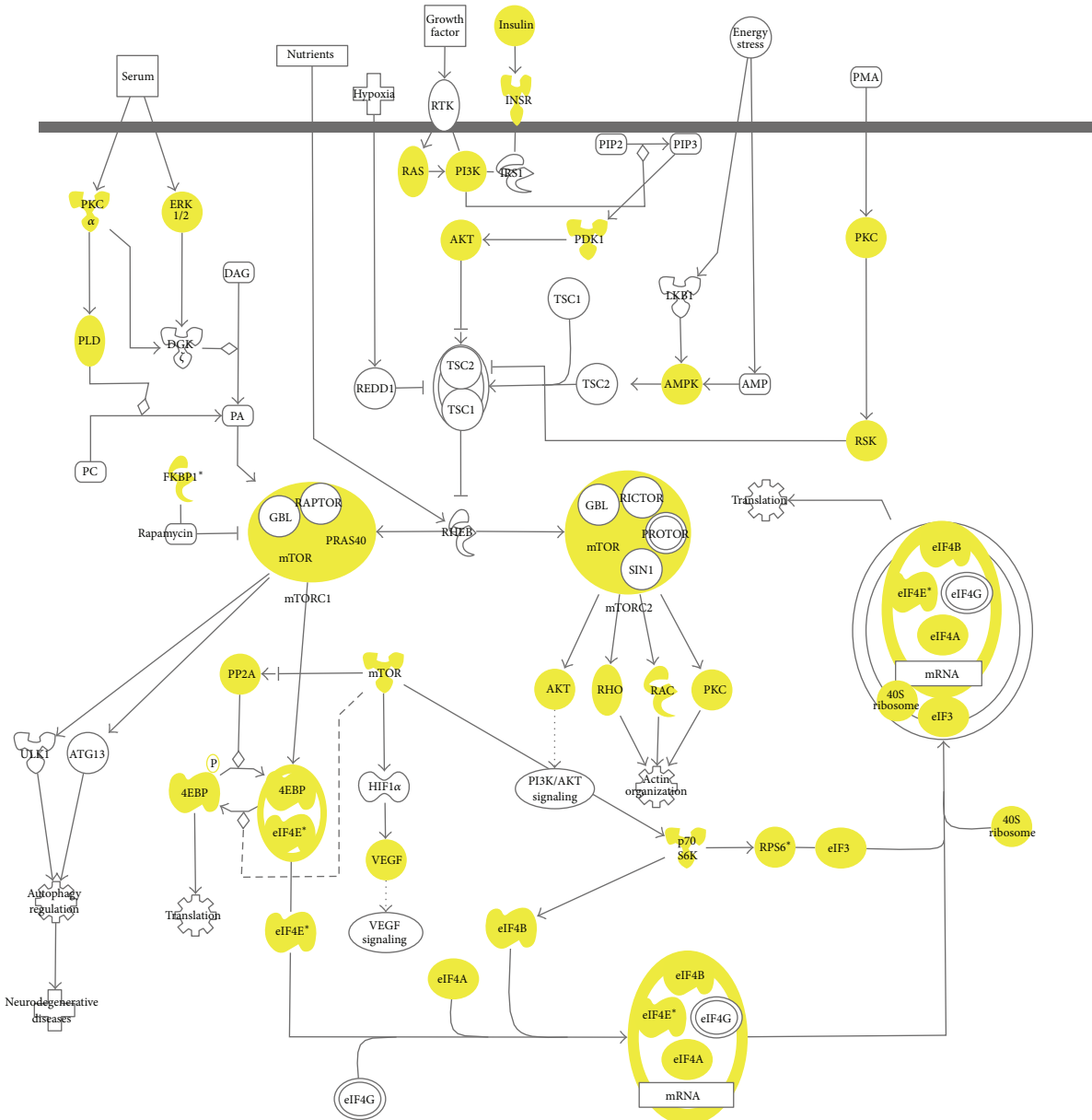


FIGURE 6: The PI3K/AKT/mTOR pathway as adapted from Ingenuity Pathway Analysis (IPA) database. The highlighted proteins in yellow depict our identified proteins from our 2D-LC-MS/MS analysis. A total of 79 proteins from our identified dataset from our 2D-LC-MS/MS are associated with this pathway.

Two of the fundamental hallmarks of cancers are the ability to sustain prolonged cell proliferation and the use of abnormal metabolic pathways to generate energy. The PI3K/AKT/mTOR pathway is documented to regulate cell growth, aging, and metabolism [28]. Furthermore, our previous study also identified the presence of dysregulated PI3K/AKT/mTOR pathway in *xmrk* zebrafish liver tumors [29]. It has been documented that this pathway is upregulated in 40–50% of hepatocellular carcinoma, which is the most common primary cancer of the liver [30–32]. Henceforth, we subjected our 2D shotgun dataset to pathway analysis using IPA. Our results showed that 79 associated proteins were identified belonging to the PI3K/AKT/mTOR pathway,

notably Ras, PI3K, AKT, mTOR, p70S6K, 4EBP, and eIF4E proteins (Figure 6). With such a high coverage of proteins associated with the PI3K/AKT/mTOR pathway, it would be highly beneficial for further studies pertaining to this pathway in relation to liver cancer. This again demonstrates the potential of our DOC-based protein extraction method in high-throughput proteomic studies to elucidate the molecular progression of diseases.

**3.5. Overview of the Strengths of DOC in Protein Extraction from Tissue Samples.** Our study demonstrated the feasibility of using DOC in the extraction of proteins from zebrafish liver tumor tissue. Figure 7 presents a general overview

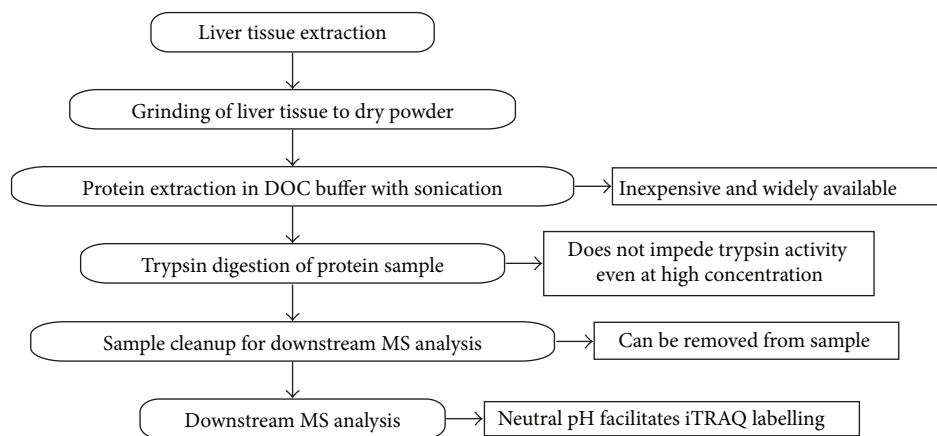


FIGURE 7: An overview of advantages of DOC as a protein extraction buffer for proteomic analysis.

of the advantages of using DOC as an extraction buffer for proteomic studies. DOC is an inexpensive and widely available denaturant. In addition, its acid-insolubility and precipitation at low pH enable its removal from the sample before LC-MS/MS analysis [24]. This is one of the key features over the more commonly used SDS. SDS is impossible to be removed by reversed-phase high performance LC, and trace amount of SDS (<0.01%) will disrupt the separation of peptides with LC [33, 34]. Moreover, SDS suppresses the ionization in matrix-assisted laser desorption/ionization and electrospray ionization MS approaches [23], causing the loss of signal that could potentially result in the low-confidence detection of proteins.

Another key to obtain a large coverage of proteins in a proteome profiling study is the complete digestion of the proteins into peptides. Thus, any chemical or solvent that impedes the activity of the enzyme (commonly trypsin) used would result in reduced enzymatic digestion and peptide numbers. The reduced amount of peptides will result in reduced detection, and hence the identification of the protein will be affected. However, the activity of trypsin is largely unaffected by high concentration of DOC solution, even up to 10% DOC [16]. This property allows the use of a higher concentration of the denaturant DOC to aid in solubilizing those hard-to-solubilize proteins.

Additionally, the pH value of 8 for DOC also facilitates trypsin digestion without the need to readjust the pH. Furthermore, it is also compatible with iTRAQ approach, which is by far the most commonly used quantitative proteomics profiling approach. The pH for iTRAQ labelling is optimally conducted at pH 8. Hence, the pH value does not need to be adjusted before iTRAQ labelling, reducing the amount of work needed as well as potential parallel sample processing variations. Interestingly, iTRAQ-based proteomic studies have a pH reduction step before applying the sample to SCX. Therefore, the reduction in pH could result in the precipitation of DOC, hence its removal.

The addition of heat during the processing of our DOC $\Delta$ X sample further improved the protein extraction efficiency of DOC as highlighted in our previous session. Heat was not applied to extraction buffers containing urea because heat

can break down urea to release isocyanate that can cause carbamylation of proteins [35]. In addition, heating of protein samples can induce protein aggregation without the presence of additives such as detergents [36]. Hence, heat could induce protein aggregation in the other lysis buffers containing the low concentration of detergents and denaturants. However, the high concentration of detergents in our SDS and DOC extraction buffers prevented potential protein aggregation with the addition of heat to our protein extraction step, further highlighting the strength of our DOC-heat-extraction method.

#### 4. Conclusions

In conclusion, the advantages of DOC coupled with heat treatment have greatly increased the number of proteins identified by mass spectrometry in proteomic studies, and this further indicated the suitability and simplicity of DOC in protein extraction of tissue from liver and other organs. Our positive evaluation of DOC is in line with the study by Proc et al. [23], who have demonstrated the high digestion efficiencies, and the highest average reproducibility in the proteins detected among other chemicals and solvents, recommending DOC as the most ideal denaturant over SDS. More importantly, we have shown the suitability of DOC in protein extraction of complex tissue (liver tumors in this study) without compromising the quality and coverage of the proteome. This is further justified by our detection of low abundant proteins, thus allowing for the detection of potential cancer biomarkers in our liver tumor samples.

#### Conflict of Interests

The authors declare that there is no conflict of interests regarding the publication of this paper.

#### Authors' Contribution

Jigang Wang and Yew Mun Lee equally contributed to this paper.

## Acknowledgments

Research of Zhiyuan Gong was supported by National Medical Research Council of Singapore. The LC/MS works were conducted in the Protein and Proteomics Centre, National University of Singapore.

## References

- [1] D. F. Stroncek, C. Burns, B. M. Martin, L. Rossi, F. M. Marincola, and M. C. Panelli, "Advancing cancer biotherapy with proteomics," *Journal of Immunotherapy*, vol. 28, no. 3, pp. 183–192, 2005.
- [2] A. Shevchenko, M. Wilm, O. Vorm, and M. Mann, "Mass spectrometric sequencing of proteins from silver-stained polyacrylamide gels," *Analytical Chemistry*, vol. 68, no. 5, pp. 850–858, 1996.
- [3] M. P. Washburn, D. Wolters, and J. R. Yates, "Large-scale analysis of the yeast proteome by multidimensional protein identification technology," *Nature Biotechnology*, vol. 19, no. 3, pp. 242–247, 2001.
- [4] M. de Wit, D. Keil, N. Remmerie et al., "Molecular targets of TBBPA in zebrafish analysed through integration of genomic and proteomic approaches," *Chemosphere*, vol. 74, no. 1, pp. 96–105, 2008.
- [5] Y. Jin, X. Zhang, D. Lu, and Z. Fu, "Proteomic analysis of hepatic tissue in adult female Zebrafish (*Danio rerio*) exposed to atrazine," *Archives of Environmental Contamination and Toxicology*, vol. 62, no. 1, pp. 127–134, 2012.
- [6] W. Kim, S. O. Lim, J. S. Kim et al., "Comparison of proteome between hepatitis B virus- and hepatitis C virus-associated hepatocellular carcinoma," *Clinical Cancer Research*, vol. 9, no. 15, pp. 5493–5500, 2003.
- [7] C. Li, Y.-X. Tan, H. Zhou et al., "Proteomic analysis of hepatitis B virus-associated hepatocellular carcinoma: identification of potential tumor markers," *Proteomics*, vol. 5, no. 4, pp. 1125–1139, 2005.
- [8] M. Wang, L. L. Chan, M. Si, H. Hong, and D. Wang, "Proteomic analysis of hepatic tissue of zebrafish (*Danio rerio*) experimentally exposed to chronic microcystin-LR," *Toxicological Sciences*, vol. 113, no. 1, Article ID kfp248, pp. 60–69, 2009.
- [9] W. Zhang, Y. Liu, H. Zhang, and J. Dai, "Proteomic analysis of male zebrafish livers chronically exposed to perfluorononanoic acid," *Environment International*, vol. 42, no. 1, pp. 20–30, 2012.
- [10] A. Abramsson, A. Westman-Brinkmalm, J. Pannee et al., "Proteomics profiling of single organs from individual adult zebrafish," *Zebrafish*, vol. 7, no. 2, pp. 161–168, 2010.
- [11] P. Carlson, D. M. Smalley, and R. J. van Beneden, "Proteomic analysis of arsenic-exposed zebrafish (*Danio rerio*) identifies altered expression in proteins involved in fibrosis and lipid uptake in a gender-specific manner," *Toxicological Sciences*, vol. 134, no. 1, pp. 83–91, 2013.
- [12] N. Wang, L. MacKenzie, A. G. De Souza, H. Zhong, G. Goss, and L. Li, "Proteome profile of cytosolic component of zebrafish liver generated by LC-ESI MS/MS combined with trypsin digestion and microwave-assisted acid hydrolysis," *Journal of Proteome Research*, vol. 6, no. 1, pp. 263–272, 2007.
- [13] J. R. Wiśniewski, A. Zougman, N. Nagaraj, and M. Mann, "Universal sample preparation method for proteome analysis," *Nature Methods*, vol. 6, no. 5, pp. 359–362, 2009.
- [14] P. G. Sadowski, T. P. J. Dunkley, I. P. Shadforth et al., "Quantitative proteomic approach to study subcellular localization of membrane proteins," *Nature Protocols*, vol. 1, no. 4, pp. 1778–1789, 2006.
- [15] Z. Li, X. Huang, H. Zhan et al., "Inducible and repressible oncogene-addicted hepatocellular carcinoma in Tet-on xmrk transgenic zebrafish," *Journal of Hepatology*, vol. 56, no. 2, pp. 419–425, 2012.
- [16] Y. Lin, J. Zhou, D. Bi, P. Chen, X. Wang, and S. Liang, "Sodium-deoxycholate-assisted tryptic digestion and identification of proteolytically resistant proteins," *Analytical Biochemistry*, vol. 377, no. 2, pp. 259–266, 2008.
- [17] N. Zhang, R. Chen, N. Young et al., "Comparison of SDS- and methanol-assisted protein solubilization and digestion methods for *Escherichia coli* membrane proteome analysis by 2-D LC-MS/MS," *Proteomics*, vol. 7, no. 4, pp. 484–493, 2007.
- [18] D. Ghosh, Z. Li, X. F. Tan, T. K. Lim, Y. Mao, and Q. Lin, "ITRAQ based quantitative proteomics approach validated the role of calcyclin binding protein (CacyBP) in promoting colorectal cancer metastasis," *Molecular and Cellular Proteomics*, vol. 12, no. 7, pp. 1865–1880, 2013.
- [19] V. N. Bhatia, D. H. Perlman, C. E. Costello, and M. E. McComb, "Software tool for researching annotations of proteins: open-source protein annotation software with data visualization," *Analytical Chemistry*, vol. 81, no. 23, pp. 9819–9823, 2009.
- [20] F. Wu, D. Sun, N. Wang, Y. Gong, and L. Li, "Comparison of surfactant-assisted shotgun methods using acid-labile surfactants and sodium dodecyl sulfate for membrane proteome analysis," *Analytica Chimica Acta*, vol. 698, no. 1–2, pp. 36–43, 2011.
- [21] B. J. Bennion and V. Daggett, "The molecular basis for the chemical denaturation of proteins by urea," *Proceedings of the National Academy of Sciences of the United States of America*, vol. 100, no. 9, pp. 5142–5147, 2003.
- [22] J. A. Gordon and W. P. Jencks, "The relationship of structure to the effectiveness of denaturing agents for proteins," *Biochemistry*, vol. 2, pp. 47–57, 1963.
- [23] J. L. Proc, M. A. Kuzyk, D. B. Hardie et al., "A quantitative study of the effects of chaotropic agents, surfactants, and solvents on the digestion efficiency of human plasma proteins by trypsin," *Journal of Proteome Research*, vol. 9, no. 10, pp. 5422–5437, 2010.
- [24] J. Zhou, T. Zhou, R. Cao et al., "Evaluation of the application of sodium deoxycholate to proteomic analysis of rat hippocampal plasma membrane," *Journal of Proteome Research*, vol. 5, no. 10, pp. 2547–2553, 2006.
- [25] M. A. Feitelson, B. Sun, N. L. Satiroglu Tufan, J. Liu, J. Pan, and Z. Lian, "Genetic mechanisms of hepatocarcinogenesis," *Oncogene*, vol. 21, no. 16, pp. 2593–2604, 2002.
- [26] R. N. Aravalli, C. J. Steer, and E. N. K. Cressman, "Molecular mechanisms of hepatocellular carcinoma," *Hepatology*, vol. 48, no. 6, pp. 2047–2063, 2008.
- [27] A. Lachenmayer, C. Alsinet, C. Y. Chang, and J. M. Llovet, "Molecular approaches to treatment of hepatocellular carcinoma," *Digestive and Liver Disease*, vol. 42, supplement 3, pp. S264–S272, 2010.
- [28] M. Laplante and D. M. Sabatini, "mTOR signaling in growth control and disease," *Cell*, vol. 149, no. 2, pp. 274–293, 2012.
- [29] W. Zheng, Z. Li, A. T. Nguyen, C. Li, A. Emelyanov, and Z. Gong, "Xmrk, Kras and Myc transgenic zebrafish liver cancer models share molecular signatures with subsets of human hepatocellular carcinoma," *PLoS ONE*, vol. 9, no. 3, Article ID e91179, 2014.

- [30] F. Sahin, R. Kannangai, O. Adegbola, J. Wang, G. Su, and M. Torbenson, "mTOR and P70 S6 kinase expression in primary liver neoplasms," *Clinical Cancer Research*, vol. 10, no. 24, pp. 8421–8425, 2004.
- [31] W. Sieghart, T. Fuereder, K. Schmid et al., "Mammalian target of rapamycin pathway activity in hepatocellular carcinomas of patients undergoing liver transplantation," *Transplantation*, vol. 83, no. 4, pp. 425–432, 2007.
- [32] A. Villanueva, D. Y. Chiang, P. Newell et al., "Pivotal role of mTOR signaling in hepatocellular carcinoma," *Gastroenterology*, vol. 135, no. 6, pp. 1972.e11–1983.e11, 2008.
- [33] K. Stone, M. LoPresti, and K. Williams, "Enzymatic digestion of proteins and HPLC peptide isolation in the subnanomole range," in *Laboratory Methodology in Biochemistry*, C. Fini, A. Floridi, V. Finelli, and B. Wittman-Liebold, Eds., pp. 181–205, CRC Press, Boca Raton, Fla, USA, 1990.
- [34] *The Handbook of Analysis and Purification of Peptides and Proteins by Reversed-Phase HPLC*, GraceVydac, Deerfield, Ill, USA, 3rd edition, 2002.
- [35] J. McCarthy, F. Hopwood, D. Oxley et al., "Carbamylation of proteins in 2-D electrophoresis—myth or reality?" *Journal of Proteome Research*, vol. 2, no. 3, pp. 239–242, 2003.
- [36] H. Hamada, T. Arakawa, and K. Shiraki, "Effect of additives on protein aggregation," *Current Pharmaceutical Biotechnology*, vol. 10, no. 4, pp. 400–407, 2009.

## Research Article

# Application of an Activated Carbon-Based Support for Magnetic Solid Phase Extraction Followed by Spectrophotometric Determination of Tartrazine in Commercial Beverages

José A. Rodríguez,<sup>1</sup> Karen A. Escamilla-Lara,<sup>1</sup> Alfredo Guevara-Lara,<sup>1</sup>  
Jose M. Miranda,<sup>2</sup> and Ma. Elena Páez-Hernández<sup>1</sup>

<sup>1</sup>Laboratorio 2, Área Académica de Química, Universidad Autónoma del Estado de Hidalgo, Carretera Pachuca-Tulancingo Km. 4.5, 42184 Mineral de la Reforma, HGO, Mexico

<sup>2</sup>Departamento de Química Analítica, Nutrición y Bromatología, Facultad de Veterinaria, Universidad de Santiago de Compostela, Pabellón 4 Planta Baja, Campus Universitario, s/n, 27002 Lugo, Spain

Correspondence should be addressed to Ma. Elena Páez-Hernández; [mpaezh@gmail.com](mailto:mpaezh@gmail.com)

Received 17 October 2014; Accepted 18 January 2015

Academic Editor: Faezeh Khalilian

Copyright © 2015 José A. Rodríguez et al. This is an open access article distributed under the Creative Commons Attribution License, which permits unrestricted use, distribution, and reproduction in any medium, provided the original work is properly cited.

A method is presented for magnetic solid phase extraction of tartrazine from nonalcoholic beverages. The method involves the extraction and clean-up by activated carbon covered with magnetite dispersed in the sample, followed by the magnetic isolation and desorption of the analyte by basified methanol. The tartrazine eluted from the magnetic support was determined by spectrophotometry. Under optimal conditions, the linear range of the calibration curve ranges from 3 to 30 mg L<sup>-1</sup>, with a limit of detection of 1 mg L<sup>-1</sup>. The method was validated by comparing the results with those obtained by HPLC. A precision of <5.0% was obtained in all cases and no significant differences were observed ( $P < 0.05$ ).

## 1. Introduction

Dyes are a group of additives used to improve the appearance of foods, textiles, and medicine allowing the homogenizing and the assertion of the color, which is the most important sensory characteristic [1]. Synthetic dyes have been used because they are more resistant to changes in temperature and acidity [2] than natural dyes. All of these compounds contain a chromophore group and different substituents resulting in a large group of synthetic dyes, each with particular chemical properties.

The azo dyes are the most commercially used group of synthetic dyes. The main feature of these compounds is the presence of an azo group ( $-N=N-$ ) and aromatic groups, resulting in a substance with high electron conjugation and a high molar absorption coefficient, making it useful at low concentrations [3].

Tartrazine, also known as yellow 5 or E 102 dye, is one of the most important synthetic azo dyes used in the food industry to confer a yellow color to food. It is soluble in water (14 mg/100 mL) giving a yellow color to the solution. It is usually applied in pastries, baked goods, snacks, drinks, biscuits, ice cream, and other sweets [4].

In spite of its useful qualities, tartrazine has also been associated with allergenic effects, hyperactivity, and attention deficit disorder [5]. For this reason, the toxicity of tartrazine was studied in the early 60s by the Expert Committee on Food Additives of FAO/WHO, which established an acceptable daily intake (ADI) of 7.5 mg kg<sup>-1</sup> of body weight per day. Moreover, since 2010, foods containing tartrazine must carry the warning “may alter the activity and attention in children.” In Mexico, this dye is regulated according to the Official Mexican Standard NOM-218-SSA1-2011 which

allows  $100 \text{ mg L}^{-1}$  as the maximum amount of tartrazine in commercial beverages [6].

In general, the methodology for the quantification of dyes involves a sample treatment, identification, and quantification steps. The chosen method depends on the type of food and the lipid, protein, and carbohydrate content. Other properties such as acid-base properties of the analyte and the interferences present in the sample matrix are also important [7]. Thus, when liquid chromatography, capillary electrophoresis, and electrochemical techniques are used, it requires a simple treatment of the sample, usually dilution and subsequent filtration. However, these instrumental methods have certain disadvantages such as the high cost of analysis (equipment and reagents) and lower analysis rate (2–4 samples per hour) [8, 9]. On the other hand, if the determination of dyes is completed using a quick and simple spectrophotometric technique, it must be considered that the presence of preservatives (sodium benzoate or citrate) and proteins may interfere significantly during the quantification step. According to this, the isolation of the sample dye using different extraction materials is critical during the analytical process [9].

Different separation strategies have been evaluated for dye extraction. Anion exchange, where acid dyes are retained by sulfonic groups present in the polymer structure [10], and liquid-liquid extraction (*n*-butanol-water) based on the formation of ion pairs with trimethyloctadecylammonium salts [11] have been proposed. Solid phase extraction is another technique used to isolate dye from complex matrices. The solid phases used for this purpose were zeolite or silica C18; the retained dye was eluted from the solid phase with methanol [12, 13].

Additionally, activated carbon has been proposed as colorant adsorbent because it has an excellent surface area and a well-defined pore structure that favors the retention of the analyte [14–17]. Despite its versatility, the activated carbon has the disadvantage of being difficult to separate from the aqueous matrix where it was dispersed. In order to facilitate separation of the extraction support from the liquid phase, Šafaříková and Šafařík [18] propose the magnetic solid phase extraction (MSPE). MSPE is based on the use of magnetite-modified activated carbon as the solid phase with paramagnetic properties. For this reason, the support can be easily isolated from the dispersion medium by applying an external magnetic field. The main advantages of MSPE are as follows: (1) presenting the possibility of using large volumes of samples, greatly reducing the time of pretreatment and the analysis result; (2) having great interaction between analytes and the solid phase with the full dispersion of the adsorbent in the sample; and (3) providing easy isolation of the adsorbent from the analytical matrix, reducing the risk of loss of analyte [19].

In spite of their promising qualities, the MSPE has been used mainly for the separation of antibiotics and other organic molecules [20]. The use for the extraction of dyes has been limited to the determination of Reactive Red 198 [21], and methylene Blue [22]. In all cases, the main advantage of the adsorbent support was its selectivity in the extraction of the analyte and the possibility of using volumes from 100 to

1000 mL [18], providing shorter analysis times as compared to conventional techniques.

According to the above-mentioned, the purpose of this work is to design a methodology based on magnetic solid phase extraction using magnetite-modified carbon for the spectrophotometric analysis of tartrazine. The method was used for the analysis of this dye in a complex matrix of nonalcoholic beverages.

## 2. Materials and Methods

**2.1. Synthesis and Characterization of Magnetite-Modified Carbon.** For the synthesis of the magnetite-modified carbon, a commercial activated vegetable carbon from Clarimex S.A. de C.V. was used. The synthesis was performed in two stages: in the first stage, magnetite was obtained by precipitation and its partial oxidation of iron (II) sulfate heptahydrate  $\text{FeSO}_4 \cdot 7\text{H}_2\text{O}$  (3.6 g). The iron precursor was dissolved in 100 mL of deionized water, stirring constantly and keeping at  $60^\circ\text{C}$ . The pH solution was adjusted to  $10.0 \pm 0.2$  and a stream of air was passed through the reaction mixture. The initial green precipitate  $(\text{Fe}(\text{OH})_2 \cdot x\text{H}_2\text{O})$  turned black after 40 minutes of reaction as a consequence of the partial oxidation of Fe(II) to Fe(III) by the action of the  $\text{O}_2$  from the air stream; the black color of the precipitate is characteristic for  $\text{Fe}_3\text{O}_4$  [23]. In the second step, 1.0 g of activated carbon was added to the reaction vessel and the mixture was stirred for 30 minutes. The magnetic phase was separated with a magnet and washed three times with distilled water. The solid phase was dried at  $60^\circ\text{C}$  for 24 h. The solid phase was pulverized in an agate mortar and stored in a desiccator until use.

In order to carry out the characterization of the synthesized magnetite-modified carbon, various instrumental techniques were used. X-ray powder diffraction analysis was performed in a Philips PW1710 instrument equipped with a copper anode and an automatic divergent opening. The conditions for the analysis were  $1.54 \text{ \AA}$   $\text{CuK}\alpha$  radiation; 40 kV voltage tube; 30 mA current tube; 0.500 intensity ratio ( $a_2/a_1$ );  $1^\circ$  divergence slit; 0.1 receiving slit; ( $2\theta^\circ$ ) 5 initial angle; ( $2\theta^\circ$ ) 70 end angle.

Morphological analysis of the solid was performed in a scanning electron microscopy (SEM) JEOL JSM-820. Qualitative analysis and determination of the distribution of magnetite in the solid were performed with a LINK QX-2000 analyzer by Energy Dispersive X-ray Spectroscopy. All spectra were obtained at 15 kV, a distance of 39 mm, and 2,500 counts; the detector angle relative to the sample in all cases was  $45^\circ$ .

**2.2. Tartrazine Extraction-Elution.** For the extraction studies, 0.05 g of magnetite-modified carbon was mixed with 20.0 mL of aqueous solution of tartrazine and stirred mechanically for 30 minutes. The pH value for tartrazine solution was varied using acetate (pH = 5.0), phosphate (pH = 7.0), and borate (pH = 9.0) solutions at  $1.0 \text{ mol L}^{-1}$  concentration. After the extraction, the solid phase was separated using a neodymium magnet and the remaining liquid phase was analyzed by spectrophotometry at a wavelength of 434 nm

in a UV-Vis spectrophotometer HACH DR-2700 with a quartz cell with 1.0 cm of path length. Thus, the remaining tartrazine was quantified by interpolation in a calibration line constructed with standard solutions of tartrazine ( $10.0\text{--}100.0\text{ mg L}^{-1}$ ) prepared in the respective buffer solution. A control experiment was carried out using activated carbon in order to evaluate the effect of the magnetic modifications in support of the tartrazine extraction.

For the elution of the retained tartrazine from the synthesized support, several eluting systems were evaluated following this procedure in triplicate: 50 mg of solid phase containing tartrazine was mixed with 2.0 mL of eluent and stirred using ultrasound for 5 minutes. 2 mL of the resulting solution was transferred to a 10 mL volumetric flask and filled with eluent solution up to the mark. The eluted tartrazine was quantified by interpolation in a calibration line constructed with absorbance values of standard solutions of tartrazine ( $10.0\text{--}100.0\text{ mg L}^{-1}$ ) prepared in the respective eluent solution.

**2.3. Analysis of Real Samples.** Six samples of commercial beverages containing tartrazine were analyzed in triplicate following this protocol: 10 mL aliquot of the drink was mixed with 2.5 mL of  $1.0\text{ mol L}^{-1}$  acetate buffer solution and transferred to a 25 mL volumetric flask and then deionized water was added up to the mark. Later, 20.0 mL of this solution was placed in a polypropylene tube containing 75 mg of magnetic support and mechanically stirred for 30 minutes in order to extract the dye. After the extraction, the solid phase was removed from the aqueous matrix using a neodymium magnet. The solid phase was then mixed with 1.0 mL of eluent and stirred for 5 minutes using ultrasound to remove the extracted tartrazine. The liquid phase was transferred to a 10 mL volumetric flask and filled with elution solution up to the mark. The concentration of tartrazine in the last solution was determined spectrophotometrically.

In order to evaluate the proposed methodology, the amount of tartrazine in the commercial beverages was also analyzed using an HPLC. This method considers a calibration line using standard solutions of tartrazine from 5 to  $20\text{ mg L}^{-1}$ . Samples were prepared as follows. An aliquot of 0.5 mL was diluted adding a mobile phase up to 5 mL. In order to introduce the samples to the chromatographic system, it was necessary to filter it using membranes of  $0.45\text{ }\mu\text{m}$  pore size.

### 3. Results and Discussion

**3.1. Characterization of Modified Carbon.** Instrumental techniques were used to provide information about the composition and structure of the magnetic modified carbon. Thus, the X-ray diffraction (XRD) studies were performed in order to determine the iron oxide form present in the solid. The XRD diffractograms from Figure 1(a) show the signals labeled as "m" that correspond to the characteristic diffraction lines of  $\text{Fe}_3\text{O}_4$  ( $2\theta = 30.1^\circ, 35.5^\circ, 43.1^\circ, 53.4^\circ, 57.0^\circ,$  and  $62.6^\circ$ ) according to the Joint Committee on Powder Diffraction Standards [24]. The broadband signal observed between  $20^\circ$

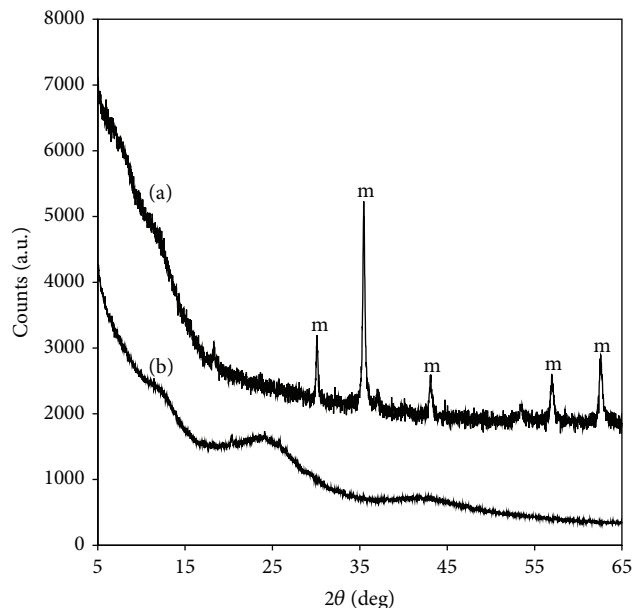


FIGURE 1: Diffractogram of (a) magnetic modified carbon support and (b) activated carbon.

and  $30^\circ$  for the  $2\theta$  angle (Figure 1(b)) is characteristic of amorphous carbon, the raw material.

The morphological study with scanning electron microscopy (SEM) for activated carbon shows a uniform phase with inhomogeneous particle sizes greater than  $20\text{ }\mu\text{m}$  (Figure 2(a)). The micrograph is consistent with SEM studies performed without modifying the activated carbon [25]. In the case of the synthesized support, it can be seen that the activated carbon is covered by a phase with a smaller size (Figure 2(b)). This was confirmed with the energy dispersive spectrum (Figure 2(c)) that shows a larger amount of carbon for the section (I), while the Fe-content is greater for the area (II), so it is concluded that the magnetite phase is covering the activated carbon.

**3.2. Study of Chemical Variables for the Extraction of Tartrazine with the Magnetic Modified Carbon Support.** The extraction of tartrazine from standard solutions using the synthesized modified carbon is shown in Figure 3. It is possible to visually verify the cleaning process of the tartrazine solution.

The capability of the synthesized modified carbon for the extraction of tartrazine was also evaluated at different pH values. The results shown in Figure 4 correspond to acidic, basic, and neutral medium adsorption isotherms constructed by plotting the concentration of tartrazine in the solution at equilibrium ( $\mu\text{M}$ ) against the concentration of the sorbate on the solid phase ( $\text{mmol kg}^{-1}$ ) after adsorption. Additionally, Table 1 shows the maximum quantity of adsorbate on the solid support at different pH values.

According to Figure 4 and Table 1, the decrease of pH values results in the increase of the amount of absorbed tartrazine. This is consequence of the interaction of tartrazine

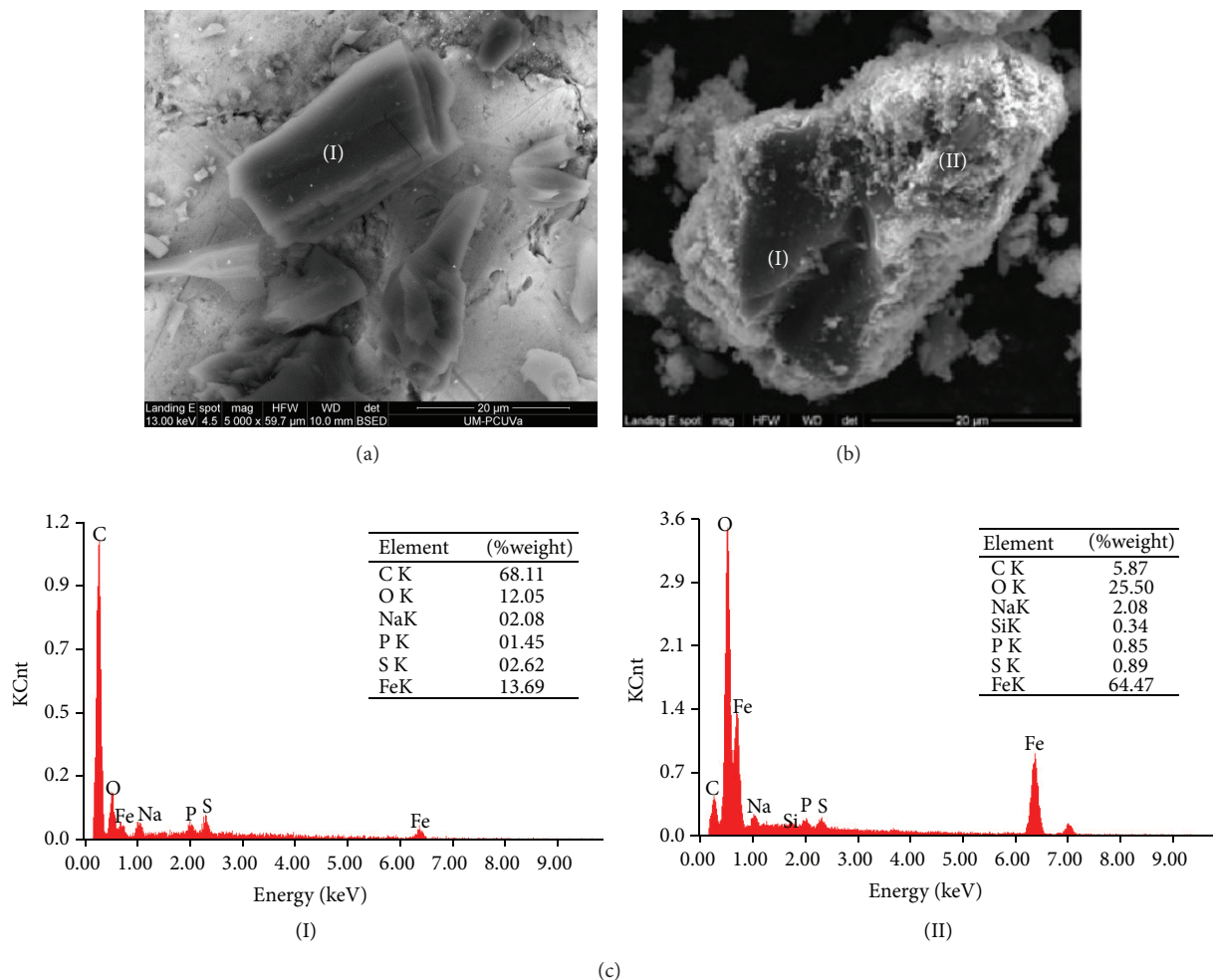


FIGURE 2: (a) Micrograph for activated carbon; (b) micrograph for magnetic modified carbon support; (c) energy dispersive spectra obtained from the analysis of zones I and II of magnetic modified carbon support.



FIGURE 3: Adsorption experiment. From left to right: dissolution of tartrazine, mixture of tartrazine with magnetic modified carbon, and magnetic support separation.

TABLE 1: Maximum adsorbed tartrazine on the adsorbent at different pH values.

pH value	Tartrazine adsorbed (mmol kg <sup>-1</sup> )
5.0	54.5
7.0	48.4
9.0	42.7

in its anionic form with the acid form of the magnetite at low pH values. In basic medium a repulsion between the negative charges of tartrazine in solution and the support is reflected in the reduction of the adsorbate retention [26]. Based on these results, pH of 5.0 was selected as the most suitable value for the retention of dye.

As part of the characterization of the MSPE-dye system, the affinity constant value between substrate and tartrazine was estimated. The analysis of the isotherm values using a Scatchard plot demonstrates the value of the affinity constant  $K_d$  for the following dissociation reaction [27]:



where TS corresponds to tartrazine adsorbed on the support, T is the tartrazine in solution, and S is the magnetic modified carbon support.

$\log K_d$  values are shown in Table 2, observing a linear trend which is associated with the homogeneity of the support. Because this is a dissociation constant, it follows that the support with a higher affinity is the activated carbon;

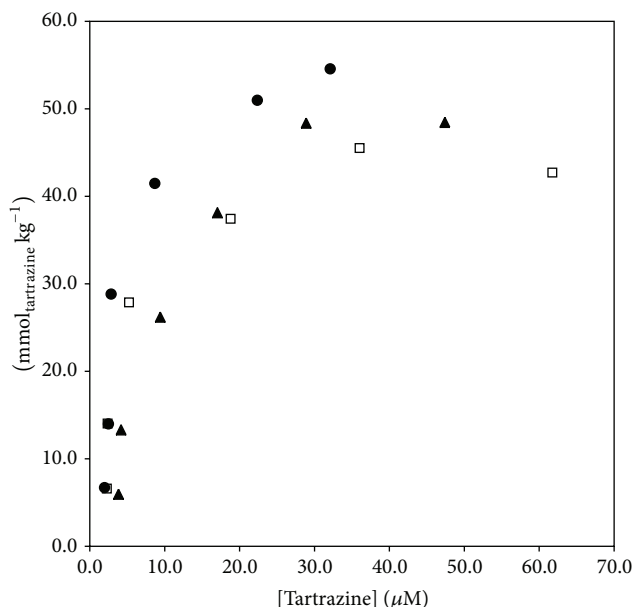


FIGURE 4: Adsorption isotherms for tartrazine on magnetic carbon modified at pH values (●) 5.0, (▲) 7.0, and (□) 9.0.

TABLE 2: Tartrazine magnetic-modified carbon support dissociation constants.

Support	$\log K_d$
Activated carbon	-28
Magnetic-modified carbon	-6.5

TABLE 3: Results of the evaluation of different systems for tartrazine elution.

Eluent	Signal 1	Signal 2	Signal 3
Methanol	0.6000	0.6010	0.6020
Basified methanol	0.7720	0.7700	0.7700
Acetonitrile	0.1460	0.1460	0.1450
Basified acetonitrile	0.4440	0.4420	0.4440

however, the synthesized support has a suitable  $\log K_d$  value because in the retention-elution methodologies design, it is recommended that the support has an average affinity to the substrate with  $\log K_d$  values between  $-7.0$  and  $-4.0$  [20].

Additional studies on the selection of the best chemical conditions for the tartrazine elution adsorbed on the magnetic modified carbon were performed. Thus, several eluting systems were evaluated for the elution step: methanol, acetonitrile, basified methanol, and basified acetonitrile [28, 29]. After the spectrophotometric analysis of the eluted tartrazine, it can be seen that basified methanol provides the greater signal (Table 3) as a consequence of removing a greater amount of tartrazine. For this reason, this eluent was chosen for elution of tartrazine in the following experiments.

**3.3. Optimization of the Physical Variables of the MSPE Process.** To optimize the conditions for the retention and elution of tartrazine involved in the MSPE system, a Taguchi

TABLE 4: Matrix obtained during optimization design for the MSPE system.

Experiment	$V_M$ (mL)	$V_E$ (mL)	$m_C$ (mg)	$C_E$ (M)	% recovery
1	10.0	1.0	50	0.0025	6.66
2	10.0	2.0	75	0.025	23.48
3	10.0	3.0	100	0.25	27.74
4	20.0	1.0	75	0.25	99.95
5	20.0	2.0	100	0.0025	7.49
6	20.0	3.0	50	0.025	44.10
7	30.0	1.0	100	0.025	31.59
8	30.0	2.0	50	0.25	90.58
9	30.0	3.0	75	0.0025	24.19

experimental design was performed. The main advantage of this technique is that it provides useful information with minimal experimentation using matrices of special design (orthogonal arrays), in which columns (factors or controllable parameters) and rows (experiments) are accommodated in such a way that a combination of factors and levels of each experiment are indicated [30].

The selected response factor was the percentage of recovery for the analysis of 20 mL of a solution of 30 mg L<sup>-1</sup> tartrazine. The selected control factors (parameters), each at 3 levels, were sample volume, volume of eluent, mass of magnetic modified carbon support, and NaOH concentration in the eluent [20]. Based on an L9 (34) Taguchi orthogonal array, the matrix design and results obtained are shown in Table 4.

Figure 5 shows a typical graph obtained by plotting the average percentage of recovery for each factor against each of its levels. According to this, the most suitable conditions for tartrazine adsorption-elution were 20 mL sample, 1 mL of eluent, 75 mg of magnetic modified carbon, and a concentration of 0.25 mol L<sup>-1</sup> NaOH for the basified methanol solution. These conditions correspond to experiment number 4, which has the highest percentage of dye recovery.

Additionally, the contribution percentage of each variable was determined by ascertaining that NaOH concentration in the eluting solution has the greater effect (45.4%), followed by the sample volume (23.6%), the mass of adsorbent (20.4%), and the eluent volume (10.6%). The higher contribution of the eluting solution in the tartrazine elution step confirms the theory of charge-repulsion between support and analyte, which is favored at a higher concentration of NaOH.

#### 3.4. Analytical Parameters of the MSPE Developed Method.

Under the optimized conditions described above, calibration lines using tartrazine standard solutions in the concentration range of 5.0 to 30.0 mg L<sup>-1</sup> were carried out. The obtained signal (AU) was measured in triplicate and the calibration lines were plotted using the average signal of the eluted tartrazine. Calibration lines show a linear dependence between the average signal and the concentration of tartrazine present

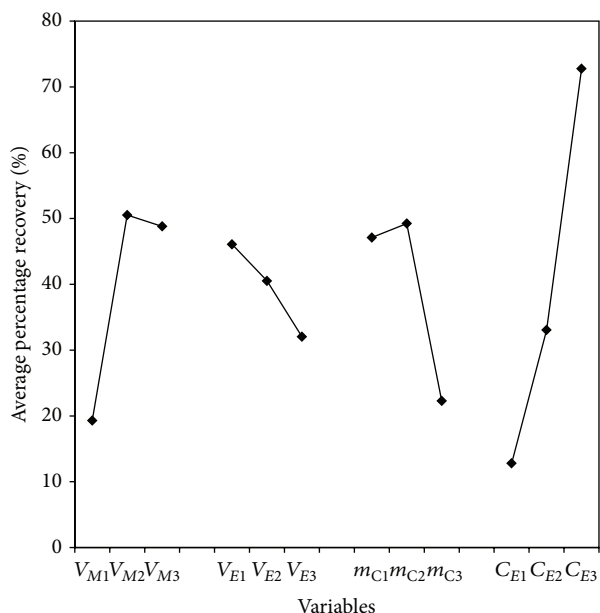


FIGURE 5: Plot of average effects in the tartrazine recovery.  $V_M$ : sample volume;  $V_E$ : eluent volume;  $m_C$ : magnetic modified carbon; and  $C_E$ : NaOH concentration in the eluent.

TABLE 5: Parameters of the regression line for signal (AU) versus tartrazine concentration ( $\text{mg L}^{-1}$ ) plot.

Parameter	Value
Root mean square deviation, $s_e$	0.013
Intercept, $b_0 \pm ts (b_0)$	$0.010 \pm 0.031$
Slope, $b_1 \pm ts (b_1)$	$0.041 \pm 0.003$
Linear interval ( $\text{mg L}^{-1}$ )	3.0–30.0
Limit of detection ( $\text{mg L}^{-1}$ )	1.0
Repeatability (%RSD, $n = 3$ , $10.0 \text{ mg L}^{-1}$ )	1.8
Reproducibility (%RSD, $n = 9$ , $10.0 \text{ mg L}^{-1}$ )	3.2

in the initial standard solution. Table 5 shows the calibration line regression parameters.

From the values reported in Table 5, it can be seen that the proposed methodology allows for the quantification of tartrazine in drinks at levels established by the Official Mexican Standard NOM-218-SSA1-2011 which allows  $100 \text{ mg L}^{-1}$  as the maximum amount of tartrazine in commercial beverages [5].

**3.5. Interference Study.** Several nonalcoholic beverages containing tartrazine also have additives as proteins and preservatives that improve physical appearance and shelf life. For this reason, the tartrazine adsorption-elution method was evaluated adding several interfering compounds. The evaluated interferents included casein, egg albumin, acesulfame K, sodium benzoate, aspartame, sodium citrate, glucose, and sucrose. Solutions of each interfering compound were prepared dissolving 10 mg in 10 mL acetate buffer.

To perform the test, 75 mg of magnetic modified carbon was mixed with 20 mL of  $30 \text{ mg L}^{-1}$  tartrazine solution and 3 mL of interferent solution. After this absorption step, 1 mL

TABLE 6: Chemical composition of the analyzed commercial beverages.

Sample	Composition
1	Soy (water and selected soy seeds), sugar, maltodextrin, concentrated pineapple juice, flavor identical to natural, pectin, and tartrazine.
2	Water, sugar, concentrated orange, tartrazine, and sodium.
3	Water, corn syrup, high fructose, concentrated pineapple juice reconstituted, citric acid, pectin, artificial flavor, acesulfame K, and yellow 5.
4	Water, high fructose corn syrup, sugar, citric acid, sodium chloride, sodium citrate, monosodium phosphate, Arabic gum, ester gum, natural lemon-lime flavor, and tartrazine.
5	Water, high fructose corn syrup, concentrated juice (7% orange and 3% pineapple), citric acid, ascorbic acid, acacia gum, ester gum, natural and artificial flavors, sodium citrate, yellow 5 (tartrazine), and beta carotene dyes.

TABLE 7: Contents of tartrazine (mean and %RSD,  $n = 3$ ) in real samples determined with the proposed methodology and comparison with HPLC reference method.

Sample	[Tartrazine] ( $\text{mg L}^{-1}$ )	
	MSPE-UV	HPLC
1	5.5 (1.3)	5.4
2	22.7 (0.8)	22.4
3	5.9 (1.8)	5.7
4	22.8 (2.3)	23.0
5	5.5 (2.6)	5.7

of basified methanol with NaOH  $0.25 \text{ mol L}^{-1}$  was used to elute tartrazine. Then 0.5 mL of the eluted solution was transferred to a 5 mL volumetric flask and filled up to the mark. This solution was analyzed by UV-Vis spectrophotometry. Results did not show a %RSD value higher than 5% of the analytical signal in a similar experiment without interferents. According to this, the proposed compounds do not interfere with the tartrazine determination following the proposed methodology.

**3.6. Analysis of Real Samples.** The tartrazine concentration in six commercially available beverages was determined. The main components of every beverage that were reported by the manufacturer are listed in Table 6.

Following the developed and optimized method, the tartrazine concentration for each beverage is shown in Table 7. This value represents the average of three independent determinations. Additionally, in Table 7 it is possible to observe the results for the analysis of samples using the HPLC reference method and MSPE-HPLC (Figure 6). For each beverage, the average concentration of tartrazine obtained using both methods was compared using a  $t$ -test with 2 degrees of freedom and 95% of confidence ( $t_{\text{tab}} = 4.3$ ). This analysis revealed no significant differences between the results from

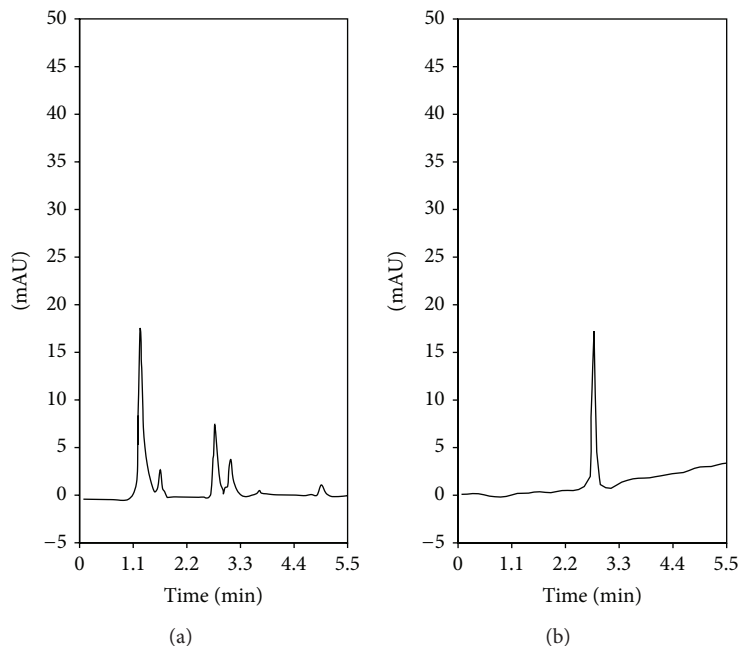


FIGURE 6: Chromatograms of (a) original sample and (b) eluted tartrazine solution after using MSPE developed method.

each method. Therefore, the methodology of MSPE is comparable with the reference methodology. Additionally, the MSPE is a robust preconcentration technique that can be coupled even to spectrophotometry or HPLC.

#### 4. Conclusions

In the present work, an activated carbon covered with magnetite support was synthesized; this support has magnetic properties that allow its separation by applying an external magnetic field.

The best conditions for the extraction and elution of tartrazine were an initial sample volume of 20 mL, buffered with acetate buffer solution, at pH 5, and mixed with 75 mg of magnetic modified carbon, tartrazine elution with 1 mL of NaOH  $0.25 \text{ mol L}^{-1}$  in methanol.

Thus, the proposed sample treatment coupled to spectrophotometric analysis is an alternative to the analysis of azo dyes in the food industry because the parameters, analytical precision, and accuracy are similar to HPLC methodologies. However, the proposed methodology saves time and is less expensive than the reference method.

#### Conflict of Interests

The authors declare that there is no conflict of interests regarding the publication of this paper.

#### Acknowledgments

The authors wish to thank CONACyT (Project INFR-2014-227999) and Consejería de Cultura, Educación e Ordenación Universitaria, and Xunta de Galicia (Project EM 2012/153) for

the financial support. Alfredo Guevara-Lara, Ma. Elena Pérez-Hernández, and José A. Rodríguez gratefully thank the SNI for the distinction of their membership.

#### References

- [1] J. Abbey, B. Fields, M. O'Mullane, and L. D. Tomaska, "Food additives: colorants," in *Encyclopedia of Food Safety*, Elsevier, New York, NY, USA, 2014.
- [2] K. Venkataraman, *The Chemistry of Synthetic Dyes*, vol. 4, Academic Press, New York, NY, USA, 1971.
- [3] N. Sekar, "Acid dyes," in *Handbook of Textile and Industrial Dyeing*, Elsevier, New York, NY, USA, 2011.
- [4] A. L. Branen, P. M. Davidson, S. Salminen, and J. Thorngat, *Food Additives*, Marcel Dekker, New York, NY, USA, 2nd edition, 2002.
- [5] L. E. Arnold, N. Lofthouse, and E. Hurt, "Artificial food colors and attention-deficit/hyperactivity symptoms: conclusions to dye for," *Neurotherapeutics*, vol. 9, no. 3, pp. 599–609, 2012.
- [6] NORMA Oficial Mexicana NOM-218-SSA1-2011, "Productos y servicios. Bebidas saborizadas no alcohólicas, sus congelados, productos concentrados para prepararlas y bebidas adicionadas con cafeína. Especificaciones y disposiciones sanitarias. Métodos de prueba," *Diario Oficial de la Federación*, 2012, [http://www.dof.gob.mx/nota\\_detalle.php?codigo=5233379&fecha=10/02/2012](http://www.dof.gob.mx/nota_detalle.php?codigo=5233379&fecha=10/02/2012).
- [7] E. C. Vidotti, W. F. Costa, and C. C. Oliveira, "Development of a green chromatographic method for determination of colorants in food samples," *Talanta*, vol. 68, no. 3, pp. 516–521, 2006.
- [8] H.-Y. Huang, Y.-C. Shih, and Y.-C. Chen, "Determining eight colorants in milk beverages by capillary electrophoresis," *Journal of Chromatography A*, vol. 959, no. 1-2, pp. 317–325, 2002.
- [9] N. Yoshioka and K. Ichihashi, "Determination of 40 synthetic food colors in drinks and candies by high-performance liquid

- chromatography using a short column with photodiode array detection," *Talanta*, vol. 74, no. 5, pp. 1408–1413, 2008.
- [10] M. Wawrzkiwicz and Z. Hubicki, "Removal of tartrazine from aqueous solutions by strongly basic polystyrene anion exchange resins," *Journal of Hazardous Materials*, vol. 164, no. 2-3, pp. 502–509, 2009.
- [11] O.-W. Lau, M. M. K. Poon, S.-C. Mok, F. M. Y. Wong, and S.-F. Luk, "Spectrophotometric determination of single synthetic food colour in soft drinks using ion-pair formation and extraction," *International Journal of Food Science & Technology*, vol. 30, no. 6, pp. 793–798, 2007.
- [12] Y. S. Al-Degs, M. I. El-Barghouthi, A. H. El-Sheikh, and G. M. Walker, "Effect of solution pH, ionic strength, and temperature on adsorption behavior of reactive dyes on activated carbon," *Dyes and Pigments*, vol. 77, no. 1, pp. 16–23, 2008.
- [13] S. Şahin, C. Demir, and Ş. Güçer, "Simultaneous UV-vis spectrophotometric determination of disperse dyes in textile wastewater by partial least squares and principal component regression," *Dyes and Pigments*, vol. 73, no. 3, pp. 368–376, 2007.
- [14] D. Xin-hui, C. Srinivasakannan, and L. Jin-sheng, "Process optimization of thermal regeneration of spent coal based activated carbon using steam and application to methylene blue dye adsorption," *Journal of the Taiwan Institute of Chemical Engineers*, vol. 45, no. 4, pp. 1618–1627, 2013.
- [15] P. Rodríguez-Estupiñan, L. Giraldo, and J. C. Moreno-Piraján, "Energetic changes in the surface of activated carbons and relationship with Ni(II) adsorption from aqueous solution," *Applied Surface Science*, vol. 286, pp. 351–357, 2013.
- [16] C. Zeng, Q. Lin, C. Fang, D. Xu, and Z. Ma, "Preparation and characterization of high surface area activated carbons from co-pyrolysis product of coal-tar pitch and rosin," *Journal of Analytical and Applied Pyrolysis*, vol. 104, pp. 372–377, 2013.
- [17] H. Duygu Ozsoy and J. Van Leeuwen, "Removal of color from fruit candy waste by activated carbon adsorption," *Journal of Food Engineering*, vol. 101, no. 1, pp. 106–112, 2010.
- [18] M. Šafaříková and I. Šafařík, "Magnetic solid-phase extraction," *Journal of Magnetism and Magnetic Materials*, vol. 194, no. 1–3, pp. 108–112, 1999.
- [19] K. Aguilar-Arteaga, J. A. Rodríguez, and E. Barrado, "Magnetic solids in analytical chemistry: a review," *Analytica Chimica Acta*, vol. 674, no. 2, pp. 157–165, 2010.
- [20] I. S. Ibarra, J. A. Rodríguez, J. M. Miranda, M. Vega, and E. Barrado, "Magnetic solid phase extraction based on phenyl silica adsorbent for the determination of tetracyclines in milk samples by capillary electrophoresis," *Journal of Chromatography A*, vol. 1218, no. 16, pp. 2196–2202, 2011.
- [21] M. Janus, E. Kusiak, J. Choina, J. Ziebro, and A. W. Morawski, "Enhanced adsorption of two azo dyes produced by carbon modification of TiO<sub>2</sub>," *Desalination*, vol. 249, no. 1, pp. 359–363, 2009.
- [22] R. Liu, X. Shen, X. Yang, Q. Wang, and F. Yang, "Adsorption characteristics of methyl blue onto magnetic Ni<sub>0.5</sub>Zn<sub>0.5</sub>Fe<sub>2</sub>O<sub>4</sub> nanoparticles prepared by the rapid combustion process," *Journal of Nanoparticle Research*, vol. 15, no. 6, article 1679, 2013.
- [23] E. Barrado, F. Prieto, M. Vega, and F. Fernández-Polanco, "Optimization of the operational variables of a medium-scale reactor for metal-containing wastewater purification by ferrite formation," *Water Research*, vol. 32, no. 10, pp. 3055–3061, 1998.
- [24] M. C. Morris, H. F. McMurdie, E. H. Evans et al., *Standard X-Ray Diffraction Powder Patterns*, National Bureau of Standards, Washington, DC, USA, 1981.
- [25] J. Zhang, X. Qiang, L. Juan, M. Yang, and Y. Xing, "Role of Ni(NO<sub>3</sub>)<sub>2</sub> in the preparation of a magnetic coal-based activated carbon," *Mining Science and Technology*, vol. 21, no. 4, pp. 599–603, 2009.
- [26] Z.-X. Sun, F.-W. Su, W. Forsling, and P.-O. Samskog, "Surface characteristics of magnetite in aqueous suspension," *Journal of Colloid and Interface Science*, vol. 197, no. 1, pp. 151–159, 1998.
- [27] A. P. Davenport, *Receptor Binding Techniques*, Humana Press, Totowa, NJ, USA, 2nd edition, 2005.
- [28] A. Mittal, J. Mittal, and L. Kurup, "Adsorption isotherms, kinetics and column operations for the removal of hazardous dye, Tartrazine from aqueous solutions using waste materials-Bottom Ash and De-Oiled Soya, as adsorbents," *Journal of Hazardous Materials*, vol. 136, no. 3, pp. 567–578, 2006.
- [29] T. Tuzimski and A. Woźniak, "Application of solid-phase extraction and planar chromatography with diode-array detection to the qualitative and quantitative analysis of dyes in beverages," *Journal of Planar Chromatography—Modern TLC*, vol. 21, no. 2, pp. 89–96, 2008.
- [30] R. K. Roy, *Design of Experiments Using the Taguchi Approach*, John Wiley & Sons, Toronto, Canada, 2001.

## Research Article

# Extraction of HCV-RNA from Plasma Samples: Development towards Semiautomation

Imran Amin,<sup>1</sup> Tania Jabbar,<sup>1,2</sup> Fawad Niazi,<sup>1</sup> and Muhammad Saeed Akhtar<sup>3</sup>

<sup>1</sup>PCR Laboratory, Punjab Institute of Nuclear Medicine (PINUM), Faisalabad 2019, Pakistan

<sup>2</sup>Department of Clinical Pathology, Punjab Institute of Nuclear Medicine (PINUM), Faisalabad 2019, Pakistan

<sup>3</sup>Nuclear Medicine Department, Punjab Institute of Nuclear Medicine (PINUM), Faisalabad 2019, Pakistan

Correspondence should be addressed to Tania Jabbar; [tania.jabbar@univie.ac.at](mailto:tania.jabbar@univie.ac.at)

Received 30 September 2014; Revised 4 February 2015; Accepted 4 February 2015

Academic Editor: Mohammad R. Pourjavid

Copyright © 2015 Imran Amin et al. This is an open access article distributed under the Creative Commons Attribution License, which permits unrestricted use, distribution, and reproduction in any medium, provided the original work is properly cited.

A semiautomated extraction protocol of HCV-RNA using Favorgen RNA extraction kit has been developed. The kit provided protocol was modified by replacing manual spin steps with vacuum filtration. The assay performance was evaluated by real-time qPCR based on Taqman technology. Assay linearity was confirmed with the serial dilutions of RTA (Turkey) containing  $1 \times (10^6, 10^5, 10^4, \text{ and } 10^3) \text{ IU mL}^{-1}$ . Comparison of test results obtained by two extraction methods showed a good correlation ( $r = 0.95$ ,  $n = 30$ ) with detection limit of  $10^2 \text{ IU mL}^{-1}$ . The semiautomated vacuum filtration based protocol demonstrated high throughput: 35 minutes for the extraction of a batch of 30 samples ( $150 \mu\text{L}$  each) with reduced labor, time, waste, and cost. Performance characteristics of semiautomated system make it suitable for use in diagnostic purpose and viral load determinations.

## 1. Introduction

The extraction process is a key component of nucleic acid detection, as it affects both the reliability and the reproducibility of target amplification. The manual extraction method (spin based) using Favorgen extraction RNA kit is time consuming and requires meticulous technical skills to achieve reproducible results [1, 2]. Therefore, demand for automated system has grown in recent years. Automated nucleic acid extraction process is potentially beneficial to reduce working time, labor cost, and risk of contamination and at the same time increases the worker safety and laboratory efficiency [3]. However, fully automated extraction system is very expensive and raises the cost of diagnosis. Therefore, developments towards semiautomation (vacuum filtration based protocol) not only reduce labor, plastic waste, and price (100 Pak Rs. or 1 US dollar) but also speed up the extraction process.

Although the introduction of real-time PCR has led to considerable progress in automating the amplification and detection steps, still nucleic acid isolation remains very labor-intensive when performed manually. Thus, the objective of the present study was to evaluate performance of vacuum

manifold system and spin based protocols for extraction of HCV-RNA using Favorgen kit high efficiency silica based spin column as reported in [4] followed by RT-qPCR. The sensitivity of two methods was compared using samples of different viral load.

## 2. Materials and Methods

In the present study, 30 EDTA anticoagulated plasma samples submitted to the Punjab Institute of Nuclear Medicine for quantitative analysis of HCV were processed. HCV-RNA had been extracted by use of the Favorgen kit according to the manufacturer's instructions [5] as shown in Figure 1. In 2 mL microcentrifuge tubes,  $150 \mu\text{L}$  plasma samples were mixed with  $575 \mu\text{L}$  of lysis buffer and appropriate amounts of internal controls. After incubation for 12 min,  $575 \mu\text{L}$  of ethanol was added to the tube for precipitation. The samples were vortexed (vortex mixer Labnet) and centrifuged (Eppendorf centrifuge 5424). Subsequently, the working solution was loaded into spin column in two steps and was separated by centrifugation at 8000 rpm (RCF) for 1 min. To remove cell debris, RNA attached to silica membrane was washed with

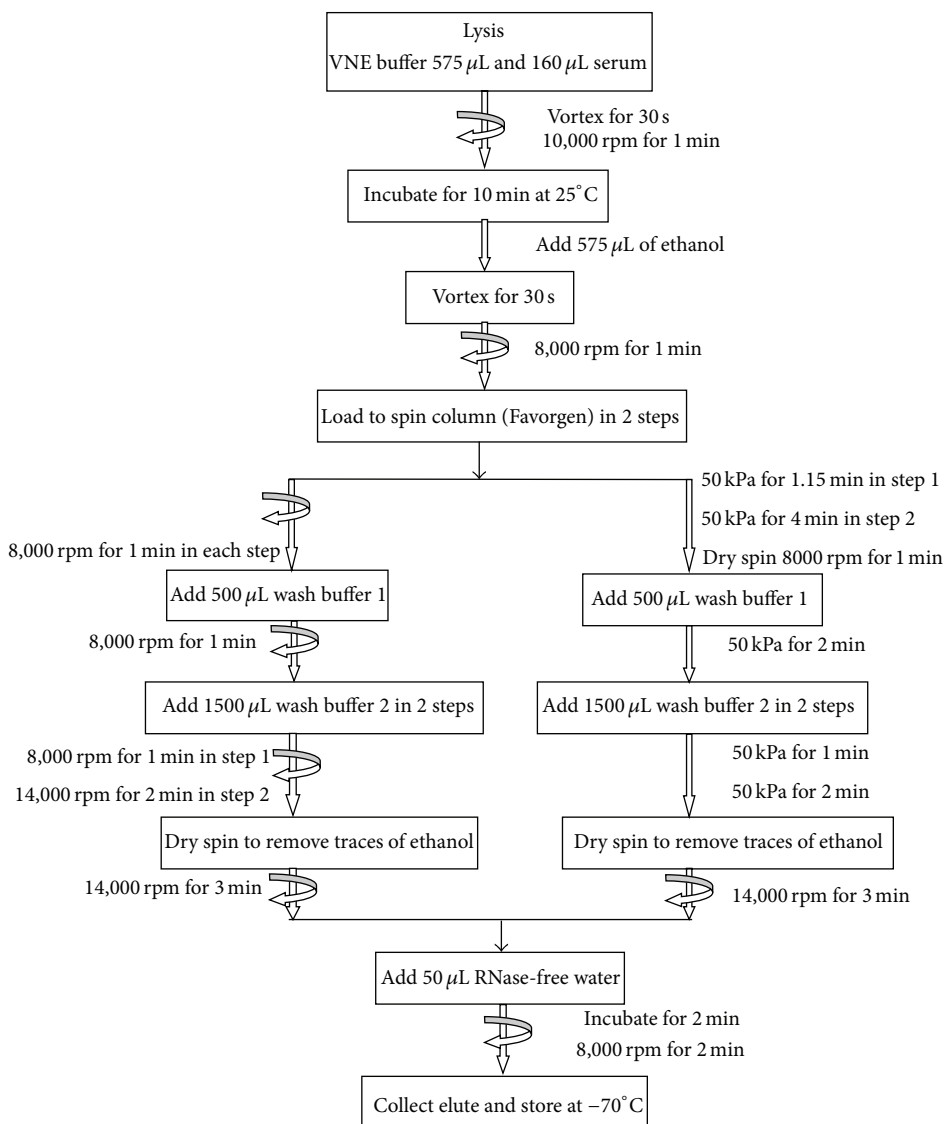


FIGURE 1: Spin and vacuum filtration based protocol for HCV-RNA extraction using Favorgen kit.

buffers 1 and 2. After complete removal of the final washing buffer by centrifugation at 14000 rpm for 3 min, RNA was eluted with RNase-free water, and the eluate was stored at  $-70^{\circ}\text{C}$ . At least 30 samples could be processed in 60 min.

**2.1. Semiautomated Extraction Protocol.** To permit a higher throughput, the manual protocol described above was implemented on vacuum filtration assembly (Welch-Ilmvac 2522) under conditions as shown in Figure 1.

**2.2. RT-qPCR.** HCV-RNA was quantified using real-time Taqman based AmpliSens HCV-FRT kits [6]. A  $15\ \mu\text{L}$  master mix containing RT-G-mix-2, RT-PCR-mix-1, RT-PCR-mix-2, polymerase (TaqF), and TM-Revertase (MMIv) was added to  $10\ \mu\text{L}$  of each eluted nucleic acid.

RT-qPCR was completed on Rotor-Gene Q 6000 (5 Plex-HRM) using the following cycling parameters: an initial cDNA synthesis by holding at 50 and  $95^{\circ}\text{C}$  for 15 min each,

followed by 45 cycles of denaturation ( $95^{\circ}\text{C}$  for 2 s), annealing ( $60^{\circ}\text{C}$  for 5 s), and extension ( $72^{\circ}\text{C}$  for 15 s). Mathematical analysis and graphical representations were performed using Rotor-Gene Q software.

### 3. Results and Discussions

Almost 30 clinical samples were subjected to RNA extraction in parallel by the spin and vacuum filtration based protocol using Favorgen kit. The experimental conditions of vacuum filtration were optimized by repeating experiments using positive control. RT-qPCR results by two extraction methods are given in Table 1. All the samples were run in duplicate and mean value was used for data analysis. Assay linearity was confirmed with the serial dilutions of RTA (Turkey) containing  $1 \times (10^6, 10^5, 10^4, \text{ and } 10^3)\ \text{IU mL}^{-1}$ . Viral load HCV-RNA was expressed in  $\text{IU mL}^{-1}$ . Although the difference of viral load was not very dramatic but rather high,

TABLE 1: RT-qPCR results using spin and vacuum filtration based protocols for HCV-RNA extraction.

Sample ID	CT	CT	CT	IU mL <sup>-1</sup>	IU mL <sup>-1</sup>	Cv %
	Internal control	Vacuum filtration	Spin	Vacuum filtration	Spin	
1	25.99	15.6 ± 0.3	18.4 ± 0.4	481,419	67,458	0.9
2	26.48	16.0 ± 0.3	17.0 ± 0.3	360,304	177,932	0.6
3	26.57	22.6 ± 0.7	24.7 ± 0.5	3,602	847	0.01
4	26.8	12.8 ± 0.2	15.1 ± 0.3	3,299,175	704,535	6.4
5	27.5	18.6 ± 0.4	19.6 ± 0.4	60,629	28,823	0.1
6	26.34	13.3 ± 0.2	15.7 ± 0.3	2,461,014	430,986	4.7
7	27.14	16.1 ± 0.3	18.8 ± 0.4	348,791	51,043	0.7
8	26.86	17.6 ± 0.3	18.6 ± 0.4	112,812	56,348	0.2
9	27.84	14.6 ± 0.2	16.8 ± 0.3	946,830	206,548	1.8
10	26.54	17.2 ± 0.3	31.8 ± 1.2	160,482	54,132	0.3
11	26.29	19.2 ± 0.4	20.4 ± 0.6	38,131	16,544	0.1
12	24.9	21.4 ± 0.6	22.18 ± 0.7	9,683	5,736	0.0
13	24.7	15.07 ± 0.3	17.2 ± 0.3	767,124	179,381	0.2
14	26.28	18.9 ± 0.4	19.8 ± 0.4	52,693	29,976	0.02
15	26.77	22.2 ± 0.7	22.6 ± 0.7	5,810	4,340	0.0
16	26.2	20.4 ± 0.6	21.2 ± 0.6	19,312	11,584	0.01
17	25.4	19.8 ± 0.4	20.0 ± 0.4	29,849	25,136	0.01
18	26.8	21.6 ± 0.6	21.8 ± 0.7	8,328	7,507	0.00
19	26.1	15.3 ± 0.3	17.1 ± 0.3	642,090	187,782	0.2
20	26.0	21.4 ± 0.6	23.4 ± 0.7	9,533	2,555	0.0
21	26.1	18.8 ± 0.4	19.0 ± 0.4	55,731	50,456	0.02
22	26.1	17.2 ± 0.3	18.3 ± 0.4	171,609	83,106	0.06
23	25.7	19.3 ± 0.4	20.1 ± 0.4	46,845	24,354	0.02
24	28.4	21.5 ± 0.6	22.5 ± 0.7	9,201	4,760	0.0
25	26.1	22.1 ± 0.6	24.3 ± 0.7	5,980	1,307	0.0
26	26.8	20.3 ± 0.6	20.7 ± 0.6	20,985	16,260	0.01
27	31.5	26.0 ± 0.9	26.9 ± 0.8	280	150	0.01
28	18.5	18.1 ± 0.3	18.5 ± 0.4	95,495	70,695	0.04
29	31.2	16.2 ± 0.3	17.5 ± 0.3	352,282	145,151	0.1
30	27.5	19.44 ± 0.4	20.5 ± 0.6	37,850	18,256	0.01

yield for the sera with amplified product was obtained by vacuum filtration based protocol with coefficient of variation of 6.4% [7]. One of the reasons that might be possible for high HCV-RNA yield is strong retention capacity of HCV-RNA on silica based membrane under employed vacuum pressure [8]. Constant amplification efficiency made the comparison reliable between two assays as demonstrated by threshold cycle of internal control CT IC.

A bivariate normal distribution fit between two assays gave diagonally distributed density ellipsoid with correlation of 95% between vacuum filtration and spin based protocols, indicating that both methods were efficient in the removal of inhibitory substance; see Figure 2.

Nevertheless, the modification of protocol from spin to vacuum filtration allowed extraction to be completed within 35 minutes. In addition, costs for consumables in

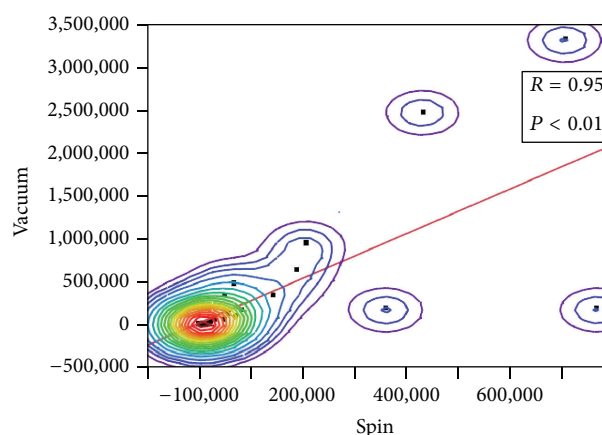


FIGURE 2: Bivariate fit between two assays.

semiautomated vacuum filtration based extraction reduced from \$1 to 0.5 with reduced labor. At the same time, this protocol is more environmentally friendly due to reduced incineration of infected collection tubes. Thus, semiautomation is a more forward looking approach for nucleic acid purification together with real-time qPCR.

#### 4. Conclusion

The performance of semiautomated vacuum filtration based extraction method was shown to permit a quick extraction process and accurate results for a quantitative assay of HCV-RNA. The method might be an alternative to an expensive full automation station for developing countries which is easy to perform and efficient. In short, costly instruments are not required to prevent contamination and to enhance the safety of worker.

#### Conflict of Interests

The authors declare that there is no conflict of interests regarding the publication of this paper.

#### Authors' Contribution

Imran Amin and Tania Jabbar have equal contributions and the names are written alphabetically.

#### References

- [1] S. C. Tan and B. C. Yiap, "DNA, RNA, and protein extraction: the past and the present," *Journal of Biomedicine and Biotechnology*, vol. 2009, Article ID 574398, 10 pages, 2009.
- [2] H. Miyachi, A. Masukawa, S. Asai et al., "Quantitative assay of hepatitis C virus RNA using an automated extraction system for specific capture with probes and paramagnetic particle separation," *Journal of Clinical Microbiology*, vol. 41, no. 2, pp. 572–575, 2003.
- [3] H. H. Kessler, A. M. K. Clarici, E. Stelzl et al., "Fully automated detection of hepatitis C virus RNA in serum and whole-blood samples," *Clinical and Diagnostic Laboratory Immunology*, vol. 9, no. 6, pp. 1385–1388, 2002.
- [4] B. Zhang, K. Chen, and E. Ni, "Comparison of three methods for extraction of HCV RNA in sera collected from individuals with hyperlipidemia, hyperbilirubinemia and hyperglobulinemia," *Journal of Virological Methods*, vol. 212, pp. 44–46, 2015.
- [5] Favorgen HCV-PCR extraction kit Instruction manual.
- [6] AmpliSens HCV-FRT PCR kit Instruction manual.
- [7] F. S. Nolte, C. Thurmond, and P. S. Mitchell, "Isolation of hepatitis C virus RNA from serum for reverse transcription-PCR," *Journal of Clinical Microbiology*, vol. 32, no. 2, pp. 519–520, 1994.
- [8] M. S. Forman and A. Valsamakis, "Verification of an assay for quantification of hepatitis C virus RNA by use of an analyte-specific reagent and two different extraction methods," *Journal of Clinical Microbiology*, vol. 42, no. 8, pp. 3581–3588, 2004.

## Research Article

# Comparison of Electrospray Ionization and Atmospheric Chemical Ionization Coupled with the Liquid Chromatography-Tandem Mass Spectrometry for the Analysis of Cholesteryl Esters

Hae-Rim Lee,<sup>1</sup> Sunil Kochhar,<sup>2</sup> and Soon-Mi Shim<sup>1</sup>

<sup>1</sup>Department of Food Science and Technology, Sejong University, 98 Gunja-dong, Seoul 143-747, Republic of Korea

<sup>2</sup>Department of Lipids & Off-Flavors, Nestlé Research Center, Nestec, Vers-chez-les-Blanc, 1000 Lausanne 26, Switzerland

Correspondence should be addressed to Sunil Kochhar; [Sunil.kochhar@rdls.nestle.com](mailto:Sunil.kochhar@rdls.nestle.com)  
and Soon-Mi Shim; [soonmishim@sejong.ac.kr](mailto:soonmishim@sejong.ac.kr)

Received 15 October 2014; Revised 15 February 2015; Accepted 15 February 2015

Academic Editor: Mohamed Abdel-Rehim

Copyright © 2015 Hae-Rim Lee et al. This is an open access article distributed under the Creative Commons Attribution License, which permits unrestricted use, distribution, and reproduction in any medium, provided the original work is properly cited.

The approach of two different ionization techniques including electrospray ionization (ESI) and atmospheric pressure chemical ionization (APCI) coupled with liquid chromatography-tandem mass spectrometry (LC-MS/MS) was tested for the analysis of cholesteryl esters (CEs). The retention time (RT), signal intensity, protonated ion, and product ion of CEs were compared between ESI and APCI. RT of CEs from both ionizations decreased with increasing double bonds, while it increased with longer carbon chain length. The ESI process generated strong signal intensity of precursor ions corresponding to  $[M+Na]^+$  and  $[M+NH_4]^+$  regardless of the number of carbon chains and double bonds in CEs. On the other hand, the APCI process produced a protonated ion of CEs  $[M+H]^+$  with a weak signal intensity, and it is selectively sensitive to detect precursor ions of CEs with unsaturated fatty acids. The ESI technique proved to be effective in ionizing more kinds of CEs than the APCI technique.

## 1. Introduction

Mother's milk is widely known as the first and essential food for infants [1]. Many studies have discovered that mother's milk provides numerous beneficial health effects including improving neurologic development, immune system against pathogens, gastrointestinal function, and obesity inhibition [1–4]. Mother's milk consists of various nutrients including cholesterol (Chl), and such components are dependent on the mother's diets and are required for infant's growth [5]. A previous study suggested that a high level of Chl intake during infancy through mother's milk can reduce the blood Chl level in adults, implying a high amount of Chl intake can decrease the risk of atherosclerosis and heart disease [5, 6].

Cholesteryl ester (CEs) is an esterified form of Chl in mother's milk and it consists of a long chain fatty acids, connecting with the hydroxyl group of Chl. It is known as

an efficient form to transport Chl through the blood stream [7]. There are two enzymes involved in the biosynthesis of CEs in humans, that is, lecithin-cholesterol acyl transferase (LCAT) and acyl-coA:cholesterol acyltransferase (ACAT). LCAT catalyzes Chl to cholesteryl esters by transferring fatty acids to Chl. In the small intestine, absorbed Chl is esterified by ACAT (Figure 1) [7–10]. The biosynthesis of CEs plays a role in the regulation of cholesterol transport and storage as well as membrane function. More importantly, it is controlled by intracellular Chl levels [11].

Many approaches have been developed that are well-suited for analyzing hydrophobic components. Gas liquid chromatography (GC) and thin-layer chromatography (TLC) have been utilized for the analysis of CEs in human milk [7, 12, 13]. Recently, high performance liquid chromatography (HPLC) condition has been optimized for the identification and quantification of CEs in various matrices such as human

meibum, human plasma, and margarine spread [14–16]. For instance, a hexyl-phenyl HPLC column with a mobile phase consisting mixture of acetonitrile and water was used with an atmospheric pressure chemical ionization (APCI) source to analyze the CEs in food matrices such as orange juice and margarine spread [13]. Butovich [15] utilized a reversed-phase (RP) C18 HPLC column with a mobile phase mixture coupled ammonium formate, acetonitrile, and propan-2-ol with an APCI source for the identification of 20 kinds of CEs in human meibum. To date, electrospray ionization (ESI) and APCI are the most common ionization sources for the coupling of LC to a tandem mass spectrometry (MS/MS) [16]. Under optimal ESI conditions, a charged liquid is formatted and sprayed for evaporating the solvent. And then, ion formation occurs in the fission of charged droplets due to the high field intensity. This technique is appropriate for analyzing polar components [17]. In optimized APCI, a mixture of solvent molecules and analyte molecules goes through a corona discharge after being dried in the gas phase. The solvent molecules are ionized to create charged solvent ions. The charge which is located with solvent ions is transferred to the analyte molecules, producing analyte ions. APCI is usually used to analyze nonpolar molecules with lower molecular weight [18]. Hence, we hypothesized that the ESI process is more adequate ionization for analysis of CEs than the APCI due to the ESI and APCI different mechanism of ionization, a potential polarity of CEs attributed to the ester group, and CEs' large molecular weight.

## 2. Materials & Method

**2.1. Chemicals.** HPLC grade acetonitrile, propan-2-ol, methanol, and water were purchased from Fisher scientific (Leicestershire, UK). Chloroform, n-hexane, ethanol, ammonium acetate, petroleum benzene, and diethyl ether were obtained from Merck-chemicals (Darmstadt, Germany). Ammonium formate and acetic acid glacial were obtained from Biosolve (Dieuze, France).

Twenty three standards of cholesterol esters (CEs) including: Chl-butyrate, Chl-valerate, Chl-heptanoate, Chl-caprylate, Chl-nonanoate, Chl-caprate, Chl-undecanoate, Chl-laurate, Chl-tridecanoate, Chl-myristate, Chl-pentadecanoate, Chl-palmitate, Chl-heptadecanoate, Chl-nonadecanoate, Chl-arachidate, Chl-heneicosanoate, Chl-behenate, and Chl-lignocerate were purchased from Nu-Chek (Elysian, MN). Chl-arachidonate, Chl-linoleate, Chl-palmitelaidate, Chl-oleate, and Chl-stearate were purchased from Sigma Aldrich (St. Louis, CA).

**2.2. Preparation of Standard Solution.** Aliquot amount of each standard was weighed and solubilized in 100% chloroform. Stock solution was consequently diluted by n-hexane/propan-2-ol (1:1, v/v) for calibration by HPLC-MS/MS (ThermoFisher Scientific, Franklin, MA).

### 2.3. Analytical Conditions

**2.3.1. High-Performance Liquid Chromatography (HPLC).** The method from Butovich [15] was adopted with certain

modifications. The samples were analyzed by using HPLC (ThermoFisher Scientific, Franklin, MA) with aria OS software (ThermoFisher Scientific, Franklin, MA). Hypersil Gold C18 column (150 mm × 2.1 mm, 5 μm) obtained from Thermo Electron (San Jose, CA) was used for the separation of CEs. Acetonitrile containing 5% of 5 mM aqueous ammonium formate was used as mobile phase A, whereas propan-2-ol contains 5% of 5 mM ammonium formate as mobile phase B. Before the injection, the column was preequilibrated with a solvent mixture (A : B, 47.4 : 52.6, v/v). The gradient rate was linearly changed to 7.6% of mobile phase A over the period of 35 min. The gradient rate was maintained for 10 min and then went back to the initial condition having 47.4% of mobile phase A within the next 1 min. It was reequilibrated for another 14 min.

**2.3.2. Mass Spectrometry (MS) Condition.** MS was conducted after separation by HPLC using Thermo LTQ having interchangeable ESI and APIC probes (Thermo Fisher Scientific Inc., San Jose, CA). The full scan with speed in events per second was carried out.

**(1) Atmospheric Pressure Chemical Ionization Source (APCI).** The entire flow was directed to the APCI ion source operating in the positive ion mode. Total ion chromatograms were recorded in the  $m/z$  range of 50 to 800. The vaporization and capillary temperature were set at 270 and 250°C, respectively. Sheath, ion sweep, and auxiliary gas pressure were set at 20, 2.0, and 5 psi, respectively. In MS<sub>2</sub> (MS/MS) experiments, the normalized collision energy was optimized for each of the compounds. Helium was used as a collision gas.

**(2) Electrospray Ionization Source (ESI).** The entire flow was directed to the Thermo LTQ ESI ion source operating in the positive ion mode (Thermo Fisher Scientific Inc., San Jose, CA). Total ion chromatograms were recorded in the  $m/z$  range of 50 to 800. ESI probe ion was used. Spray voltage was set to 4000 V. Vaporization and capillary temperature was set at 240 and 280°C, respectively. Sheath (N<sub>2</sub>), ion sweep, and auxiliary gas (N<sub>2</sub>) pressure were, respectively, set at 10, 2.0, and 5 psi. In MS<sub>2</sub> (MS/MS) experiments, the normalized collision energy was optimized for each of the compounds. The particular transitions, the collision energy, and the tube lens settings were specific for each analyte and obtained using the TSQ Tune Master software in the optimization MS + MS/MS mode. These were shown in Table 1.

## 3. Results and Discussion

**3.1. Comparison of Retention Time, Intensity, and Ion Fragmentation of CEs between ESI and APCI Mass Spectra.** ESI is one of the primary ionization techniques for the coupling of LC to MS, while APCI is a supplementary technique to electrospray and suitable for thermally stable polar and nonpolar compounds due to no generation of charged ions. ESI is particularly suited for polar organic compounds and is sensitive to matrix effects. High molecular weight compounds can be observed as multicharged molecular ions in ESI. In contrast to ESI, the APCI technique is used to analyze

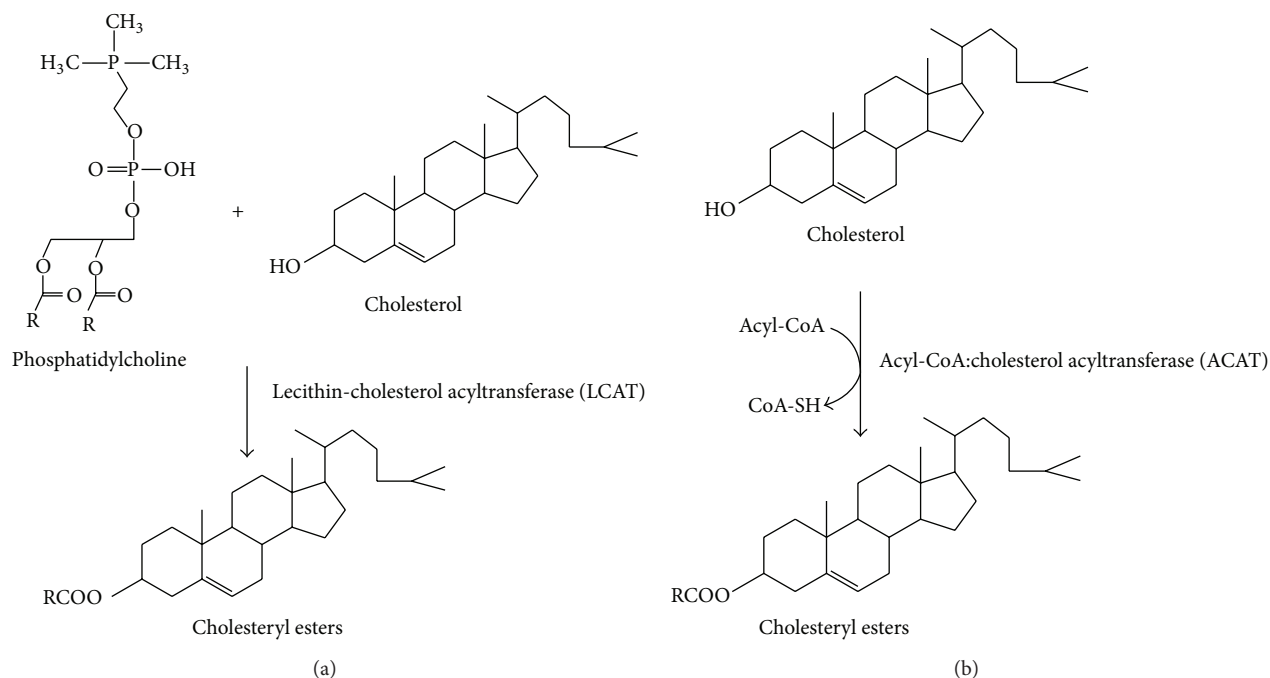


FIGURE 1: Biosynthesis of cholesterol esters (CEs) in human by two enzymes: lecithin-cholesterol acyl transferase (LCAT) (a) and acyl-CoA:cholesterol acyltransferase (ACAT) (b).

smaller molecular compared to ESI technique [16, 19, 20]. Owing to different ionization mechanism and characteristics of CEs, we hypothesized that ESI is more suitable for isolation and identification of CEs than APCI; firstly, polarity of CEs is due to the ester group. Secondly, the least molecular weight of CEs is 428.7, which is combined cholesterol with acetic acid (C2:0).

The retention time (RT) of CEs by using both ESI and APCI process is expressed in Table 1. Overall, RT of CEs on total ion chromatogram (TIC) was affected by a number of carbon chains and double bonds. The Chl-lignocerate (C24:0) appeared at 28.49 min of RT, while Chl-myristate was separated at 16.06 min of RT. RT increased with longer carbon chain lengths. CEs containing the same number of carbons with different number of double bonds such as Chl-linoleate (C18:2), Chl-oleate (C18:1), and Chl-stearate (C18:0) appeared at 15.55, 18.13, and 21.31 min of RT, respectively. The present double bonds reduced RT. These findings are similar to a previous study in which fatty acid's chain length and double bond influenced the RT in the analysis fatty acid [21, 22].

Under ESI technique, both full and product ion scan of CEs standards were demonstrated to generate protonated molecular ions such as  $[M+Na]^+$  and  $[M+NH_4]^+$  (Table 1). Among the protonated ions,  $[M+Na]^+$  was the most abundant for 18 CEs:  $m/z$  479 for Chl-butyrate,  $m/z$  493 for Chl-valerate,  $m/z$  521 for Chl-heptanoate,  $m/z$  535 for Chl-caprylate,  $m/z$  549 for Chl-nonanoate,  $m/z$  563 for Chl-caprate,  $m/z$  577 for Chl-undecanoate,  $m/z$  519 for Chl-laurate,  $m/z$  605 for Chl-tridecanoate,  $m/z$  619 for Chl-myristate,  $m/z$  633 for Chl-pentadecanoate,  $m/z$  647 for Chl-palmitate,  $m/z$  661 for Chl-heptadecanoate,  $m/z$  675

for Chl-stearate,  $m/z$  689 for Chl-nonadecanoate,  $m/z$  703 for Chl-arachidate,  $m/z$  717 for Chl-heneicosanoate, and  $m/z$  731 for Chl-behenate. As shown in Table 1, 5 other CEs including Chl-palmitelaidate, Chl-linoleate, Chl-oleate, Chl-arachidonate, and Chl-lignocerate were detected corresponding to  $[M+NH_4]^+$  at  $m/z$  690, 666, 640, 668, and 754, respectively. This adduct ion ( $[M+NH_4]^+$ ) appeared to have stronger intensity than other proton adducts such as  $[M+Na]^+$  and  $[M+H]^+$ . In the HPLC-ESI-MS/MS analysis of CEs, all standards lost its fatty acid as well as created a specific fragment with  $m/z$  369 derived from Chl. The product ion at  $m/z$  369 is supposed to be Chl upon its dehydration, corresponding to  $[M-H_2O+H]^+$  and suggesting that Chl produces the specific daughter ion with an  $m/z$  369 by using ESI technique. Up to now, only 20 kinds of CEs in human medium have been analyzed by APCI linked to HPLC-MS [15]. To our knowledge, there is no study regarding the analysis of various CEs using ESI as a source.

APCI ion source hardware is quite similar to that of ESI. The differences are both the APCI probe, which consists of a heated ceramic tube where the effluent is evaporated and a corona needle [23]. Thus, the difference in signal intensity and product ion of CEs between APCI and ESI source was investigated. In the current study, 23 CEs were analyzed according to the APCI technique (Table 1). All CEs standards created the protonated molecule,  $[M+H]^+$ , showing a lower signal intensity at the same concentration compared to the consequence of the ESI source. This implies that the insufficient parent ion of CEs was produced using APCI. Nevertheless, CEs containing double bonds were observed to have relatively strong signal intensity from APCI

TABLE 1: Time-scheduled SIM conditions,  $m/z$  ions and corresponding structures used in the LC-ESI-MS/MS analysis of CEAs.

Compound	Retention time (RT, min)	Molecular weight (Mw)	SRM transitions		Coll. energy (v)		Corresponding structure		NL		Fatty acid
			$(m/z)$ Precursor ion	Product ion	ESI	APCI	ESI	APCI	ESI	APCI	
Chl-butyrate	7.02	456.8	479.4 → 119	457.5 → 105.20	40	62	[M+Na] <sup>+</sup>	[M+H] <sup>+</sup>	2.82E + 03	1.22E + 02	4:0
			479.4 → 369	457.5 → 369	5	7					
Chl-valerate	7.69	470.8	493.4 → 105	471 → 369	39	20	[M+Na] <sup>+</sup>	[M+H] <sup>+</sup>	8.14E + 03	9.54E + 01	5:0
			493.4 → 369	—	9						
Chl-heptanoate	8.93	498.8	521.4 → 147	499.6 → 369	31	8	[M+Na] <sup>+</sup>	[M+H] <sup>+</sup>	1.28E + 04	1.14E + 01	7:0
			521.4 → 369	—	9						
Chl-caprylate	9.77	512.8	535.5 → 147	514 → 369	22	10	[M+Na] <sup>+</sup>	[M+H] <sup>+</sup>	1.44E + 04	2.94E + 01	8:0
			535.5 → 369	—	13						
Chl-nonanoate	10.64	526.9	549.5 → 105	528 → 369	42	5	[M+Na] <sup>+</sup>	[M+H] <sup>+</sup>	1.24E + 04	6.03E + 01	9:0
			549.5 → 369	—	10						
Chl-caprate	11.64	540.9	563.5 → 107	542 → 369	30	11	[M+Na] <sup>+</sup>	[M+H] <sup>+</sup>	1.50E + 04	2.88E + 02	10:0
			563.5 → 369	—	18						
Chl-undecanoate	12.51	555	577.5 → 161	556 → 369	32	8	[M+Na] <sup>+</sup>	[M+H] <sup>+</sup>	1.76E + 04	3.42E + 02	11:0
			577.5 → 369	—	14						
Chl-laurate	13.68	569	591.5 → 161	570 → 146.9	32	32	[M+Na] <sup>+</sup>	[M+H] <sup>+</sup>	1.50E + 04	1.40E + 03	12:0
			591.5 → 369	570 → 369	13	10					
Chl-arachidionate	13.98	673.11	690.6 → 109	674 → 147.14	43	36	[M+NH <sub>4</sub> ] <sup>+</sup>	[M+H] <sup>+</sup>	5.03E + 05	2.46E + 04	20:4
			690.6 → 369	674 → 369	10	14					
Chl-tridecanoate	15.09	583	605.5 → 105	584 → 369	46	10	[M+Na] <sup>+</sup>	[M+H] <sup>+</sup>	1.22E + 04	1.96E + 02	13:0
			605.5 → 369	—	13						
Chl-linoleate	15.55	649.08	666.6 → 161	650 → 373.26	30	15	[M+NH <sub>4</sub> ] <sup>+</sup>	[M+H] <sup>+</sup>	2.77E + 05	1.14E + 04	18:2
			666.6 → 369	650 → 361.26	9	15					
Chl-palmitelaidate	15.92	623.05	640.6 → 108	624 → 335.21	35	15	[M+NH <sub>4</sub> ] <sup>+</sup>	[M+H] <sup>+</sup>	6.73E + 04	4.10E + 03	16:2
			640.6 → 369	624 → 369	9	13					
Chl-myristate	16.06	597	619.5 → 108	598 → 369	39	14	[M+Na] <sup>+</sup>	[M+H] <sup>+</sup>	1.57E + 04	2.61E + 02	14:0
			619.5 → 369	—	16						
Chl-pentadecanoate	17.52	611.1	633.6 → 369	612 → 369	12	5	[M+Na] <sup>+</sup>	[M+H] <sup>+</sup>	5.06E + 03	1.75E + 03	15:0
			633.6 → 369	612 → 369	12	5					
Chl-oleate	18.13	651.1	668.6 → 147	652 → 363.28	33	20	[M+NH <sub>4</sub> ] <sup>+</sup>	[M+H] <sup>+</sup>	1.62E + 05	8.79E + 03	18:1
			668.6 → 369	652 → 369	8	11					
Chl-palmitate	18.6	625.1	647.6 → 147	626 → 161.1	28	23	[M+Na] <sup>+</sup>	[M+H] <sup>+</sup>	1.17E + 04	2.23E + 03	16:0
			647.6 → 369	626 → 369	14	11					
Chl-heptadecanoate	19.92	639.1	661.6 → 105	640 → 146.89	69	32	[M+Na] <sup>+</sup>	[M+H] <sup>+</sup>	1.43E + 04	1.67E + 03	17:0
			661.6 → 369	640 → 369	16	10					
Chl-stearate	21.31	653.1	675.6 → 135	654 → 273.16	38	31	[M+Na] <sup>+</sup>	[M+H] <sup>+</sup>	9.78E + 03	7.03E + 02	18:0
			675.6 → 369	654 → 369	15	6					
Chl-nonadecanoate	22.53	667.2	689.6 → 119	668 → 147	45	28	[M+Na] <sup>+</sup>	[M+H] <sup>+</sup>	1.24E + 04	7.34	19:0
			689.6 → 369	668 → 369	19	9					
Chl-arachidate	23.85	681.2	703.6 → 335	682 → 228.75	16	33	[M+Na] <sup>+</sup>	[M+H] <sup>+</sup>	7.32E + 04	6.00E + 02	20:0
			703.6 → 369	682 → 369	15	5					
Chl-heneicosanoate	25.14	695.2	717.7 → 349.5	696 → 272.6	17	31	[M+Na] <sup>+</sup>	[M+H] <sup>+</sup>	5.94E + 04	2.92E + 03	21:0
			717.7 → 369	696 → 369	19	14					
Chl-behenate	26.39	709.2	731.7 → 363	710 → 386.13	17	14	[M+Na] <sup>+</sup>	[M+H] <sup>+</sup>	6.73E + 04	1.82E + 03	22:0
			731.7 → 369	710 → 369	23	9					
Chl-lignocerate	28.49	737.3	754.7 → 132	738 → 108.96	50	28	[M+NH <sub>4</sub> ] <sup>+</sup>	[M+H] <sup>+</sup>	4.86E + 04	5.01E + 03	24:0
			754.7 → 369	738 → 369	11	16					

source. For example, signal intensity of Chl-arachidonate (C20:4) was higher than that of Chl-arachidate (C20:0) in the MS<sub>1</sub> experiment of their [M+H]<sup>+</sup> ions. The same patterns occurred among Chl-linoleate (C18:2), Chl-oleate (C18:1), and Chl-stearate (C18:0) as shown in Table I. The precursor ion of CEs with unsaturated fatty acids seems to be sensitively detected compared to CEs with saturated fatty acid by the APCI technique. Butovich [15] found that the fragmentation of CEs containing saturated fatty acids did not generate clear specific product ions except for *m/z* 369 because of the very low intensity of their precursor ions [M+H]<sup>+</sup>.

In conclusion, the ESI technique produced two protonated ions of CEs such as [M+Na]<sup>+</sup> and [M+NH<sub>4</sub>]<sup>+</sup> with strong signal intensity; otherwise, the APCI technique generated protonated ion [M+H]<sup>+</sup>. The ESI process coupled with LC-MS more effectively ionized CEs than the APCI process regardless of number of carbon chains and double bonds. However, there is a limitation for comparison in the ESI and APCI source regarding which one is appropriate ionization on analyzing of CEs. It is necessary to study the comparison in the limit of detection, limit of quantification, matrix effects of ESI, and APCI for providing a suitable MS to LC conditions for CEs.

## Conflict of Interests

The authors do not have any conflict of interests related to this paper.

## Authors' Contribution

Sunil Kochhar and Soon-Mi Shim contributed equally to the study.

## References

- [1] R. Y. Nishimura, G. S. F. de Castro, A. A. Jordão Jr., and D. S. Sartorelli, "Breast milk fatty acid composition of women living far from the coastal area in Brazil," *Jornal de Pediatria*, vol. 89, no. 3, pp. 263–268, 2013.
- [2] C. G. Perrine and K. S. Scanlon, "Prevalence of use of human milk in US advanced care neonatal units," *Pediatrics*, vol. 131, no. 6, pp. 1066–1071, 2013.
- [3] I. Ojeda, M. Moreno-Guzmán, A. González-Cortés, P. Yáñez-Sedeño, and J. M. Pingarrón, "A disposable electrochemical immunosensor for the determination of leptin in serum and breast milk," *Analyst*, vol. 138, no. 15, pp. 4284–4291, 2013.
- [4] U.-J. Yang, S. Ko, and S.-M. Shim, "Vitamin C from standardized water spinach extract on inhibition of cytotoxicity and oxidative stress induced by heavy metals in HepG2 cells," *Journal of the Korean Society for Applied Biological Chemistry*, vol. 57, no. 2, pp. 161–166, 2014.
- [5] A. M. Kamelska, R. Pietrzak-Fiećko, and K. Bryl, "Variation of the cholesterol content in breast milk during 10 days collection at early stages of lactation," *Acta Biochimica Polonica*, vol. 59, no. 2, pp. 243–247, 2012.
- [6] Y. Arad, J. J. Badimon, L. Badimon, W. C. Hembree, and H. N. Ginsberg, "Dehydroepiandrosterone feeding prevents aortic fatty streak formation and cholesterol accumulation in cholesterol-fed rabbit," *Arteriosclerosis, Thrombosis, and Vascular Biology*, vol. 9, no. 2, pp. 159–166, 1989.
- [7] J. Bitman, D. L. Wood, N. R. Mehta, P. Hamosh, and M. Hamosh, "Comparison of the cholesteryl ester composition of human milk from preterm and term mothers," *Journal of Pediatric Gastroenterology and Nutrition*, vol. 5, no. 5, pp. 780–786, 1986.
- [8] T.-Y. Chang, B.-L. Li, C. C. Y. Chang, and Y. Urano, "Acyl-coenzyme A: cholesterol acyltransferases," *The American Journal of Physiology—Endocrinology and Metabolism*, vol. 297, no. 1, pp. E1–E9, 2009.
- [9] C. Pramfalk, M. Eriksson, and P. Parini, "Cholesteryl esters and ACAT," *European Journal of Lipid Science and Technology*, vol. 114, no. 6, pp. 624–633, 2012.
- [10] S. Kunnen and M. van Eck, "Lecithin: cholesterol acyltransferase: old friend or foe in atherosclerosis?" *Journal of Lipid Research*, vol. 53, no. 9, pp. 1783–1799, 2012.
- [11] J. D. Horton, J. L. Goldstein, and M. S. Brown, "SREBPs: activators of the complete program of cholesterol and fatty acid synthesis in the liver," *The Journal of Clinical Investigation*, vol. 109, no. 9, pp. 1125–1131, 2002.
- [12] R. M. Clark and K. E. Hundrieser, "Changes in cholesteryl esters of human milk with total milk lipid," *Journal of Pediatric Gastroenterology & Nutrition*, vol. 9, no. 3, pp. 347–350, 1989.
- [13] E. A. Emken, R. O. Adlof, D. L. Hachey, C. Garza, M. R. Thomas, and L. Brown-Booth, "Incorporation of deuterium-labeled fatty acids into human milk, plasma, and lipoprotein phospholipids and cholesteryl esters," *Journal of Lipid Research*, vol. 30, no. 3, pp. 395–402, 1989.
- [14] I. Mezine, H. Zhang, C. Macku, and R. Lijana, "Analysis of plant sterol and stanol esters in cholesterol-lowering spreads and beverages using high-performance liquid chromatography-atmospheric pressure chemical ionization-mass spectroscopy," *Journal of Agricultural and Food Chemistry*, vol. 51, no. 19, pp. 5639–5646, 2003.
- [15] I. A. Butovich, "Cholesteryl esters as a depot for very long chain fatty acids in human meibum," *Journal of Lipid Research*, vol. 50, no. 3, pp. 501–513, 2009.
- [16] O. A. Ismaiel, M. S. Halquist, M. Y. Elmamly, A. Shalaby, and H. Thomas Karnes, "Monitoring phospholipids for assessment of ion enhancement and ion suppression in ESI and APCI LC/MS/MS for chlorpheniramine in human plasma and the importance of multiple source matrix effect evaluations," *Journal of Chromatography B: Analytical Technologies in the Biomedical and Life Sciences*, vol. 875, no. 2, pp. 333–343, 2008.
- [17] W. M. A. Niessen and A. P. Tinke, "Liquid chromatography-mass spectrometry. General principles and instrumentation," *Journal of Chromatography A*, vol. 703, no. 1-2, pp. 37–57, 1995.
- [18] A. Garcia-Ac, P. A. Segura, L. Viglino, C. Gagnon, and S. Sauvé, "Comparison of APPI, APCI and ESI for the LC-MS/MS analysis of bezafibrate, cyclophosphamide, enalapril, methotrexate and orlistat in municipal wastewater," *Journal of Mass Spectrometry*, vol. 46, no. 4, pp. 383–390, 2011.
- [19] J. M. Purcell, C. L. Hendrickson, R. P. Rodgers, and A. G. Marshall, "Atmospheric pressure photoionization fourier transform ion cyclotron resonance mass spectrometry for complex mixture analysis," *Analytical Chemistry*, vol. 78, no. 16, pp. 5906–5912, 2006.
- [20] M. E. Rybak, D. L. Parker, and C. M. Pfeiffer, "Determination of urinary phytoestrogens by HPLC-MS/MS: a comparison of atmospheric pressure chemical ionization (APCI) and electrospray ionization (ESI)," *Journal of Chromatography B*, vol. 861, no. 1, pp. 145–150, 2008.

- [21] M. I. Avelano, M. VanRollins, and L. A. Horrocks, "Separation and quantitation of free fatty acids and fatty acid methyl esters by reverse phase high pressure liquid chromatography," *Journal of Lipid Research*, vol. 24, no. 1, pp. 83–93, 1983.
- [22] F. B. Jungalwala, V. Hayssen, J. M. Pasquini, and R. H. McCluer, "Separation of molecular species of sphingomyelin by reversed-phase high-performance liquid chromatography," *Journal of Lipid Research*, vol. 20, no. 5, pp. 579–587, 1979.
- [23] R. T. Gallagher, M. P. Balogh, P. Davey, M. R. Jackson, I. Sinclair, and L. J. Southern, "Combined electrospray ionization-atmospheric pressure chemical ionization source for use in high-throughput LC-MS applications," *Analytical Chemistry*, vol. 75, no. 4, pp. 973–977, 2003.

## Research Article

# Sample Preparation and Extraction in Small Sample Volumes Suitable for Pediatric Clinical Studies: Challenges, Advances, and Experiences of a Bioanalytical HPLC-MS/MS Method Validation Using Enalapril and Enalaprilat

**Bjoern B. Burckhardt and Stephanie Laeer**

*Institute of Clinical Pharmacy and Pharmacotherapy, Heinrich-Heine-University, 40225 Düsseldorf, Germany*

Correspondence should be addressed to Bjoern B. Burckhardt; [bjoern.burckhardt@uni-duesseldorf.de](mailto:bjoern.burckhardt@uni-duesseldorf.de)

Received 31 October 2014; Revised 5 February 2015; Accepted 5 February 2015

Academic Editor: Mohamed Abdel-Rehim

Copyright © 2015 B. B. Burckhardt and S. Laeer. This is an open access article distributed under the Creative Commons Attribution License, which permits unrestricted use, distribution, and reproduction in any medium, provided the original work is properly cited.

In USA and Europe, medicines agencies force the development of child-appropriate medications and intend to increase the availability of information on the pediatric use. This asks for bioanalytical methods which are able to deal with small sample volumes as the trial-related blood lost is very restricted in children. Broadly used HPLC-MS/MS, being able to cope with small volumes, is susceptible to matrix effects. The latter restrains the precise drug quantification through, for example, causing signal suppression. Sophisticated sample preparation and purification utilizing solid-phase extraction was applied to reduce and control matrix effects. A scale-up from vacuum manifold to positive pressure manifold was conducted to meet the demands of high-throughput within a clinical setting. Faced challenges, advances, and experiences in solid-phase extraction are exemplarily presented on the basis of the bioanalytical method development and validation of low-volume samples (50  $\mu$ L serum). Enalapril, enalaprilat, and benazepril served as sample drugs. The applied sample preparation and extraction successfully reduced the absolute and relative matrix effect to comply with international guidelines. Recoveries ranged from 77 to 104% for enalapril and from 93 to 118% for enalaprilat. The bioanalytical method comprising sample extraction by solid-phase extraction was fully validated according to FDA and EMA bioanalytical guidelines and was used in a Phase I study in 24 volunteers.

## 1. Introduction

For the last years both competent authorities, the US Food and Drug Administration (FDA) and the European Medicines Agency (EMA), force the development of high quality child-appropriate medications and intend to improve the availability of information on the pediatric use. Due to the current lack of sufficient evidence-based pharmacotherapy in children, sophisticated clinical investigations in all pediatric age groups (particularly in neonates and infants) are required to overcome this drawback.

Unfortunately, most bioanalytical assays are not yet tailored to meet current ethical and analytical burdens for research in children. Although the blood sample volume for determination of drug concentration is limited to microliters, it is essential for a valuable determination in pediatric patients

to keep the calibration range as broad as or even broader than in assays applied in adult studies. HPLC-MS/MS is a predestinated analytical technique that appears to be the most suitable to deal with small sample volumes obtained from children and is linked with high selectivity for the quantification of the analytes of interest in diverse biological matrices. However, both the chromatographic equipment and the mass spectrometer (MS) encounter problems caused by the matrix. For example, the lifetime of the HPLC column is reduced if the sample purification is insufficient. Additionally, the detection by MS is susceptible to matrix effects leading to ionization suppression or enhancement [1, 2]. The matrix has a profound impact and restrains a precise quantification especially at the lower concentration levels. This ends up in nonrobust methods that do not encompass the broadest calibration range possible.

Therefore, the role played by proper sample preparation and extraction is important to overcome and control the interference caused through the biological matrices. A sophisticated sample clean-up removes material that chromatographically interferes with the analyte, enables appropriate recoveries, and erases matrix compounds that shorten column lifetime and affect the detection by MS. Attempts to simplify sample preparation and to reduce the preparation time ended in the awareness that this process accounts for less accuracy and precision in quantification [3]. Biological fluids like plasma, serum, urine, and saliva present a varying composition of, for example, lipids, proteins, electrolytes, cells, coeluting metabolites, impurities, and degradation products. All of these components might interfere with the analyte of interest. To reduce this interference several approaches had been developed in the past. Commonly used extraction techniques are protein precipitation (PPT), liquid/liquid extraction (LLE), and solid-phase extraction (SPE).

The purpose of the present work was to illustrate the importance of sample preparation exemplified by solid-phase extraction for the bioanalytical method development of low-volume assays for pediatric studies according to international agency guidelines. Using the method validation of enalapril, enalaprilat, and benazepril (internal standard), the encountered challenges and advances in sample preparation and solid-phase extraction as well as their effects on bioanalytical method validation of small volume samples were emphasized.

## 2. Methods

**2.1. Material.** The drug substances enalapril maleate CRS and enalaprilat dihydrate CRS (both European Pharmacopoeia Reference Standards) were purchased at the European Directorate for the Quality of Medicine & Healthcare (Strasbourg, France). Benazepril hydrochloride ( $\geq 98\%$ , HPLC) and ethyl acetate (100% p.a.) were obtained from Sigma-Aldrich (Seelze, Germany). Methanol (HiPerSolv Chromanorm HPLC grade), water (super gradient grade), and acetone (AnalaR Normapur) were purchased from VWR (Germany). Alternative supplier of methanol (HPLC grade) was Fisher Scientific (Loughborough, United Kingdom). Formic acid (98–100% p.a.) was delivered by AppliChem (Gatersleben, Germany). Ammonium formate (99%, HPLC grade) was obtained from Fluka (Seelze, Germany). Blank human serum was provided by employees of the Institute of Clinical Pharmacy and Pharmacotherapy (Düsseldorf, Germany). Oasis 96-well plates (30 and 10 mg) and XBridge BEH C18 3.5  $\mu\text{m}$  columns (3.0 mm  $\times$  150 mm) were obtained from Waters (Eschborn, Germany).

**2.2. Preparation of Standard and Quality Control.** Stock solutions of enalapril, enalaprilat, and benazepril (internal standard) were prepared at 0.10 mg/mL in methanol. These stock solutions were diluted with water to obtain working solutions with 10  $\mu\text{g}/\text{mL}$  enalapril and enalaprilat as well as 166 ng/mL benazepril. For the calibration curve, blank serum was spiked with the analytes of interest and serially diluted.

The final calibration range of the mass spectrometry was 0.2–200 ng/mL enalapril and 0.18–180 ng/mL enalaprilat. Quality control (QC) samples were independently prepared at four concentration levels over the whole calibration range (LLOQ, low, medium, and ULOQ).

**2.3. Sample Preparation, Extraction, and Scale-Up.** Based on preliminary investigations on the degree of sample dilution prior to solid-phase extraction a dilution ratio of 1:23 using water led to a robust method with high recovery rates for all analytes of interest.

Solid-phase extraction was chosen for the extraction process of the biological fluid owing to the superior purification performance if compared to protein precipitation or liquid-liquid extraction. Based on the compound properties of enalapril and enalaprilat, strong mixed-mode ion exchangers were chosen as sorbent material for the purification. Both a cation exchanger that interacts with the carboxylic acid groups and an anion exchanger that binds with the amino group of all above-mentioned substances were evaluated on their applicability (Oasis MCX and MAX material). The SPE protocol included a conditioning step utilizing methanol to enable optimal wetting of the cavernous sorbent material. For the subsequent equilibration step, different pH values and acids in aqueous solutions were tested to warrant for best interaction conditions prior the aqueous sample was loaded into the cavity. Namely, 2% formic acid (v/v), 4% phosphoric acid (v/v), 0.2 N hydrochloric acid, and pure water were evaluated. To purify the sample as much as possible, washing steps from hydrophilic to lipophilic properties were evaluated (water, 2% formic acid, hydrochloric acid, methanol, isopropanol, acetone, ethyl acetate, and mixtures of the aforementioned). Elution was assessed by acidified methanol for MAX sorbent material and ammonium in methanol for MCX sorbent material. The kind of acid (or base), its concentration, and the corresponding elution volumes were investigated to obtain all analytes within one fraction by reducing the coeluted residual matrix to a minimum.

To meet current demands in sample throughput within a clinical study, the scale-up to offline positive pressure extraction was conducted. The switch to 96-well format came along with a changeover from vacuum extraction to positive pressure extraction. SPE-formats with higher amounts of SPE cavities per plate were commercially not available. For the critical steps of sample load, washing, and sample elution, the positive pressure was kept between 1 and 2 psi to warrant an intensive interaction between analyte and sorbent material as well as reproducible flow rate. Figure 1 illustrates the corresponding scale-up.

**2.4. Chromatographic and Mass Spectrometric Conditions.** The utilized modular HPLC system (Shimadzu Deutschland GmbH, Duisburg, Germany) consisted of a controller SCL-10Avp, two separate pumps LC-10ADvp, three-channel online degasser DGU-20A<sup>3</sup> prominence, autosampler SIL-10ADvp, and a column oven (L-2300, VWR/Hitachi). For the separation of enalapril and enalaprilat an XBridge BEH C18 3.5  $\mu\text{m}$  column (3.0 mm  $\times$  150 mm) was used. After injection

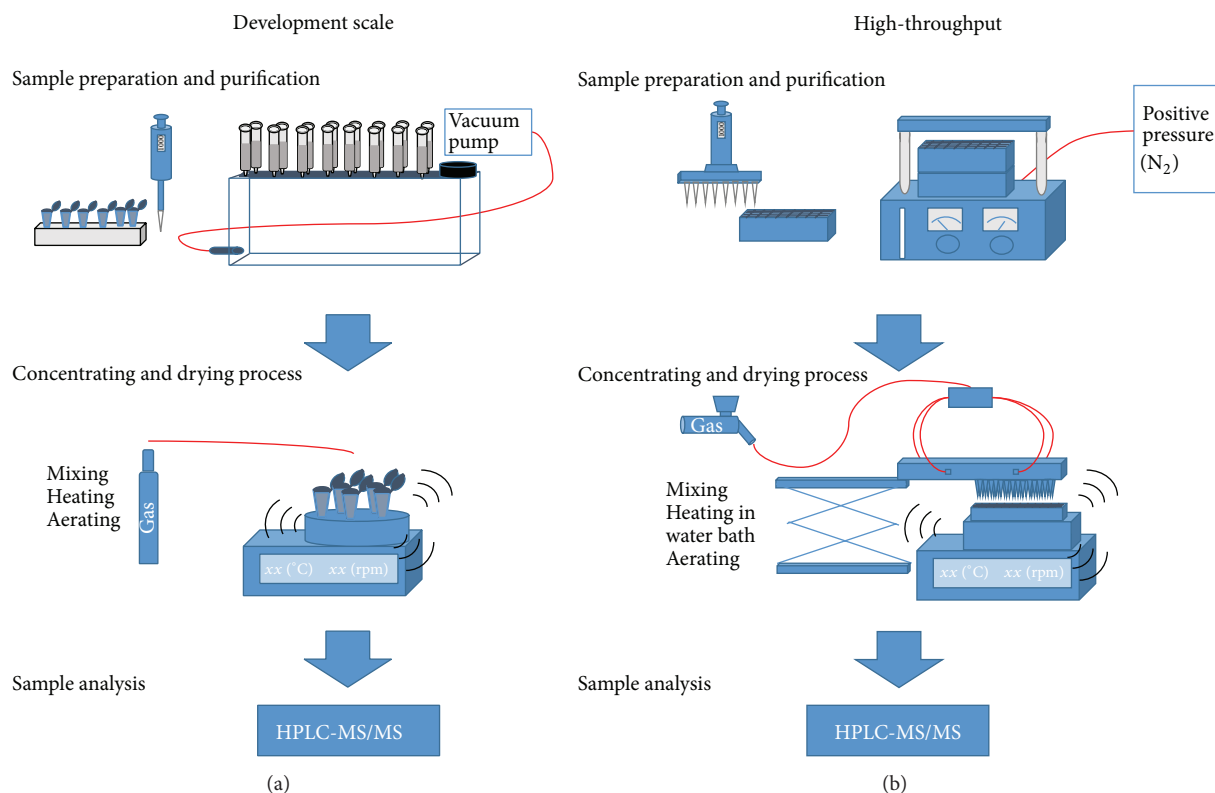


FIGURE 1: Scale-up process and optimization steps to establish a high-throughput approach of all bioanalytical assays utilizing solid-phase extraction. On the left side the development approach of sample preparation and purification is illustrated (a). The solid-phase extraction is performed by cartridges using the vacuum manifold. By contrast the scale-up is shown on the right side (b). Samples were prepared in 96-well approaches utilizing multichannel pipettes. The purification is conducted on a positive pressure manifold with 96-well plates. For the drying process the applied thermomixer was modified by a heatable water bath and a special drying top frame to deal with the deep-well collection plates (in-house development).

of 10  $\mu\text{L}$  sample solution (methanol/water 40 : 60, v/v) the samples were separated under gradient conditions within 6-minute run time utilizing a methanol/water mixture (40 : 60, v/v) buffered with formic acid (1%, v/v) and ammonium formate (2 mM). The applied gradient started with 40% of methanol and increased stepwise after 0.5 minute to 60% and after 1 minute to 80%. Between 1 and 4 minutes the amount of methanol was continuously increased to 95% and reduced at 4.5 minutes to 40% of methanol again. It stayed at this level till the end of the run time. The flow rate was 0.4 mL/min and the column temperature was maintained at 50°C which resulted in a moderate back pressure of 125 bar. Triple-quadrupole tandem mass spectrometric detection was performed on an Applied Biosystems SCIEX API 2000 (Applied Biosystems/MDS SCIEX, Concord, Canada) with an electrospray ionization (ESI) interface running in positive ionization mode. The device screened the transitions channels 377.2 to 234.2  $m/z$  (enalapril), 349.1 to 206.1  $m/z$  (enalaprilat), and 425.3 to 351.2  $m/z$  (benazepril) in multiple reaction monitoring (MRM) mode. All dwell times were set to 250 ms.

**2.5. Validation.** The bioanalytical method was fully validated according to current FDA and EMA bioanalytical guidelines

as a quantitative confirmatory method in terms of linearity, specificity, accuracy, precision, recovery, matrix effect, and stability [4, 5]. A main focus during validation was on the extraction process. The latter was in particular validated on recovery of the extraction process and absolute plus relative matrix effect. Additionally, extraction process efficiency and interference caused by hyperlipidemic and hemolyzed samples were evaluated.

The ratio of peak area of serum spiked with analyte prior to solid-phase extraction ( $\text{Area}_A$ ) with the peak area of blank serum spiked with analyte after the extraction ( $\text{Area}_B$ ) yielded the recovery of the assay. Recovery was determined at four concentration levels with five replicates per level. Calculation was performed as follows:

$$\text{RE} [\%] = \left( \frac{\text{Area}_A}{\text{Area}_B} \right) * 100, \quad (1)$$

where RE = recovery;  $\text{Area}_A$  = peak area of serum spiked with analyte prior to extraction;  $\text{Area}_B$  = peak area of blank serum spiked with analyte after the extraction.

Although the blood composition and pH value are strongly controlled and vary only slightly within a healthy subject, the overall consequence of all compounds in a biological sample matrix contributes to the matrix effect

that alters the accurate and precise determination of the analyte of interest. Therefore, a suitable sample preparation and purification by SPE contributes extremely to a robust method being less-sensitive to the effect. Apart from broadly investigated absolute matrix effect, the investigation of the relative matrix effect appears in this context more relevant for precise and robust methods for the analysis of biological samples [2].

Calculation of the absolute matrix effect was conducted by calculating the ratio of the peak area of extracted human serum postspiked with analyte ( $Area_x$ ) to the peak area of the analyte in the same concentration dissolved in mobile phase ( $Area_y$ ). The absolute matrix effect was determined at four concentration levels with five replicates per level. The absolute matrix effect was calculated according to the equation by Matuszewski et al. [2]:

$$ME [\%] = \left( \frac{Area_x}{Area_y} \right) * 100, \quad (2)$$

where ME = matrix effect;  $Area_x$  = detected peak area of extracted human serum postspiked with analyte;  $Area_y$  = detected peak area of dissolved analyte in mobile phase.

To distinguish between ion suppression and ion enhancement caused by the matrix, the calculated matrix effect was subtracted by 100. A value < 0 indicated ion suppression caused by the matrix while ion enhancement was present if the calculated value was > 0.

According to international guidelines, the absolute matrix effect should be evaluated but is not limited to a certain range. However, the applicant needs to be able to estimate the effect of the matrix on the assay's performance.

By contrast the European Medicines Agency provides a guidance mentioning fixed acceptance criteria for the relative matrix effect. The intersubject variability of the internal standard normalized relative matrix effect (IS-ME) of processed samples should be maximum 15% and is expressed as coefficient of variation (CV) [4]. The calculation of the latter was done by evaluation of the individual IS-normalized matrix effect being defined as the matrix factor of the analyte divided by the matrix factor of the IS. The matrix factor represents the ratio of the peak area in the presence and the absence of the matrix of the corresponding substance. The CV of the IS-normalized matrix effects of seven subjects was used to assess the relative ME. The relative matrix effect was evaluated at 0.39 ng/mL enalapril and 0.35 ng/mL enalaprilat (low concentration level) as well as at 200 ng/mL enalapril and 180 ng/mL enalaprilat (ULOQ). Per concentration level three replicates per subject were analysed:

$$\begin{aligned} IS-ME [\%] &= \left( \left( \frac{\text{Peak area of analyte}_{\text{Presence of matrix}}}{\text{Peak area of analyte}_{\text{Absence of matrix}}} \right) \right. \\ &\quad \left. * \left( \frac{\text{Peak area of IS}_{\text{Presence of matrix}}}{\text{Peak area of IS}_{\text{Absence of matrix}}} \right)^{-1} \right) * 100, \end{aligned} \quad (3)$$

where IS-ME = internal standard normalized matrix effect.

To calculate the process efficiency of the solid-phase extraction the following equation by Taylor [1] was used:

$$PE [\%] = RE [\%] * \frac{(100 - ME [\%])}{100}, \quad (4)$$

where PE = process efficiency; RE = recovery; ME = absolute matrix effect.

Further validation parameters, as listed in the international bioanalytical guidelines, were investigated as follows: linearity was evaluated by measuring freshly spiked human serum with enalapril and enalaprilat at 11 concentration levels. The bioanalytical method was evaluated on four different days by four different runs on accuracy and precision. Therefore, five independently prepared quality control samples were assessed on four concentration levels (enalapril: 0.2, 3.13, 25, and 200 ng/mL; enalaprilat: 0.18, 2.81, 22.5, and 180 ng/mL) per run. The precision was determined by ANOVA while the accuracy was described by percentage deviation of the mean value to the nominal values of each concentration level. A maximum deviation of  $\pm 15\%$  ( $\pm 20\%$  at the LLOQ) was regarded as acceptable [4]. The selectivity was assessed by check for interaction caused by 7 human serum samples spiked with 11 common comedications. The long-term stability of the drugs was evaluated at  $-80^\circ\text{C}$  for at least 60 days, short-term stability conducted at  $20^\circ\text{C}$  for 24 h, and autosampler stability for 24 h also at  $20^\circ\text{C}$ . Additionally, the stability of the dried eluate after sample extraction was investigated at  $-20^\circ\text{C}$  for 24 h.

**2.6. Application.** The high-throughput approach was applied to a Phase I study in 24 healthy volunteers. Both urine and serum samples were withdrawn and analyzed after administration of 10 mg enalapril maleate. With focus on sample extraction, the applicability was evaluated on the time required to run the extraction, the occurrence of any clotting of the cavity during extraction, and the goodness of extraction by checking for any shift in retention time in samples of different volunteers and different sample conditions (e.g., hemolyzed samples).

### 3. Results and Discussion

**3.1. Sample Preparation.** Preliminary investigations on the degree of sample dilution had been shown to influence the extraction performance and accounted highly for a robust method with high recovery. Investigations on suitable sample dilution solvents (formic acid, phosphoric acid, hydrochloric acid, and water) and their mixing ratio with the sample itself were conducted. To determine the best suitable mixing ratio of acids or pure water, the ratio was varied between 1:1 and 1:23. The conducted investigations on the most appropriate dilution solvent showed that water is sufficient if high dilution factors were applied. By increasing the mixing ratio, the detected peak areas of enalapril and enalaprilat increased in parallel (Figure 2). A mixing ratio of 1:10 and 1:23 worked best with regard to sample recovery. The highest dilution ratio resulted in a total sample volume of about 1.2 mL. Owing to the maximum capacity of a cavity ( $\sim 1.4$  mL), a higher degree

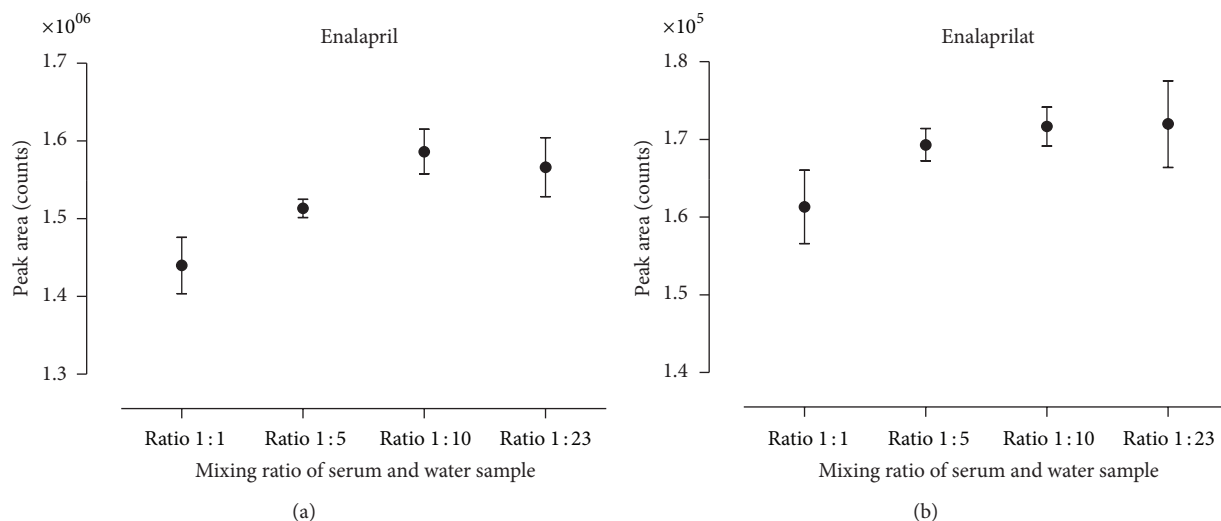


FIGURE 2: Comparison of mixing ratios of serum and water on resulting peak areas. The detected peak areas of enalapril (a) and enalaprilat (b) of purified serum samples are presented. The mixing ratio was varied between 1:1 and 1:23. Each determination was conducted by three independently prepared quality control samples. The mean and corresponding standard deviations are shown.

of dilution is not recommended for routine. It increases the risk of carryover and rises the likelihood of sample mix-up as the sample solution needs to be pipetted at least in two parts into the cavity. The final composition of the diluted sample solution consisted of 50  $\mu\text{L}$  serum being mixed with 5  $\mu\text{L}$  benazepril working solution (IS) and 1100  $\mu\text{L}$  water.

**3.2. Sample Extraction.** Specifically, if small biological sample volumes like in pediatric research require purification, the sample extraction plays a particular role. Commonly, protein precipitation (PPT), liquid/liquid extraction (LLE), and solid-phase extraction (SPE) are applied as extraction techniques. PPT is a fast and simple approach but works best only in protein-rich matrices such as whole blood, plasma, or serum. Nevertheless, the PPT is nonselective and does not remove matrix interferences other than proteins. In the investigations by Dams et al., PPT in combination with LC-MS/MS had the greatest matrix effect amongst the investigated purification approaches [3]. It is a useful and fast technique to optimize lifetime of the equipment but does not increase the analytical sensitivity which is important for low-volume LC-MS/MS assays. LLE allows separation of analytes of interest from proteins and other hydrophilic components, but if emulsions are formed, the separation of the organic solvent becomes difficult and might result in incomplete and various-analyte diffusion. Jessome and Volmer emphasized the cumbersome sample preparation by LLE and LC-MS/MS [6]. Especially the complex adjustment of the pH value for the transfer in the organic phase, extraction of highly polar substances and necessary multiple extraction steps are some challenges faced. In particular for high-throughput analytics—as it is useful in clinical study approaches—the LLE is not the first choice. Consequently, SPE was selected owing to its superior purification properties and flexibilities in extraction protocols to cope with diversity of analytes, purifications solvents, and biological fluids.

The selected drug combination (calculated log  $P$  values of enalapril: 2.5; enalaprilat:  $-0.9$ ; benazepril: 3.5) carried the risk of improper binding to the sorbent due to Coulomb repulsion, losing hydrophilic analytes during too extensive and not well-balanced washing steps or by incomplete recovery of the more lipophilic compounds from the sorbent material during elution. All this may be attributed to low recovery or bad reproducibility which in turn narrows the calibration range, because especially lower concentrations might not conform to international guideline requirements. Available sorbent phases characterized by different interaction possibilities (van der Waals forces, ionic interaction, etc.) and different amounts of sorbent per cavity and the high flexibility in the SPE protocol on how intensive the purification of sample needs to be conducted represent some of many useful tools to overcome those drawbacks.

First extraction attempts were undertaken by utilizing Oasis MCX. This polymeric material is characterized by a strong cation exchanger (on sulfonic acid base) binding the carboxylic acids groups of the analytes of interest. However, purified samples showed a split peak for the selected transition of enalaprilat if determined by HPLC-MS/MS. The corresponding chromatograms revealed a peak occurring at an earlier retention time plus a second peak at the expected retention time of the compound (Figure 3).

The peak area and intensity of the first peak did not alter with different enalaprilat concentrations per sample and accounted therefore most likely for a residual serum matrix component. It was not possible to erase the peak neither by thought-out SPE nor by any number of different LC gradients or by different HPLC columns featured with opposed chromatographic properties (Atlantis T3, XBridge, and XSelect). The checks for contamination in mobile phase, autosampler, or solutions for SPE were additionally negative. At the lowest concentration level of the calibration curve, the first peak and the one of enalaprilat were comparable

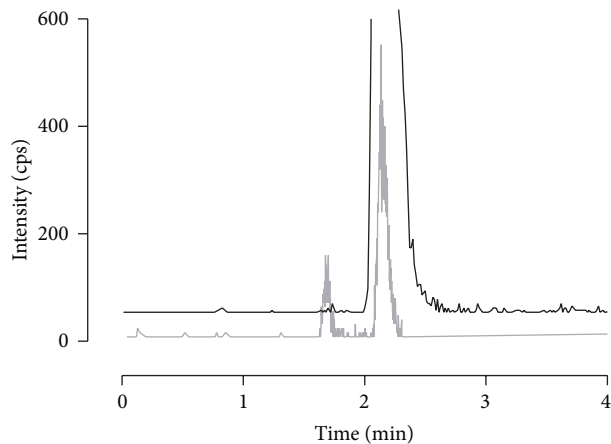


FIGURE 3: Determined split peak in serum with the transition  $349.1 \rightarrow 206.1$   $m/z$  during method development. The split peak was measured on several HPLC columns after SPE purification by Oasis MCX. In grey, the ion count of a low enalaprilat concentration in serum is shown that clearly identifies the split peak. As reference, the enalaprilat standard solved in mobile phase is presented by the black line without any split peak (base line is nudged to prevent overlap).

in shape, intensity, and peak area. This phenomenon carried the risk of less robustness if automated integration of the chromatogram is preferred. After also scanning for the second most intense transition of enalaprilat ( $349.1 \rightarrow 303.1$   $m/z$ ), clarity was brought to question as the first peak did not belong to enalaprilat. However, quantification with two transitions would have resulted in a higher LLOQ which was undesired as very low concentration levels are expected in the scheduled pediatric studies. Therefore, the sorbent material of the SPE was changed from cation exchanger to strong anion exchanger (MAX) and a new extraction protocol was developed. This brought success to the method, as the compound with the same transition as enalaprilat ( $349.1 \rightarrow 206.1$   $m/z$ ) could be detached by SPE and consequently the split peak was removed.

At this stage an excuse to an already established and fully validated extraction method for the same drug entities in urine (amongst others) is made to introduce another useful approach to purify the sample matrix, to reduce the relative matrix effects, and to meet the current EMA bioanalytical guideline [4]. A two-step solid-phase extraction by a weak anion exchanger followed by a strong cation exchanger significantly reduced the internal standard normalized matrix effect compared to the purification by MCX only (Figure 4). The more hydrophilic the compound was the merrier the improvement of the matrix effect was pronounced. However, it expounds how diverse the several biological fluids are and emphasizes the high required effort in method development to reduce the relative matrix effect. By applying the final two-step extraction the following results for the relative matrix effect were obtained: at the LLOQ the CV was 4.04% and 6.62% for enalapril and enalaprilat, respectively. A CV of 1.26% for enalapril and 1.25% for enalaprilat was calculated at the ULOQ and was therefore well within the EMA requirements of 15% [7]. This bioanalytical urinary method was fully

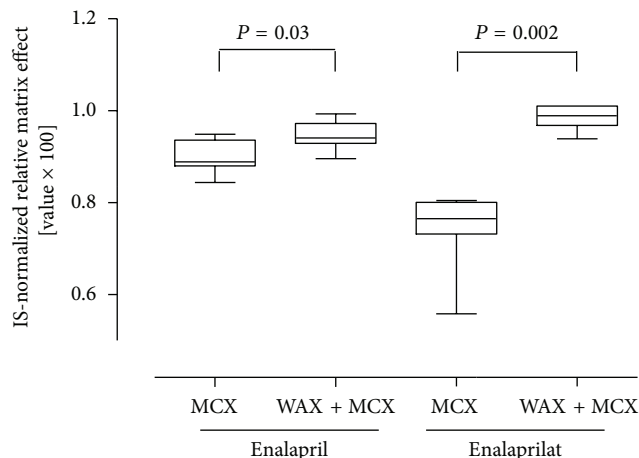


FIGURE 4: Comparison of different extraction methods on the internal standard normalized matrix effect. The SPE extraction by Oasis MCX is compared to the two-step extraction by Oasis WAX + MCX. Each boxplot describes median, 25th, 75th percentile + 10th, and 90th percentile as whisker.  $N = 9$  measurements per boxplot. Statistical analysis was performed by a Mann-Whitney- $U$  test (two-tailed  $P$  value).

validated according to the strictest validation parameters of EMA and FDA bioanalytical guidance [7].

At an early development stage of the extraction protocol in serum at which the extraction was not methodologically sound, we encountered some deviation in retention time when comparing the chromatograms of analyte solved in mobile phase to extracted analyte in serum (Figure 5). By increasing the amount of organic washing steps as well as the elution force of the used organic solvents (methanol, acetone, and ethyl acetate), this timely shift could be eliminated (Figure 5). Even the intensities and peak areas of both, the analyte in mobile phase and the analyte in purified serum, were finally comparable. This pointed out the gained high degree of sample purification and accounted for a very limited signal suppression by the residual matrix compound in the final extract. However, it illustrates that matrix effects not only affect the signal intensities of the mass spectrometer but can also alter the chromatographic performance. A comparable effect was recently published by Fang et al. [8].

Finally, the conducted investigations on the most appropriate elution solvent and its volume yielded 0.4 mL acidified methanol (2% formic acid, v/v). This elution step did not only served to elute the analytes of interest but also acted as a final step to fraction the analytes of interest and other interfering residual compounds. Hereby the choice and elution force of the solvent as well as the amount of solvent were investigated on their effect to attribute to a rugged, reliable, and selective protocol. As illustrated in Figure 6, there was a reciprocal relationship between the elution volume of acidified methanol and the detected peak areas of the analytes of interest. The obtained smaller peak areas—after the sorbent material was eluted with higher volumes of acidified methanol—might be explained by the fact that more interfering matrix was coeluted. The interference induced by the matrix led to ion suppression and smaller peak areas.

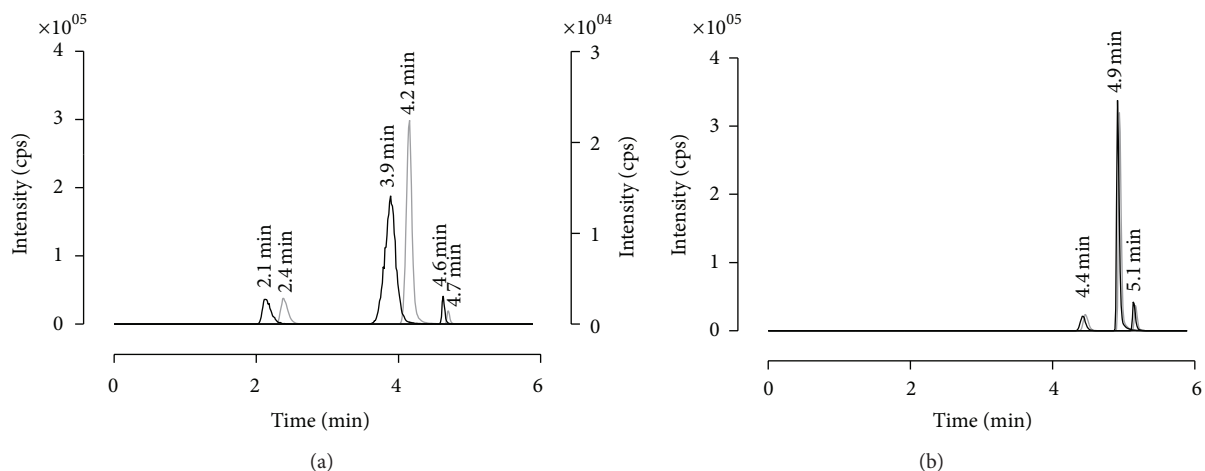


FIGURE 5: Multiple reaction monitoring scan chromatograms of enalapril, enalaprilat, and benazepril. The left graph illustrates the shift in retention time detected by comparing the analytes solved in mobile phase versus the analytes in purified matrix during first extraction attempts. Right graph shows the final chromatogram by comparing also the analytes in mobile phase versus analytes in purified serum. A timely shift in retention time was not detectable anymore. MRMs: 377.2  $\rightarrow$  234.2  $m/z$  (enalapril), 349.1  $\rightarrow$  206.1  $m/z$  (enalaprilat), and 425.3  $\rightarrow$  351.2  $m/z$  (benazepril). The black line identifies the extracted serum samples and the grey line illustrates the drug substances dissolved in mobile phase. Cps: counts.

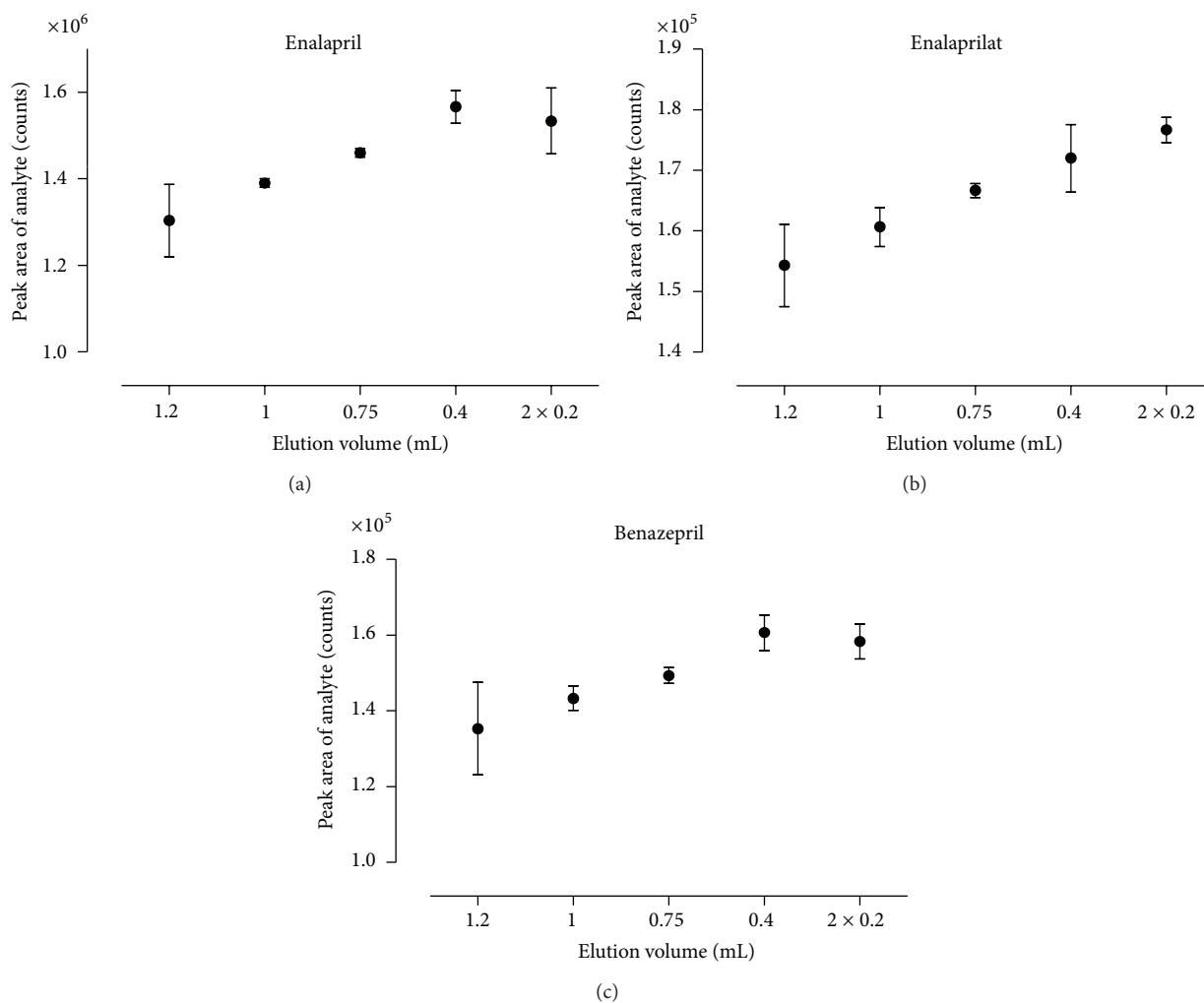


FIGURE 6: Effect of elution volume on peak area of the analytes of interest. The peak areas of enalapril (a), enalaprilat (b), and benazepril (c) after elution are presented with different volumes of 2% formic acid in methanol. Each determination was conducted by three independently prepared quality control samples. The mean and corresponding standard deviations are shown.

The final protocol for the serum method was destined to the following approach: the samples were extracted with Oasis MAX solid-phase extraction cartridges (10 mg, 1 mL)—a mixed mode, reverse-phase, and strong anion exchanger (on quarternary amine base). The MAX 96-well plates chosen allowed for high sample throughput and were primed with 1 mL of formic acid in methanol (2%, v/v) followed by an equilibration step with 1 mL water. On the one hand, this aqueous step prior to sample load ensured that, for example, no denaturation and therefore clotting of sample matrix on the sorbent material happened. On the other hand, it offered the best interaction conditions with the sorbents. After the sample mixture was loaded into the cartridges and passed, the sorbent of the cartridges was washed by 1.0 mL of water, 1.0 mL of methanol-acetone mixture (60 : 40, v/v), 1.0 mL of ethyl acetate, and 500  $\mu$ L of methanol. The increasing elution force of the investigated organic solvents was used mainly to wash out phospholipids that are known to be responsible for a large part of matrix effect in blood, serum, and plasma [9]. Finally the analytes were eluted from the cartridges once with 0.4 mL of formic acid in methanol (2%, v/v). The eluate was evaporated to dryness under a gentle stream of compressed air while shaking at 550 rpm at 40°C. The residue was reconstituted with 100  $\mu$ L of methanol and water (40 : 60, v/v).

**3.3. Scale-Up of Sample Preparation and Extraction to 96-Well Setting.** For reproducible and high-quality solid-phase extraction (SPE) with a high run-to-run consistency as desired for clinical studies, the switch from single cartridges by vacuum extraction to 96-well positive pressure extraction was conducted. This scaling presented the highest possible offline scaling for the used SPE material. SPE-formats with higher amounts of SPE cavities per plate were commercially not available. The conventional vacuum manifold had the disadvantage of irreproducible analyte recoveries due to variable processing times in the columns. For the highest possible reproducibility during extraction, the controlled and appropriate flow rate is much more essential than applying either vacuum or positive pressure. However, the positive pressure manifold had the advantage of being equipped with a monitor to check for the flow rate of the liquid. Specifically the sample load, washing, and elution step are known to be the most sensitive and critical steps regarding the flow rate. The exact adjustment of the flow rate of the liquids was important to generate a well-balanced setting of high reproducibility, best extraction speed and duration of sample extraction.

The transfer from vacuum extraction to positive pressure not only enabled a semiautomated extraction but also highly increased the sample amount up to about thousand samples which can be purified per week by one laboratory technician. Since appropriate equipment for rapid and continuous drying was not commercially available, required equipment for the drying process was self-developed to suit best the laboratory preconditions and needs. Figure 1 is enclosed illustrating the scale-up from single cartridges using vacuum technique to the positive pressure extraction in 96-well formate. As indicated in Figure 7, the scale-up is a mandatory step in

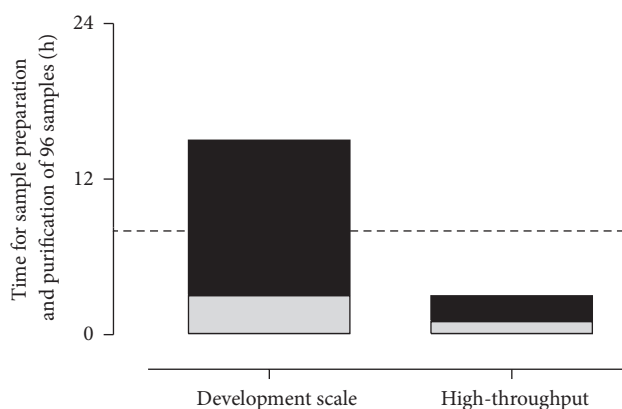


FIGURE 7: Comparison of required time for bioanalysis between development scale by applying single cartridges and the high-throughput approach with 96-well plate. The calculation bases on a sample amount of 96 samples. The black areas mark the required time for sample purification by solid-phase extraction and grey areas identify the time frame required for sample preparation. The dashed line represents one full working day (8 hours). By applying the high-throughput approach the sample preparation and purification is finalized within 2 hours while the same amount of samples is impossible to purify within one working day by one lab technician using the previous development scale.

method development if the assay will be applied to analyze hundreds or thousands of samples. In our positive pressure approach, it took about 2 hours from raw sample to sample preparation and extraction to the final sample solution ready to be determined by HPLC-MS/MS. In such a run, 96 samples could be prepared which required much more than one full working day (8 h) of one laboratory technician to prepare the same amount by the previously used vacuum manifold approach. The applied pressures of 1–3 psi were fully sufficient to ensure a continuous and appropriate flow rate of solvent/sample solution through the sorbent material. The scale-up enabled a nearly sixfold higher sample throughput.

**3.4. Validation.** The chosen calibration range of 0.2–200 ng/mL enalapril and 0.18–180 ng/mL enalaprilat, respectively, showed guideline-conforming linearity over all eleven concentration levels. Best fit of the linear regression was gained by  $1/x^2$  weighting for both analytes. No additional peaks above the guideline limits within  $\pm 0.3$  minutes of the retention time of enalapril, enalaprilat, and benazepril were observed in the spiked serum samples with coadministered drugs (acetylsalicylic acid, aliskiren, ramipril, ramiprilat, candesartan, atenolol, bisoprolol, metoprolol, pantoprazole, and pravastatin). No interferences in blank samples of the different sources were detected and the signal-to-noise ratios of spiked to blank samples of all sources were above 5 : 1. Obtained results by one-way ANOVA for the intrarun precision ranged from 2.2 to 5.0% for enalapril and from 4.9 to 18.0% for enalaprilat. These precision results conformed all to the current bioanalytical guidelines. Mean accuracy results of the quality control samples were likewise within the guideline requirements of  $\pm 15\%$  at all concentration levels (at

TABLE 1: Results for recovery, absolute matrix effect, and process efficiency.

	Concentration [ng/mL]	Absolute matrix effect $\pm$ S.D. [%]	Mean recovery $\pm$ S.D. [%]	Mean process efficiency [%]
Enalapril	0.195	$-12.6 \pm 11.9$	$77.1 \pm 0.7$	67.4
	3.13	$-8.9 \pm 2.2$	$103.5 \pm 3.7$	94.3
	25	$-19.8 \pm 4.4$	$102.9 \pm 6.3$	77.6
	200	$-17.5 \pm 3.5$	$92.0 \pm 6.9$	72.5
Enalaprilat	0.175	$-1.5 \pm 10.8$	$99.9 \pm 7.8$	98.4
	2.81	$0.3 \pm 3.7$	$118.3 \pm 4.6$	118.7
	22.5	$10.5 \pm 4.9$	$102.4 \pm 4.7$	113.2
	180	$2.2 \pm 3.5$	$92.9 \pm 9.2$	94.9
Benazepril	25	$-7.2 \pm 2.8$	$76.9 \pm 2.3$	71.3

Data compiled as mean or mean  $\pm$  standard deviation (S.D.).

TABLE 2: Relative matrix effect obtained in seven different human sources.

Donor	Enalapril		Enalaprilat	
	0.39 ng/mL	200 ng/mL	0.35 ng/mL	180 ng/mL
Healthy adults				
29–86 years old				
♂ Donor 1	106.7	96.8	162.5	135.9
♂ Donor 2	99.1	95.7	122.1	108.2
♂ Donor 3	96.6	96.6	120.9	119.4
♀ Donor 4	111.1	97.6	132.1	126.6
♀ Donor 5	107.2	97.8	121.0	114.5
♀ Donor 6	98.8	94.5	123.1	112.1
♂ Donor 7	98.4	92.8	114.4	106.7
Mean value of normalized relative ME $\pm$ S.D. [%]	$102.6 \pm 5.6$	$96.0 \pm 1.8$	$128.0 \pm 16.1$	$117.6 \pm 10.5$
CV [%] within donors	5.49	1.87	12.56	8.96

ME: matrix effect; S.D.: standard deviation; CV: coefficient of variation.

the LLOQ  $\pm 20\%$ ). Hemolyzed blood as well as hyperlipidemic blood samples had no detectable influence on the specific MS-channels of enalapril, enalaprilat, and IS, respectively. Obtained stability results of enalapril and enalaprilat for long-term storage ( $-80^\circ\text{C}$ , 60 days), for short-term storage ( $20^\circ\text{C}$ , 24 h), and in the autosampler ( $20^\circ\text{C}$ , 24 h) proved the drug stability. Additionally, both drug substances showed no significant degradation if they were stored as dried elution extract at  $-20^\circ\text{C}$  for 24 h.

The effect of the matrix on the determination of enalapril and enalaprilat was evaluated at the LLOQ (0.2 ng/mL; 0.18 ng/mL), one low concentration (3.13 ng/mL; 2.81 ng/mL), one middle concentration (25 ng/mL; 22.5 ng/mL), and at the ULOQ (200 ng/mL; 180 ng/mL). By combining SPE and chromatographic separation the matrix effect was observably reduced in this setting, leading to an ion suppression of  $-8.9$  to  $-19.8\%$  for enalapril and of  $-7.2 \pm 2.8\%$  for the internal standard benazepril. The sample matrix had no or a slight ion enhancing effect on detection of enalaprilat. It ranged between  $-1.5$  and  $10.5\%$ . All analytes were almost fully recovered from the sorbent of the mixed-mode anion exchanger, resulting in a process efficiency of 67 to 94% for enalapril, 95–119% for enalaprilat, and 71% for benazepril. Details are arranged in Table 1.

The relative matrix effects of the extracted serum samples at a low concentration level (0.39 ng/mL enalapril and 0.35 ng/mL enalaprilat, resp.) were 5.49% (CV) for enalapril and 12.56% for enalaprilat. At the ULOQ, coefficients of variation of 1.87% for enalapril and 8.96% for enalaprilat were evaluated for all seven different human sources. All findings complied with EMA bioanalytical guideline. Details are arranged in Table 2.

**3.5. Application.** For the Phase I study, in total approximately 1600 serum and 600 urinary samples were analyzed. No clotting of serum sample solution in any SPE cavity was noticed. A shift in the retention times of enalapril, enalaprilat, and benazepril in purified serum samples of 24 different sources was not detected during the analysis by HPLC-MS/MS and allowed for an automated intergration. Furthermore, hemolyzed samples did not affect the extraction run negatively and showed no significant interference during analysis. The determined pharmacokinetic results of the Phase I study will be used to apply a new marketing authorization and remain therefore confidential. However, during sample determination 22 calibration curves in serum and 7 in urine were required to quantify the drug concentration in the corresponding samples. Obtained results of the calibration

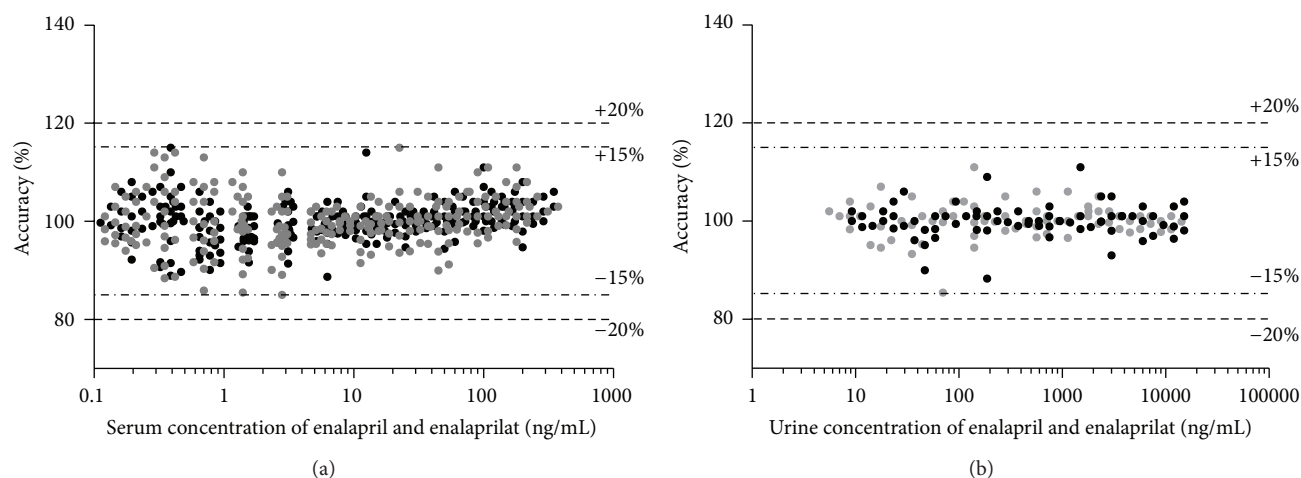


FIGURE 8: The plots show the accuracy results of 22 serum calibration curves and the accuracy results of 7 urinary calibration curves (each covering 11 concentration levels per drug substance) of enalapril (black) and enalaprilat (grey) used for the evaluation of the obtained results of the conducted Phase I study. Additionally the accuracy thresholds (dashed lines) according to FDA and EMA bioanalytical guidelines for all concentrations levels ( $\pm 15\%$ ) and the LLOQ ( $\pm 20\%$ ) are indicated.

curves on intra- and interrun accuracy proved the applicability of the established bioanalytical method comprising the good sample extraction and their suitable preparation. Figure 8 shows the accuracy results for the serum and urine calibration curves.

Furthermore, these tailored low-volume assays will be applied to pediatric Phase II and III studies. The available pediatric study investigating the pharmacokinetics of enalapril and its active metabolite enalaprilat in hypertensive children was published by Wells et al. using a radioimmunoassay [10]. They found mean concentrations between 2 and 25 ng/mL enalaprilat. Lloyd et al. reported enalaprilat concentration values between 0.9 and 12.7 ng/mL in children with heart failure [11]. Both reported ranges are covered by the linear range of the assay presented and confirm its applicability for pediatric research. The required sample volume of 50  $\mu\text{L}$  serum for reliable determination appears additionally well suitable for clinical trials in all age groups, especially for neonates and newborns. The required sample volumes of published LC-tandem mass spectrometry assays on enalapril and enalaprilat range between 200 and 1000  $\mu\text{L}$  blood [12–17].

#### 4. Conclusion

Using the example validation of the low-volume bioanalytical method of enalapril and enalaprilat, pitfalls as well as improvements of the extraction protocol were shown. The aim of an accurate and precise low-volume method encompassing a broad calibration range with very low limits of quantification was only gained by complex extraction protocols. The calibration range of the established assay covers reported enalapril and enalaprilat concentrations in pediatric patients and proves its applicability for pediatric research. It was shown that the undertaken efforts for a sophisticated extraction protocol utilizing solid-phase

extraction resulted in a high recovery and high reduction of matrix effect. Controlling the latter—amongst others—warranted for a valuable and reliable bioanalytical method in serum. It allowed successful validation of a low-volume bioanalytical HPLC-MS/MS method according to the FDA and EMA bioanalytical guidelines. The applicability of the high-throughput approach was proven by a clinical study in 24 volunteers.

#### Conflict of Interests

There is no conflict of interests regarding the publication of this paper.

#### Acknowledgment

The research leading to these results has received funding from the European Union Seventh Framework Programme (FP7/2007-2013) under Grant Agreement no. 602295 (LENA).

#### References

- [1] P. J. Taylor, “Matrix effects: the Achilles heel of quantitative high-performance liquid chromatography-electrospray-tandem mass spectrometry,” *Clinical Biochemistry*, vol. 38, no. 4, pp. 328–334, 2005.
- [2] B. K. Matuszewski, M. L. Constanzer, and C. M. Chavez-Eng, “Strategies for the assessment of matrix effect in quantitative bioanalytical methods based on HPLC-MS/MS,” *Analytical Chemistry*, vol. 75, no. 13, pp. 3019–3030, 2003.
- [3] R. Dams, M. A. Huestis, W. E. Lambert, and C. M. Murphy, “Matrix effect in bio-analysis of illicit drugs with LC-MS/MS: influence of ionization type, sample preparation, and biofluid,” *Journal of the American Society for Mass Spectrometry*, vol. 14, no. 11, pp. 1290–1294, 2003.

- [4] European Medicines Agency, *Guideline on Bioanalytical Method Validation: (EMA/CHMP/EWP/192217/2009)*, 2012.
- [5] Food and Drug Administration, *Guidance for Industry: Bioanalytical Method Validation*, U.S. Department of Health and Human Services, 2001.
- [6] L. L. Jessome and D. A. Volmer, "Ion suppression: a major concern in mass spectrometry," *LC-GC North America*, vol. 24, no. 5, pp. 498–510, 2006.
- [7] B. B. Burckhardt, J. Tins, and S. Laeer, "Simultaneous quantitative and qualitative analysis of aliskiren, enalapril and its active metabolite enalaprilat in undiluted human urine utilizing LC-ESI-MS/MS," *Biomedical Chromatography*, vol. 28, no. 12, pp. 1679–1691, 2014.
- [8] N. Fang, S. Yu, and M. J. Ronis, "Matrix effects break the LC behaviour rule for analytes in LC-MS/MS analysis of biological samples," *Experimental Biology and Medicine*. In press.
- [9] E. Chambers, D. M. Wagrowski-Diehl, Z. Lu, and J. R. Mazzeo, "Systematic and comprehensive strategy for reducing matrix effects in LC/MS/MS analyses," *Journal of Chromatography B: Analytical Technologies in the Biomedical and Life Sciences*, vol. 852, no. 1-2, pp. 22–34, 2007.
- [10] T. Wells, R. Rippley, R. Hogg et al., "The pharmacokinetics of enalapril in children and infants with hypertension," *Journal of Clinical Pharmacology*, vol. 41, no. 10, pp. 1064–1074, 2001.
- [11] T. R. Lloyd, L. T. Mahoney, D. Knoedel, W. J. Marvin Jr., J. E. Robillard, and R. M. Lauer, "Orally administered enalapril for infants with congestive heart failure: a dose-finding study," *The Journal of Pediatrics*, vol. 114, no. 4, pp. 650–654, 1989.
- [12] S. Ramusovic, G. Thielking, and S. Læer, "Determination of enalapril and enalaprilat in small human serum quantities for pediatric trials by HPLC-tandem mass spectrometry," *Biomedical Chromatography*, vol. 26, no. 6, pp. 697–702, 2012.
- [13] C. Ghosh, I. Jain, C. P. Shinde, and B. S. Chakraborty, "Rapid and sensitive liquid chromatography/tandem mass spectrometry method for simultaneous determination of enalapril and its major metabolite enalaprilat, in human plasma: application to a bioequivalence study," *Drug Testing and Analysis*, vol. 4, no. 2, pp. 94–103, 2012.
- [14] Q. Gu, X. Chen, D. Zhong, and Y. Wang, "Simultaneous determination of enalapril and enalaprilat in human plasma by liquid chromatography-tandem mass spectrometry," *Journal of Chromatography B: Analytical Technologies in the Biomedical and Life Sciences*, vol. 813, no. 1-2, pp. 337–342, 2004.
- [15] D. M. Lima, I. M. Mundim, P. C. B. V. Jardim, T. S. V. Jardim, D. G. A. Diniz, and E. M. Lima, "A high performance liquid chromatography-tandem mass spectrometry (LC-MS/MS) method using solid phase extraction for the simultaneous determination of plasma concentrations of enalapril and enalaprilate in hypertensive patients treated with different pharmaceutical formulations," *Therapeutic Drug Monitoring*, vol. 31, no. 6, pp. 710–716, 2009.
- [16] S. Lu, K. Jiang, F. Qin, X. Lu, and F. Li, "Simultaneous quantification of enalapril and enalaprilat in human plasma by high-performance liquid chromatography-tandem mass spectrometry and its application in a pharmacokinetic study," *Journal of Pharmaceutical and Biomedical Analysis*, vol. 49, no. 1, pp. 163–167, 2009.
- [17] N. M. Najib, N. Idkaidek, A. Adel et al., "Bioequivalence evaluation of two brands of enalapril 20 mg tablets (Narapril and Renitec) in healthy human volunteers," *Biopharmaceutics and Drug Disposition*, vol. 24, no. 7, pp. 315–320, 2003.

## Research Article

# QuEChERS Method Followed by Solid Phase Extraction Method for Gas Chromatographic-Mass Spectrometric Determination of Polycyclic Aromatic Hydrocarbons in Fish

Mona Khorshid,<sup>1</sup> Eglal R. Souaya,<sup>2</sup> Ahmed H. Hamzawy,<sup>1</sup> and Moustapha N. Mohammed<sup>1</sup>

<sup>1</sup>Central Laboratory of Residue Analysis of Pesticides and Heavy Metals in Food (QCAP), Agricultural Research Center, Ministry of Agriculture and Land Reclamation, 7 Nadi Elsaid Street, Dokki, Giza 12311, Egypt

<sup>2</sup>Department of Chemistry, Faculty of Science, Ain Shams University, Cairo 11566, Egypt

Correspondence should be addressed to Mona Khorshid; monakhorshed1@hotmail.com and Ahmed H. Hamzawy; ahmed\_qcap@yahoo.com

Received 30 September 2014; Revised 4 December 2014; Accepted 6 December 2014

Academic Editor: Mohammad R. Pourjavid

Copyright © 2015 Mona Khorshid et al. This is an open access article distributed under the Creative Commons Attribution License, which permits unrestricted use, distribution, and reproduction in any medium, provided the original work is properly cited.

A gas chromatography equipped with mass spectrometer (GCMS) method was developed and validated for determination of 16 polycyclic aromatic hydrocarbons (PAHs) in fish using modified quick, easy, cheap, effective, rugged, and safe (QuEChERS) method for extraction and solid phase extraction for sample cleanup to remove most of the coextract combined with GCMS for determination of low concentration of selected group of PAHs in homogenized fish samples. PAHs were separated on a GCMS with HP-5ms Ultra Inert GC Column (30 m, 0.25 mm, and 0.25  $\mu$ m). Mean recovery ranged from 56 to 115%. The extraction efficiency was consistent over the entire range where indeno(1,2,3-cd)pyrene and benzo(g,h,i)perylene showed recovery (65, 69%), respectively, at 2  $\mu$ g/kg. No significant dispersion of results was observed for the other remaining PAHs and recovery did not differ substantially, and at the lowest and the highest concentrations mean recovery and RSD% showed that most of PAHs were between 70% and 120% with RSD less than 10%. The measurement uncertainty is expressed as expanded uncertainty and in terms of relative standard deviation (at 95% confidence level) is  $\pm 12\%$ . This method is suitable for laboratories engaged daily in routine analysis of a large number of samples.

## 1. Introduction

Polycyclic aromatic hydrocarbons (PAHs) are a large group of organic compounds that are included in the European Union (EU) and US Environmental Protection Agency (US EPA) priority pollutant list due to their mutagenic and carcinogenic properties [1]. The most important sources of PAHs have been identified as coke ovens in the production of aluminum, iron, and steel; heating in power plants and residences; cooking; motor vehicle traffic; environmental tobacco smoke; and the incineration of waste material [2]. Cooking and food processing at high temperatures have been shown to generate various kinds of genotoxic substances or cooking toxicants including PAHs [3]. A number of PAHs are known for their carcinogenic, mutagenic, and teratogenic properties like benzo(a)anthracene, benzo(b)fluoranthene,

benzo(k)fluoranthene, benzo(g,h,i)perylene, benzo(a)pyrene, chrysene, dibenzo(a,h)anthracene, and indeno(1,2,3-cd)pyrene [4]. PAHs containing up to four fused benzene rings are known as light PAHs and those containing more than four benzene rings are called heavy PAHs. Heavy PAHs are more stable and more toxic than light ones [5]. Light PAHs are more volatile, water soluble, and less lipophilic than the heavy PAHs, so PAHs migrate through the food chain into hydrophobic compartments and thus accumulate in lipid components due to their lipophilic nature [6–8].

Seven of the PAHs have been classified by the US EPA as compounds of probable human carcinogens. These are benzo(a)anthracene, benzo(b)fluoranthene, benzo(k)fluoranthene, chrysene, benzo(a)pyrene, dibenzo(a,h)anthracene, and indeno(1,2,3-cd)pyrene [9]. With the aim of minimizing harmful effects on human health, recently, the European

Union established a maximum level of 2 ng/g wet weight for benzo(a)pyrene (the marker used for carcinogenic risk of PAHs) in muscle meat of fish [10].

In 2008, a scientific opinion adopted by the European Food Safety Authority (EFSA, 2008) concluded that benzo(a)pyrene alone is not a suitable indicator for the occurrence and toxicity of PAHs in food and that eight specified PAHs (PAH<sub>8</sub>), for which oral carcinogenicity data are available, and/or a subgroup of these, PAH<sub>4</sub>, are more suitable markers. It was further concluded that PAH<sub>8</sub> would not provide much added value compared to PAH<sub>4</sub> (the sum of benzo(a)pyrene, chrysene, benz(a)anthracene, and benzo(b)fluoranthene) [11]. In September 2012, benz(a)anthracene, benzo(b)fluoranthene, and chrysene were included in the assessment and recorded together with benzo(a)pyrene as a sum parameter (group of "PAH<sub>4</sub>"), as per Regulation (EU) number 835/2011.

Developed analytical methods include soxhlet extraction [12], dispersed solid phase extraction [13], and accelerated solvent extraction coupled to sample cleanup using gel permeation chromatography [14] which had been used to assess most of PAHs in different matrices by changing the technique of cleanup from coextracted interferences that may cause false positive results, but most of these techniques are expensive, use chlorinated solvent for extraction, and are time and chemicals consuming. In 2013 a simple solid phase extraction (SPE) method [15] followed by comprehensive two-dimensional gas chromatography coupled to time-of-flight mass spectrometry has been developed for analysis of (15 + 1) carcinogenic polycyclic aromatic hydrocarbons (PAHs). This method includes three critically assessed sample preparation approaches: (i) gel permeation chromatography (GPC), (ii) GPC followed by silica based SPE, and (iii) SPE employing PAHs-dedicated molecularly imprinted polymers (MIPs).

Also in 2013, two of the most relevant analytical methods including different extraction procedures such as ultrasound-assisted solvent extraction (USAE) and ultrasound-assisted emulsification microextraction (USAEME) for determination of 11 mutagenic and carcinogenic PAHs were optimized by the selected extraction techniques. The recoveries ranging from 70% to 100% by USAE and from 70% to 108% by USAEME with estimated quantification limits between 0.020 and 2.6 µg/kg were achieved [16].

A few researches on the development of QuEChERS analytical method for determination of PAHs levels in fish have been previously published in the literature. The streamline of QuEChERS (quick, easy, cheap, effective, rugged, and safe) method for extraction of pesticides in tissues of high fat (>3.5%) encourages scientists to apply modifications and develop this method in order to extract veterinary drugs [17] and PAHs from seafood such as shrimp [18] and in fish by using QuEChERS for extraction followed by dispersive SPE analysis by GCMS in SIM mode for quantification [19].

The aim of this study is to adapt and validate QuEChERS method [20] for extraction followed by solid phase extraction for sample purification and gas chromatography mass spectrometer GCMS for determination of 16 PAHs in fish at low LOQ level.

## 2. Materials and Methods

**2.1. Sample Preparation.** The edible parts (head, bones, and removable skin were removed) of nonsmoked blank Herring fish were obtained and completely homogenized in a food mixer as a blank sample and then stored in a freezer at -20°C.

**2.2. Chemicals and Reagents.** Acetone (Riedel-de Hën, purity 99.8%), acetonitrile (Sigma-Aldrich, purity > 99.9%), toluene (Merck), dichloromethane chromatography grade, and n-hexane (purity > 99.0%) were the solvents used. Agilent QuEChERS salts and buffers were prepackaged in anhydrous packages for EN 15662 containing 4 g magnesium sulfate (MgSO<sub>4</sub>), 1 g sodium chloride (NaCl), 1 g sodium citrate, and 0.5 g disodium citrate sesquihydrate. Silica gel (60–120 mesh, Fluka) was activated at 150°C for 12 hours prior to use.

A 1000 µg/mL stock solution of 14 PAHs includes naphthalene, fluorene, fluoranthene, benz(a)anthracene, chrysene, pyrene, benzo(b)fluoranthene, benzo(k)fluoranthene, benzo(a)pyrene, acenaphthene, phenanthrene, anthracene, acenaphthylene, and pyrene-d<sub>10</sub> (surrogate standard) and reference standards obtained from Sigma-Aldrich with purity > 95% were prepared, while benzo(g,h,i)perylene and dibenz(a,h)anthracene were obtained as readymade of 100 µg/mL in methylene chloride and indeno[1,2,3-cd]pyrene 200 µg/mL in methanol. A 1 µg/mL working solution of all 16 PAHs was prepared in toluene. Calibration mixtures with concentration 2, 10, 50, 100, and 500 ng/mL were prepared from serial dilution of the working solution in toluene where pyrene-d<sub>10</sub> maintained at level 50 ng/mL in all calibration levels and all stored in refrigerator at 4°C.

**2.3. Apparatus.** PFTE or polyethylene 50 mL tubes with screw cap and 15 mL tubes contain 1 g magnesium sulfate were obtained for sample extraction. Centrifuge up to 4000 rpm (Heraeus Labofuge 400), Vortex, Automatic Pipettes (Hirschmann Laborgerate) suitable for handling volumes of 10 µL to 100 µL and 100 µL to 1000 µL, 10 mL solvent-dispenser (Hirschmann Laborgerate) for Acetonitrile. The glassware were washed with detergent and water then rinsed with acetone and dried at 90°C before use.

**2.4. Sample Extraction Steps.** The validation procedure needs to be considered, the context of fitness for purpose and cost benefit criteria [21]. About 10 g of fish sample was weighted in 50 mL Teflon centrifuge tube, 50 µL of 10 µg/mL pyrene-d<sub>10</sub> was added which acts as surrogate standard of 50 µg/Kg, and each set of 6 replicates was spiked with 20, 100, and 500 µL of 1 µg/mL spiking mixture to get 2, 10, and 50 µg/kg, respectively. 10 mL of acetonitrile was used for extraction, shaken for 2 minutes, mixed with Agilent QuEChERS, shaken for 1 minute, and centrifuged at 4000 rpm for 5 minutes. Aliquots of the resulting supernatant were transferred to Teflon tube containing MgSO<sub>4</sub>, vortexed for 30 seconds, and centrifuged at 4000 rpm for 2 minutes; 4 mL of the acetonitrile layer was transferred into 50 mL flask and then evaporated near to dryness.

**2.5. Cleanup of PAHs Samples by Packed Solid Phase Extraction (SPE) Steps.** All fish extracts were subjected to packed solid phase cleanup cartridge which was prepared in-house as follows. Plug a glass wool on 10 mL length syringe; 1g 20% deactivated silica gel and 0.2 MgSO<sub>4</sub> were weighted and conditioned with 5 mL of n-hexane/dichloromethane (3 : 2), the sample extract loaded to the cartridge using 10 mL of elute (n-hexane/dichloromethane). Collect fractions in a 50 mL flask, evaporate on rotary evaporator at 40°C near to dryness and dissolve in 2 mL toluene and then apply to GCMS for analysis.

**2.6. GC-MSD Conditions.** Agilent 6890N series gas chromatography instrument equipped with 5975 series mass selective detector and Agilent GC Column of model J&W HP-5ms Ultra Inert with the specifications (30 m length, 0.25 mm internal diameter, 0.25 μm film thickness) were used for both qualitative and quantitative determination of PAHs. Helium gas was used as the carrier gas; the column was maintained at a constant flow rate of 1.3 mL/min. The back injector line was maintained at 260°C. Injection volumes were 1.0 μL in the splitless mode. The column temperature was initially held at 90°C for 2 min, ramping to 180°C at a rate of 15°C/min, held at 180°C for 15 min, ramping to 250°C at a rate of 10°C/min, held for 2 min, ramping to 290°C at a rate of 10°C/min, and held for 10 min. The mass spectrometer was operated in the ionization mode and spectra were acquired using a mass range of 45–450 m/z. SIM acquisition was carried out by comparison of the base peak of each targeted PAH as shown in Table 1.

Quality control and assurance of each patch were passed by monitoring the performance of the GCMS and the mass selective detector daily by tuning the mass detector and monitoring the sensitivity and linearity of the calibration curve, respectively, and also analyzing blank sample to confirm that there is no contamination effect on the results during analysis.

### 3. Results and Discussion

**3.1. Chromatographic Results.** Figure 1 represents overlay between blank and spike fish at level 50 μg/kg samples to show the separation of 16 PAHs by GCMS in 35 minutes using Agilent J&W HP-5ms Ultra Inert GC Column (30 m length, 0.25 mm internal diameter, and 0.25 μm film thicknesses). PAHs corresponding to chromatogram numbers can be found in Table 1. This representative chromatogram of PAHs in fish matrix indicates good cleanup separation techniques with minimum interference of coextract that may influence the accuracy of the result. Matrix matched standards were used in order to compensate the matrix enhancement effect. This indicates good selectivity and specificity of the method.

**3.2. Method Linearity.** The linearity was obtained by plotting the peak area of each analyte versus its concentration.

The linearity of all PAHs indicates that both dibenz(a,h)anthracene and indeno(1,2,3-cd)pyrene compounds had  $r^2$  values of 0.996; all others were 0.998 or higher within measurement range of 2–50 μg/L indicating excellent linearity.

TABLE 1: Representing the PAHs used and respective analytical ions used for quantification.

Compounds name	CAS number	Target compound monitored SIM ions ( $m/z$ )	
		Quant.	Confirm.
Naphthalene	91-20-3	276	277, 274
Acenaphthene	83-32-9	153	154, 152
Acenaphthylene	208-96-8	152	151, 150
Fluorene	86-73-7	166	165, 167
Phenanthrene	85-01-8	178	176, 179
Anthracene	120-12-7	178	176, 179
Fluoranthene	206-44-0	202	203, 200
Pyrene	129-00-0	202	200, 203
Benz(a)anthracene	56-55-3	228	226, 229
Chrysene	218-01-9	228	226, 229
Benzo(b)fluoranthene	205-99-2	252	253, 250
Benzo(k)fluoranthene	207-08-9	252	253, 250
Benzo(a)pyrene	50-32-8	252	253, 250
Indeno(1,2,3-c,d)pyrene	193-39-5	128	127, 129
Dibenzo(a,h)anthracene	53-70-3	278	279, 276
Benzo(g,h,i)perylene	191-24-2	276	277, 274
Pyrene-d <sub>10</sub>	1718-52-1	212	211, 208

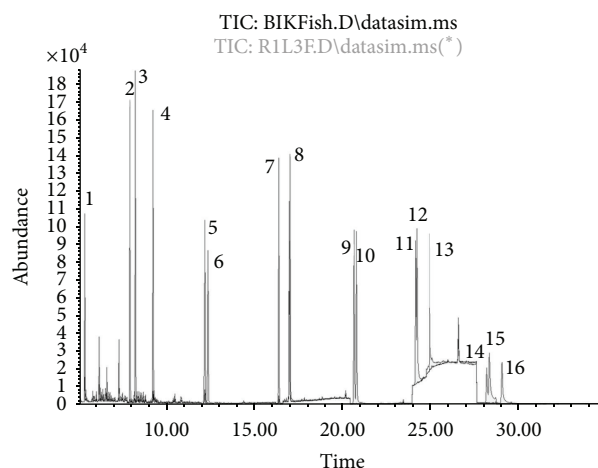


FIGURE 1: Representing total ion chromatogram of 16 PAHs in fish sample at level 50 μg/kg by weight.

**3.3. The Limit of Determination (LOD).** It is the minimum concentration of analyte in the test sample that can be measured with a stated probability that the analyte is present at a concentration above that in the blank sample. Limits of detection expressed as three multiplied by SD of the recovery replicates at the lowest expected concentrations ranging between 0.09 and 1.94 μg/kg are shown in Table 2.

**3.4. The Limit of Quantitation (LOQ).** It is the lowest concentration of analyte that can be determined with an acceptable level of uncertainty according to Eurachem guideline and it

TABLE 2: Retention times (RT), regression coefficient ( $r^2$ ), regression equation, limit of detection (LOD), and standard deviation (SD) obtained for standards in toluene calibration.

Compounds	RT (min)	$r^2$	Regression equation	LOD	SD
(1) Naphthalene	5.241	0.998	$Y = 2.68e4X + 2.67e5$	1.22	0.41
(2) Acenaphthylene	7.815	0.999	$Y = 1.14e0X + 1.56e2$	0.36	0.12
(3) Acenaphthene	8.092	0.999	$Y = 1.53e4X + 4.47e4$	1.17	0.39
(4) Fluorene	9.040	0.999	$Y = 1.80e4X + 2.69e4$	1.64	0.55
(5) Phenanthrene	11.803	0.999	$Y = 2.48e4X + 7.34e4$	0.74	0.25
(6) Anthracene	11.984	0.999	$Y = 2.23e4X + 8.11e4$	1.94	0.65
(7) Fluoranthene	16.077	0.999	$Y = 2.55e4X - 3.26e4$	0.95	0.32
(8) Pyrene	16.720	0.999	$Y = 2.53e4X - 3.12e4$	0.50	0.17
(9) Benzo(a)anthracene	20.285	0.999	$Y = 8.37e1X - 9.44e2$	0.75	0.25
(10) Chrysene	20.409	0.999	$Y = 9.17e1X - 7.76e3$	0.33	0.11
(11) Benzo(b)fluoranthene	23.792	0.998	$Y = 6.34e1X - 9.62e2$	0.57	0.19
(12) Benzo(k)fluoranthene	23.861	0.999	$Y = 8.40e1X + 6.26e2$	0.58	0.19
(13) Benzo(a)pyrene	24.612	0.998	$Y = 7.78e1X - 9.25e2$	0.37	0.12
(14) Indeno(1,2,3-cd)pyrene	27.809	0.996	$Y = 3.86e1X - 8.83e2$	0.44	0.15
(15) Dibenz(a,h)anthracene	27.870	0.996	$Y = 5.10e1X - 8.85e2$	0.90	0.30
(16) Benzo(g,h,i)perylene	28.534	0.999	$Y = 7.98e1X - 5.45e2$	0.09	0.03

TABLE 3: Representing recovery percentage, relative standard deviation (RSD%), and  $RSD_{pooled}\%$  results of  $n = 6$  replicates on each spiking level.

Compounds	Recovery $\pm$ RSD%			$RSD_{pooled}\%$
	2.0 $\mu\text{g/Kg}$	10.0 $\mu\text{g/Kg}$	50.0 $\mu\text{g/Kg}$	
(1) Naphthalene	95 $\pm$ 16	96 $\pm$ 11	88 $\pm$ 5	5
(2) Acenaphthene	96 $\pm$ 5	108 $\pm$ 10	113 $\pm$ 11	5
(3) Acenaphthylene	107 $\pm$ 12	118 $\pm$ 3	97 $\pm$ 5	4
(4) Fluorene	85 $\pm$ 10	117 $\pm$ 11	114 $\pm$ 10	5
(5) Phenanthrene	102 $\pm$ 12	109 $\pm$ 5	116 $\pm$ 10	5
(6) Anthracene	87 $\pm$ 10	112 $\pm$ 10	115 $\pm$ 10	5
(7) Fluoranthene	102 $\pm$ 12	106 $\pm$ 13	115 $\pm$ 9	5
(8) Pyrene	101 $\pm$ 13	111 $\pm$ 12	115 $\pm$ 10	5
(9) Benzo(a)anthracene	96 $\pm$ 6	99 $\pm$ 4	105 $\pm$ 2	2
(10) Chrysene	89 $\pm$ 19	88 $\pm$ 6	103 $\pm$ 2	4
(11) Benzo(b)fluoranthene	76 $\pm$ 6	72 $\pm$ 4	105 $\pm$ 3	3
(12) Benzo(k)fluoranthene	89 $\pm$ 10	76 $\pm$ 6	97 $\pm$ 6	4
(13) Benzo(a)pyrene	70 $\pm$ 8	74 $\pm$ 13	106 $\pm$ 5	4
(14) Indeno(1,2,3-cd)pyrene	65 $\pm$ 9	61 $\pm$ 7	98 $\pm$ 5	4
(15) Dibenz(a,h)anthracene	74 $\pm$ 9	72 $\pm$ 9	97 $\pm$ 5	4
(16) Benzo(g,h,i)perylene	69 $\pm$ 3	56 $\pm$ 9	96 $\pm$ 5	4

is usually the lowest point on the calibration curve which is  $2\mu\text{g/kg}$ . The analytes were considered to be quantitative when their abundance confirmation ion signal to noise is  $S/N \geq 3$  with an accurate quantitation of  $\pm 20\%$  of their true value in the calibration standard. Sample residues that met all criteria but had  $S/N < 3$  were reported as less than the limit of quantification ( $<LOQ$ ) while those which had not fit any criteria were reported as not detected (N.D.).

3.5. Recovery and Relative Standard Deviation (RSD). The recovery of ( $n = 6$ ) replicates at each level was calculated and

summarized in Table 3 which shows very good recovery and excellent RSD.

From Table 3, the recovery of each set of 6 replicates was in the range of 56–115% where the lower spiking level was selected in order to include the lower concentration of PAHs fish muscle fixed at  $2\mu\text{g/Kg}$ . The extraction efficiency was consistent over the entire range with indeno(1,2,3-cd)pyrene and benzo(g,h,i)perylene being the most affected compounds where their recovery at lower level was 65 and 69%, respectively, and at the second level was 61 and 56%. No significant dispersion of results was observed for the other

remaining PAHs and recovery did not differ substantially at the lowest and the highest concentrations.

According to Commission Regulation (EC) number 1881/2006 and (EC) number 333/2007 [22, 23], the maximum level for the determination of PAHs in fish was  $2 \mu\text{g}/\text{kg}$  wet weight and the recovery range of the methods used should be 50–120%, indicating that the validated method complies with these criteria.

Where  $\text{RSD}_{\text{pooled}}$  can be calculated [21] as

$$\text{RSD}_{\text{pooled}} = \sqrt{\frac{\text{RSD}_1^2(n_1 - 1) + \text{RSD}_2^2(n_2 - 1) + \dots}{(n_1 - 1) + (n_2 - 1) + \dots}} \quad (1)$$

RSD is the relative standard deviation,  $n$  is the number of samples, and the equation used to calculate the recovery is [24]

$$\text{Recovery}\% = \frac{C_f}{C_e} \times 100, \quad (2)$$

where  $C_f$  is the found concentration and  $C_e$  is the expected concentration.

Figures 2, 3, and 4 represent mean recovery and RSD% ranges; most of the PAHs recovery was between 70 and 120% with most of RSD less than 10%.

The reported results provide evidence that the adapted QuEChERS method achieved for most of the PAHs gives good recoveries, repeatability, and reproducibility.

**3.6. Method Uncertainty Calculation.** Using these equations the following was found.

Relative standard uncertainty  $U_{\text{Rec}} = 3.6\%$  and

$$U_{(\text{Rec})} = \frac{s}{\sqrt{n}} \quad (3)$$

Combined uncertainty  $U_c$  is

$$U_c = \sqrt{(U_p)^2 + (U_{\text{Rec}})^2 + U_{\text{Ref}}^2} = 6.2\% \quad (4)$$

$U_c$  is combined uncertainty.  $U_{\text{Rec}}$  is the uncertainty due to recovery.  $U_{\text{Ref}}$  is the uncertainty due to reference standard preparation.  $U_p$  is the uncertainty due to precision experiments.

The uncertainty due to reference standard preparation  $U_{\text{Ref}} = 0.7$ .

$U_p$  which is the relative standard uncertainty due to precision experiments expressed as relative standard deviation was found to be less than 5% (the highest pooled RSD% for pyrene).

Expanded uncertainty is obtained by multiplying the combined uncertainty by a coverage factor  $k$ . For confidence level of 95%  $k$  is 2. The expanded uncertainty (at 95% confidence level) was found to be  $\pm 12\%$ .

The higher sample weight used in the proposed method (10 g) with accepted solid phase extraction cleanup techniques compared with E1 and E2 QuEChERS acetonitrile based extraction method (1 g) [19] facilitates the ability of

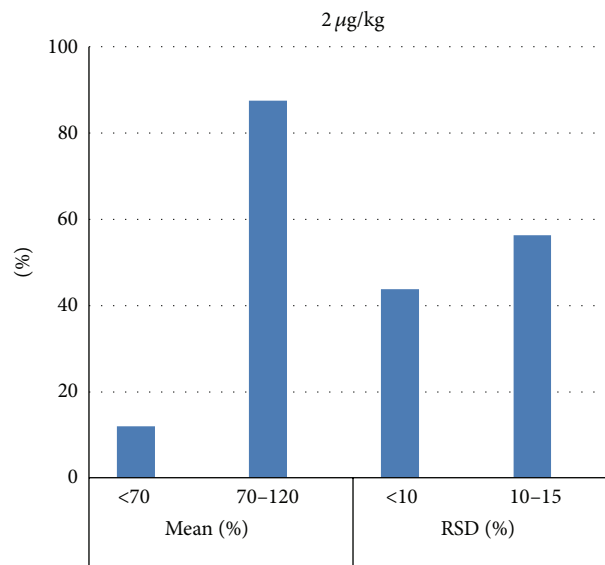


FIGURE 2

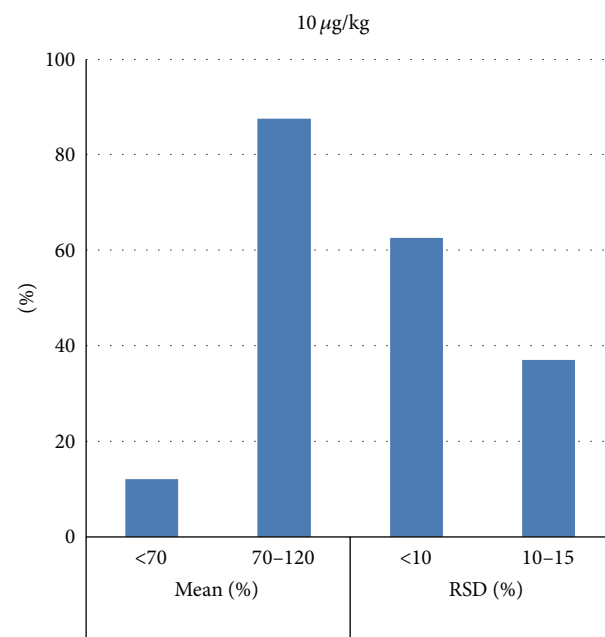


FIGURE 3

lowering the limits of quantification for PAHs where the recoveries obtained at  $500 \mu\text{g}/\text{Kg}$  for traditional acetonitrile based QuEChERS extraction using extraction scheme E1 (1% acetic acid in acetonitrile and AOAC salts) yield average recoveries less than 67%, with individual PAHs recoveries typically ranging from 35 to 87%, also for extraction scheme E2 (acetonitrile and EN salts) performed equally poorly, with average PAHs recoveries being less than 68% and individual PAHs recoveries ranging from 24 to 88%, while for the proposed method the individual PAHs recoveries range from 65 to 107% at the LOQ limits ( $2 \mu\text{g}/\text{Kg}$ ) with method uncertainty equal to  $\pm 12$  (at 95% confidence level) indicating

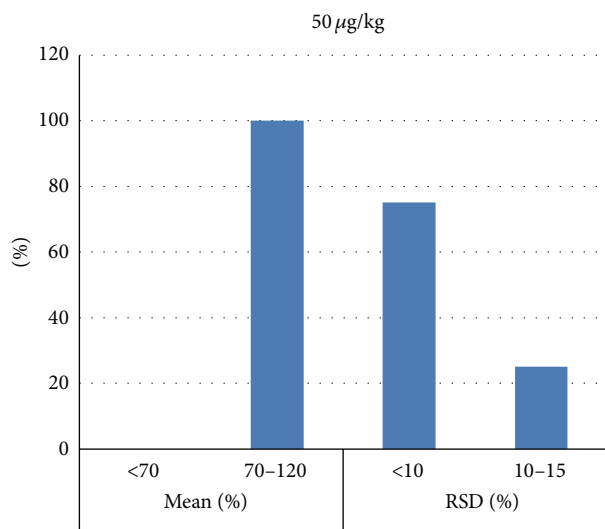


FIGURE 4

that the method is quite fit for purpose with acceptable LOQ, precision, and accuracy according to Commission Regulation (EC) number 1881/2006 and (EC) number 333/2007.

#### 4. Conclusion

The results found were very promising; it may be concluded that modified QuEChERS method of extraction followed by cleanup silica gel packed solid phase extraction combined with GCMS for quantitation is an efficient method for determination of low concentration of selected group of PAHs in homogenized fish samples. This method is suitable for laboratories engaged daily in routine analysis of a large number of samples, and the LOQ of the method is sufficiently attained low in order to be used in the national monitoring program of Egypt for determination of PAHs in fish as well as in imported and exported fish following Codex regulations.

#### Conflict of Interests

The authors declare that there is no conflict of interests regarding the publication of this paper.

#### Acknowledgments

The authors gratefully appreciate the financial support of Central Laboratory of Residue Analysis of Pesticides and Heavy Metals in Food (QCAP), Agricultural Research Center of Egypt, continuous support of Dr. Ashraf El Marsafy (lab director), and technical support of Dr. Emad Attallah.

#### References

- [1] United States Environmental Protection Agency (U.S. EPA), "Guidance for assessing chemical contaminant data for use in fish advisories," Tech. Rep. EPA/823/b-00/007, 2000.
- [2] WHO, Environmental Health Criteria 202, Selected Non-heterocyclic PAHs, 1998, <http://www.inchem.org/documents/ehc/ehc/ehc202.htm>.
- [3] M. Jägerstad and K. Skog, "Genotoxicity of heat-processed foods," *Journal of Mutation Research—Fundamental and Molecular Mechanisms of Mutagenesis*, vol. 574, no. 1-2, pp. 156–172, 2005.
- [4] A. Luch, *The Carcinogenic Effects of Polycyclic Aromatic Hydrocarbons*, Imperial College Press, London, UK, 2005.
- [5] T. Wenzl, R. Simon, E. Anklam, and J. Kleiner, "Analytical methods for polycyclic aromatic hydrocarbons (PAHs) in food and the environment needed for new food legislation in the European Union," *TrAC—Trends in Analytical Chemistry*, vol. 25, no. 7, pp. 716–725, 2006.
- [6] E. Ferrarese, G. Andreottola, and I. A. Oprea, "Remediation of PAH-contaminated sediments by chemical oxidation," *Journal of Hazardous Materials*, vol. 152, no. 1, pp. 128–139, 2008.
- [7] S. R. Wild and K. C. Jones, "Polynuclear aromatic hydrocarbons in the United Kingdom environment: a preliminary source inventory and budget," *Environmental Pollution*, vol. 88, no. 1, pp. 91–108, 1995.
- [8] European Commission (EC), European Commission Regulation: O. J. (L835), 2011.
- [9] USEPA, US Environmental Protection Agency. Federal Register, 59 FR 1788, 1994.
- [10] European Commission, "Commission regulation No 208/2005: regards polycyclic aromatic hydrocarbons," *Official Journal of the European Union*, vol. L34, pp. 3–5, 2005.
- [11] EFSA, Scientific opinion of the panel on contaminants in the food chain on a request from the European Commission on Polycyclic Aromatic Hydrocarbons in Food, 2008, <http://www.efsa.europa.eu/de/efsajournal/pub/724.htm>.
- [12] United States Environmental Protection Agency (U.S. EPA), *Method 3540C, Soxhlet Extraction*, United States Environmental Protection Agency (U.S. EPA), Washington, DC, USA, 1996.
- [13] D. Smith and K. Lynam, Agilent Technologies Application note, 5990-6668EN, 2010.
- [14] J. Sanz-Landaluze, L. Bartolome, O. Zuloaga, L. González, C. Dietz, and C. Cámara, "Accelerated extraction for determination of polycyclic aromatic hydrocarbons in marine biota," *Analytical and Bioanalytical Chemistry*, vol. 384, no. 6, pp. 1331–1340, 2006.
- [15] L. Drabova, M. Tomaniova, K. Kalachova, V. Kocourek, J. Hajslova, and J. Pulkrabova, "Application of solid phase extraction and two-dimensional gas chromatography coupled with time-of-flight mass spectrometry for fast analysis of polycyclic aromatic hydrocarbons in vegetable oils," *Food Control*, vol. 33, no. 2, pp. 489–497, 2013.
- [16] I. Yebra-Pimentel, E. Martínez-Carballo, J. Regueiro, and J. Simal-Gándara, "The potential of solvent-minimized extraction methods in the determination of polycyclic aromatic hydrocarbons in fish oils," *Journal of Food Chemistry*, vol. 139, no. 1–4, pp. 1036–1043, 2013.
- [17] G. Stubbings and T. Bigwood, "The development and validation of a multiclass liquid chromatography tandem mass spectrometry (LC-MS/MS) procedure for the determination of veterinary drug residues in animal tissue using a quechers (Quick, Easy, Cheap, Effective, Rugged and Safe) approach," *Analytica Chimica Acta*, vol. 637, no. 1-2, pp. 68–78, 2009.
- [18] M. Smoker, K. Tran, and R. E. Smith, "Determination of polycyclic aromatic hydrocarbons (PAHs) in shrimp," *Journal of*

*Agricultural and Food Chemistry*, vol. 58, no. 23, pp. 12101–12104, 2010.

- [19] N. D. Forsberg, G. R. Wilson, and K. A. Anderson, “Determination of parent and substituted polycyclic aromatic hydrocarbons in high-fat salmon using a modified QuEChERS extraction, dispersive SPE and GC-MS,” *Journal of Agricultural and Food Chemistry*, vol. 59, no. 15, pp. 8108–8116, 2011.
- [20] M. Anastassiades, S. J. Lehotay, D. Stajnbaher, and F. J. Schenck, “Fast and easy multiresidue method employing acetonitrile extraction/partitioning and dispersive solid-phase extraction for the determination of pesticide residues in produce,” *Journal of AOAC International*, vol. 86, no. 2, pp. 412–431, 2003.
- [21] Eurachem Guide, *The Fitness for Purpose of Analytical Methods*, English Edition 1.0., 1998.
- [22] European Commission, “Setting maximum levels for certain contaminants in foodstuffs,” Commission Regulation (EC) No. 1881/2006, 2006.
- [23] European Union, “Commission Regulation (EC) no. 401/2006 laying down the methods of sampling and analysis for the official control of the levels of mycotoxins in foodstuffs,” *Official Journal of the European Union*, vol. L 70, pp. 12–34, 2007.
- [24] E. D. Prudnikov, “Theoretical calculation of the standard deviation in atomic emission spectroscopy,” *Journal of Spectrochimica Acta*, vol. 36, no. 4, pp. 385–392, 1981.

## Research Article

# A High Throughput Method for Measuring Polycyclic Aromatic Hydrocarbons in Seafood Using QuEChERS Extraction and SBSE

Edward A. Pfannkoch,<sup>1</sup> John R. Stuff,<sup>1</sup> Jacqueline A. Whitecavage,<sup>1</sup> John M. Blevins,<sup>2</sup> Kathryn A. Seely,<sup>2</sup> and Jeffery H. Moran<sup>2,3</sup>

<sup>1</sup>GERSTEL Inc., 701 Digital Drive, Suite J, Linthicum, MD 21090, USA

<sup>2</sup>Arkansas Department of Health, Public Health Laboratory, 201 S. Monroe Street, Little Rock, AR 72205, USA

<sup>3</sup>Department of Pharmacology and Toxicology, University of Arkansas for Medical Sciences, 4301 W. Markham Street, Little Rock, AR 72205, USA

Correspondence should be addressed to Edward A. Pfannkoch; [eapfannkoch@gerstelus.com](mailto:eapfannkoch@gerstelus.com)

Received 30 September 2014; Revised 15 January 2015; Accepted 17 January 2015

Academic Editor: Shahram Seidi

Copyright © 2015 Edward A. Pfannkoch et al. This is an open access article distributed under the Creative Commons Attribution License, which permits unrestricted use, distribution, and reproduction in any medium, provided the original work is properly cited.

*National Oceanic and Atmospheric Administration (NOAA) Method NMFS-NWFSC-59 2004* is currently used to quantitatively analyze seafood for polycyclic aromatic hydrocarbon (PAH) contamination, especially following events such as the Deepwater Horizon oil rig explosion that released millions of barrels of crude oil into the Gulf of Mexico. This method has limited throughput capacity; hence, alternative methods are necessary to meet analytical demands after such events. Stir bar sorptive extraction (SBSE) is an effective technique to extract trace PAHs in water and the quick, easy, cheap, effective, rugged, and safe (QuEChERS) extraction strategy effectively extracts PAHs from complex food matrices. This study uses SBSE to concentrate PAHs and eliminate matrix interference from QuEChERS extracts of seafood, specifically oysters, fish, and shrimp. This method provides acceptable recovery (65–138%) linear calibrations and is sensitive (LOD = 0.02 ppb, LOQ = 0.06 ppb) while providing higher throughput and maintaining equivalency between NOAA 2004 as determined by analysis of NIST SRM 1974b mussel tissue.

## 1. Introduction

When the Deepwater Horizon oil rig exploded off the northern coast of the Gulf of Mexico on April 20, 2010, millions of barrels of crude oil were released into the gulf before the well was capped, and later sealed, almost six months later. Fragile ecosystems, air and water quality, food supplies, human health, and economies in and around the Gulf of Mexico are still being impacted by this spill [1]. Without effective monitoring of food and water quality after such spills, fisheries could remain closed unnecessarily or products from unmonitored fisheries may enter the general food supply, leading to potential endangerment of public health. Nine PAHs were initially selected as markers for contamination in seafood harvested in and around potentially impacted areas [2]. Regulatory limits and established safe levels of exposure for each of these analytes are summarized in Table 1.

The National Oceanic and Atmospheric Administration is responsible for closing and opening Federal waters for seafood harvest. The NOAA Office of Response and Restoration (OR&R) publication entitled *Managing Seafood Safety after an Oil Spill* [3] and input from NOAA, the Food and Drug Administration, the Environmental Protection Agency, and several state authorities were used to establish criteria for analytically screening seafood for oil contamination as part of the Deepwater Horizon explosion. NOAA currently recommends using *NOAA Method NMFS-NWFSC-59 2004* [4] as the preferred method for quantifying polycyclic aromatic hydrocarbons (PAHs) in seafood harvested from potentially oil-impacted areas. This gas chromatography/mass spectrometry (GC/MS) method recommends running batches of only 12 to 14 samples where assay preparation, sample preparation, and extensive sample cleanup require multiple

TABLE 1: United States PAH regulatory limits for reopening impacted areas.

Chemical <sup>1</sup>	Levels of concern (ppm)			
	mg/kg/day	13 g/day (shrimp and crabs)	12 g/day (oysters)	49 g/day (finfish)
Naphthalene	0.02	123	133	32.7
Fluorene	0.04	246	267	65.3
Anthracene/phenanthrene	0.3	1846	2000	490
Fluoranthene	0.3	246	267	65.3
Pyrene	0.03	185	200	49
Benz[ <i>a</i> ]anthracene	0.0002	1.32	1.43	0.35
Chrysene	0.02	132	143	35
Benzo[ <i>a</i> ]pyrene	0.00002	0.132	0.143	0.035

<sup>1</sup>Includes alkylated homologues, specifically C-1, C-2, C-3, C-4 naphthalenes; C-1, C-2, C-3 fluorenes; C-1, C-2, C-3 anthracenes/phenanthrenes; C-1, C-2 pyrenes.

Table modified from FDA 2010 [2].

days of work to complete. Additionally, size-exclusion high-performance liquid chromatography is completed prior to GC/MS analysis for further sample cleanup. Lastly, the GC/MS method is almost an hour long for each sample [4]. All of these steps result in a low-throughput method. Hence, there is concern that the NOAA 2004 method may not have the throughput capacity necessary during an emergency response. Other methods have been utilized to extract PAHs from seafood, like solid-liquid extraction with *n*-hexane or dichloromethane with a mandatory solid phase extraction cleanup step [5], but larger volumes of chlorinated solvents are necessary and relative standard deviations (RSDs) are high for some compounds. Also, solid-phase microextraction (SPME) has been utilized to extract PAHs from seafood, which eliminates the need for solvents and a separate cleanup step [6], but is not high throughput since the SPME fiber is exposed to a single sample for 60 minutes.

As a result of the Deepwater Horizon explosion, a new PAH screening method was developed using liquid chromatography/fluorescence (LC/FL) technology [2]. Although the LC/FL method is fast and high throughput, this method lacks quantification and mass spectral confirmation and is only used for screening purposes [7]. Incorporating existing extraction procedures like QuEChERS (quick, easy, cheap, effective, robust, and safe) may retain the throughput capacity of this method and add much needed quantification capabilities.

QuEChERS was first developed to extract a broad spectrum of pesticides from fruits and vegetables and has been shown to yield high recovery of apolar compounds from a variety of plant materials [8]. The technique has since been extended to other analytes including PAHs in fish tissue with recoveries of >90% [9, 10]. QuEChERS uses a water-miscible solvent to extract analytes of interest but requires dispersive solid phase extraction (dSPE) for further sample cleanup. In dSPE procedures, primary secondary amine (PSA) adsorbent is typically used to remove organic acids while C18 or graphitized carbon black can be included to remove fats and pigments [11–13].

In 1999, Baltussen et al. developed a microextraction technique commonly referred to as stir bar sorptive extraction (SBSE) [14], which initially was used to extract compounds

from liquid matrices [15]. This technique uses 1-2 cm magnetic stir bars coated with a 0.5 or 1.0 mm film of polydimethylsiloxane (PDMS), a commonly used sorptive material, to extract compounds with high octanol : water partition coefficients ( $\log K_{o/w} > 2$ ) [14, 16]. SBSE is easy to use and parts per billion detection levels for apolar pollutants, like PAHs, in aqueous solutions are possible when combined with GC/MS [17, 18]. Also, SBSE has been successfully applied for the detection and quantification of trace levels of numerous analytes in food, environmental, and forensic applications [15, 19, 20]. Further, the United States Environmental Protection Agency Region 7 Laboratory concluded that SBSE can meet *EPA Method 625* performance criteria for all 18 PAHs listed [21].

The purpose of this study is to determine if QuEChERS and SBSE technology can be combined to provide an extraction and concentration procedure for PAHs from fish and shellfish that can be coupled to GC/MS. This new extraction method will result in a high throughput approach, unlike the NOAA 2004 method, with quantifiable results and mass spectral confirmation, unlike the LC/FL method. This method is the first to combine QuEChERS with SBSE technology to successfully develop a method to minimize matrix interference and significantly increase sample throughput while maintaining quantifiable results for low level measurements.

## 2. Materials and Methods

**2.1. Reagents and Chemicals.** Analytical PAH standards (part number 31458) and deuterated Semi-Volatile Internal Standard Mix (part number 31006) were from Restek (Bellefonte, PA, USA), while optima LC-MS grade acetonitrile (ACN), methanol, dichloromethane, and sodium hydrogen carbonate were all purchased from Sigma Aldrich (St. Louis, Missouri, USA). Deionized (DI) water used for this work was purified to 18.2 M $\Omega$ -cm resistivity. NIST (Gaithersburg, MD, USA) standard reference material was organics in mussel tissue (SRM 1974b). QuEChERS AOAC extraction kits containing 6.0 g MgSO<sub>4</sub> and 1.5 g sodium acetate were provided as generous gifts from Agilent Technologies (Santa Clara, CA,

USA). Stir bars were conditioned using a TC-2 tube conditioner (GERSTEL, Linthicum, MD, USA). Unless otherwise specified all other chemicals and reagents were of reagent grade or higher.

**2.2. Equipment.** Studies were performed in two different laboratories with slightly different instrumentation as follows: Sample tissue was homogenized using (1) equal parts sample and DI water using a Waring (Lancaster, PA, USA) model LB10S variable speed steel bowl lab blender, or (2) homogenized frozen with a Robot Coupe (Jackson, MS, USA) RSI 2Y1 laboratory grade blender by incorporating a small amount of dry ice. Samples were agitated either manually or with an ATR (Laurel, MD, USA) RKVSD Rotamix rotating inverter. All extracts were centrifuged with either a Thermo Fisher Scientific (Waltham, MA, USA) Sorvall Evolution RC centrifuge or Eppendorf (Hamburg, Germany) 5430R centrifuge. SBSE was performed at room temperature with GERSTEL Twister stir bars in 10 mL headspace vials on a 20 position magnetic stir plate. Stir bars were thermally desorbed using a TDU thermal desorption unit with a CIS 4 programmed temperature vaporizing inlet and analysis automated using an MPS 2 autosampler with Maestro software (GERSTEL, Linthicum, MD, USA). Lastly, an Agilent (Santa Clara, CA, USA) 7890 GC interfaced with either an Agilent 5975 or 5973 MS was used.

**2.3. Standard and Sample Preparation.** Samples of frozen gulf shrimp, fresh oysters, and Atlantic croaker (*Micropogonias undulatus*) were either obtained from local markets or as a generous gift from the Alabama Public Health Laboratory. Seafood obtained at local markets was purchased whole to verify identification prior to being homogenized. Sample tissue (fresh or partially frozen) was homogenized either with equal parts water or by using dry ice in a laboratory grade blender. No difference in results was seen between either of preparation methods. Dry ice was sublimed from homogenized samples at  $-20^{\circ}\text{C}$  prior to analysis. Homogenates equivalent to  $3.0 \pm 0.1\text{ g}$  tissue (or  $6.0 \pm 0.1\text{ g}$  of water homogenate) were weighed into 50 mL conical tubes. Internal standard and PAH standard solutions were spiked directly onto the tissue in the tube.

Stock solutions of PAH standards, quality controls, and internal standards were prepared by diluting original solutions in ACN to yield 0.3, 3.0, 15, 30, and 75 ng/ $\mu\text{L}$  spiking solutions. Stock solutions of deuterated PAH standards used as internal standards were prepared by diluting original solutions in ACN to yield a spiking solution of 3.75 ng/ $\mu\text{L}$ . Adding 20  $\mu\text{L}$  of internal standard to 3.0 g tissue (or 6.0 g of water homogenized tissue) yielded an internal standard concentration of 25 ng/g in tissue. Adding 10  $\mu\text{L}$  of each standard spike level to 3.0 g tissue (or 6.0 g water homogenized tissue) yielded spike levels of 1.0, 10, 50, 100, and 250 ng/g.

We performed the standard AOAC version of QuEChERS without further optimization by following package insert directions. In brief, DI water was added to samples to normalize final weight at 15 g. Samples were vortexed for 30 seconds and further diluted with 15 mL of ACN and vortexed

for an additional minute. The contents of the QuEChERS salt packet (6.0 g  $\text{MgSO}_4$  and 1.5 g sodium acetate) were added to the sample and shaken 1 minute. Samples were mixed on an ATR rotator for 10 minutes and centrifuged at approximately 4000  $\times\text{g}$  for 5 minutes at  $5.0^{\circ}\text{C}$ . The upper ACN layer was collected and stored up to 48 hours prior to analysis.

Prior to use, Twister stir bars were conditioned at  $300^{\circ}\text{C}$  under 80 mL/min zero grade nitrogen flow in the tube conditioner for 2 hours. SBSE was accomplished by transferring 1.0 mL aliquots of the upper ACN layer to a 10 mL headspace vial containing a conditioned, precoated stir bar and 4.0 mL of 0.1 M  $\text{NaHCO}_3$  to reduce organic acid interference. Samples were stirred at room temperature for 90 minutes at approximately 1200 rpm. Stir bars were removed with clean tweezers, rinsed briefly with DI water, blotted dry, and placed into clean glass desorption tubes for analysis.

Calibration of the thermal desorption unit was performed by spiking a known amount of PAH standard mix onto Tenax TA adsorbent tubes (Supelco, Bellefonte PA, USA) and desorbing under the same conditions as used for the Twister desorption, as described below. The total recovery of the combined QuEChERS/SBSE procedure was determined by using this calibration to quantify the PAHs recovered from the spiked oyster matrix.

**2.4. Stir Bar Desorption and GC/MS Conditions.** Stir bars were thermally desorbed at 100 mL/minute into the GC using the thermal desorption unit in splitless mode heated at  $720^{\circ}\text{C}/\text{minute}$  from  $40^{\circ}\text{C}$  (0.2 min) to  $300^{\circ}\text{C}$  (5 minutes). Analytes were refocused in the inlet at  $-120^{\circ}\text{C}$  on a quartz wool-filled liner in solvent venting mode and transferred to the column by heating the inlet at  $720^{\circ}\text{C}/\text{minute}$  to  $300^{\circ}\text{C}$  (3 minutes) with a 10:1 split ratio. Since the focus of this study was the extraction and cleanup procedure, adequate chromatographic separation was performed on a Restek DB 5MS or 5XI 5SIL MS column (30 m  $\times$  0.25 mm  $\times$  0.25  $\mu\text{m}$ ) with zero grade helium carrier at 1 mL/minute constant flow unless otherwise noted. The column was held at  $60^{\circ}\text{C}$  for 1 minute and then heated at  $15^{\circ}\text{C}/\text{min}$  to  $325^{\circ}\text{C}$  and held for 3 minutes for a total run time of 21.7 minutes. Simultaneous detection was performed using selective ion mode (SIM)/Scan mode from 50–400 amu. Specific SIM parameters including the quantifier and two qualifier ions are provided in Table 2.

**2.5. GERSTEL Twister Stir Bar Cleaning Procedures.** After use, stir bars were cleaned by soaking 10–40 stir bars overnight in 40 mL of a 50% methylene chloride in 50% methanol solution. The liquid was poured off and stir bars were carefully spread out on a clean watch glass in the fume hood to allow excess solvent to evaporate for 2 hours. Twisters were thermally conditioned at  $300^{\circ}\text{C}$  in the tube conditioner under a stream of nitrogen (80 mL/min per tube) for 2 hours and allowed to cool for 15 minutes under nitrogen flow before being stored individually in 2 mL vials. Stir bars analyzed after cleaning showed no detectable PAH carryover (data not shown).

TABLE 2: MSD SIM method conditions; quantifier in bold.

Group	RT <sup>1</sup> (min)	Ions monitored
1	2.5	(102, 50), (126, 50), ( <b>128</b> , 50)
2	7.6	(115, 50), (141, 50), ( <b>142</b> , 50)
3	9.0	(151, 20), ( <b>152</b> , 20), (153, 20), (154, 20)
4	10.0	(165, 50), ( <b>166</b> , 50), (167, 50)
5	11.5	(176, 50), ( <b>178</b> , 50), (179, 50)
6	13.5	(200, 50), ( <b>202</b> , 50), (203, 50)
7	15.5	(226, 50), ( <b>228</b> , 50), (229, 50)
8	17.4	(126, 50), ( <b>252</b> , 50), (253, 50)
9	19.2	(138, 20), (139, 20), ( <b>276</b> , 20), (277, 20), (278, 20), (279, 20)

Group 1: naphthalene; Group 2: 2-methylnaphthalene; Group 3: acenaphthylene, acenaphthene; Group 4: fluorene; Group 5: phenanthrene, anthracene; Group 6: fluoranthene, pyrene; Group 7: benzo[*a*]anthracene, chrysene; Group 8: benzo[*b*]fluoranthene, benzo[*k*]fluoranthene, Benzo[*a*]pyrene; Group 9: benzo[*ghi*]perylene.

<sup>1</sup>RT is the retention time for the start of the SIM group window.

### 3. Results and Discussion

Combining QuEChERS and SBSE technology increases sample throughput with quantitative results. Data show that the combination of QuEChERS and SBSE is a viable approach for the determination of important PAH markers in oysters and other seafood that eliminates extensive sample preparation and increases quantitative throughput capabilities.

Although the QuEChERS technique has been used previously to extract PAHs in fish [10, 22], the procedure does not provide additional concentration unless the final sample is evaporated and reconstituted, which also simultaneously concentrates any remaining matrix interferences. Furthermore, using a dSPE cleanup step appears to leave some amount of matrix compounds in the sample extract that may interfere with the analysis [22, 23]. Large volume injection has been used to improve the detection limits for pesticides after QuEChERS extraction [24, 25], but retention time shifts were reported after only three injections on the GC/MS unless back-flushing was used to eliminate interference from high molecular weight matrix contaminants [23]. These initial attempts at using only QuEChERS failed to provide adequate detection limits; therefore, we incorporated SBSE as a dual cleanup and concentrating step.

**3.1. Optimizing SBSE Conditions.** Since PAHs are ubiquitous, precautions must be taken to ensure background contamination is minimized. Oysters were chosen as the first matrix to test the QuEChERS/SBSE method in seafood because oysters are considered a difficult matrix since the high fat content in oysters may introduce high background interferences [12]. Prior to this study, we have performed SBSE in aqueous solutions containing water-miscible organic solvents for compounds with high  $K_{o/w}$  and found the relative percentage of organic solvent must be optimized for efficient extraction of the target analytes. Based on our previous studies and a study by Ochiai et al. [16], 20% ACN was selected because the

$\log K_{o/w}$  for the PAHs of interest ranged between 3.3 and 6.75. Therefore, to perform the SBSE on the QuEChERS extracts, 1.0 mL of the acetonitrile layer was diluted into 4.0 mL water or buffer resulting in a final solution containing 20% ACN. When the optimized extraction conditions were used with the oyster matrix, including the addition of 0.1 M NaHCO<sub>3</sub>, excellent signal to noise ratio in the SIM mode was obtained (Figure 1). SBSE also provided a concentration factor up to 1000x compared to liquid injection, which enabled quantification of very low levels of analytes. Preliminary SBSE extraction studies evaluated extraction times of 30, 60, and 90 minutes, 4 hours, and 16 hours (overnight) to estimate near-equilibrium conditions. Based on these studies, SBSE extraction time for this matrix was evaluated at 90 minutes or 16 hours. No significant improvement in signal was seen with overnight extraction (data not shown); therefore, a 90-minute extraction was used for all subsequent testing. In addition, incorporating 0.1 M NaHCO<sub>3</sub> during SBSE greatly reduced interference due to organic acids and improved signal-to-noise ratios (Figure 2 (A and B)). With routine instrument maintenance, the optimized conditions provided stable chromatography for >200 samples.

**3.2. Method Linearity and Recovery.** GC/MS analysis was used to determine extraction performance, but optimization of the GC/MS parameters was secondary to investigating the combination of QuEChERS and SBSE as a novel extraction procedure for PAHs in seafood. The Agilent 5975 GC/MS configuration used in this study was ideal due to the ease of use to evaluate extraction performance and general availability and robust high throughput nature of the instrumentation. The described extraction procedure can be used to introduce sample into any optimized GC/MS configuration where the columns, GC/MS conditions, or other instrumentation, like GC/QQQ, could be used to analyze these extracts. Normalizing instrument responses to deuterated PAH internal standards produced linear calibrations and accounted for varying extraction efficiencies (Table 3). The QuEChERS/SBSE method provides linear calibration with concentrations of 1, 10, 50, 100, and 250 ng/g matrix for 9 target PAHs (Table 3) with recoveries of 65.5–138.4% for concentrations spiked at 2.5, 50, and 250 ng/g in oysters (Table 3,  $n = 3$  for each spiked concentration), which is consistent with previous studies using this technology [10, 17, 18].

**3.3. Method Trueness and Precision.** Trueness and precision of these determinations were further assessed by measuring PAH concentrations in oysters spiked at 2.5, 50, and 250 ng/g (Table 3). Analysis of a NIST standard reference material performed over a period of several weeks illustrates the accuracy and precision of the method using certified reference material (Table 4). This analysis provided excellent recovery for total PAH (98%,  $n = 11$ ) with high precision (7–19% RSD) that meets the guidelines expressed in the NOAA reference method and National Institute of Standards and Technology Deepwater Horizon study [1, 26]. Only two PAH values, naphthalene and anthracene, were outside the target range.

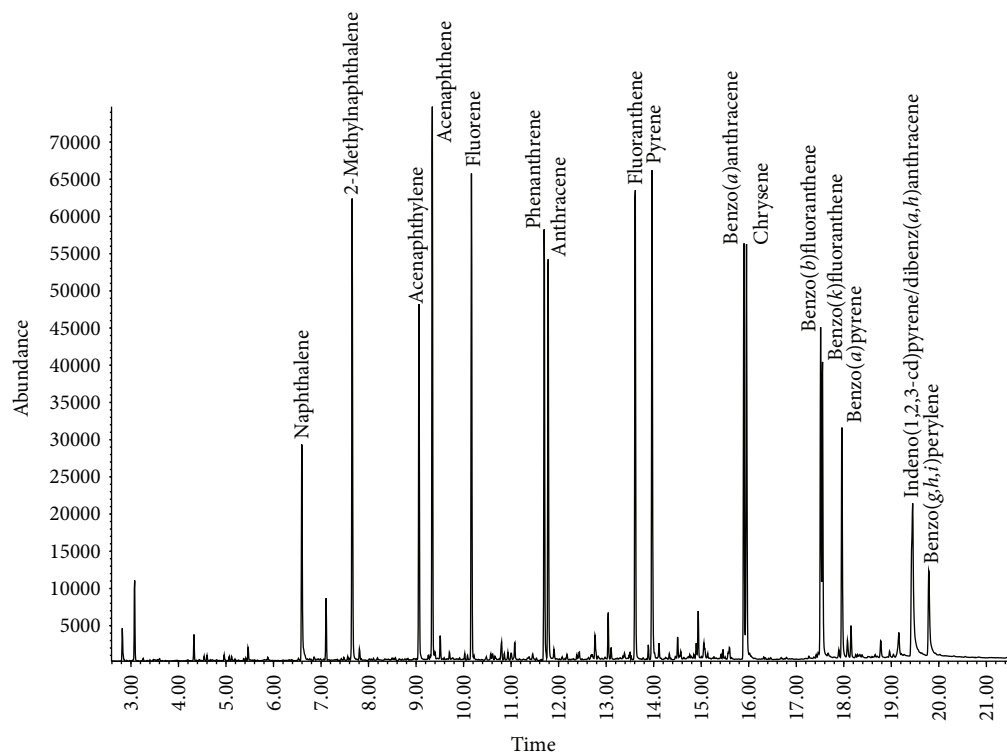


FIGURE 1: Total ion chromatography of PAHs in oysters spiked at 25 ng/g.

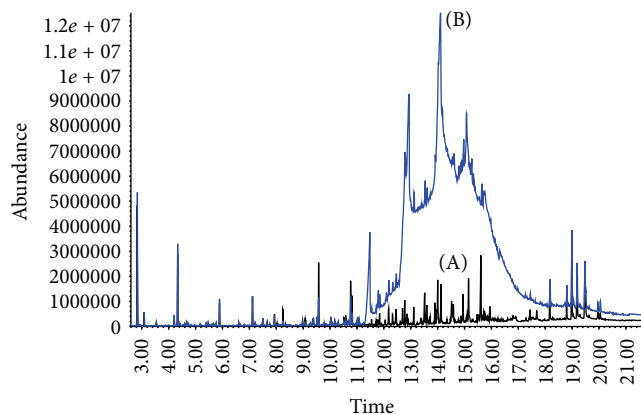


FIGURE 2: Matrix interference is reduced in oysters during SBSE with use of 0.1 M  $\text{NaHCO}_3$  (A) instead of water (B).

Naphthalene exhibited the highest variability (19% RSD) which may have been due to losses during the extra 10-minute shake in our QuEChERS procedure and the relatively high volatility of naphthalene. Although the value for fluorene is within range of the NIST standard reference material, the fluorene values reported in Table 4 were only detected using a 60 m column ( $n = 3$ ) because of coelution of other analytes, such as PCBs, that was difficult to separate using the shorter 30 m column. Anthracene was overestimated due to coelution of contaminants when a shorter GC separation was employed for the study. The presence of a coeluting contaminant in

the stir bar extract was confirmed by comprehensive GC  $\times$  GC analysis on a Leco Pegasus 4D system (data not shown). All of the PAHs were detected, even anthracene, much below the lowest regulatory limits. The limits of detection for the PAHs were found to be 0.020 ppb and the limits of quantification 0.060 ppb, based on  $s/n$  ratios of 3 : 1 and 10 : 1, respectively.

**3.4. Testing Additional Matrices.** Since the SBSE method was successfully validated in both spiked oysters and in NIST standard reference material (mussel tissue) the method was repeated in other seafood matrices using croaker (a finfish) and shrimp. Table 5 shows the linear regression data with 1–250 ng/g spiked tissues with mean  $r^2$  values from 0.9905–0.9948 ( $n = 3$ ). Also, percent recoveries ranged from 63.1 to 93.6% when croaker and shrimp were spiked with 50 ng/g of analyte, a concentration below the regulatory level of concern. Even though further inter- and intralaboratory studies are needed to fully test the utility of this new extraction procedure, these results with oysters, croaker, and shrimp show significant promise for increasing analytical capacity for assessing petroleum contamination in potentially impacted seafood.

The SBSE method is successful with difficult matrices, like seafood, by not only decreasing matrix interference, but also concentrating the analytes. The method and theory of SBSE has been described in detail elsewhere [27]. Briefly, the PDMS coating on the stir bar acts as an immobilized liquid into which apolar analytes in an aqueous matrix can partition. Because of the apolar nature of the PDMS, polar matrix

TABLE 3: Retention time, linear regression, and recovery in oysters.

	RT <sup>1</sup> (min)	Mean $r^2$	Percent recovery (mean $\pm$ SEM <sup>2</sup> )		
			2.5 ng/g	50 ng/g	250 ng/g
Naphthalene	5.5	0.9916	125.6 $\pm$ 0.08	71.6 $\pm$ 0.03	82.4 $\pm$ 0.02
Fluorene	9.25	0.9912	92.8 $\pm$ 0.02	75.3 $\pm$ 0.3	84.5 $\pm$ 0.03
Phenanthrene	10.93	0.9957	118 $\pm$ 0.07	69.8 $\pm$ 0.02	81.5 $\pm$ 0.02
Anthracene	11.02	0.9960	95.6 $\pm$ 0.03	66.8 $\pm$ 0.01	79.9 $\pm$ 0.02
Fluoranthene	13.02	0.9937	138.4 $\pm$ 0.02	88.7 $\pm$ 0.03	100.9 $\pm$ 0.03
Pyrene	13.42	0.9937	131.1 $\pm$ 0.03	86.1 $\pm$ 0.03	97.6 $\pm$ 0.03
Benz[ <i>a</i> ]anthracene	15.52	0.9930	90.7 $\pm$ 0.02	69.4 $\pm$ 0.01	84.3 $\pm$ 0.02
Chrysene	15.58	0.9934	103.7 $\pm$ 0.03	66.3 $\pm$ 0.01	80.7 $\pm$ 0.02
Benzo[ <i>a</i> ]pyrene	17.86	0.9940	70.8 $\pm$ 0.09	65.5 $\pm$ 0.01	81.1 $\pm$ 0.03

<sup>1</sup>RT is the retention time.<sup>2</sup>SEM is the standard error of the mean.

TABLE 4: Analysis on SRM mussel tissue.

Analyte	Acceptable range (ng/g)	Certificate of analysis (ng/g)	QuEChERS-SBSE (ng/g)	%RSD
Naphthalene	1.6–3.3	2.4	1.0	18.5
Fluorene	0.3–0.7	0.49	0.35 <sup>1</sup>	14.7
Phenanthrene	1.7–3.5	2.6	1.9	11.1
Anthracene	0.3–0.8	0.53	2.4 <sup>2</sup>	15.2
Fluoranthene	11.5–23.1	17	19.2	7.0
Pyrene	12.2–24.2	18	19.0	7.2
Benz[ <i>a</i> ]anthracene	2.9–6.9	4.7	3.7	7.2
Chrysene + Triphenylene	7.4–13.8	10.6	8.8	6.8
Benzo[ <i>a</i> ]pyrene	2.0–3.6	2.8	1.7	10.4
Total		<b>59.12</b>	<b>58.05</b>	

<sup>1</sup> $n = 3$  (only detected using 60 m column).<sup>2</sup>Possible coelution.TABLE 5: Analysis of finfish and shrimp matrices,  $n = 3$ .

Spike level ( $\eta$ g/g)	Croaker	Shrimp	Croaker	Shrimp
	50	50	Mean $r^2$	
Percent recovery				
Naphthalene	70.5 $\pm$ 0.001	70.5 $\pm$ 0.017	0.9943	0.9905
Fluorene	63.1 $\pm$ 0.003	78.6 $\pm$ 0.024	0.9912	0.9930
Phenanthrene	70.7 $\pm$ 0.007	67.3 $\pm$ 0.004	0.9948	0.9932
Anthracene	69.1 $\pm$ 0.008	67.7 $\pm$ 0.003	0.9951	0.9810
Fluoranthene	93.6 $\pm$ 0.024	78.2 $\pm$ 0.008	0.9919	0.9940
Pyrene	85.7 $\pm$ 0.024	76.3 $\pm$ 0.009	0.9918	0.9920
Benz[ <i>a</i> ]anthracene	64.4 $\pm$ 0.016	68.7 $\pm$ 0.008	0.9908	0.9929
Chrysene	65.3 $\pm$ 0.023	66.9 $\pm$ 0.011	0.9916	0.9933
Benzo[ <i>a</i> ]pyrene	64.1 $\pm$ 0.006	65.2 $\pm$ 0.007	0.9919	0.9915

components (including inorganic salts, carbohydrates, ionized acids, and amines) do not partition well into the PDMS and therefore do not interfere with the analysis. Furthermore, since loading capacity is based on the volume of PDMS on the stir bar, not the surface area, high molecular weight apolar components such as triglycerides and peptide fragments, which do not diffuse effectively into the PDMS layer, will not interfere with the analysis. Hence, SBSE provides sample cleanup as well as sample concentration and achieves low detection limits in complex sample matrices.

**3.5. Method Workflow and Throughput.** The QuEChERS/SBSE method is inexpensive since the stir bars can be cleaned and reused for 30–50 samples, resulting in an estimated cost of <\$10 per sample for all consumables, including QuEChERS kits. In addition, we propose that the QuEChERS/SBSE procedure can provide high sample throughput. The workflow possible by a single analyst is illustrated in Figure 3. The red bars represent the sample processing steps for a single batch of 20 samples prepared by first performing QuEChERS extractions on a batch of 20 samples followed by unattended

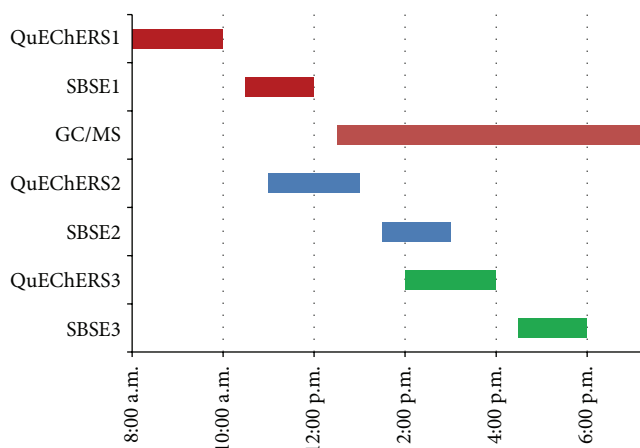


FIGURE 3: Flowchart demonstrating high throughput application of QuEChERS/SBSE method with one technician completing about 60 samples per workday.

SBSE for 90 minutes. Samples are loaded onto the GC/MS and an automated analysis is started. It is possible for a single analyst to prepare a second batch of 20 samples (blue bars) and even a third 20-sample batch (green bars) per day which can be added to the automated GC/MS analysis. The length of the GC/MS method, or other analysis, may vary, but results can be obtained for about 60 samples per day.

#### 4. Conclusion

The QuEChERS/SBSE method presented is a viable alternative to the NOAA method and the LC/FL method to maintain sensitivity, accuracy, and precision while efficiently quantifying PAH contamination in seafood. The QuEChERS extraction strategy was used to effectively extract PAHs from complex seafood matrices including mollusks, crustaceans, and finfish. This study uses a novel SBSE with a buffered diluent to concentrate PAHs and eliminate matrix interference from QuEChERS extracts of seafood, specifically oysters, fish, shrimp, and mussels. This method provides acceptable recovery (65–138%) and linear calibrations and is sensitive (LOD = 0.02 ppb, LOQ = 0.06 ppb) while providing higher throughput and maintaining equivalency between NOAA 2004 as determined by analysis of NIST SRM 1974b mussel tissue.

#### Conflict of Interests

The authors declare that there is no conflict of interests regarding the publication of this paper.

#### Acknowledgments

This work was supported by the Centers for Disease Control contract, 200-2007-21729 (Jeffery H. Moran), and the Bioterrorism Cooperative Agreement, U90/CCU616974-07 (Jeffery H. Moran). The authors also thank Agilent Technologies for providing GC/MS instrumentation and QuEChERS

extraction kits and the Alabama Public Health Laboratory for the specimens used in some of these studies. Cynthia M. Pfannkoch (J. Craig Venter Institute) provided invaluable technical assistance with sample tissue preparation and QuEChERS extractions.

#### References

- [1] National Commission on the BP Deepwater Horizon Oil Spill and Offshore Drilling, *Deep Water: The Gulf Oil Disaster and the Future of Offshore Drilling*, National Commission on the BP Deepwater Horizon Oil Spill and Offshore Drilling, 2011.
- [2] FDA, *Protocol for Interpretation and Use of Sensory Testing and Analytical Chemistry Results for Reopening Oil-Impacted Areas Closed to Seafood Harvesting Due to The Deepwater Horizon Oil Spill*, Food and Drug Administration, 2010.
- [3] R. J. Yender, J. Michel, and C. Lord, *Managing Seafood Safety after an Oil Spill*, National Oceanic and Atmospheric Administration, Hazardous Materials Response Division, Office of Response and Restoration, Seattle, Wash, USA, 2002.
- [4] C. A. Sloan, D. W. Brown, R. W. Pearce et al., "Extraction, cleanup, and gas chromatography/mass spectrometry analysis of sediments and tissues for organic contaminants," U.S. Department of Commerce, NOAA Technical Memo NMFS-NWFSC-59, 2004.
- [5] P. Plaza-Bolaños, A. G. Frenich, and J. L. M. Vidal, "Polycyclic aromatic hydrocarbons in food and beverages. Analytical methods and trends," *Journal of Chromatography A*, vol. 1217, no. 41, pp. 6303–6326, 2010.
- [6] N. Aguinaga, N. Campillo, P. Viñas, and M. Hernández-Córdoba, "Evaluation of solid-phase microextraction conditions for the determination of polycyclic aromatic hydrocarbons in aquatic species using gas chromatography," *Analytical and Bioanalytical Chemistry*, vol. 391, no. 4, pp. 1419–1424, 2008.
- [7] S. Gratz, A. Mohrhous, B. Gamble et al., "Screen for the presence of polycyclic aromatic hydrocarbons in select seafoods using LC-fluorescence," FDA Laboratory Information Bulletin 4475, U.S. Food and Drug Administration, 2010.
- [8] M. Anastassiades, S. J. Lehotay, D. Štajnbaher, and F. J. Schenck, "Fast and easy multiresidue method employing acetonitrile extraction/partitioning and "dispersive solid-phase extraction" for the determination of pesticide residues in produce," *Journal of AOAC International*, vol. 86, no. 2, pp. 412–431, 2003.
- [9] B. O. Pule, L. C. Mmualefe, and N. Torto, "Analysis of polycyclic aromatic hydrocarbons in fish with agilent sampliQ QuEChERS AOAC kit and HPCL-FLD," Agilent Application Note, 2010.
- [10] M. J. Ramalhosa, P. Paíga, S. Morais, C. Delerue-Matos, and M. B. P. P. Oliveira, "Analysis of polycyclic aromatic hydrocarbons in fish: evaluation of a quick, easy, cheap, effective, rugged, and safe extraction method," *Journal of Separation Science*, vol. 32, no. 20, pp. 3529–3538, 2009.
- [11] F. J. Schenck and V. Howard-King, "Rapid solid phase extraction cleanup for pesticide residues in fresh fruits and vegetables," *Bulletin of Environmental Contamination and Toxicology*, vol. 63, no. 3, pp. 277–281, 1999.
- [12] E. Björklund, C. Von Holst, and E. Anklam, "Fast extraction, clean-up and detection methods for the rapid analysis and screening of seven indicator PCBs in food matrices," *TrAC—Trends in Analytical Chemistry*, vol. 21, no. 1, pp. 39–52, 2002.
- [13] F. J. Schenck, S. J. Lehotay, and V. Vega, "Comparison of solid-phase extraction sorbents for cleanup in pesticide residue

- analysis of fresh fruits and vegetables,” *Journal of Separation Science*, vol. 25, no. 14, pp. 883–890, 2002.
- [14] E. Baltussen, P. Sandra, F. David, and C. Cramers, “Stir bar sorptive extraction (SBSE), a novel extraction technique for aqueous samples: theory and principles,” *Journal of Microcolumn Separations*, vol. 11, no. 10, pp. 737–747, 1999.
- [15] F. David and P. Sandra, “Stir bar sorptive extraction for trace analysis,” *Journal of Chromatography A*, vol. 1152, no. 1-2, pp. 54–69, 2007.
- [16] N. Ochiai, K. Sasamoto, H. Kanda et al., “Optimization of a multi-residue screening method for the determination of 85 pesticides in selected food matrices by stir bar sorptive extraction and thermal desorption GC-MS,” *Journal of Separation Science*, vol. 28, no. 9-10, pp. 1083–1092, 2005.
- [17] B. Kolahgar, A. Hoffmann, and A. C. Heiden, “Application of stir bar sorptive extraction to the determination of polycyclic aromatic hydrocarbons in aqueous samples,” *Journal of Chromatography A*, vol. 963, no. 1-2, pp. 225–230, 2002.
- [18] J. I. Cacho, N. Campillo, P. Viñas, and M. Hernández-Córdoba, “Use of headspace sorptive extraction coupled to gas chromatography-mass spectrometry for the analysis of volatile polycyclic aromatic hydrocarbons in herbal infusions,” *Journal of Chromatography A*, vol. 1356, pp. 38–44, 2014.
- [19] N. Barco-Bonilla, R. Romero-González, P. Plaza-Bolaños, J. L. Fernández-Moreno, A. G. Frenich, and J. L. M. Vidal, “Comprehensive analysis of polycyclic aromatic hydrocarbons in wastewater using stir bar sorptive extraction and gas chromatography coupled to tandem mass spectrometry,” *Analytica Chimica Acta*, vol. 693, no. 1-2, pp. 62–71, 2011.
- [20] A. Kende, Z. Csizmazia, T. Rikker, V. Angyal, and K. Torkos, “Combination of stir bar sorptive extraction—retention time locked gas chromatography—mass spectrometry and automated mass spectral deconvolution for pesticide identification in fruits and vegetables,” *Microchemical Journal*, vol. 84, no. 1-2, pp. 63–69, 2006.
- [21] L. Iverson, L. Webb, M. S. Germain, and E. Pfannkoch, “Stir bar sorptive extraction (Twister), thermal desorption, and GC/MS analysis of semi-volatile organic compounds in surface water: a comparison with EPA methods,” in *Proceedings of the American Society of Mass Spectrometry Conference*, Salt Lake City, Utah, USA, 2010.
- [22] N. D. Forsberg, G. R. Wilson, and K. A. Anderson, “Determination of parent and substituted polycyclic aromatic hydrocarbons in high-fat salmon using a modified QuEChERS extraction, dispersive SPE and GC-MS,” *Journal of Agricultural and Food Chemistry*, vol. 59, pp. 8108–8116, 2011.
- [23] E. A. Pfannkoch, J. R. Stuff, J. A. Whitecavage, and F. Foster, “Automated QuEChERS extraction for the determination of pesticide residues in foods using gas chromatography/mass spectrometry,” Gerstel Technical Memo, 2011.
- [24] T. Cajka, K. Mastovská, S. J. Lehotay, and J. Hajslová, “Use of automated direct sample introduction with analyte protectants in the GC-MS analysis of pesticide residues,” *Journal of Separation Science*, vol. 28, no. 9-10, pp. 1048–1060, 2012.
- [25] S. C. Cunha, S. J. Lehotay, K. Mastovska, J. O. Fernandes, M. Beatriz, and P. P. Oliveira, “Evaluation of the QuEChERS sample preparation approach for the analysis of pesticide residues in olives,” *Journal of Separation Science*, vol. 30, no. 4, pp. 620–632, 2007.
- [26] M. K. J. Schantz, “Interlaboratory analytical comparison study to support deepwater horizon natural resource damage assessment: description and results for mussel tissue QA10TIS01,” Tech. Rep. 7819, 2011.
- [27] E. Baltussen, F. David, P. Sandra, and C. Cramers, “On the performance and inertness of different materials used for the enrichment of sulfur compounds from air and gaseous samples,” *Journal of Chromatography A*, vol. 864, no. 2, pp. 345–350, 1999.

## Research Article

# Estimation of Measurement Uncertainties for the DGT Passive Sampler Used for Determination of Copper in Water

Jesper Knutsson, Sebastien Rauch, and Gregory M. Morrison

Department of Water Environment Technology, Division of Civil and Environmental Engineering,  
Chalmers University of Technology, 412 96 Göteborg, Sweden

Correspondence should be addressed to Jesper Knutsson; [jesper.knutsson@chalmers.se](mailto:jesper.knutsson@chalmers.se)

Received 20 May 2014; Accepted 24 July 2014; Published 1 September 2014

Academic Editor: Mohammad R. Pourjavid

Copyright © 2014 Jesper Knutsson et al. This is an open access article distributed under the Creative Commons Attribution License, which permits unrestricted use, distribution, and reproduction in any medium, provided the original work is properly cited.

Diffusion-based passive samplers are increasingly used for water quality monitoring. While the overall method robustness and reproducibility for passive samplers in water are widely reported, there has been a lack of a detailed description of uncertainty sources. In this paper an uncertainty budget for the determination of fully labile Cu in water using a DGT passive sampler is presented. Uncertainty from the estimation of effective cross-sectional diffusion area and the instrumental determination of accumulated mass of analyte are the most significant sources of uncertainty, while uncertainties from contamination and the estimation of diffusion coefficient are negligible. The results presented highlight issues with passive samplers which are important to address if overall method uncertainty is to be reduced and effective strategies to reduce overall method uncertainty are presented.

## 1. Introduction

The overall goal of environmental management programs is to provide a framework for assessing environmental status, identifying problem areas, and to continuously assess quality indicators to ensure that those are within established acceptable limits which ensure a “good and nondeteriorating status.” One of the indicators of environmental quality outlined by the Water Framework Directive of the European Union is heavy metal concentration in water bodies, including Cu, Pb, Cd, and Ni [1]. There is therefore a stated need to measure and assess the environmental concentration of these metals. This should be done using a method that is representative and that provides comparable results across EU member states, though the directive does not specify what level of uncertainty is considered sufficient.

A passive sampler is a device used to collect a target analyte *in situ*, both in gaseous and liquid media. Recently, passive samplers have found increasing use in the determination of metals and organic contaminants in water [2–4]. However, measurement uncertainty, relatively little investigated, is a perceived limitation of passive sampling in comparison to the more conventional grab and automated bottle sampling procedures. The work presented here aims at

characterizing and assessing the uncertainty associated with the determination of time-weighted concentrations of labile metal ions in freshwater using passive sampling.

A passive sampler for metal sampling is typically composed of a membrane filter, a diffusion layer gel, and a receiving phase placed in a sampler housing, like the DGT (diffusive gradients in thin films) technique (Figure 1). The DGT passive sampler was first described by Allan et al. [4] and since then the technique has been used in a wide range of applications and is one of the most widely used passive sampler techniques for quantification and speciation of metals in aquatic environments. The analyte accumulates on the receiving phase as a result of the chemical affinity of the analyte for the solid receiving phase. The amount of analyte accumulated is proportional to the average concentration of labile analyte in the water, the time the sampler is exposed, and other aquatic environmental factors such as temperature and turbulence. After sampler retrieval and determination of the collected amount of metal, the average bulk concentration of metal can be calculated (see [3–5])

$$c_b = \frac{(M_{\text{acc}} - M_{\text{blank}})(D^w \Delta g + D^{\text{MDL}} \delta)}{t D^w D^{\text{MDL}} A_e}. \quad (1)$$

See [6].

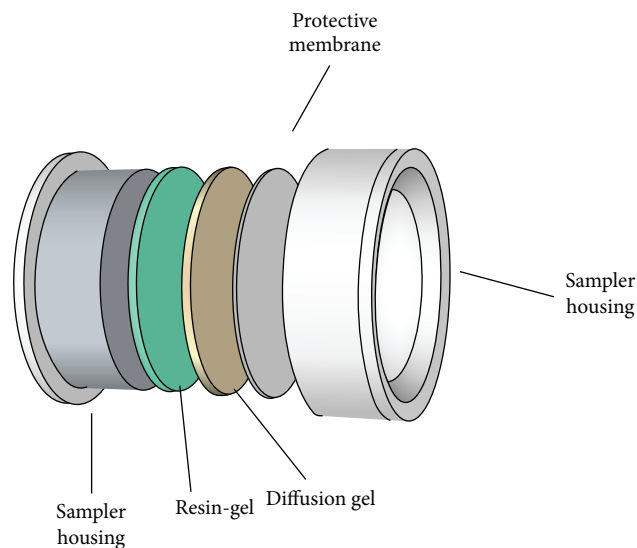


FIGURE 1: A schematic render of a DGT passive sampler showing its principal components.

In (1),  $c_b$  denotes the bulk concentration of the analyte in the water body,  $M_{\text{acc}}$  is the mass of the analyte accumulated on the sampler,  $D^W$  is the diffusion coefficient of the analyte in water at 20°C,  $\Delta g$  is the thickness of material diffusion layer (MDL, consisting of membrane filter and diffusion layer gel),  $D^{\text{MDL}}$  is the diffusion coefficient of the analyte in the MDL,  $\delta$  is the effective thickness of the diffusion boundary layer that is formed at the water-sampler interface,  $t$  is the time of exposure, and  $A_e$  is the effective sectional area of diffusion.

Although there has been some consideration of overall uncertainty in passive sampler measurements [7], there is no published study evaluating the components of this uncertainty. The identification of key components contributing to overall uncertainty can support the improvement of procedures based on passive samplings, as well as reducing potential concerns about performance and reliability [7].

## 2. Materials and Methods

For the purpose of this study, a simple case was assumed; a DGT passive sampler with characteristics listed in Table 1 was used to determine dissolved Cu concentration in water ( $c_b = 1.28 \pm 0.16 \times 10^{-6} \text{ gl}^{-1}$ ). We note that the estimation of uncertainty resulting from metal-ligand interactions is out of the scope of this paper and Cu is therefore considered fully labile and present as  $\text{Cu}^{2+}$ . In the absence of metal complexes, the time weighted average concentration can be derived using (1).

The uncertainty budget presented here was estimated for a generic passive sampler under predefined environmental conditions (Table 1). The characteristics of the passive samplers were chosen based on the characteristics of existing commercially available samplers (DGT Research Ltd.) and the availability of data. Similarly, environmental conditions were selected based on the availability of data for specific

samplers. Although a number of passive sampler technologies have been described in the literature [8–11], the general methodology presented in this work should be applicable to estimate measurement uncertainty for a broad range of passive samplers, even if the specific conclusions for the passive sampler system assessed here does not necessarily hold true for other types.

Uncertainty in passive sampling is expected from all steps in the analytical process, including preparation of the samplers, deployment, analyte extraction, analysis, and estimation of diffusion rates and pathways. Overall, the estimation of uncertainties and the propagation of uncertainties were based on standard methodology [12]. Input data for the calculation were obtained from the literature and our own results, depending on availability. A cause and effect diagram was created to visualize the sources of uncertainty in the analytical chain when using a passive sampler to determine time weighted average bulk concentration (Figure 2). A list of relevant parameters (see Table 2) was identified from the cause and effect diagram and the model equation as a basis for the construction of the uncertainty budget.

## 3. Results and Discussion

### 3.1. Uncertainties in Analyte Accumulation

**3.1.1. Diffusional Pathway.** When deploying a prepared passive sampler, the fully labile metal ion ( $\text{Cu}^{2+}$ ) accumulates on the receiving phase and the accumulation rate is governed by diffusion across a diffusion boundary layer (DBL, see Figure 3), a membrane filter of known thickness (0.135 mm), and a gel layer of a known thickness (0.80 mm). No assessment was found of the uncertainty of  $\Delta g$ , but a low uncertainty level was assumed for the combined membrane filter and gel layer ( $0.935 \pm 0.05 \text{ mm}$ ) based on the authors judgement [12].

The DBL is the water layer closest to the passive sampler-water interface that is not affected by the mixing conditions in the bulk water phase. This measure is a representation of the effective DBL as this is neither evenly distributed layer across the surface nor a true unmixed layer but rather a velocity gradient. The effective thickness of the DBL is subject to uncertainty. The uncertainty can be reduced by deploying several devices with varying  $\Delta g$ , as described by Zhang et al. [13], but this procedure increases the scope and cost of measurement considerably. Therefore in the hypothetical scenario presented here, the DBL thickness was estimated to be  $0.26 \pm 0.05 \text{ mm}$ , covering a wide range of flow regimes, from fast flowing water to slow moving lake epilimnion [6]. The diffusion coefficient of the metal ion  $\text{Me}^{2+}$  depends in turn on the water temperature and on which media it is diffusing in. The total accumulated amount ( $M$ ) depends on the accumulation rate and the length of the exposure in time ( $t$ ).

**3.1.2. Diffusion Coefficients.** The diffusion coefficients  $D^W$  and  $D^{\text{MDL}}$  are usually determined experimentally in a separate experiment. The determination itself is associated with

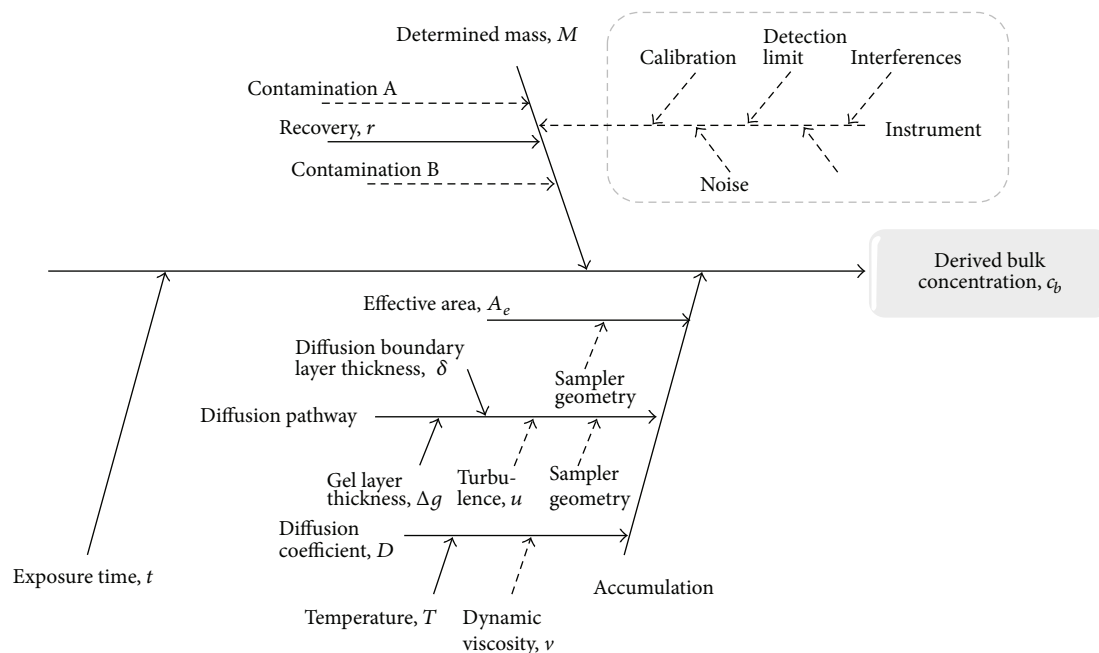


FIGURE 2: Cause and effect diagram describing the uncertainties associated with the determination of bulk concentration  $c_b$ , using a passive sampler. Dashed arrows indicates parameters whose uncertainty contribution was included in another parameter. The dashed box shows the uncertainty from instrument determination of analyte. Uncertainty analysis of the ICP-MS technique has been performed previously [19, 22] and was therefore not treated separately in this paper.

TABLE 1: Predefined passive sampler characteristics and environmental conditions used as a basis in the uncertainty calculations.

Parameter	Property/Value
Passive sampler	
Diameter	2 cm
Diffusion layer	Acrylamide gel with APA cross-linker (APA2) [23]
Cellulose nitrate membrane	135 $\mu\text{m}$ thickness and 0.45 $\mu\text{m}$ pore size
Receiving phase	Resin-gel containing Chelex resin
Environmental conditions	
pH	7.5
Water temperature	25° C/298 K
Turbulence	Estimated

TABLE 2: Parameters for which uncertainty is determined and respective units.

Parameter	Unit	Definition
$A_e$	$\text{m}^2$	Effective area of diffusional cross-section
$D^{\text{MDL}}$	$\text{m}^2 \text{s}^{-1}$	Diffusion coefficient of the $\text{Cu}^{2+}$ ion in the MDL
$D^{\text{W}}$	$\text{m}^2 \text{s}^{-1}$	Diffusion coefficient of the $\text{Cu}^{2+}$ ion in water
$M$	g	Accumulated amount of $\text{Cu}^{2+}$ determined from sample
$M_{\text{blank}}$	g	Contamination determined from field blank
$r$		Recovery during the extraction phase
$T$	K	Temperature in bulk water phase
$t$	hours	Exposure time
$\delta$	m	Diffusional boundary layer thickness
$\Delta g$	m	Diffusional pathway thickness of the MDL

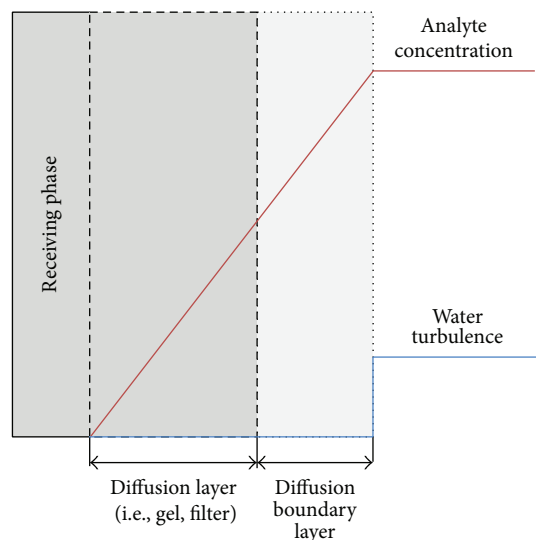


FIGURE 3: Schematic representation of the concentration gradient that forms over the diffusional pathway.

uncertainty, and results are typically reported without associated uncertainty. A typical relative uncertainty of diffusion coefficients has been reported in the range 1.3–6.4% [14, 15] and for the purpose of this assessment we will use a  $D^{\text{MDL}}$  value of  $6.42 \times 10^{-10} \text{ m}^2 \text{ s}^{-1}$ , which is the diffusion coefficient of  $\text{Cu}^{2+}$  in APA2 gel (a polyacrylamide hydrogel containing 15 % vol acrylamide and 0.3% agarose-derived cross-linker) and the upper value in the uncertainty interval, that is, 6.4% [15]. The diffusion coefficient of  $\text{Cu}^{2+}$  in water ( $D^{\text{W}}$ ) is reported to be 1.14 times larger at  $7.30 \times 10^{-10} \text{ m}^2 \text{ s}^{-1}$  [15]. For the purpose of this paper that same relative uncertainty was applied to both  $D^{\text{MDL}}$  and  $D^{\text{W}}$ . It should be noted that effective diffusion coefficients may also be significantly affected in low ionic strength solutions (<1 mM).

The diffusion coefficient  $D$  depends on water temperature as described by the Stokes-Einstein equation:

$$D = \frac{k_b T}{3\pi\mu d}, \quad (2)$$

where  $k_b$  is the Boltzmann constant ( $\text{m}^2 \text{ kg s}^{-2} \text{ K}^{-1}$ ),  $T$  is the temperature (K),  $\mu$  is the viscosity of the medium ( $\text{kg s}^{-1} \text{ m}^{-1}$ ), and  $d$  is the spherical diameter of the diffusing particle.

The uncertainty introduced from variability of  $T$  was analysed ( $D(T)$ ). The uncertainty in the experimental determination of  $D$  was also estimated. The standard uncertainty in  $D^{\text{W}}$  from uncertainty in water temperature was calculated to be  $0.06 \times 10^{-10} \text{ m}^2 \text{ s}^{-1}$ , and the combined standard uncertainty from the determination of  $D^{\text{W}}$  and temperature was calculated through summation in quadrature to be  $7.30 \pm 0.47 \times 10^{-10} \text{ m}^2 \text{ s}^{-1}$ . A similar treatment of  $D^{\text{MDL}}$  resulted in  $6.42 \pm 0.10 \times 10^{-10} \text{ m}^2 \text{ s}^{-1}$ .

**3.1.3. Effective Area.** The effective area of the section through which diffusion occurs has been reported to be somehow

larger than the nominal area due to lateral diffusion; that is, diffusion occurs in three dimensions [6, 7]. Warnken et al. report that the radius of the effective diffusion window is  $1.02 \pm 0.024 \text{ cm}$  and also note that the gel disc diameter had shrunk on average 0.12 cm ( $n = 6$ ) during drying prior to determination of the radius [16]. No estimate on uncertainty was given for this measure, so a 0.05 cm uncertainty was assumed based on the number of significant figures reported, and a rectangular distribution was selected due to the lack of information on the measurement.

Summation in quadrature was used to combine the uncertainties from the determination of effective radius and the estimation of the shrinkage in order to calculate the total uncertainty associated with the effective area [17]. The divisor  $\sqrt{3}$  was used to get the standard uncertainty of the shrinkage because of the assumed rectangular distribution, followed by summation in quadrature:

$$U_c = \sqrt{u_i(r_{\text{disc}})^2 + \left(\frac{u_i(r_{\text{shrinkage}})}{\sqrt{3}}\right)^2}. \quad (3)$$

The combined uncertainty of the effective radius was calculated to be 0.0449 cm, making the effective radius of the sampler  $1.08 \pm 0.04 \text{ cm}$ . Using the derivative of the circle area function to calculate the uncertainty of the effective area,  $A_e$ , gave the value  $3.66 \pm 0.30 \text{ cm}^2$ .

## 3.2. Uncertainties in Determination of Mass

**3.2.1. Preparation and Handling.** During preparation, transport, storage, and handling of the passive sampler devices there is a risk of contamination. The best assessment of the uncertainty from these sources comes from the use of field blanks [18]. The field blanks can be used to correct for contamination issues. We have estimated during field trials that the associated relative uncertainty resulting from contamination is typically in the order of 24% for passive sampler devices, with field blank values of  $8.1 \pm 2.0 \text{ ng Cu}^{2+}$  ( $n = 3$ ) (unpublished data).

**3.2.2. Extraction.** The analyte ( $\text{Cu}^{2+}$ ) is subsequently extracted from the receiving phase using a small volume of nitric acid. The recovery factor,  $r$ , has been reported previously ( $0.793 \pm 0.051$ ) [5]. The uncertainty was reported as an interval, and therefore a rectangular distribution was assumed.

**3.2.3. Analysis/Determination.** The resulting extract is diluted to a suitable volume concentration before analysis by a selected analytical technique. Inductively coupled plasma-mass spectrometry (ICP-MS) is widely used for the determination of trace metal concentrations in environmental samples and therefore, we estimate uncertainty for ICP-MS analysis in this paper. The ICP-MS instrument is calibrated using calibration standards prepared from certified standard solutions.

Generally, the analytical procedure using ICP-MS is subject to known and unknown interferences of which some

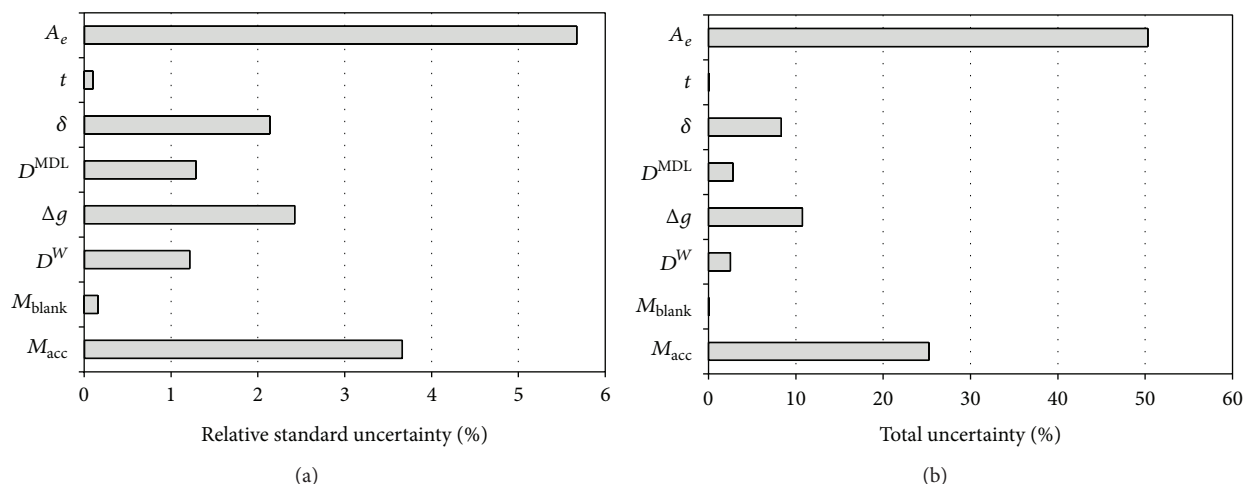


FIGURE 4: Relative standard uncertainty (a) and percentage of total uncertainty (b) for the variables in the model equation.

TABLE 3: Uncertainty budget for  $M_{\text{acc}}$  showing relative uncertainties for the variables and the combined standard uncertainty.

Symbol	Source of uncertainty	Type*	Standard uncertainty $u(x_i)$	Distribution	Divisor	Relative uncertainty
$m_{\text{icp-ms}}$	Estimated mass from ICP-MS analysis	A	$1.0 \times 10^{-8}$ g	Normal	1	0.008
$r$	Recovery factor	B	0.0293	Rectangular	$\sqrt{3}$	0.064
Uc (M)	Combined standard uncertainty	A	$6.15 \times 10^{-8}$ g	Normal		0.038

\* Note: type of uncertainty refers to types A and B, using standard vocabulary for statistically evaluated uncertainty (A) and uncertainty evaluated by other methods (B).

can be compensated for, while others may persist, depending on specific instrument capabilities [18]. Furthermore, instrument drift, stability of stock solutions, and density of stock solutions will contribute to uncertainty [18] and the uncertainty budget of the instrumental analysis is a comprehensive topic in its own right. A simplified view is given in Figure 2 to highlight the importance of the analytical step. However, instrument performance and the typical uncertainty of the method have been addressed elsewhere [19] and are not repeated here. The reported standard relative uncertainty for Ni solutions containing  $10 \text{ ng g}^{-1}$  or more was 7.5%, which was used for the calculations in this paper.

The estimated accumulated mass and mass on blank samples was determined using ICP-MS and then corrected for by the recovery factor according to

$$M_{\text{acc/blank}} = \frac{m_{\text{icp-ms}}}{r}. \quad (4)$$

Using the rule for uncertainty propagation in quotients the estimate for  $M_{\text{acc}}$  becomes  $1.63 \pm 0.06 \times 10^{-6}$  g (see Table 3). A similar treatment of  $M_{\text{blank}}$  resulted in  $0.010 \pm 0.003 \times 10^{-6}$  g.

**3.3. Total Combined Uncertainty of the Passive Sampler Measurement.** To estimate the combined standard uncertainty of the bulk concentration  $c_b$ , the relation in the model equation (1) was used. Since it was a mixed expression, the rule of

uncertainty propagation states that the combined uncertainty can be calculated using

$$\partial Q = \sqrt{\left(\frac{\partial q}{\partial x} \delta x\right)^2 + \dots + \left(\frac{\partial q}{\partial z} \delta z\right)^2}. \quad (5)$$

See [20].

This means that the combined uncertainty is equal to the root square sum of the partial derivatives of the variables. However, it is also possible to derive a numerical solution as suggested by Kragten [21]. The approximation derived from this numerical method assumes linearity and small values of relative uncertainty,  $u(x_i)/x_i$ . While this is not always the case, the accuracy of the solution is still acceptable for most practical purposes [21].

A summary of the quantities and the associated standard uncertainties is presented in Table 4.

During calculations values were not rounded to avoid the introduction of additional uncertainty. The output of the numerical treatment of combined uncertainties can be seen in Table 5. The measurement output with associated uncertainty was  $c_b = 1.32 \pm 0.100 \mu\text{g l}^{-1}$ . Using a coverage factor  $k = 2$  the result was instead  $1.32 \pm 0.200 \mu\text{g l}^{-1}$  (confidence interval  $\approx 95\%$ ), or a relative uncertainty of 7.6% at  $k = 1$ .

When plotting the relative standard uncertainties of the components graphically (Figure 4) it is obvious that the largest uncertainty was introduced from the effective cross-sectional area estimate ( $A_e$ ). The combined estimated uncertainties resulting from the determination of the lateral

TABLE 4: Quantities, nominal values, and their associated uncertainty used in this work.

Quantity	Value	Standard uncertainty	Comment
$A$	3.66 cm <sup>2</sup>	0.30 cm <sup>2</sup>	See previous section and [16]
$D^{\text{MDL}}$	$6.42 \times 10^{-10}$ m <sup>2</sup> /s	$0.09 \times 10^{-10}$ m <sup>2</sup> /s	Empirical value [15]
$D^{\text{W}}$	$7.30 \times 10^{-10}$ m <sup>2</sup> /s	$0.47 \times 10^{-10}$ m <sup>2</sup> /s	Empirical value [15]
$M_{\text{acc}}$	$1.29 \times 10^{-6}$ g	$0.01 \times 10^{-6}$ g	Observation
$M_{\text{blank}}$	$0.008 \times 10^{-6}$ g	$0.002 \times 10^{-6}$ g	Observation
$r$	0.793	0.051	Observation [5]
$t$	168 h	0.3 h	Covers the time it takes to deploy and retrieves 5 passive samplers
$T$	25°C/298 K	4 K	Standard deviation of the measured temperature
$\delta$	$0.26 \times 10^{-3}$ m	$0.05 \times 10^{-3}$ m	Estimate [16]
$\Delta g$	$0.9 \times 10^{-3}$ m	$0.05 \times 10^{-3}$ m	Estimate

TABLE 5: Uncertainty budget for determination of time weighted average concentration of Cu<sup>2+</sup> in water using a DGT passive sampler.

Symbol	Source of uncertainty	Type	Standard uncertainty $u(x_i)$	Distribution	Divisor	$U_i$ (M) $\mu\text{g L}^{-1}$
$M_{\text{acc}}$	Determination of accumulated mass	A	$6.14 \times 10^{-8}$ g	Normal	1	0.49
$M_{\text{blank}}$	Determination of contamination	A	$2.55 \times 10^{-9}$ g	Normal	1	0.02
$D^{\text{W}}$	Diffusion coefficient in water	A	$4.73 \times 10^{-11}$ m <sup>2</sup> /s	Normal	1	0.16
$\Delta g$	Thickness of material diffusion layer (MDL)	B	$2.89 \times 10^{-5}$ m	Rectangular	$\sqrt{3}$	0.33
$D^{\text{MDL}}$	Diffusion coefficient in MDL	A	$1.03 \times 10^{-11}$ m <sup>2</sup> /s	Normal	1	0.16
$\delta$	Diffusion boundary layer	B	$2.89 \times 10^{-5}$ m	Rectangular	$\sqrt{3}$	0.29
$t$	Time	B	624 s	Rectangular	$\sqrt{3}$	0.01
$A_e$	Effective area	A	$2.08 \times 10^{-5}$ m <sup>2</sup>	normal	1	0.69
Uc ( $c_b$ )	Combined standard uncertainty			Normal		0.98
Uc ( $c_b$ )	Expanded standard uncertainty			Normal ( $k = 2$ )		1.95

TABLE 6: Results from sensitivity analysis, showing the effect on total uncertainty of the passive sampler measurement from reductions in uncertainty of selected parameters.

Parameter	Change in uncertainty	Result on total uncertainty
Effective area, $A_e$	50% reduction	Reduction from 7.6% to 6.1% in overall relative uncertainty
Recovery factor, $r$	50% reduction	Reduction from 7.6% to 6.9% in overall relative uncertainty
Diffusion boundary layer, $\delta$	From 0.05 mm to 0.014 mm standard uncertainty	Reduction from 7.6% to 7.3% in overall relative uncertainty
Diffusion pathway thickness	50% reduction	Reduction from 7.6% to 7.3% in overall relative uncertainty
Diffusion pathway thickness	4 times increase	Increase from 7.6% to 12.2% in overall relative uncertainty

diffusion round the edges and the shrinkage of the gel resulted in an uncertainty that largely affects the end result, as it accounts for nearly 50% of the total uncertainty (see Figure 4). Uncertainties from the estimation of  $M_{\text{acc}}$  account for roughly 25% of the total uncertainty, with the most significant factor being the estimation of extraction recovery.

A sensitivity analysis shows that halving the uncertainty for the effective radius and shrinkage in the determination of  $A_e$  would reduce the contribution of  $A_e$  to the overall uncertainty to roughly 20% ( $1.32 \pm 0.08 \mu\text{g l}^{-1}$  or 6.0% relative overall uncertainty). Similarly, a reduction in the uncertainty in the recovery factor,  $r$ , by 50%, would reduce the contribution from  $M_{\text{acc}}$  to overall uncertainty from 25% to approximately 9% ( $1.32 \pm 0.09 \mu\text{g l}^{-1}$  or 6.8% relative overall uncertainty). On the other hand, an increase in the uncertainty for diffusion layer thickness from 0.05 mm to

0.2 mm would result in  $1.32 \pm 0.16 \mu\text{g l}^{-1}$  or 12.2% relative overall uncertainty. This is a significant increase in overall uncertainty and illustrates the sensitivity of the method to inconsistencies in the gel-membrane layer interface. Furthermore, the effects of uncertainty changes in DBL and diffusive layer thickness are shown in Table 6.

The sensitivity analysis shows that overall method uncertainty can be significantly reduced by addressing the proper sources of uncertainties and also that deterioration in diffusion layer consistency can have significant negative effects on overall method uncertainty.

#### 4. Conclusion

An uncertainty analysis was performed for passive sampling of a metal ion in water to highlight critical steps in the method

and to identify key factors for potential improvement. In the analysis performed here the uncertainty of the effective cross-sectional diffusion area  $A_e$  was identified as the main contributor to overall uncertainty. Uncertainties in analyte recovery and material diffusion ranked second and third, respectively. An improvement in the estimation of  $A_e$  was found to be an important step toward achieving a reduction in uncertainty in passive sampling. Optimization of the extraction procedure will provide a further reduction in overall uncertainty.

## Conflict of Interests

The authors declare that there is no conflict of interests regarding the publication of this paper.

## References

- [1] European Commission, 2000/60/EC, 2000.
- [2] H. Zhang and W. Davison, "Direct in situ measurements of labile inorganic and organically bound metal species in synthetic solutions and natural waters using diffusive gradients in thin films," *Analytical Chemistry*, vol. 72, no. 18, pp. 4447–4457, 2000.
- [3] L. B. Blom, G. M. Morrison, J. Kingston et al., "Performance of an in situ passive sampling system for metals in stormwater," *Journal of Environmental Monitoring*, vol. 4, no. 2, pp. 258–262, 2002.
- [4] I. J. Allan, J. Knutsson, N. Guigues, G. A. Mills, A. Fouillac, and R. Greenwood, "Evaluation of the chemcatcher and DGT passive samplers for monitoring metals with highly fluctuating water concentrations," *Journal of Environmental Monitoring*, vol. 9, no. 7, pp. 672–681, 2007.
- [5] H. Zhang and W. Davison, "Performance characteristics of diffusion gradients in thin films for the in situ measurement of trace metals in aqueous solution," *Analytical Chemistry*, vol. 67, no. 19, pp. 3391–3400, 1995.
- [6] W. Davison and H. Zhang, "Progress in understanding the use of diffusive gradients in thin films (DGT) back to basics," *Environmental Chemistry*, vol. 9, no. 1, pp. 1–13, 2012.
- [7] C. Miège, S. Schiavone, A. Dabrin et al., "An in situ intercomparison exercise on passive samplers for monitoring metals, polycyclic aromatic hydrocarbons and pesticides in surface waters," *Trends in Analytical Chemistry*, vol. 36, pp. 128–143, 2012.
- [8] W. Davison and H. Zhang, "In situ speciation measurements of trace components in natural waters using thin-film gels," *Nature*, vol. 367, no. 6463, pp. 546–548, 1994.
- [9] W. G. Brumbaugh, J. D. Petty, T. W. May, and J. N. Huckins, "A passive integrative sampler for mercury vapor in air and neutral mercury species in water," *Chemosphere—Global Change Science*, vol. 2, no. 1, pp. 1–9, 2000.
- [10] J. K. Kingston, R. Greenwood, G. A. Mills, G. M. Morrison, and L. B. Persson, "Development of a novel passive sampling system for the time-averaged measurement of a range of organic pollutants in aquatic environments," *Journal of Environmental Monitoring*, vol. 2, no. 5, pp. 487–495, 2000.
- [11] J. Rozemeijer, Y. van der Velde, H. de Jonge, F. van Geer, H. P. Broers, and M. Bierkens, "Application and evaluation of a new passive sampler for measuring average solute concentrations in a catchment scale water quality monitoring study," *Environmental Science and Technology*, vol. 44, no. 4, pp. 1353–1359, 2010.
- [12] S. L. R. Ellison and A. Williams, "Eurachem/CITAC guide: Quantifying Uncertainty in Analytical Measurement," 2012.
- [13] H. Zhang, W. Davison, R. Gadi, and T. Kobayashi, "In situ measurement of dissolved phosphorus in natural waters using DGT," *Analytica Chimica Acta*, vol. 370, no. 1, pp. 29–38, 1998.
- [14] E. R. Unsworth, H. Zhang, and W. Davison, "Use of diffusive gradients in thin films to measure cadmium speciation in solutions with synthetic and natural ligands: comparison with model predictions," *Environmental Science and Technology*, vol. 39, no. 2, pp. 624–630, 2005.
- [15] S. Scally, W. Davison, and H. Zhang, "Diffusion coefficients of metals and metal complexes in hydrogels used in diffusive gradients in thin films," *Analytica Chimica Acta*, vol. 558, no. 1–2, pp. 222–229, 2006.
- [16] K. W. Warnken, H. Zhang, and W. Davison, "Accuracy of the diffusive gradients in thin-films technique: diffusive boundary layer and effective sampling area considerations," *Analytical Chemistry*, vol. 78, no. 11, pp. 3780–3787, 2006.
- [17] I. J. Allan, J. Knutsson, N. Guigues, G. A. Mills, A. Fouillac, and R. Greenwood, "Chemcatcher and DGT passive sampling devices for regulatory monitoring of trace metals in surface water," *Journal of Environmental Monitoring*, vol. 10, no. 7, pp. 821–829, 2008.
- [18] S. Nelms, *Inductively Coupled Plasma Mass Spectrometry Handbook*, Blackwell, 2005.
- [19] V. J. Barwick, S. L. R. Ellison, and B. Fairman, "Estimation of uncertainties in ICP-MS analysis: a practical methodology," *Analytica Chimica Acta*, vol. 394, no. 2–3, pp. 281–291, 1999.
- [20] J. R. Taylor, *An Introduction to Error Analysis*, University Science books, Sausalito, Calif, USA, 1997.
- [21] J. Kragten, "Tutorial review. Calculating standard deviations and confidence intervals with a universally applicable spreadsheet technique," *The Analyst*, vol. 119, no. 10, pp. 2161–2165, 1994.
- [22] P. Evans and B. Fairman, "High resolution ID-ICP-MS certification of an estuary water reference material (LGC 6016) and analysis of matrix induced polyatomic interferences," *Journal of Environmental Monitoring*, vol. 3, no. 5, pp. 469–474, 2001.
- [23] H. Zhang and W. Davison, "Diffusional characteristics of hydrogels used in DGT and DET techniques," *Analytica Chimica Acta*, vol. 398, no. 2–3, pp. 329–340, 1999.